UNIVERSITÉ DU QUÉBEC À MONTRÉAL

INVESTIGATING THE METABOLOME AND PROTEOME OF COLON AND FECAL SAMPLES FROM HEALTHY MICE BY LC-MS/MS

MASTER'S THESIS

PRESENTED

AS PARTIAL FULFILLMENT

OF THE MASTER'S IN BIOCHEMISTRY

BY

ORIANA ZAMBITO

MAY 2024

UNIVERSITÉ DU QUÉBEC À MONTRÉAL

ÉTUDE DU MÉTABOLOME ET DU PROTÉOME DES ÉCHANTILLONS DE CÔLON ET DE FÈCES DE SOURIS SAINES PAR LC-MS/MS

MÉMOIRE

PRÉSENTÉE

COMME EXIGENCE PARTIELLE

À LA MAÎTRISE EN BIOCHIMIE

PAR

ORIANA ZAMBITO

MAI 2024

REMERCIEMENTS

I am deeply grateful to Prof. Lekha Sleno for generously welcoming me into her academic realm and providing me with the invaluable opportunity to learn under her guidance. Her support, patience, and dedication have been pivotal throughout my studies and research, inspiring me to persist on this academic path. Special thanks extend to the members of Prof. Lekha Sleno's lab, including Maggy Lépine, Kahina Chabi, Nathan Ghafari, Ikram Benhadji, Myriam Mireault, Carina Lima, Kathrina Mae Kumaresan, Ons Ousji and Said Matar, along with a notable mention of Leanne Ohlund.

I would also like to say a big thank you to our collaborators Prof. Nicolas Pilon, Nejia Lassoued, and Rodolphe Soret for their crucial contributions to this project. This project would not have been realised without their vital contribution.

I extend my gratitude to my family and my partner, without whom this academic journey would not have been possible. Their consistent support, unwavering presence, and unconditional love have never gone unnoticed. Through the highs and lows of these past two years, they have been a source of joy, laughter, and support as a constant, grounding force that has enabled me to overcome challenges and continue my academic path.

TABLE DES MATIÈRES

LISTE DES FIGURES

LISTE DES TABLEAUX

LISTE DES ABRÉVIATIONS, DES SIGLES ET DES ACRONYMES

ABC	Ammonium bicarbonate buffer
ACN	Acetonitrile
APCI	Atmospheric pressure chemical ionization
Arg	Arginine
BMI	Body mass index
CE	Collision energy
CI	Chemical ionization
CID	Collision induced dissociation
CNS	Central nervous system
COX	Cyclooxygenase
CRC	Colorectal cancer
DC	Direct current
DIA	Data independent acquisition
DTT	Dithiothreitol
ECM	Extracellular matrix
EI	Electronic ionization
ENS	Enteric nervous system
ESI	Electrospray ionization
EtOH	Ethanol
FA	Formic acid

FDR	False discovery rate
GC	Gas chromatography
GI	Gastrointestinal tract
HLB	Hydrophilic-lipophilic balance
HPLC	High resolution liquid chromatography
HRMS	High resolution mass spectrometry
IAM	Iodoacetamide
IBD	Irritable bowel disease
IBS	Irritable bowel syndrome
IDA	Information dependent acquisition
IMA	Inferior mesenteric artery
K8	Keratin type II cytoskeletal 8
K18	Keratin type II cytoskeletal 18
K19	Keratin type II cytoskeletal 19
K20	Keratin type II cytoskeletal 20
LC-MS/MS	Liquid chromatography coupled to tandem mass spectrometry
Lys	Lysine
MeOH	Methanol
MRM	Multiple reaction monitoring
MS	Mass spectrometry
MS/MS	Tandem mass spectrometry

NMR	Nuclear magnetic resonance
PCA	Principal component analysis
PCR	Polymerase chain reaction
PFP	Pentafluorophenyl
PGA1	Prostaglandin A1
PGA2	Prostaglandin A2
PGB1	Prostaglandin B1
PGD1	Prostaglandin D1
PGE1	Prostaglandin E1
PGE2	Prostaglandin E2
PGF2a	Prostaglandin F2alpha
PGH2	Prostaglandin H2
PGI2	Prostaglandin I2
15deltaPGJ2	15-deoxy-DELTA 12,14-prostaglandin J2
QqTOF	Quadrupole time-of-flight mass analyzer
RF	Radio frequency
RPLC	Reverse-phase liquid chromatography
SPE	Solid phase extraction
SSRI	Selective serotonin reuptake inhibitor
TLC	Thin layer chromatography
TOF	Time-of-Flight

LISTE DES SYMBOLES ET DES UNITÉS

m/z	Mass-to-charge ratio
rpm	Revolutions per minute
ppm	Parts per million
%	Percent
ºC	Degrees Celsius
mg	Milligram
g	Gram
ml	Millilitre
L	Litre
Q	Quadrupole
RT	Retention time
Psi	Pound-force per square inch
V	Voltage
Min	Minute
cm	Centimetre
pH	Potential of hydrogen

RÉSUMÉ

Les perturbations du microbiome intestinal suscitent un intérêt croissant, car elles peuvent être reliées à plusieurs maladies intestinales et constituer des marqueurs de la santé intestinale globale. Compte tenu de la présence de divers micro-organismes dans le côlon et dans les matières fécales, ces types d'échantillons sont idéaux pour étudier le microbiome intestinal, ce qui les rend d'un grand intérêt à étudier. De plus, les régions proximaux et distaux de ces types d'échantillons peuvent également fournir une compréhension supplémentaire des voies biologiques se produisant dans différentes parties de l'intestin. Dans cette étude, des analyses LC-MS/MS non ciblées ont été effectuées sur des échantillons de selles et de côlon proximaux et distaux provenant de souris saines pour le profilage métabolomique et protéomique. Lors d'une étape d'homogénéisation suivi par la précipitation de protéines, les surnageants résultants ont été utilisés pour l'analyse métabolomique non ciblée et les culots protéiques ont servi pour l'analyse protéomique ascendante quantitative. Les protéines ont été solubilisées et leurs quantités normalisées avant la digestion trypsique et l'extraction en phase solide des peptides résultants. Les analyses métabolomiques et protéomiques ont été effectuées sur une plate-forme quadripôle temps de vol. Pour l'analyse métabolomique, les échantillons ont été injectés sur une colonne à mode mixte à phase inverse d'échange d'ions ainsi que sur une colonne pentafluorophényle avec une séparation optimisée pour l'analyse de métabolites polaires. Les deux colonnes ont fourni des résultats complémentaires, augmentant la couverture des métabolites détectés. Le logiciel Sciex OS a été utilisé pour la recherche de pics non ciblés et leur correspondance spectral à l'aide de base de données pour l'identification de métabolites putatifs. Suivant une analyse statistique, 153 métabolites du côlon et 23 métabolites fécaux ont été filtrés selon leurs différences quantitatives entre les régions proximales et distales du côlon. Pour l'analyse protéomique, les peptides ont été séparés à l'aide d'une colonne C18 en phase inverse. À partir de ces données, 1103 protéines de souris ont été quantifiés dans les échantillons du côlon, dont 158 se sont révélées significativement changeantes entre les régions distales et proximales. Pour les échantillons fécaux, une analyse métaprotéomique a été réalisée pour identifier des espèces bactériennes uniques provenant des différentes régions de l'intestin et pour déterminer qu'il n'y avait pas des différences significatives au niveau de ces espèces dans les différentes régions du côlon. Ce mémoire explique la méthodologie détaillée utilisée, y compris les étapes de traitement des données, ainsi que les résultats élucidés grâce à cette étude.

Mots clés : Intestin, Côlon, Microbiome, Fèces, Métabolomique, Protéomique, LC-MS/MS

ABSTRACT

There is a growing interest in gut microbiome perturbations as they can be related to several intestinal diseases and be markers of overall gut health. Fecal and colon samples can mirror or reflect gut health, including changes at the microbiome level, and are therefore of great interest to study. Proximal and distal locations of these sample types can also provide additional understanding of the biological pathways occurring in different parts of the gut. In this study, untargeted LC-MS/MS analyses were performed on proximal and distal fecal and colon samples from healthy mice for metabolomic and proteomic profiling. Proximal and distal fecal and colon samples were collected from healthy mice prior to sample homogenisation and protein precipitation. Resulting supernatants were used for untargeted metabolomics, and protein pellets were used for quantitative proteomics. Proteins were solubilized and amounts normalized prior to trypsin digestion and solid-phase extraction of resulting peptides. Metabolomic and proteomic analyses were performed on a quadrupole time-of-flight platform. For the untargeted metabolomics, samples were separated on ion exchange-reverse phase mixed-mode and pentafluorophenyl columns using optimized solvent gradients for the analysis of polar metabolites. The two columns provided complementary results, increasing the coverage of detected metabolites. Sciex OS software was employed for untargeted peak finding and searching small molecule spectral libraries for putative metabolite identification, in which 966 colon metabolites and 1183 fecal metabolites were putatively identified. Performing statistical analyses demonstrated that 153 colon and 23 fecal metabolites were changing quantitively between proximal and distal regions. For proteomics analyses, peptides were separated using a reverse-phase C18 column with quantitative SWATH analysis. From the resulting data, 1103 mouse proteins were quantified in the colon samples, 158 of which were significantly changing between distal and proximal regions. Identification and quantification of several bacterial species was possible through metaproteomics analysis of the fecal samples, although no differentially expressed species were determined between the distal and proximal regions. The methodology, results and data processing pipelines used in this study are outlined in this Master's thesis.

Keywords : Gut, Microbiome, Feces, Colon, Metabolomics, Proteomics, LC-MS/MS

CHAPITRE 1
INTRODUCTION

With intestinal diseases on the rise, it is critical to understand the biological implications and variability occurring within the gut. This chapter includes an introduction on the gastrointestinal system and the analytical technique (LC-HRMS/MS) used in the context of this thesis to study the gut. Metabolomics and proteomics were performed to provide insight into the proteomic and metabolic profiles occurring in colon tissue and fecal samples. Before diving into the results and methodologies used in of this project, it is important to introduce the anatomy, previous research, and analytical methods used to understand the results in later chapters.

1.1 Gastrointestinal Tract

The gastrointestinal (GI) system includes some of the most complex organs in the human body, responsible for digestive, absorptive, and excretive processes, all of which are essential for human health (Cheng *et al.*, 2010; Ogobuiro *et al.*, 2023). The gastrointestinal (GI) tract which is the largest component of the gastrointestinal system is composed of two large sections: the upper GI tract and the lower GI tract. The upper GI tract is composed of the mouth, esophagus, stomach, and part of the small intestine (duodenum, jujenum and ileum) with the lower GI tract being composed of the colon, rectum, and anus (Greenwood-Van Meerveld *et al.*, 2017). The oral cavity is responsible for processing/breaking down ingested food in a manner that can be efficiently moved down the esophagus by peristalsis to the stomach for efficient nutrient absorption through the action of various digestive enzymes present (Greenwood-Van Meerveld *et al.*, 2017; Livovsky *et al.*, 2020; Ogobuiro *et al.*, 2023). The processed material in the stomach (chyme) is then passed into the small intestine where the digestion procedures continue, in which the majority of nutrient absorption occurs notably in the jejunum (Ogobuiro *et al.*, 2023). Any ingested material that hasn't been digested or absorbed throughout the GI tract is directed to the large intestine, or colon, where water from undigested food will be absorbed, leading to the formation of fecal matter that is designated for excretion (Greenwood-Van Meerveld *et al.*, 2017; Livovsky *et al.*, 2020; Ogobuiro *et al.*, 2023). Accessory organs that are not directly part of the GI tract such as the liver and pancreas are responsible for releasing essential digestive enzymes, bile acids and lipases that are key contributors to the digestive process (Ogobuiro *et al.*, 2023). In addition to water absorption in the colon, undigested materials act as a source of nutrition for the various microbiome species present in the large intestine (Thursby et Juge, 2017).

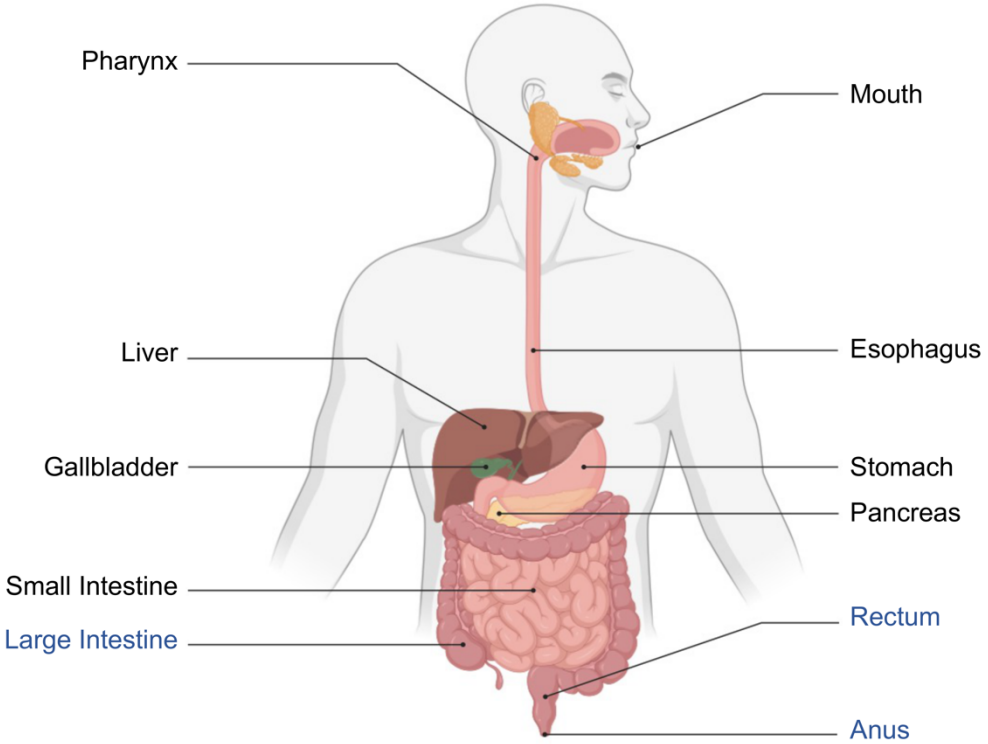

Figure 1.1 Diagram of organs of the gastrointestinal tract (upper GI organs shown in black, lower GI organs shown in blue)

The GI tract plays a large role in the human body's overall immunity and immune response, as it acts as a barrier between the external environment and the body's internal homeostasis (Di Tommaso *et al.*, 2021; Dieterich *et al.*, 2018; Monteiro et Batterham, 2017; Thursby et Juge, 2017). The GI tract can protect the body against invading pathogens and antigens by distinguishing harmful from beneficial microorganisms and sending signals based on ingested/exposed matter to the brain (Dieterich *et al.*, 2018). Changes in microbiome composition along the GI tract can have a large effect on signals conveyed to the brain and can thus alter immune responses and the performance of absorptive, digestive, and excretive processes, highlighting its importance in health and disease. (Di Tommaso *et al.*, 2021; Hillman *et al.*, 2017; Viggiano *et al.*, 2015). Although the GI tract harbors up to trillions of different microorganisms, not all organs have the same species or relative amount of different organisms (Rinninella *et al.*, 2019; Thursby et Juge, 2017). For example, the stomach has a very small amount of microorganisms present (10^1 bacteria/gram) due to its acidic environment, whereas large intestine presents much higher amounts (10^{12}

bacteria/gram) as the environment is ideal for microorganism survival (Dieterich *et al.*, 2018; Hillman *et al.*, 2017; Rinninella *et al.*, 2019). The type of microorganisms that reside in the GI tract vary from bacteria, fungi, and viruses (Hou *et al.*, 2022). It was shown that 75% of all human encoding genes were expressed at the intestinal level (Gremel *et al.*, 2015). Due to factors such as age, genetics, diet, lifestyle habits and environmental exposures that can alter microbiome composition, the GI tract and notably the colon is highly heterogeneous from one individual to another. The gut-brain axis which enables the communication between the GI tract and the brain, can occur through signals from the enteric nervous system (ENS) and the central nervous system (CNS) (Geng *et al.*, 2022). The ENS has been shown to be heavily involved within the gut in which millions of ganglia and neural cells are rooted (Holland *et al.*, 2021). The colon harbours the largest population of microorganisms in the GI tract. Over the last several decades, there has been a large rise in gastrointestinal diseases with many of these diseases being expressed in the colon, including Crohn's, Ulcerative Colitis, Irritable Bowel Syndrome, and Colorectal Cancer (Cosnes *et al.*, 2011; Dieterich *et al.*, 2018; Huang, Z. *et al.*, 2022; Kuipers *et al.*, 2015). These intestinal diseases and conditions often involve microbial dysbiosis occurring in the colon (Thursby et Juge, 2017).

1.2 Anatomy of The Large Intestine

The large intestine also named the colon, is very large and presents significant heterogeneity between one individual from another. The colon can be separated into several different parts notably the proximal region (right-sided colon) and the distal region (left-sided colon). The proximal region is made up of the cecum, ascending and transverse colon, whereas the distal portion of the colon is made up of the descending colon, sigmoid colon, and the rectum. Separation at the splenic flexure is the boundary between the two distinct portions of the colon (Figure 1.2) (Kahai *et al.*, 2023). The superior mesenteric artery (SMA) provides blood and nutrients for the cecum, ascending colon and two thirds of the transverse colon, all of which are formed by the midgut (Kahai *et al.*, 2023; Malone *et al.*, 2023). On the distal side, the remaining third of the transverse colon, the descending colon, sigmoid colon, and the rectum are formed from the hindgut and are supplied blood by the inferior mesenteric artery (IMA) (Kahai *et al.*, 2023; Malone *et al.*, 2023).

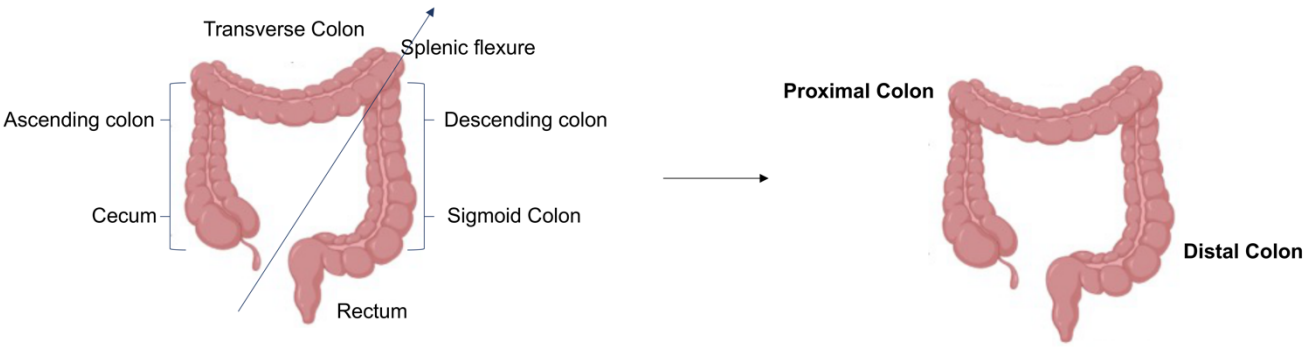

Figure 1.2 Anatomy of colon and its distinct regions when separated at the splenic flexure

In the colon, fecal formation occurs predominantly in the proximal region of the colon where remaining water and other nutrients are absorbed. The formed feces will then move towards the distal region of the colon where they are mainly stored and awaiting excretion out of the rectum (Azzouz et Sharma, 2023).

1.2.1 Variability in the Large Intestine

The colon is a very large organ with high heterogeneity between individuals due to the differences in genetics and exposures. As previously mentioned, intestinal diseases that are expressed in the colon such as ucerative colitis, Crohn's, irritable bowel syndrome (IBS), and colorectal cancer (CRC) have been on the rise for the past few decades and more research has been dedicated for diagnostic and prognostic purposes of these diseases. Expression of intestinal diseases as well as prognosis has been shown to differ between the two distinct regions (Koutroubakis, 2010; Lotfollahzadeh *et al.*, 2023; Loupakis *et al.*, 2015; Petrelli *et al.*, 2017; Soret *et al.*, 2020).

Many studies on CRC have been published showing that prognosis differs greatly on tumor location in the colon. Overall, the outcome is far worse for patients with tumors residing in the proximal region as opposed to the distal region (Arnold *et al.*, 2017; Duraes *et al.*, 2022; Loupakis *et al.*, 2015; Petrelli *et al.*, 2017). *Arnold et al.* performed a study on 2159 patients with location specific CRC (515 patients with tumors in proximal region and 1644 patients with tumors in the distal region) to observe how the survival rates and response rates of varying therapies, differed

between patients with tumours located in the two regions. They were able to conclude that overall and progression-free survival rates were significantly worse for patients with tumors located in the proximal region of the colon. Additionally, they tested the effects of treatment on tumors from both regions, and found that overall treatment was the most successful only on distal tumors (Arnold *et al.*, 2017).

Hirschsprung's disease, which affects 1/5000 newborns is characterized by the absence of neural ganglionic cells of the ENS which prevents peristalsis in the colon, leading to a major blockage (Klein et Varga, 2020; Lotfollahzadeh *et al.*, 2023; Soret *et al.*, 2020). In most cases (≈ 80%), this disease is mainly expressed in the distal region of the colon, mainly in the recto sigmoidal region or the sigmoidal region. It is only in very rare cases that the entire colon is affected by this absence of neural ganglion cells, also touching the proximal region (Kessmann, 2006; Lotfollahzadeh *et al.*, 2023). Ulcerative colitis which is a type of irritable bowel disease (IBD) is characterized by chronic inflammation in the colon causing symptoms such as bloody diarrhea, stomach pain and fecal incontinence, shows an increased prevalence in the distal region (recto sigmoidal) (Koutroubakis, 2010). The proximal region can be affected in much rarer cases of ulcerative colitis (Feuerstein *et al.*, 2019; Koutroubakis, 2010). These examples demonstrate the variability occurring within the colon notably when diseases are involved.

1.3 Liquid Chromatography Coupled to High Resolution Tandem Mass Spectrometry (LC-HRMS/MS)

1.3.1 High Performance Liquid Chromatography

Chromatography is a powerful separation technique that utilizes a stationary phase and a flowing mobile phase to separate compounds in a complex matrix. There are various types of chromatography that can be employed depending on the nature of the sample and compounds to be separated. Four of the most commonly used types of chromatography include liquid chromatography (LC), gas chromatography (GC), and thin-layer chromatography (TLC) (Coskun, 2016). In the scope of this project, liquid chromatography was employed and will therefore be the type of chromatography further explained.

High performance liquid chromatography (HPLC) implies the use of liquid chromatography at high pressures with the use of high performance pumps. This technique is widely used for non-volatile and thermolabile compounds. Separation occurs on the basis that some molecules present in the sample will interact more with the stationary phase and be more highly retained, while other

molecules will be eluted more quickly. Properties such as polarity, charge, and molecular size of a molecule will affect its affinity to adhere to the stationary phase and will dictate its elution time (time retained on the column). Although there are many types of liquid chromatography, normal phase, reverse phase (RPLC), and ion-exchange chromatography are some examples of very widely used types (Bird, 1989; Snyder *et al.*, 2010). Normal phase employs a polar stationary phase and non-polar mobile phases resulting in polar compounds having more retention and thus longer retention times. The opposite can be said for RPLC where a rather non-polar stationary phase is used, and rather polar mobile phases are used. In RPLC, polar compounds will elute much earlier as their interaction with the polar mobile phase is favoured, whereas non-polar compounds will adhere to the non-polar stationary phase resulting in their later elution. Reverse-phase liquid chromatography was employed in the scope of this project and will therefore be further discussed. RPLC is the most common type of liquid chromatography employed since the solvents required for normal phase are generally incompatible with LC-MS/MS analysis. RPLC yields an efficient separation of a broad range of metabolites and if specific types of metabolites are targeted for separation, the stationary phase can always be changed to tailor the analysis. Non-polar stationary phases used in RPLC are often packed with silica-based particles. There are columns that vary in the amount of carbon atoms that are bound to the silica particles from C_4, C_8, and C_{18}. The larger carbon chain will result in a more hydrophobic stationary phase (Snyder *et al.*, 2010). Three different chromatographic columns were used in the context of this project, an Aeris Peptide C_{18} column, a Scherzo SM-C18 column and a Luna PFP column. Each of these columns separate compounds differently, with the Aeris column being a classic C_{18} column used for RPLC with solid core particles. Although the Scherzo SM-C18 (mixed-mode) utilizes some of the same concepts as a traditional C_{18}, it also offers the advantage of anion/cation exchange interactions resulting in the separation of basic/acidic compounds as well. The Luna PFP column employs a pentafluorophenyl phase resulting in good retention for aromatic and conjugated molecules. The Scherzo mixed-mode and Luna PFP columns were employed for metabolomic analyses to maximize metabolite coverage from complex samples, as metabolite structures, their polarities, and acid/base properties can vary greatly.

Mobile phases used in RPLC are composed of water and an organic solvent such as acetonitrile (ACN) or methanol (MeOH). The mobile phases can be passed through the stationary phase either with a constant percentage of organic solvent (isocratic elution), or with increasing percentages of organic solvent over time (gradient elution) allowing very hydrophobic molecules to be able to elute out of the column. As the analytes elute from the column, a retention time and peak intensity

is recorded, representative to each eluted molecule used for qualitative and quantitative purposes respectively (Snyder *et al.*, 2010).

1.3.2 High Resolution Tandem Mass Spectrometry

Mass spectrometry is a very powerful analytical tool that separates ionized molecules based on their respective mass to charge ratio (*m/z*). Tandem mass spectrometry when coupled to liquid chromatography (LC-MS/MS) yields important information about compounds as it allows for the identification, quantification and structural elucidation of the molecules present in a complex sample matrix (Ho *et al.*, 2003). Mass spectrometry is a powerful tool due to its potential for high resolving power and sensitivity allowing for the detection of exact masses. This allows for the differentiation of molecules that have the same nominal masses, but not the same exact mass, making it an ideal tool for the study of metabolites and proteins (Sleno, 2012).

When molecules separated by liquid chromatography elute, an ionization step is essential to bring them to gaseous phase and give them a positive or negative charge to these compounds. Once all compounds are ionized, they are then able to pass through the mass analyzer which can differ from one instrument to another and a mass spectrum will be produced as shown in Figure 1.3. The mass spectrum displays peaks respective to the *m/z* of ions (*x-axis*) and their abundance (peak intensity) (*y-axis*).

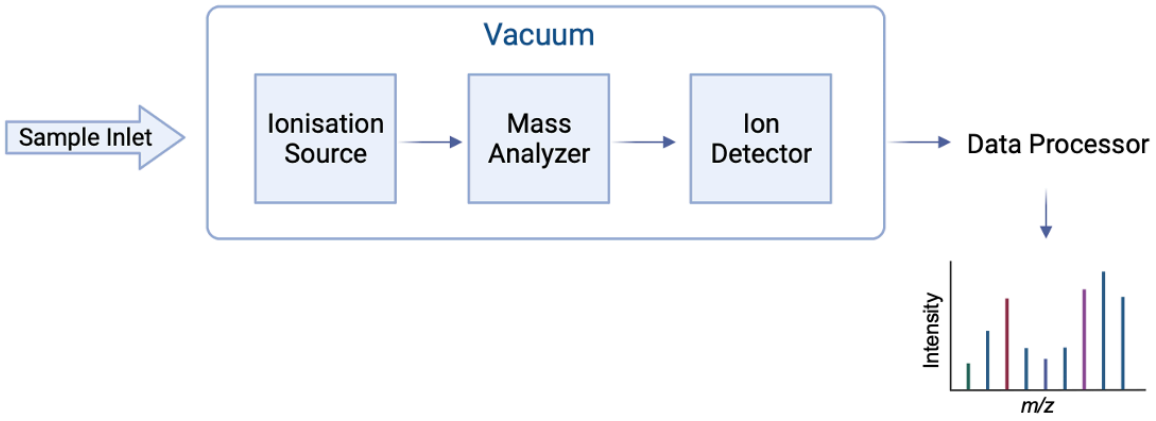

Figure 1.3 General overview of the components of a mass spectrometer

There are several different ionization sources that can be employed where soft ionization sources are most appropriate when tandem mass spectrometry is employed, in order to limit in-source

fragmentation. Hard ionization sources will fragment the molecular ion using electron bombardment, but this can often lead to the fragmentation and loss of the molecular ion from being detected. Soft ionization sources will ionise particularly thermally labile and non-volatile molecules in a gentler way resulting in the majority of cases, the molecular ion intact and able to be detected (Garg et Zubair, 2023).

Electrospray ionization (ESI) is one of the most utilized ionization techniques in modern mass spectrometry and was used in this project. Although ESI is useful for metabolomics studies, it is also perfectly suited to proteomic studies (Banerjee et Mazumdar, 2012). Molecules incoming from liquid chromatography separation travel through a fine capillary or needle-like tube where an energy potential is applied, resulting in charged droplets when these molecules exit the capillary almost in the form of an aerosol. As there is still solvent surrounding these charged droplets, nitrogen gas is used to help with the solvent evaporation process. The droplets will continuously decrease in size as the solvent continues to evaporate with a large charge accumulation occurring in the droplet. This results in a coulombic explosion releasing all the gaseous phase ions out of the droplet. These ions are then directed into the mass analyzer for separation and sorting based on their respective *m/z* (Banerjee et Mazumdar, 2012; Ho *et al.*, 2003; Hoffmann et Stroobant, 2007). This overall process is demonstrated in a simplified manner in Figure 1.4.

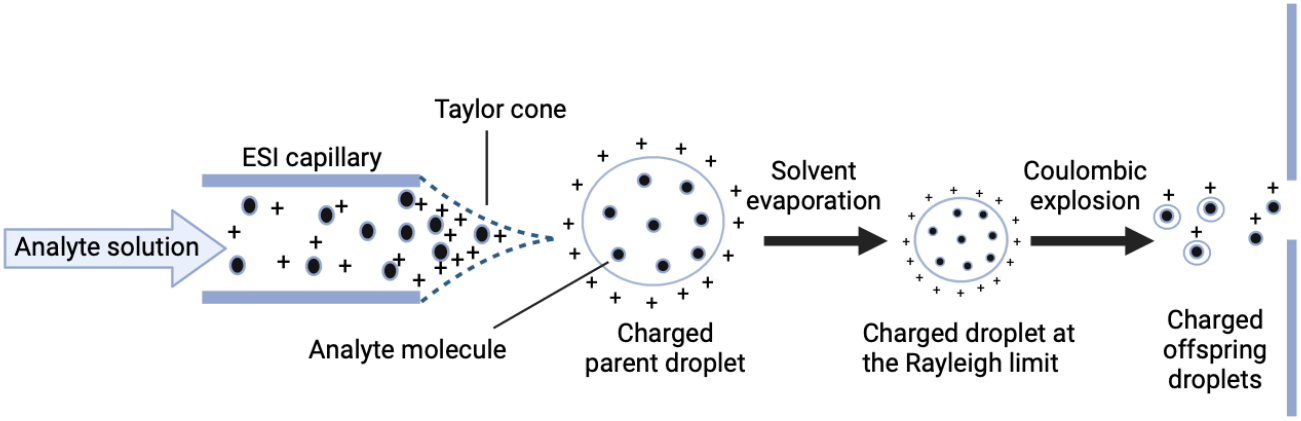

Figure 1.4 Simplified diagram demonstrating the steps for compound ionization via electrospray ionization (ESI)

Many mass analyzers exist such as quadrupole, time-of-flight (TOF), and Orbitrap analyzers to name a few, and each type has their own set of features (mass range, resolving power, mass

accuracy) making them suitable for different types of analyses (Haag, 2016). One feature that is highly important when considering mass analyzers is the mass accuracy which essentially describes how accurate the *m/z* detected for a given compound is when compared to the theoretical *m/z* value of that given compound This goes hand in hand with the resolving power of the mass analyzer, as a higher resolving power will be able to distinguish exact masses that are very close in value to each other, also leading to more accurate *m/z* values detected when adequate mass calibration is performed (Hoffmann et Stroobant, 2007).

The combination of different mass analyzers is often employed to exploit their different features. In this project, a hybrid quadrupole-time of flight (QqTOF) system was used. Although quadrupole analyzers operate at unit resolution, they are great for isolating ions of interest that are within a defined range of *m/z* (Haag, 2016). Quadrupole analyzers are composed of four parallel circular rods (with opposite charges) that have alternating radiofrequency (RF) and direct current (DC) voltages applied. At these applied voltages, ions that possess a *m/z* that is within the defined range will be able to oscillate through the field without encountering the charged rods. Ions that have a *m/z* outside the defined range, will oscillate into the rods neutralizing their charge, and expelling them from the analyzer. A second quadrupole (q2) acts as a collision cell (only RF applied) where precursor ions that were able to pass through the first quadrupole (Q1) will get fragmented producing product ions yielding tandem mass spectrometry (MS/MS) data (Haag, 2016; Ho *et al.*, 2003). Triple quadrupole mass analyzers also exist and are widely used for targeted analyses in which selectivity is extremely high when performing multiple reaction monitoring (MRM) (Ho *et al.*, 2003). TOF mass analyzers differentiate ions based on the speed at which they travel in a field free flight tube (Figure 1.5). Prior to entry into the flight tube, all ions acquire the same kinetic energy as they are accelerated into the field free flight tube in which the ions are then separated based on the speed at which they travel to the detector. Ions with smaller *m/z* will travel much quicker than ions with larger *m/z* (Gross, 2010; Hoffmann et Stroobant, 2007). The combination of both the quadrupole (Qq) and TOF analyzers is widely used in metabolomic and proteomic studies due to the high sensitivity, resolving power, and robustness (Hoffmann et Stroobant, 2007). With the combination of both these mass analyzers, both MS and MS/MS spectra can be acquired. In TOF-MS mode, the quadrupole does not filter any ions and simply passes all ions into the TOF for separation of precursor ions formed in the source. In MS/MS mode, the first quadrupole (Q1) will act as a mass filter selecting precursor ions to enter into the second quadrupole (q2) for fragmentation by collision-induced dissociation (CID), where residual

precursor ions and fragment ions will enter the TOF analyzer for separation (Gross, 2010; Hoffmann et Stroobant, 2007).

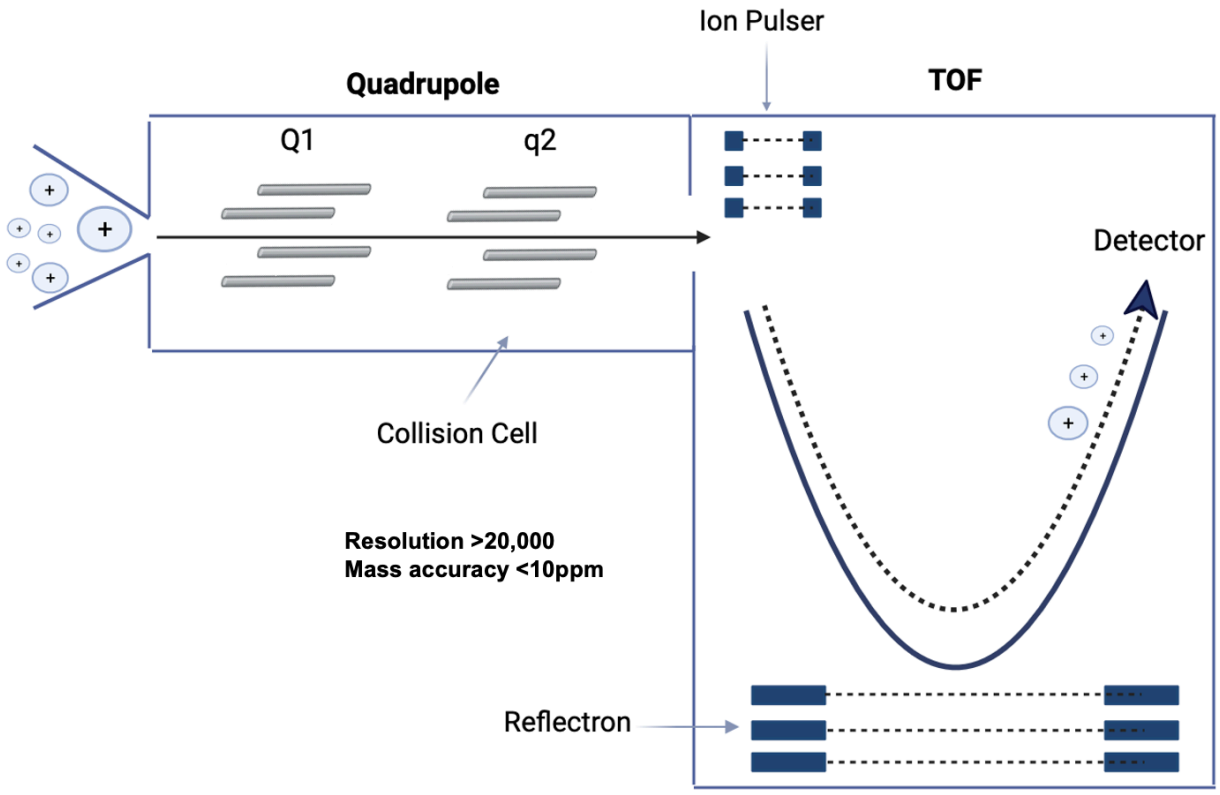

Figure 1.5 Diagram of a quadrupole time-of-flight mass analyzer in MS/MS mode (QqTOF)

In untargeted acquisitions such as global metabolomics and proteomics as performed in the scope of this project, tandem MS is crucial as it generates MS/MS spectra of compounds in which each spectrum can help elucidate the structure of a compound or peptide sequence. Many molecules can have the same exact mass, if not very close ones meaning that there's no way to distinguish these molecules from the MS1 spectrum obtained, even with high resolution instruments as the one used in this study. One way to confirm the identity of a compound is through structural elucidation which can be done with MS/MS spectra as it shows how each compound fragments based on their structure. An example is shown of structural elucidation in Figure 1.6 with succinic acid.

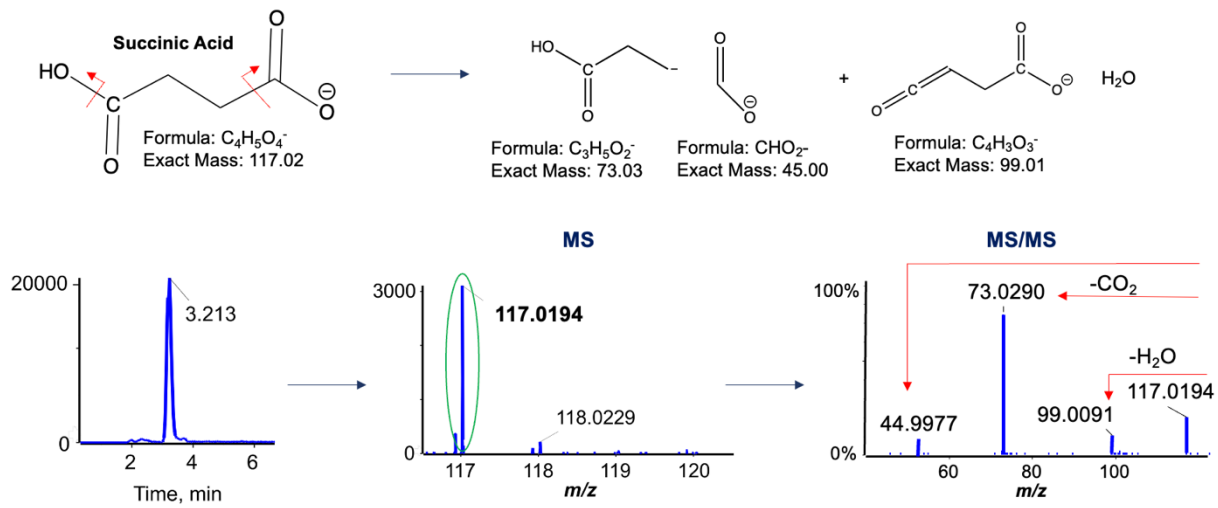

Figure 1.6 Structural elucidation of succinic acid by accurate mass measurements and MS/MS fragmentation

MS/MS spectra can be produced via two types of acquisition modes when doing untargeted analyses. Samples can be run in information-dependent (IDA) or in data-independent acquisition (DIA, SWATH) modes. In IDA, the mass spectrometer will select only certain precursor ions to get fragmented in the collision cell. This selection is based on parameters set within the method in which the user will specify that in one cycle, for example, only the ten highest intensity ions will be selected for fragmentation. This parameter can change to any given number depending on what the user is interested in. This usually leads to good quality MS/MS spectra as it avoids interference from other ions outside of the narrow selection window (usually around 0.7 Da) that could potentially be in the same *m/z* window. In contrast, DIA acquisition will select a wider window of precursor ions (as specified by the user) to get fragmented in the collision cell to produce MS/MS spectra. This is beneficial in some cases as it can lead to a higher coverage of compounds having MS/MS spectra, but it can also lead to more complicated spectra to analyze (Zhu *et al.*, 2014). The difference between these two acquisition types is shown in Figure 1.7.

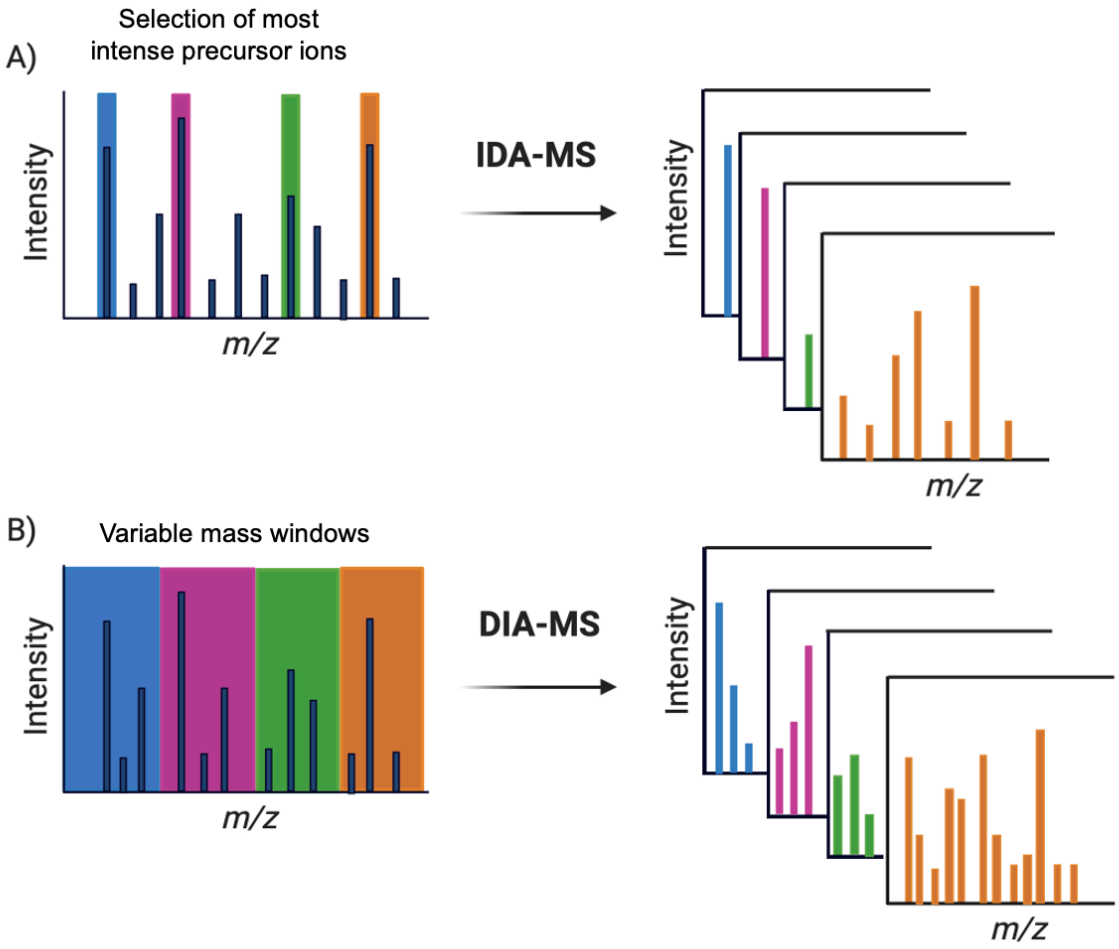

Figure 1.7 Comparison of information dependent acquisition (IDA) and data-independent acquisition (DIA, SWATH)

1.4 Metabolomic Analysis

Metabolomics comprises the study of metabolites, also known as small molecules from biological matrices that are end products of compounds originating from the host (endogenous metabolites) or compounds originating from the external environment such as food, contaminants, drugs, and pollution (exogenous metabolites) (Johnson *et al.*, 2016). There are several “omic” studies: genomics, transcriptomics, proteomics and metabolomics which are generally described in Figure 1.8 (Dettmer *et al.*, 2007). Studying metabolites is of high interest as the variation of certain metabolites can often be the result of a perturbation occurring from genomic or proteomic changes, in which these metabolites allow a different view of what the effects of these perturbations are.

This makes metabolomics ideal for use in precision medicine, drug development/monitoring and biomarker discovery for a plethora of diseases.

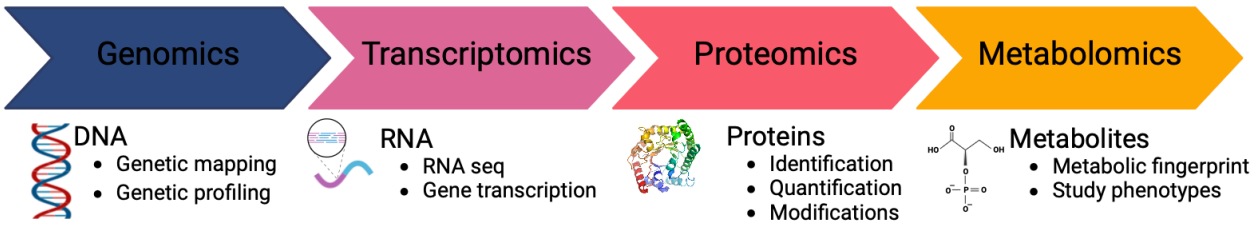

Figure 1.8 Different "*omic*" technologies and their applications

Moreover, because metabolites are essentially the endpoint from the other "omics", metabolites are the key to understand phenotypes and phenotypical changes that often times cannot be understood from genomics as metabolomics is the closest link to phenotype (Clish, 2015; Dettmer *et al.*, 2007; Guijas *et al.*, 2018). Metabolites can also predict certain phenotypes as their change in abundance or even presence can occur prior to phenotypic changes occurring, which is essential for prevention in the context of health and disease (Wang, Z. et Yu, 2019).

Metabolomics, in the scope of this project, is done so using liquid chromatography coupled to high resolution tandem mass spectrometry (LC-HRMS/MS) due to its robustness, sensitivity and versatility, but other analytical techniques such as nuclear magnetic resonance (NMR) can also be utilized (Johnson *et al.*, 2016; Wishart, 2008). The overall metabolomics processing workflow when using LC-HRMS/MS as the analytical technique of choice is composed of several steps (Figure 1.9): *1)* sample preparation for metabolite extraction, *2)* injection of samples into LC-MS/MS for separation and characterization, *3)* putative metabolite identification by spectral matching between experimental MS/MS spectra with MS/MS spectra from various databases, *4)* statistical analysis to find changing metabolites for biomarker discovery with pathway analysis (mainly in the context of disease) (Wishart, 2008). Sample preparation in metabolomics is quite simple including a step to homogenize the samples using buffer and then precipitate proteins with organic solvents such as methanol (MeOH), ethanol (EtOH) or acetonitrile (ACN), to name a few. Following a centrifugation step, the supernatant is evaporated and reconstituted for metabolomic analysis. Method development is often required to optimize the chromatographic separation a given set of samples as well as the optimization of mass spectrometer parameters.

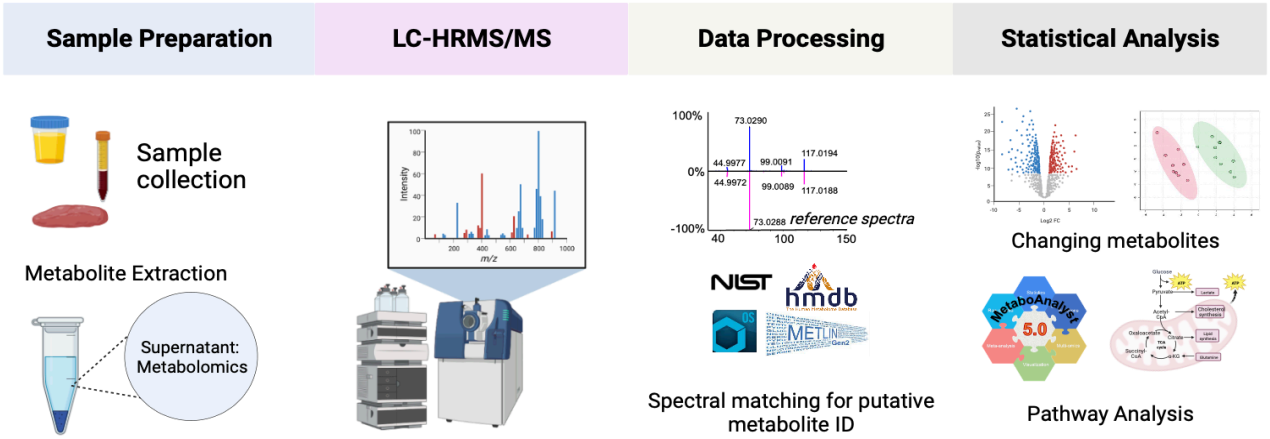

Figure 1.9 Untargeted LC-HRMS/MS metabolomics workflow

A key goal when performing untargeted metabolomics is to identify as many metabolites as possible in a given sample set. The initial goal is to maximize the metabolite coverage in order to try an understand the overall profile of what can be detected within a given sample type. This also leads to the ability to compile an in-house database of a variety of metabolites which can be extremely useful for later metabolomic studies. Metabolite identification is putatively done when matching MS/MS spectra from experimental samples with those available from various databases such as NIST, HMDB and Metlin, to name a few (Scalbert *et al.*, 2009). When identifications are made this way, they are known as putative because they are not a direct comparison between experimental spectra and spectra from authentic standards. This is a limitation in metabolomics notably when performing untargeted metabolomics. The datasets obtained in untargeted metabolomics are often very large and authentic standards can be very costly. Therefore, the goal is to characterize as many metabolites as possible and to create in-house databases for future work of metabolite characterization on different sample types. With databases that have very high metabolite coverage identified from varying chromatography columns and mass spectrometry methods, it allows the possibility to perform targeted metabolomic analyses with higher reproducibility and quantitative measurements, as well as limited data size. Another advantage of is the fact that the contents of the database will be based off of results originating from same instrumentation and methods being run for actual samples, allowing for a more accurate metabolite identification. This is a way to work around the large limitation of very large datasets,

by putatively identifying as many metabolites as possible in the untargeted acquisition and then focusing in on a group of metabolites of interest in subsequent sample sets. For example, performing statistical analysis to find a smaller subset of metabolites of interest or metabolites of a pathway of interest that can then be studied in a targeted manner, and confirmed with metabolite standards for accurate metabolite confirmation. The use of authentic standards also aids greatly in establishing the correct retention times of metabolites, a factor in which can be a source of error in metabolite databases and spectral libraries due to differing separation methods being used which can lead to different retention times reported for the same metabolite (Scalbert *et al.*, 2009).

The metabolome constitutes a very large number of metabolites in which there is a large variability in their structures and properties. Metabolites can range from lipids of varying chain lengths, amino acids, small peptides, to name only a few (Gonzalez-Covarrubias *et al.*, 2022). Evidently this makes a large subset of molecules to study when performing untargeted metabolomics, as the goal is to identify as many metabolites as possible. Due to the vast variability in properties that all these metabolites possess, it is impossible to use only one chromatographic separation method or column to identify all these metabolites with varying properties. To account for the differing properties of metabolites, different separation columns are often used with the aim at observing complementary separation to identify a larger range of metabolites as employed in the scope of this project (Scalbert *et al.*, 2009).

Although metabolomics poses several technical challenges and limitations, it remains an essential technique to study how metabolites vary within various tissues and biofluids to discover new biomarkers of disease, development of new drugs and new treatments for the ever-evolving world, as well as play a large role in precision medicine. In the scope of this project, metabolomics was performed to study the variations within the respective regions of the colon of healthy subjects, for further understanding of the baseline metabolic variations before the introduction of disease as well as compile an in-house database of which metabolites can be detected in these sample types, for subsequent studies to come.

1.5 Proteomic Analysis

Contrary to metabolomics, proteomics involves the study of proteins which unlike metabolites, are very large molecules in which their composition can range from 50 to over 2000 amino acids. When using LC-HRMS/MS to perform proteomic analysis, protein identification, quantification as well as the study of post-translational modifications is possible (Matthiesen et Bunkenborg, 2013).

Much like metabolomics, changes or perturbations occurring in the body (Figure 1.9) can reflect altered protein expression levels giving rise to the identification of potential biomarkers and pathways involved in various diseases. Additionally, proteomics offers great complementarity to transcriptomic analysis since reported mRNA abundance levels of genes does not necessarily mean these same levels are expressed at the protein level. Proteins carry out key functions and biological processes in the body (such as enzymes), therefore it is advantageous to study changes in the levels of expressed proteins allowing for a more comprehensive understanding of what types of biological processes are occurring (Karpievitch *et al.*, 2010; Macklin *et al.*, 2020).

Due to the large size of proteins, the sample preparation workflow for optimal protein identification, quantification and characterization in complex sample matrices is quite different to the one for metabolomic analysis. For proteomic analysis by LC-HRMS/MS two main types of LC-MS/MS proteomics can be employed: top-down proteomics and bottom-up proteomics where the latter was performed in the scope of this project. Top-down proteomics involves studying intact proteins, whereas bottom-up proteomics involves digesting the proteins into peptides and studying the resulting peptides (Figure 1.10). Bottom-up proteomics will be the focus of this section. Peptides can be studied through digestion of proteins which involves a protease that will cleave proteins at known sites, such as trypsin that cleaves proteins at C-terminal arginine (Arg) and lysine residues (Lys) and is the most common protease used for this task (Matthiesen et Bunkenborg, 2013).

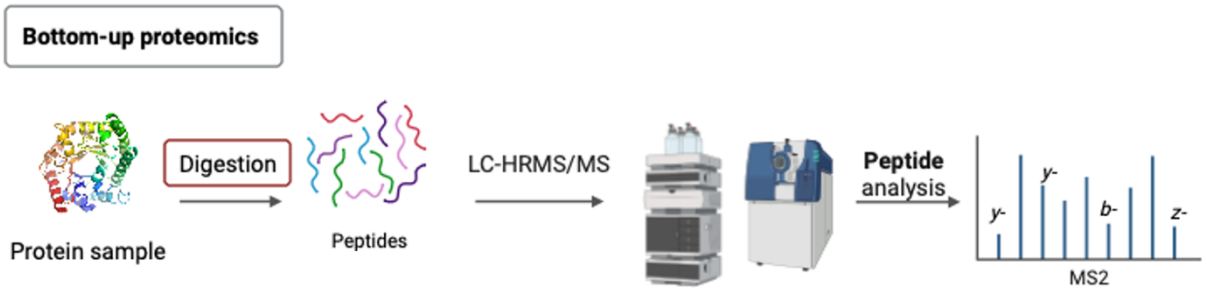

Figure 1.10 Simplified bottom-up proteomics workflow

Following sample preparation, samples are injected into the LC-HRMS/MS system for peptide separation and characterization. The separated peptides can be sequenced through MS/MS spectra obtained, in which the *m/z* fragments correspond to the differences in mass of linked amino acids of the peptide sequences (Matthiesen et Bunkenborg, 2013). When peptides are

selected for fragmentation in the mass spectrometer, the peptide bond linking amino acids is broken, resulting most commonly in a series of *y* and *b* ions, when collision-induced dissociation is employed, as in most MS/MS experiments. The *y* ions denote the charge remaining with the C-terminal end peptide sequence and *b* ions have the charge remaining on the N-terminal end, allowing the direction of the peptide sequence to be deduced when sequencing peptides from the MS/MS spectra (Cleveland et Rose, 2013; Dupree *et al.*, 2020). Proteins are then able to be identified by matching these sequenced peptides using several databases and softwares such as UniProt and ProteinPilot. The databases will identify these proteins based on unique peptide sequences with some peptides mapping to multiple proteins and therefore showing a protein group instead of a unique protein being identified in some instances (Tuli et Ressom, 2009).

1.5.1 Metaproteomic Analysis of Microbial Species

The term metaproteomics is used for many applications and is defined as the identification and quantification of proteins from microbial species, in which it can be done using LC-HRMS/MS (Kleiner, 2019). Although major breakthroughs in microbiome studies have been achieved using 16S rRNA technology for assessing microbial taxonomy, metaproteomics has shown extreme potential for being able to touch on certain aspects regarding the microbiome that are challenging by 16S rRNA. For example, metaproteomics offers strain specific information through the proteins expressed, which is challenged when using 16S rRNA (Cortes *et al.*, 2019). Another challenge that has been reported with 16S rRNA is the innacurate taxonomic classification for certain bacterial species such as *Enterobacter* and *Klebsiella* for example*,* which have a very high 16S rRNA gene similarity. In cases like these where there is high similarity in 16S rRNA gene sequences between genera, complimentary metaproteomic analysis could be beneficial (Cortes *et al.*, 2019; Zwittink *et al.*, 2017). Abundance levels of expressed proteins mapping to unique microbial species can also be measured with metaproteomics, allowing for a better picture of the abundance and activities of species. This adds a more comprehensive view of the microbial species (Kleiner, 2019). Although metaproteomics shows promise for advancing the scientific community into further understand the microbiome and its dynamic nature for the understanding of diseases, there are many challenges associated. These challenges include characterization of low abundance microbial proteins, the high heterogeneity between samples (notably in feces), the lack of developed metaproteomic databases, and the data processing time needed (Armengaud, 2023; Lai, L. A. *et al.*, 2019). Despite these challenges, metaproteomics still acts as an important complimentary analysis to 16S rRNA for comprehensive microbiome research.

1.6 Literature on Metabolomics and Proteomics in the Colon

Although many studies have been conducted on the colon and the microbiome by LC-MS/MS, to our knowledge no studies have combined the metabolomic, proteomic, and metaproteomic variations between the different regions of the colon using whole colon tissue and fecal samples from the distal and proximal regions in healthy mice. To date, many studies that involve metabolomic or proteomic analyses studying the colon have been in human patients with an intestinal disease such as colorectal cancer, ulcerative colitis, and IBD, with very few combining multiple analyses (Ang *et al.*, 2010; Busi *et al.*, 2023; Folz *et al.*, 2023; Marshall *et al.*, 2021; Su *et al.*, 2022). Additionally, some studies do not study explicitly the proximal and distal regions of the colon, but rather parts of the small intestine compared to the proximal region of the large intestine such as in the study performed by *Folz et al (Folz et al., 2023)*.

A study performed by *van der Post et al.* studied membrane protein profiles of the distinct regions of the colon by LC-MS/MS in which they were able to find distinct proteomic patterns distinct to each region of the colon in humans. They also studied the transverse and sigmoid colon regions separately along with the ascending and descending colon. Although, this study has some similarities to the one performed in this project, there are important differences. In the study presented by *van der Post et al.* they mainly focus on membrane proteins in the four differing regions of the colon as opposed to studying the whole proteome, as well as the metabolome (van der Post et Hansson, 2014).

Additionally, a study by *Baxter et al*. included untargeted metabolomics to explore differences among individuals undergoing colonoscopy procedures. This involved colon biopsies from both proximal and distal regions, along with self-collected stool samples. The study observed considerable diversity among individuals, particularly related to BMI, and identified distinct metabolites associated with different colon regions (Baxter *et al.*, 2020)

1.7 Mouse Model System

Murine models have been used extensively in research due to their genetic, anatomic, and physiological similarities to humans and their ability to be serve as models to study various diseases. Murine models are essential to study biological perturbations since human samples are often not available (Meier *et al.*, 2023).

In this project, a murine model was used to study the metabolic and proteomic variations between the proximal and distal colon. Increasingly, murine models are being used for research into host-microbiome interactions and disease driven by microbiome dysbiosis, as it is possible to control the diet and treatments (Hugenholtz et de Vos, 2018; Nguyen *et al.*, 2015). Although murine models do present many similarities to humans as previously mentioned, there are some limitations when applying knowledge obtained from murine models to humans.

As this project focused on the gut, it is important to outline some differences between the murine and human gut. The size of the murine GI is much smaller than the human GI, and although anatomically they are quite similar, some differences are presented lower in the GI tract. Firstly, humans don't possess a non-glandular forestomach like mice do, although the glandular stomach in mice is like the one in humans. Another difference is at the cecum. In mice, the cecum is large relative to the size of the GI tract, whereas in humans the cecum is quite small. This also leads to differences where principal fermentation occurs between mice and humans. In mice, seeing as the cecum is quite large, a big portion of fermentation is occurring in the cecum, whereas in humans this is not the case (Hugenholtz et de Vos, 2018; Nguyen *et al.*, 2015).

Along with anatomical differences in the GI tract, microbiome composition also differs between mice and humans. Although, 79 genera are found in common to both mouse and human gut, their abundances differ greatly, where it was reported that *Prevotella, Faecalibacterium, Succinivibrio, Dialister, and Ruminococcus* genera were shown to be highly abundant in human microbiota whereas in mice they were shown to be much less abundant. *Lactobacillus,* on the other hand, is highly abundant in mice compared to humans, presenting a limitation when bridging the gap between gut microbiome studies in mice to humans (Hugenholtz et de Vos, 2018; Nguyen *et al.*, 2015).

In this project, FVB/N mice strains (from Charles River Laboratories) were used as they are very suitable for transgenic experiments. The mice were sacrificed at 20 days post-natal pre-weaning for sample collection to avoid changes in diet or microbiome composition when they wean at 21 days. Sex was not considered in most of this study, although a small analysis was done to compare the fecal metabolomic variations between female and male mice.

1.8 Objectives

As previously noted, the prevalence of intestinal diseases like colorectal cancer, IBS, Crohn's, and ulcerative colitis has increased in recent decades. While numerous studies have explored their prevalence, diagnostics, and potential treatments, there is a notable gap in understanding the internal heterogeneity within distinct regions of the colon in healthy individuals.

Prognosis and expression of disease can differ greatly between the proximal and distal regions of the colon. Therefore, it is crucial to comprehend the baseline differences present in a healthy colon before diseases manifest. A baseline understanding of how heterogeneous a healthy colon is could potentially help accelerate understanding of the perturbations being seen in the colon when intestinal diseases are introduced. The objective of this project is to investigate the metabolome and proteome of colon and fecal samples from the proximal and distal regions in healthy mice using untargeted LC-MS/MS. This involves examining the overall detectable metabolome and proteome coverage across all colon and fecal samples, alongside conducting statistical analyses to identify the predominant metabolites and proteins in the distinct regions of the colon. This comprehensive approach will shed light on unique pathways and biological processes in these different regions of the colon.

The project also delves into the gut microbiome, aiming to perform metaproteomics to identify unique microbial species and observe their dominance in respective colon regions. Given that factors like diet, environmental exposure, medication use, age, and stress can influence metabolic, proteomic, and microbiome profiles in subjects, this study is conducted on mice where these variables were kept constant to ensure more reliable results. These studies in healthy mice could be employed for future work on mouse models of human diseases or environmental exposures. Few studies have integrated metabolomics and proteomics for this purpose, making this project a valuable contribution to an important area of research. The results and methodology will be detailed in Chapter 2.

CHAPITRE 2

SCIENTIFIC ARTICLE: PROTEOMIC AND METABOLOMIC ANALYSIS OF COLON AND FECES FROM PROXIMAL AND DISTAL REGIONS IN HEALTHY MICE

Oriana Zambito, Nejia Lassoued, Rodolphe Soret, Nicolas Pilon, Lekha Sleno

Proteomic and Metabolomic Analysis of Colon and Feces from Proximal and Distal Regions in Healthy Mice

Oriana Zambito[1,3], Nejia Lassoued[2,3], Rodolphe Soret[2,3], Nicolas Pilon[2,3], Lekha Sleno[1,3]

1) *University of Quebec in Montreal (UQAM)*, Chemistry Department, PO Box 8888 Downtown Station, Montreal, H3C 3P8, Canada, sleno.lekha@uqam.ca

2) *University of Quebec in Montreal (UQAM)*, Biology Department, PO Box 8888 Downtown Station, Montreal, H3C 3P8, Canada

3) *CERMO-FC*, Centre d'Excellence de Recherches sur les Maladies Orphelines-Fondation Courtois

Oriana Zambito is the principal author of this article. She carried out all bibliographical research, laboratory manipulations, preparation of figures and tables as well as the writing of the article. Nejia Lassoued, Rodolphe Soret and Nicolas Pilon were all implicated in providing the samples required for this article as it is the result of a collaboration between Prof. Pilon's and Prof. Sleno's research groups. Prof. Lekha Sleno guided and supervised the project, as well as revised the manuscript.

2.1 Résumé

Le système gastro-intestinal fait partie des systèmes les plus complexes du corps humain, avec une grande hétérogénéité entre les individus en raison des expositions environnementales et de la génétique. Une forte hétérogénéité est observée au sein des régions distinctes du côlon, notamment avec l'introduction de maladies avec des pronostics et des options de traitement différents. Dans cette étude, la chromatographie liquide couplée à la spectrométrie de masse en tandem haute résolution (LC-HRMS/MS) a été utilisée pour étudier la couverture globale du métabolome et du protéome dans une analyse non ciblée de tissus du côlon et d'échantillons fécaux chez des souris en bonne santé, ainsi que pour étudier l'homogénéité des régions distales et proximales du côlon pour étudier les profils de base dans l'intestin sain. Des échantillons de selles et de côlon ont été prélevés sur dix souris saines avant la précipitation des protéines. Les surnageants résultants ont été utilisés pour la métabolomique non ciblée, et les culots de protéines ont été utilisées pour la protéomique quantitative. Des analyses métabolomiques et protéomiques ont été effectuées sur une plateforme quadripolaire de temps de vol. La métabolomique a été réalisée avec deux méthodes chromatographiques complémentaires, en modes d'ionisation par électrospray négatif et positif, suivies d'une correspondance spectrale et d'une analyse statistique. TOF-MS/MS a été collecté en mode dépendant des données et en mode SWATH ciblé. Plus de 900 métabolites putatifs ont été identifiés, dans lesquels une distinction claire entre les régions proximales et distales a été démontrée pour 153 métabolites du tissu du côlon. Une tendance similaire a été observée à partir d'une analyse protéomique quantitative, avec 1103 protéines du côlon de souris quantifiées, dont 158 présentaient des niveaux significativement différents entre les deux régions. Bien qu'une couverture élevée du métabolome a été obtenue à partir d'échantillons fécaux, avec plus de 1100 métabolites putatifs mesurés, un degré d'hétérogénéité beaucoup plus faible a été observé dans les métabolites fécaux. La métaprotéomique des échantillons fécaux a révélé la capacité d'identifier les espèces au-delà de la taxonomie et a permis de résoudre les informations sur les espèces et de quantifier leurs peptides uniques. D'après les résultats quantitatifs de SWATH, aucune distinction dans les profils du microbiome n'a été observée entre les selles proximales et distales de souris saines.

2.2 Abstract

The GI tract is amongst the most complex systems in the human body with high heterogeneity between individuals due to environmental exposures and genetics. High heterogeneity is observed within the distinctive regions of the colon notably with the introduction of disease with different prognoses and treatment options. In this study, liquid chromatography coupled to high resolution tandem mass spectrometry (LC-HRMS/MS) was employed to study the overall metabolome and proteome coverage in an untargeted analysis of colon tissue and fecal samples in healthy mice, as well as to investigate the homogeneity of the distal and proximal colon regions to study baseline profiles within a healthy gut. Fecal and colon samples were collected from ten healthy mice prior to protein precipitation. Resulting supernatants were used for untargeted metabolomics, and the protein pellets were used for quantitative proteomics. Both metabolomic and proteomic analyses were performed on a quadrupole time-of-flight platform. Metabolomics was performed with two complementary chromatographic methods, in both negative and positive electrospray ionisation modes, followed by spectral matching and statistical analysis. TOF-MS/MS was collected in data-dependent mode, and targeted SWATH mode. Over 900 putative metabolites were identified in which a clear distinction between proximal and distal regions was shown for 153 colon tissue metabolites. A similar trend was observed from quantitative proteomic analysis, with 1103 mouse colon proteins quantified, 158 of which had significantly different levels between the two regions. Although high metabolome coverage was obtained from fecal samples, with over 1100 putative metabolites measured, a much lower degree of heterogeneity was seen in the fecal metabolites. Metaproteomics of fecal samples revealed the ability to identify species beyond taxonomy and was able to resolve species information and quantify unique peptides from each of these species. From the quantitative SWATH results, no distinction in microbiome profiles was seen between proximal and distal feces from healthy mice.

2.3 Introduction

The gastrointestinal (GI) tract is composed of many complex organs, having specific functions in digestion, absorption, and elimination, acting as a critical connection between the external environment and the body (Cheng *et al.*, 2010; Monteiro et Batterham, 2017; Thursby et Juge, 2017). Along with these functions, the GI tract is essential in various immune responses for protecting against pathogens and antigens, and its microbiome composition exhibits a significant role in intestinal homeostasis (Mason *et al.*, 2008; Wu et Wu, 2012). Due to the complexity of the

GI tract and factors such as diet, age, genetics, lifestyle and other environmental exposures that can affect its microbial communities, it is highly heterogenous being different individuals, and even within the same individuals over time (Hou *et al.*, 2022; Thursby et Juge, 2017; Weiss et Hennet, 2017). The upper GI tract is composed of the mouth, esophagus, stomach, and the first part of the small intestine, while the lower GI tract runs from the small intestine to the colon, rectum, and anus (Greenwood-Van Meerveld *et al.*, 2017). The colon is home to the largest microbiome population in the GI tract and its dysbiosis is the source of many inflammatory intestinal diseases, such as Crohn's, ulcerative colitis and colorectal cancer, all of which have been on the rise over the last several decades (Agrawal et Jess, 2022; Cosnes *et al.*, 2011; Dieterich *et al.*, 2018; Huang, Z. *et al.*, 2022; Kuipers *et al.*, 2015; Thursby et Juge, 2017). Untargeted metabolomic and proteomics analyses using liquid chromatography coupled to high resolution tandem mass spectrometry was performed on colon and fecal samples with the objectives of characterizing which proteins and metabolites can be detected through untargeted approaches in these two sample types, as well as looking specifically at the differences within two regions of the colon.

The colon, also known as the large intestine is composed of six major segments; the cecum, ascending colon, transverse colon, descending colon, sigmoid colon and the rectum (Vadlamudi *et al.*, 2012). The first three segments make up the proximal colon (ascending colon), and the latter three portions make up the distal colon (descending colon) (Vadlamudi *et al.*, 2012). Fecal samples can also originate from both these regions of the colon as their formation starts in the late proximal region and is then stored and excreted further down the distal region (Azzouz et Sharma, 2023). Certain diseases such as Hirschsprung's disease, a rare disorder characterized by an underdeveloped enteric nervous system in the gut leading to impaired peristalsis, and ulcerative colitis affect more commonly the distal region of the colon(Koutroubakis, 2010; Soret *et al.*, 2020). Severity of disease can also be distinct between locations as seen in colorectal cancer, where different prognostic rates are recorded between the two regions for reasons that are not yet fully understood (Deng, K. *et al.*, 2018; Duraes *et al.*, 2022; Huang, Y. *et al.*, 2021; Lee *et al.*, 2017; Petrelli *et al.*, 2017; Su *et al.*, 2022). Investigating the differences between metabolomic and proteomic profiles in healthy mice can serve as a foundation to better understand the biological pathways involved and highlight the importance of region specificity within the colon, notably when intestinal diseases are present.

To date, many metabolomic or proteomic studies have been performed to study these perturbations in different regions of the colon by studying fecal, and colon samples from individuals

possessing a disease, such as colorectal cancer, and irritable bowel disease, but very few studies have involved healthy subjects to investigate variations within the colon without the presence of disease (Deng, K. *et al.*, 2018; Su *et al.*, 2022). A recent study used untargeted metabolomics to investigate differences in individuals undergoing colonoscopy procedures, by collecting colon biopsies from the proximal and distal regions, as well as self-collected stool samples, noting high interindividual diversity especially based on BMI, as well as specific characteristic metabolites correlating with different regions (Baxter *et al.*, 2020). By performing the analysis on healthy wild-type mice, otherwise confounding factors such as diet, environmental stress, age, and medications are limited. There is extensive literature combining various "omics" studies, such as proteogenomics and metagenomics, comparing proximal and distal colon regions, however the majority of studies compare profiles in disease *vs.* healthy tissue. Imperial *et al.* conducted proteogenomics to investigate differing gene mutations and proteins between proximal, distal, and rectal colorectal cancers (Imperial *et al.*, 2018). Huang *et al.* compared proximal and distal colon profiles in patients with colorectal cancer by studying transcriptomic and gene mutational differences (Huang, Y. *et al.*, 2021). Parigi *et al.* performed transcriptomic analysis using quantitative PCR on healthy and colitis-induced mice to understand transcriptomic differences across different regions of the colon and how this profile changes upon introduction of disease (Parigi *et al.*, 2022). A large portion of studies investigate the differences between regions in the context of disease, but not in healthy subjects, highlighting the importance of understanding baseline variations. Very few have employed a combination of proteomics and metabolomics for this purpose (Busi *et al.*, 2023; Huang, Y. *et al.*, 2021; Marshall *et al.*, 2021; Xu *et al.*, 2022).

2.4 Experimental Methods

2.4.1 Chemicals

Sequencing-grade, TPCK-treated trypsin (from bovine pancreas), iodoacetamide (IAM) and dithiothreitol (DTT), as well as HPLC grade acetonitrile (ACN), methanol (MeOH), ethanol (EtOH), ammonium bicarbonate (ABC), and formic acid (FA), were obtained from Sigma-Aldrich (Oakville, ON, Canada). Ultrapure water was obtained from a Millipore Synergy UV system (Billerica, MA, USA).

2.4.2 Sample Collection

Colon and fecal samples from proximal and distal regions were collected from five female healthy FVB/N mice (Taketo *et al.*, 1991). Additional fecal samples were collected for simultaneous

preparation of metabolite extracts and peptide digests from six FVB/N mice (3 male, 3 female). These latter samples were necessary, since we noted that protein pellets from feces stored in the freezer following metabolite extraction for several days prior to digestion into peptides did not yield satisfactory proteome coverage. Before dissection, all mice were euthanized using carbon dioxide. Regarding colon samples, mesenteric fat was first removed and then the colon was divided into the proximal and distal regions, each 1.5 cm in length. Each region of the colon was opened longitudinally for feces collection. All mice were obtained from Charles River Laboratories (Senneville, QC, Canada) and fed standard rodent chow diet #5075 (Charles River). Mice were maintained at the animal facility at *Université du Québec à Montréal* (UQAM), and sample collection was performed at 20 days postnatal (pre-weaning). All samples were collected into pre-weighed 1.5 mL Safe-Lock polypropylene tubes (Eppendorf, Mississauga, ON, Canada) and stored at -80°C. Distal and proximal colon samples weighed an average of 93 $\pm$ 19 mg and 128 $\pm$ 26 mg, respectively. Distal and proximal fecal samples weighed an average of 50 $\pm$ 25 mg and 55 $\pm$17 mg, respectively.

2.4.3 Sample Preparation

2.4.3.1 Metabolite extraction

An initial volume of 100 mM ammonium bicarbonate (ABC) buffer (pH 8.5) was added to tissues collected, corresponding to half the weight of tissue collected (0.5 µl per mg) for colon samples and 1 µl per mg weight for fecal samples, followed by vortex mixing (5 s) and bath sonication for 15 minutes. Proteins were then precipitated using 3 times the volume of buffer with 100% MeOH. All colon samples were probe sonicated using a QSonica XL-2000 CML-4 sonicator (5 cycles, 5s each) for further tissue homogenization. All samples (colon and fecal) were centrifuged (8 minutes, 4°C, 14000 rpm) where the supernatant was kept for metabolomic analysis, and the resulting protein pellet used for proteomic analysis. Supernatants were dried with a universal vacuum concentrator (Fisher Scientific, Mississauga, ON, Canada) and reconstituted in 25% MeOH with reconstitution volume either matching or doubling the supernatant volume taken for colon and fecal samples, respectively. Prepared sample extracts were stored at -30°C prior to analysis.

2.4.3.2 Protein solubilisation and digestion

A solution of 7 M urea and 2 M thiourea (100 µl) was added to each dried protein pellet followed by vortex mixing (10 s) and sonication in a water bath for 15 minutes. ABC buffer (300 µl) was then added to each sample followed by probe sonication for five 5 s cycles. Quantitation of protein

in resulting extracts was performed by the Bradford protein assay, with appropriate dilutions to cover the dynamic range from 20-140 µg/ml protein. A normalized sample size of 100 µg protein was then aliquoted into a new tube and volumes completed to 400 µl with ABC buffer, followed by 15 µl of 100 mM DTT (15 min at 37°C), and 20 µl of 100 mM IAM (30 min at 37°C in the dark) for reductive alkylation. Digestion was initiated with the addition of 20 µl trypsin solubilized in 50 mM acetic acid with overnight incubation at 37°C and continual mixing at 650 rpm on an Eppendorf thermomixer. Following digestion, samples were diluted with water to 1 mL followed by solid phase extraction (SPE) on OASIS HLB cartridges (30 mg/mL) from Waters Limited (Mississauga, ON, Canada). Cartridges were conditioned with 1 mL each of 100% MeOH and nanopure water, followed by sample loading. Cartridges were washed with 1 mL of nanopure water and eluted with 2 volumes of 500 µl of 100% MeOH. Samples were dried (SpeedVac) and reconstituted in 120 µl of 10% ACN, 0.2% formic acid (FA), and stored at -30°C prior to LC-MS/MS analysis.

2.4.4 LC-HRMS/MS Analysis

2.4.4.1 Metabolomics

Metabolite extracts (10 µl) were analyzed on a Nexera UHPLC (Shimadzu, Columbia, MD, USA) coupled to a quadrupole time-of flight (TripleTOF 5600) mass spectrometer (Sciex, Concord, ON, Canada) equipped with a DuoSpray ion source in both ionization electrospray modes. Chromatographic separation of metabolites employed an Imtakt Scherzo SM-C18 column (100 x 3 mm, 3 µm) with a flow rate of 0.3 mL/min, column temperature of 40ºC, and gradient elution with water (A) and ACN (B), both containing 0.1% FA. Complementary chromatographic separation was performed using a Phenomenex Luna Reverse-Phase PFP column (150 x 2.1 mm, 3 µm) at a flow rate of 0.25 mL/min and gradient elution with water containing 0.1% FA (A) and 100% MeOH (B). The gradient elution for both columns was initiated at 3% B at 2.0 min, increased linearly to 65% at 15 min followed by an increase to 95% within 0.5 min, then held for 2.5 min, followed by column re-equilibration at starting conditions.

Ion source parameters were set at 450ºC for source temperature, 5000 (or -4500) V for ionspray voltage and 80 V for declustering potential (DP), 35 psi for curtain gas, 50 psi for nebulizer gas (nitrogen) and drying gases. Information dependent acquisition (IDA) was employed with TOF-MS data for *m/z* 80-980 (200 ms accumulation time) followed by MS/MS acquisition for *m/z* 40-800 for the 8 most intense ions (100 ms accumulation time) with a cycle time of 1.1 s, with collision offset voltage set to 30 $\pm$ 10 V. An in-house standard mix (from *m/z* 120-922*)* was injected every four samples for auto-calibration in MS and MS/MS mode.

2.4.4.2 Proteomics

Samples (20 µl) were analyzed on a Nexera UHPLC (Shimadzu, Columbia, MD, USA) coupled to a quadrupole time-of flight (TripleTOF 5600) mass spectrometer (Sciex, Concord, ON, Canada) equipped with a DuoSpray ion source in positive electrospray mode. Gradient elution of water and acetonitrile with 0.1% FA were used as mobile phases A and B respectively, on a Phenomenex Aeris PEPTIDE XB-C18 column (100 x 2.1mm, 1.7µm) with a SecurityGuard ULTRA C18 peptide guard (2.1 x 2mm) (Phenomenex, Torrance, CA, USA) at a flow rate of 0.30 mL/min and column temperature of 40°C. Gradient elution was initiated at 5% B at 2.5 min, increased to 30% at 40 min followed by an increase to 50% at 42 min, increase to 90% at 44 min and held for 3 min, followed by decrease to 5% at 47 min for column re-equilibration for 8 min.

Ion source parameters were set at 500ºC for source temperature, 5000 V for ionspray voltage and 80V for declustering potential (DP), 35 psi for curtain gas, 50 psi for nebulizer gas (nitrogen) and drying gases. An in-house standard mix was injected every four samples for auto-calibration in MS and MS/MS mode. Information-dependent acquisition (IDA) and data-independent acquisition (SWATH) were both employed for high resolution mass spectrometry analysis. TOF-MS data for IDA acquisition was acquired from *m/z* 140-1250 with an accumulation time of 250 ms, followed by MS/MS acquisition from *m/z* 80-1300 of the 15 most intense ions. Collision-offset voltage was set to 30 $\pm$ 10 V. Pooled samples were prepared for distal and proximal colon and fecal samples for ion library creation from IDA analyses. For SWATH acquisition, TOF-MS scan from *m/z* 140-1250 with an accumulation time of 150 ms, followed by MS/MS experiments (100) with variable Q1 windows from *m/z* 80-1500 for a total cycle time of 2.7 s. Collision-offset voltage was set to 30 $\pm$ 5 V.

2.4.5 Data Processing

2.4.5.1 Metabolomics

Data was acquired using Sciex Analyst TF (v1.7.1) software and data visualization used PeakView (v2.2) with MasterView 1.1 from Sciex. For untargeted data processing, MarkerView (v1.2.1, Sciex) software was used for peak picking to find unique features (*m/z*, RT) and for normalization. Putative identification of metabolites was performed by importing feature lists and data into Sciex OS-Q for spectral matching using several databases (Sciex *all-in-one* HR-MS metabolite library, NIST and an in-house library of standard metabolites). Putative metabolite identifications used mass error cutoff within $\pm$ 10 ppm for protonated or deprotonated precursor ions and a library

score of 80% for MS/MS spectral matching. Peak verification was performed for each putative metabolite to ensure adequate signal/noise and proper integration using MultiQuant software (Sciex), and results were then imported into MarkerView for MLR (most likely ratio) normalization prior to statistical analysis using a Welch corrected *t*-test and Principal Component Analysis (PCA).

For further coverage of metabolite features that did not yield a putative metabolite hit by spectral matching of IDA data, a different approach was taken by first using MarkerView (v1.2.1, Sciex) software to process raw data to find statistically significant peaks (using thresholds of $p < 0.01$, fold change $\geq |2|$ following t-test). Peak verification was then performed on these features using Multiquant. The remaining features (*m/z*, RT pairs) that did not have previous putative metabolite assignments were targeted using SWATH acquisition with 1 Da windows, for subsequent spectral matching within Sciex OS-Q as previously described.

Heat maps were constructed using NG-CHM Builder from MD Anderson Cancer Centre (Houston, TX, USA) (Ryan *et al.*, 2019). An excel file was uploaded with defined peak areas of each compound for each sample. Peak areas were annotated as percentage relative to the highest peak area for a given compound. Hierarchical clustering was applied to row ordering options specifying Euclidean distance metric and Ward agglomeration with original order specified for column ordering options. No covariates were assigned.

Enrichment analysis of metabolites was performed using MetaboAnalyst 5.0 (Montreal, Canada) (Pang *et al.*, 2021). The Human Metabolome Database (HMDB) numbers corresponding to metabolites were inputted for analysis with Small Molecule Pathway Database (SMPDB) based pathways selected and using metabolite sets containing at least 2 entries.

2.4.5.2 Proteomics

Raw data visualization was performed with PeakView 2.2 with MasterView 1.1 from Sciex. OneOmics Suite 3.1 cloud-based program was used for protein identifications from IDA data with UniprotKB database released February 2022. Criteria specified for protein identification for colon samples was as follows: mouse species, iodoacetamide cysteine alkylation, trypsin digestion, 1% global protein and peptide false discovery rate with up to 4 peptides per protein and 3 transitions per peptide. For fecal samples, the same parameters were employed for protein identification, except no species were specified, and results were filtered to identify proteins from bacterial

species as well as mouse. Heat maps were constructed using the same process as previously mentioned.

2.5 Results and Discussion

2.5.1 Untargeted Metabolomics

Colon and fecal samples from five healthy mice were analyzed by LC-MS/MS to characterize the coverage of our untargeted metabolomics workflows as well as to study the variations between two distinct regions of the colon. Raw LC-HRMS/MS data were first processed to find unique features (*m/z*, retention time) present in the samples. These features were then searched against HRMS/MS spectral databases for putative metabolite identification (Figure 2.1). Due to the limitations in proper peak integration with automated peak picking, each metabolite peak was verified to ensure adequate signal-to-noise and consistent integrations throughout the dataset. This step was essential for subsequent statistical analyses. Overall, 307, 215, 272, and 217 colon metabolites, as well as 416, 208, 386, and 225 fecal metabolites identified in Scherzo (+), Scherzo (-), PFP (+) and PFP (-) datasets, respectively. These results are summarized in Supplemental Tables 2.8 and 2.9, listing each metabolite name, library score, mass error, and formula, and which dataset they were from. It is important to note that these tables list metabolite IDs from four datasets in which overlapping metabolites can be present.

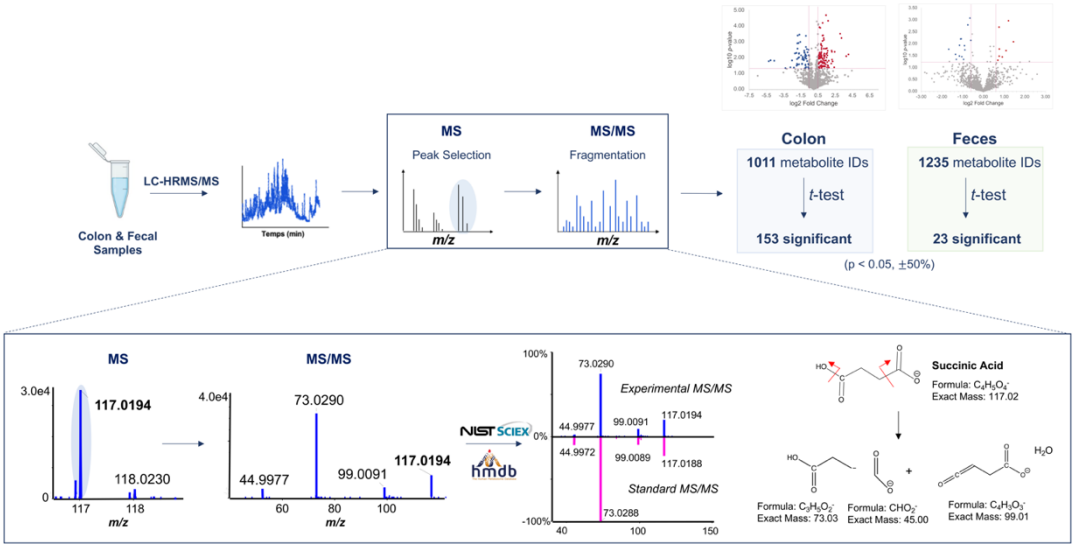

Figure 2.1 Untargeted metabolomics workflow of colon and fecal samples from sample preparation to data processing, with an example of spectral matching for succinic acid

Separation of metabolites was performed using two chromatographic columns for complementary separation. Both columns serve different roles as the Scherzo mixed-mode column exhibits good retention of polar compounds having either acidic or basic groups, due its ion exchange and reverse phase characteristics, whereas the PFP column separates based on polarity with preferential retention of aromatic and conjugated compounds. As seen in Figure 2.2a, there are 162 putative colon metabolites uniquely identified with the Scherzo column, 140 identified metabolites unique to the PFP column, and 212 identified metabolites common to both columns. The same complementarity was seen from fecal samples (Figure 2.2b**),** where 179 and 163 metabolites are unique to the Scherzo and PFP columns, respectively, with 282 metabolites in common. When comparing putative metabolite identifications between the two chromatographic columns, retention times were not considered explaining the discrepancy of total number of metabolites.

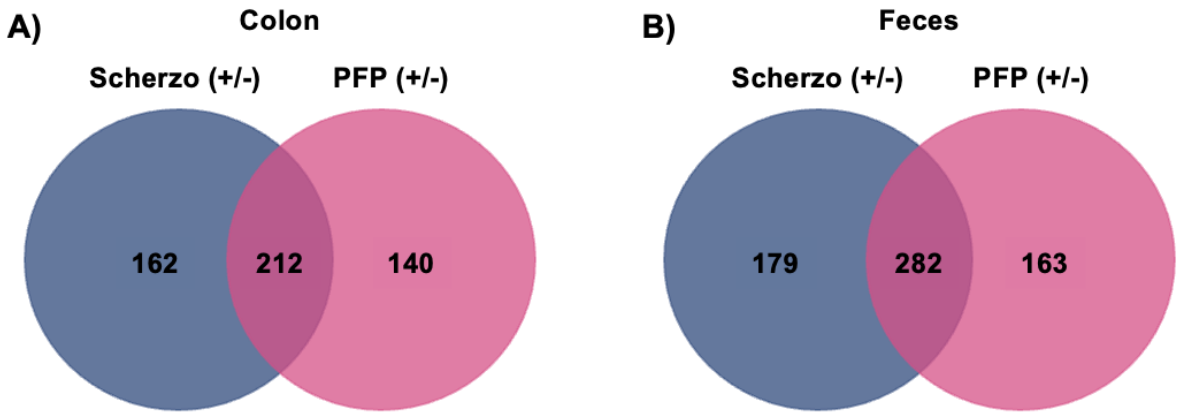

Figure 2.2 Venn diagrams representing unique and common metabolites with putative identifications by MS/MS spectral matching, from combined positive and negative ion modes, using Scherzo and PFP columns for colon (a) and fecal (b) samples

When all metabolites were compiled, the highest proportion represent organic acids and derivatives (HDMB metabolite superclass), more specifically, carboxylic acids and derivatives (class), and amino acids and peptides (subclass). This dataset also covered many organoheterocyclic compounds and lipid-like molecules as seen in Figure 2.3. Regarding lipid molecules in colon and fecal samples, fatty acyls, such as eicosanoids and fatty acids, were the major sub-classes. Glycerophospholipids and steroids were seen to have better coverage with the

Scherzo column whereas organic acids notably in fecal samples has better cover from the PFP column but not in colon samples.

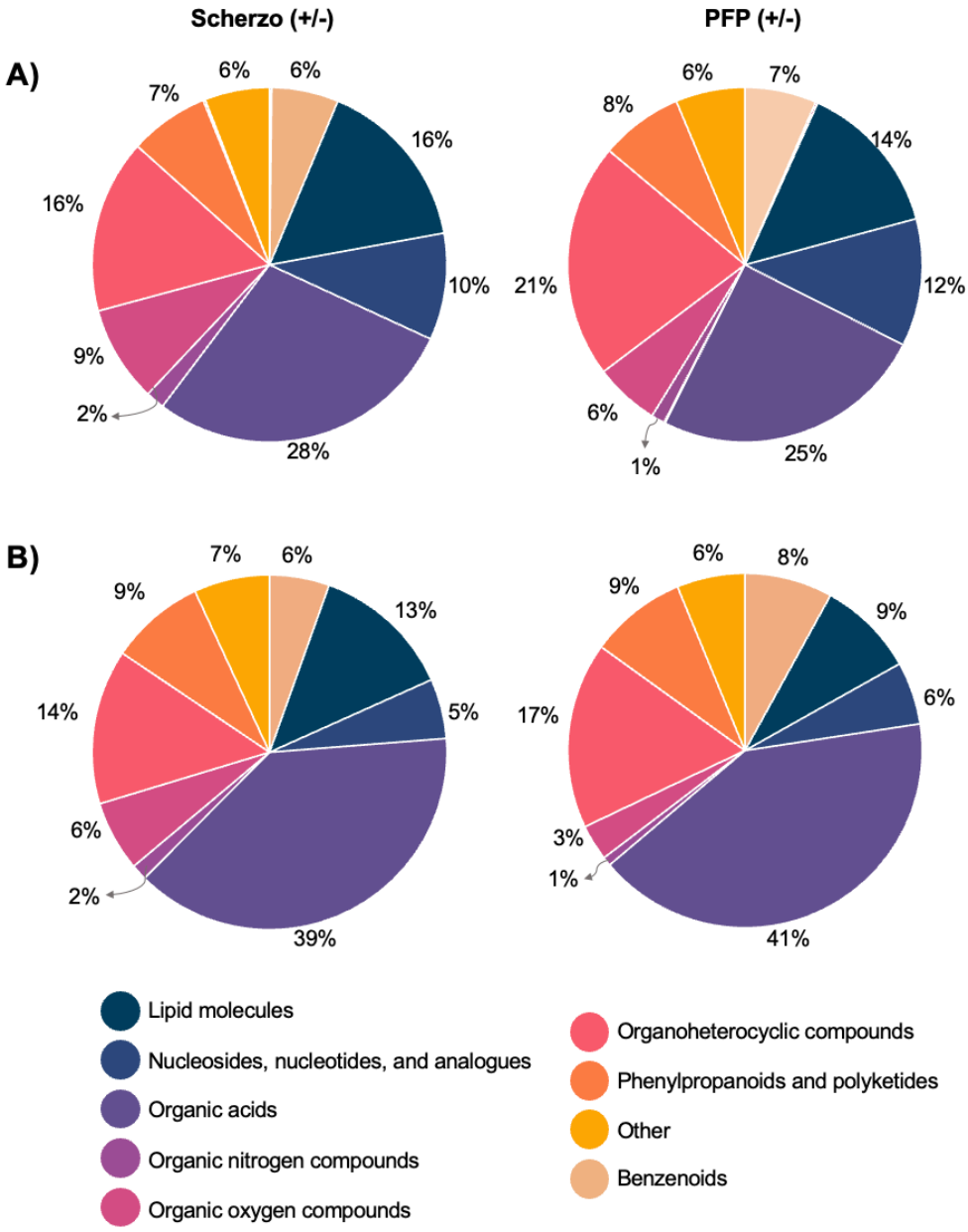

Figure 2.3 Classification of metabolite superclasses from combined putative identifications from Scherzo and PFP datasets in positive and negative modes from colon (a) and fecal (b) samples

Principal Component Analysis (PCA) was performed on the quantitative data to determine if there was any clustering of proximal and distal samples. For colon, there is already a clustering of samples from the two regions based on using all metabolites, whereas for feces, no distinction was seen (Figure 2.4). This indicates that at the tissue level, certain metabolites are differing between the two regions causing the groups to cluster into their respective areas of the PCA plot, whereas in the fecal samples, less clustering between groups is observed overall. Although PCA plots greatly help to visualize the clustering pattern of large data sets, it is used in this case as a visual aid to get a generalized view of the data obtained.

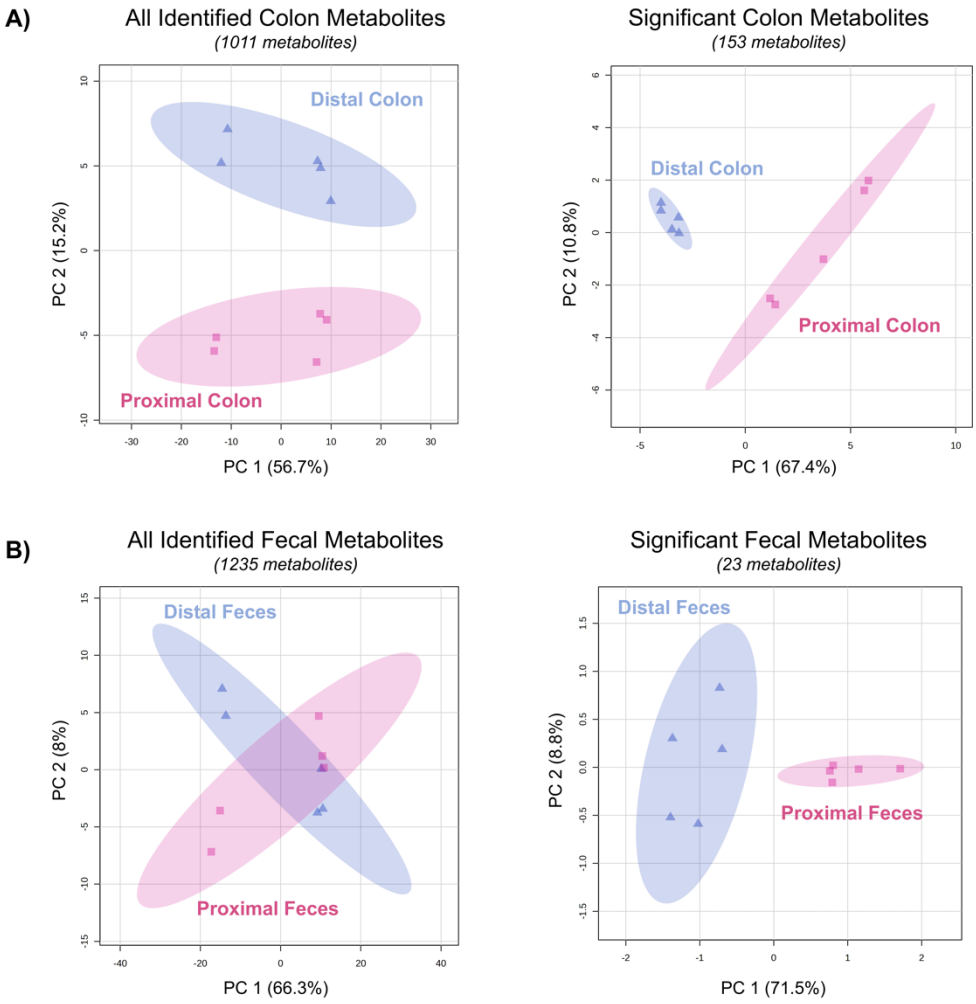

Figure 2.4 Unsupervised PCA plots of all identified and statistically significant metabolite IDs from Scherzo and PFP columns of a) colon, and b) fecal samples

2.5.1.1 Metabolite Differences Between Distal and Proximal Regions

Statistical analysis was performed to observe which metabolites are shown to increase or decrease in the distal portion of the colon compared to proximal samples. In Figure 2.4, we are able to observe the difference in the generated PCA plots when only the statistically significant metabolites are used in the analysis. When a threshold of *p-value* < 0.05 and fold change greater than ± 50% was set, 153 colon and 23 fecal metabolites were found to be significantly changing between the two regions. Regarding colon samples, 100 metabolites were increased and 53 were decreased in the distal region. Of the 23 fecal metabolites, 9 increased and 14 decreased. These results are summarized in Supplemental Tables 2.10 and 2.11. Heatmaps with hierarchical clustering were used to visualize the changes in levels in the individual samples. The Welch *t*-test allows inter-individual variation to be considered when finding significant differences between groups. The Welch *t*-test will consider inter-individual variation and compare two given groups of samples (West, 2021).

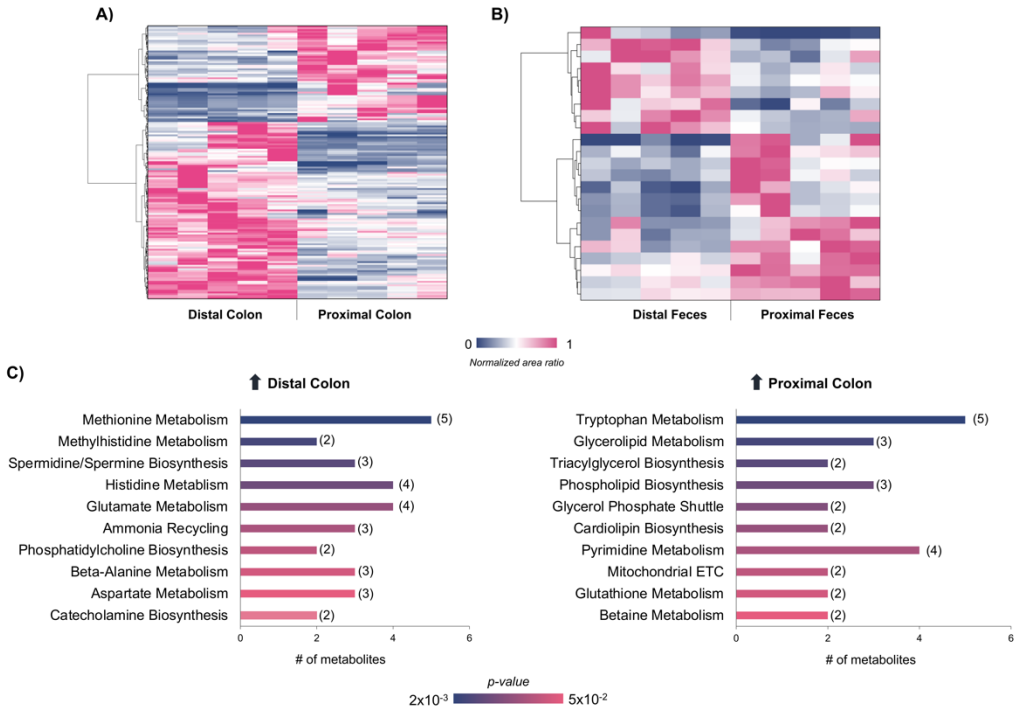

Figure 2.5 a) Heatmap of 153 statistically significant colon metabolites; b) Heatmap of 23 statistically significant fecal metabolites; c) Enrichment analysis using MetaboAnalyst 5.0 of statistically significant metabolites that are increased in distal and proximal colon

As shown in Figure 2.5a, there is a shift in abundance in the colon tissue for many metabolites. The same extent of variability is not seen in fecal samples as shown in Figure 2.5b, both in terms of number of statistically significant metabolites but also in the variation within the same region of these metabolites. This lack of significant variability between regions from fecal samples can be potentially explained by how fecal formation occurs in the colon. Fecal formation starts in the proximal portion of the colon, where the proximal colon will absorb nutrients and water from matter incoming from the small intestine, forming feces that are then stored in the distal portion of the colon waiting to be expelled (Azzouz et Sharma, 2023). There should not, in fact, be much variation of the level of metabolites in the feces in the absence of disease. This finding can also be due to the large complexity of fecal metabolome (most of which is not even contained in metabolite databases, and therefore not a subject of this study). With such highly complex samples, it is increasingly difficult to detect differences in low abundance metabolites.

Performing an enrichment analysis revealed certain specific pathways that were affected as seen in Figure 2.5. For example, methionine metabolism is a highly enriched pathway in the distal colon, whereas metabolites involved in tryptophan metabolism have higher levels in the proximal region. Tryptophan is metabolised through the serotonin, kynurenine, and indole pathways. Metabolites involved in the serotonin and kynurenine pathways were increased in the proximal region as shown in Figure 2.6 and Table 2.1 (Wang, S. *et al.*, 2023). Figure 2.6 and Table 2.1 also show the overlap and complementarity between the four datasets. For example, 5-hydroxyindoleacetic acid and kynurenine are well detected (and identified through spectral matching) in three of four datasets with similar results between proximal and distal regions. However, serotonin was only idenfied in Scherzo (+) dataset, and xanthurenic acid was seen uniquely in PFP (-) dataset.

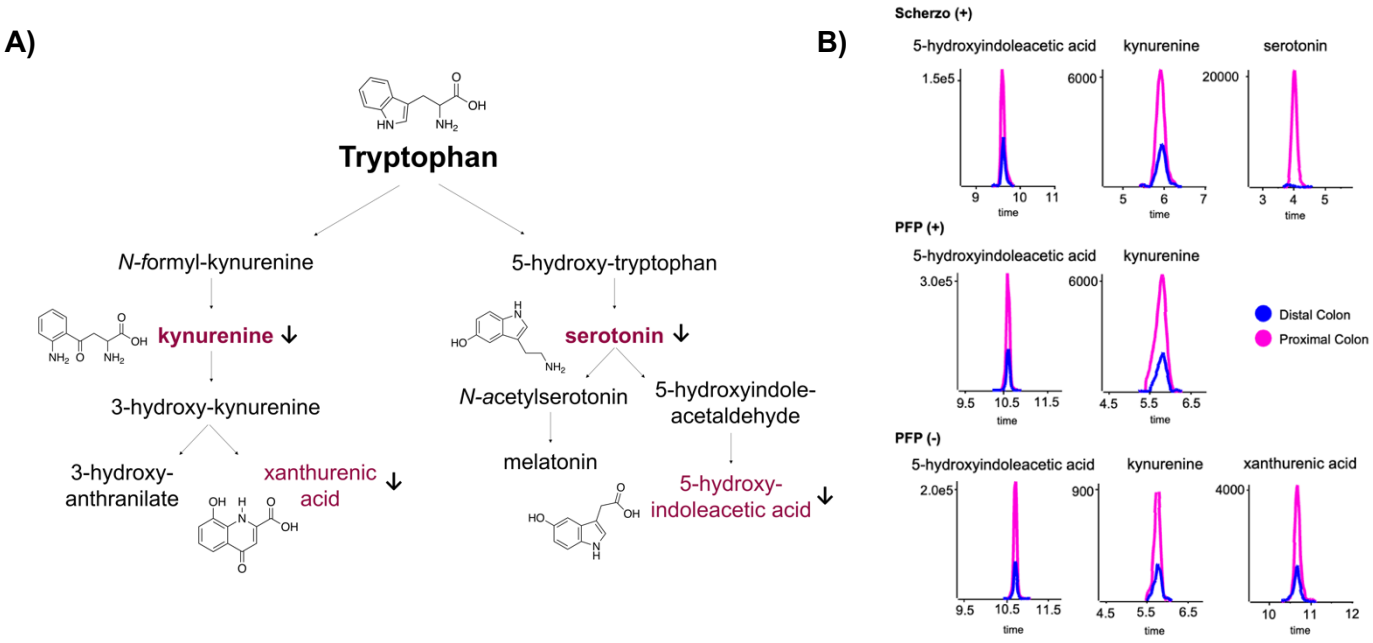

Figure 2.6 a) Tryptophan metabolism via serotonin and kynurenine pathways with metabolites identified (kynurenine, xanthurenic acid, serotonin, and 5-hydroxyindole-acetic acid) shown to be increased in the proximal region of the colon (decreased in distal colon). Other metabolites in the respective pathways were not identified in any datasets. b) Relative peak intensities between distal and proximal colon of identified metabolites are shown as extracted ion chromatograms for representative samples.

Table 2.1 Metabolites Increased in Proximal Colon Involved in Tryptophan Metabolism

Metabolite ID	Chemical Formula	Retention Time (min)	Fold Change DC/PC	*p*-value	Column (+/-)
Serotonin	$C_{10}H_{12}N_2O$	4.1	-23.8	$1.6x10^{-2}$	Scherzo (+)
5-hydroxyindoleacetic acid	$C_{10}H_9NO_3$	9.6	-3.5	$1.1x10^{-2}$	Scherzo (+)
		10.6	-3.3	$5.2x10^{-3}$	PFP (+)
		10.7	-3.7	$1.0x10^{-3}$	PFP (-)
Kynurenine	$C_{10}H_{12}N_2O_3$	5.9	-3.9	$3.2x10^{-2}$	Scherzo (+)
		5.7	-3.8	$2.5x10^{-2}$	PFP (+)
		5.7	-3.3	$2.6x10^{-2}$	PFP (-)
Xanthurenic acid	$C_{10}H_7NO_4$	10.7	-4.5	$5.4x10^{-3}$	PFP (-)

Specific metabolites, such as serotonin, 5-hydroxyindoleacetic acid, kynurenine and xanthurenic acid, were shown to have higher levels in the proximal colon. Kynurenine is implicated in the inflammatory response, as well as being a crucial player in the gut-brain axis (Deng, Y. *et al.*, 2021). Tryptophan is converted into kynurenine by the enzyme indoleamine 2,3-dioxygenase, which has been shown to be an oncogenic protein as its levels are elevated in colorectal cancer, leading to depleted tryptophan and elevated kynurenine levels (Bishnupuri *et al.*, 2019; Venkateswaran *et al.*, 2019; Zhang, X. *et al.*, 2021). Kynurenine is capable of modulating immune responses during tumour growth by inactivating immune cells such as T-cells allowing cancerous cells to continuously proliferate (Bishnupuri *et al.*, 2019; Venkateswaran et Conacci-Sorrell, 2020; Zhang, X. *et al.*, 2021). Due to kynurenine's role in the gut-brain axis, altered tryptophan metabolism and kynurenine via intestinal microbiota dysbiosis has also been shown to lead to neurological diseases (Deng, Y. *et al.*, 2021). Tryptophan can also be metabolized into serotonin, with implications in both neurological and gastrointestinal signaling, where serotonin in the gut surprisingly accounts for over 90% of the serotonin produced in the body (Fouquet *et al.*, 2019; Gershon et Tack, 2007; Reigstad *et al.*, 2015; Roth *et al.*, 2021). Although all of these metabolites exhibited at least over 300% increase in peak area, serotonin was seen to have the highest fold change with peak areas in proximal colon 24-fold higher than in distal colon samples. Serotonin is produced from enterochromaffin cells (EC) in the intestinal mucosa in the gut and plays a large role in colonic motility, secretion, signalling, sensation, and immune activity (Gao *et al.*, 2022; Mawe et Hoffman, 2013; Roth *et al.*, 2021). Atypical levels of serotonin are a growing area of research due to their implications in various intestinal diseases, such as colorectal cancer, ulcerative colitis, and irritable bowel syndrome (IBS) (Manocha et Khan, 2012). IBS symptoms can be expressed either through constipation or diarrhea, two symptoms of different extremities (Bonetto *et al.*, 2021; Manocha et Khan, 2012; Saha, 2014). Serotonin levels associated with symptoms of constipation IBS are shown to decrease, whereas serotonin is increased in IBS patients with diarrhea symptoms (Bonetto *et al.*, 2021; Manocha et Khan, 2012; Saha, 2014; Spiller, 2008). Metabolites resulting from tryptophan degradation are thus largely implicated in intestinal diseases and are a group of molecules that are continuously studied to further understand their implication in pathogenesis and treatment of these intestinal diseases. This study has shown that these metabolites are increased in the proximal region of the colon. A study by Wei *et al.*, demonstrated similar results that elevated levels of EC cells and serotonin are found in the proximal colon and that their altered levels led to significant differences in colon motility and contractions resulting in delayed gastric excretions from the proximal region (Wei *et al.*, 2021).

Prostaglandins are another group of metabolites that showed significant changes between the two regions. Five prostaglandin molecules (PGA1, PGA2, PGD1, PGE1, and PGH2 respectively, at several different retention times) were shown to be higher in the distal colon (prostaglandin E1, A1, A2, and H2) (Figure 2.7, Table 2.2). Prostaglandins can be synthesized from arachidonic acid or dihomo-gamma linolenic acid through cyclooxygenase (COX) enzymes. Prostaglandin A2 (PGA2) and H2 (PGH2) are products of arachidonic acid metabolism, whereas prostaglandin A1 (PGA1), and prostaglandin E1 (PGE1) are products of dihomo-gamma linolenic acid metabolism, the direct precursor of arachidonic acid (Figure 2.7a) (Schröder, R. *et al.*, 2012; Straus et Glass, 2001; Wang, W. *et al.*, 2021). Interestingly, prostaglandins can either be pro or anti-inflammatory depending on the type of prostaglandin (Ricciotti et FitzGerald, 2011; Wang, D. et DuBois, 2008). For example, prostaglandin E2 (PGE2) is pro-inflammatory and can contribute to chronic inflammation and can be pro-tumorigenic in certain cases, whereas prostaglandin E1 (PGE1) has been shown to have beneficial effects on tissue injury (Hao *et al.*, 2018; Levin *et al.*, 2002; Ricciotti et FitzGerald, 2011; Wang, D. et DuBois, 2008). Unlike PGE2, prostaglandin A2 (PGA2) can have anti-tumorigenic and anti-inflammatory effects. Elevated levels of prostaglandin E synthases have been reported in colorectal cancer, in which PGA2 was shown to cause a decrease in prostaglandin E synthase enzyme levels (Gorospe *et al.*, 1996; Sasaki et Fukushima, 1994; Schröder, O. *et al.*, 2006). Like PGA2, PGE1 and PGA1 also have anti-inflammatory properties in cases of colorectal cancer and irritable bowel syndrome (Kunkel *et al.*, 1979; Mandal *et al.*, 2005; Rossi *et al.*, 2000; Sasaki et Fukushima, 1994). These anti-inflammatory prostaglandins (PGA2, PGE1, PGA1) that are increased in the distal colon could potentially play a role as to why morbidity rates and tumor progression for colorectal cancer in the distal colon have more favourable outcomes compared to those affecting the proximal colon. This highlights once more the heterogeneity between the two distinct regions and that prostaglandin metabolites are molecules of interest when studying diseases affecting the gut. As shown in Figure 2.7a, PGH2 is also a precursor for many prostaglandins, such as PGI2, PGF2, PGE2, PGD2, 15ΔPGJ2, as well as various thromboxanes (TXA2) (not shown). PGH2 being increased in distal colon can lead to a potential cascade of formation of other prostaglandins leading to potential cases of pro or anti inflammatory action in the distal colon (Jara-Gutiérrez et Baladrón, 2021; Rajakariar *et al.*, 2007; Simon, 1999).

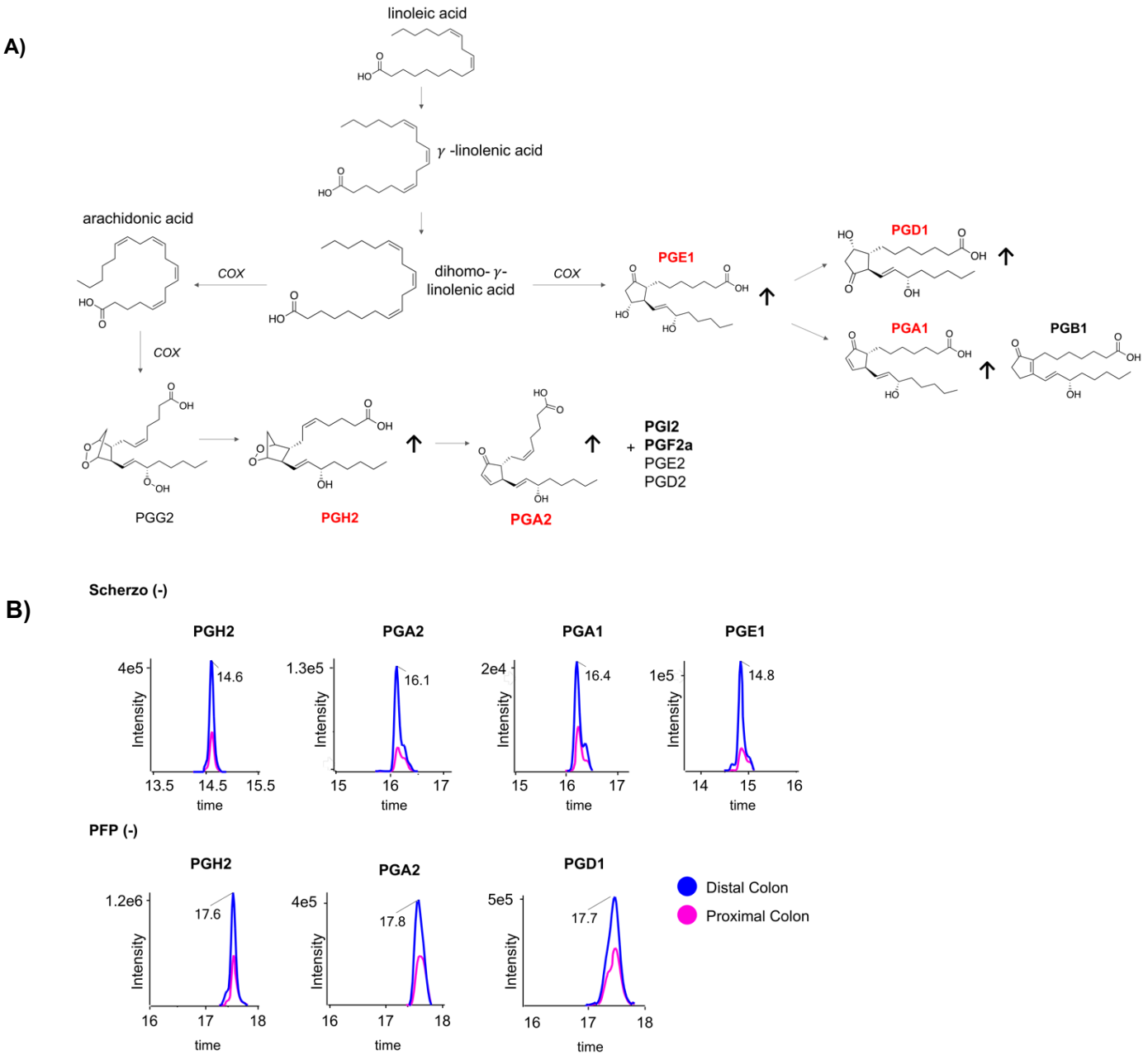

Figure 2.7 a) Arachidonic acid metabolism (Adapted from (Surh et al., 2011)). Prostaglandins in red have increased levels in the distal colon and other bolded prostaglandins were identified in the dataset but did not show statistical significance between the two regions b) Relative peak intensities between distal and proximal colon of identified metabolites are shown as extracted ion chromatograms for representative samples.

Table 2.2 All Identified Prostaglandin Metabolites in Colon from All Metabolite Datasets

Metabolite ID	Retention Time (min)	Chemical Formula	Fold Change DC/PC	*p*-value	Column (+/-)
.DELTA.17-6-Ketoprostaglandin F1.alpha.	12.3	$C_{20}H_{32}O_6$	1.0	$8.5x10^{-1}$	Scherzo (-)
13,14-Dihydro-15-ketoprostaglandin A2	16.8	$C_{20}H_{30}O_4$	1.1	$6.0x10^{-1}$	Scherzo (+)
13,14-Dihydro-15-ketoprostaglandin A2	16.8		1.0	$7.8x10^{-1}$	Scherzo (-)
13,14-Dihydro-15-ketoprostaglandin A2	15.4		-1.2	$3.1x10^{-1}$	Scherzo (-)
15-Deoxy-.DELTA.12,14-prostaglandin J2 (in-source fragment)	**17.8**	**$C_{20}H_{28}O_3$**	**2.5**	**$2.2x10^{-2}$**	**PFP (-)**
15-Deoxy-.DELTA.12,14-prostaglandin J2	17.1		1.6	$1.1x10^{-1}$	Scherzo (-)
15-Deoxy-.DELTA.12,14-prostaglandin J2 (in-source fragment)	**16.1**		**2.7**	**$9.2x10^{-6}$**	**Scherzo (-)**
15-Deoxy-.DELTA.12,14-prostaglandin J2 (in-source fragment)	**14.6**		**2.3**	**$6.7x10^{-4}$**	**Scherzo (-)**
5-Isoprostaglandin-F2.alpha.-VI	14.4	$C_{20}H_{34}O_5$	1.4	$3.3x10^{-3}$	Scherzo (-)
5-Isoprostaglandin-F2.alpha.-VI	17.1		1.2	$1.2x10^{-1}$	PFP (-)
5-Isoprostaglandin-F2.alpha.-VI	13.9		1.2	$2.6x10^{-1}$	Scherzo (-)
8-iso-Prostaglandin A1 (in-source fragment)	**14.8**	**$C_{20}H_{32}O_4$**	**1.8**	**$1.6x10^{-3}$**	**Scherzo (-)**
9-Oxoprosta-5Z,10,12Z,14E-tetraenoic acid (in-source fragment)	**17.8**	**$C_{20}H_{28}O_3$**	**2.0**	**$4.0x10^{-4}$**	**PFP (+)**
9-Oxoprosta-5Z,10,12Z,14E-tetraenoic acid (in-source fragment)	**16.1**		**2.8**	**$5.9x10^{-3}$**	**Scherzo (+)**
Bicyclo-prostaglandin E2	15.3	$C_{20}H_{30}O_4$	-1.2	$2.4x10^{-1}$	Scherzo (+)
Prostaglandin A1	**16.4**	**$C_{20}H_{32}O_4$**	**1.6**	**$1.1x10^{-2}$**	**Scherzo (-)**
Prostaglandin A2	**16.1**	**$C_{20}H_{30}O_4$**	**2.7**	**$2.1x10^{-5}$**	**Scherzo (-)**
Prostaglandin A2	**17.8**		**2.1**	**$3.9x10^{-4}$**	**PFP (-)**
Prostaglandin A2 (in-source fragment)	**14.6**		**2.3**	**$7.6x10^{-4}$**	**Scherzo (-)**
Prostaglandin B1	15.6	$C_{20}H_{32}O_4$	1.2	$3.1x10^{-1}$	Scherzo (-)
Prostaglandin D1	**17.7**	**$C_{20}H_{34}O_5$**	**1.5**	**$1.4x10^{-3}$**	**PFP (-)**
Prostaglandin E1	**14.8**	**$C_{20}H_{34}O_5$**	**1.5**	**$2.8x10^{-2}$**	**Scherzo (-)**
Prostaglandin H2	**14.6**	**$C_{20}H_{32}O_5$**	**2.2**	**$5.9x10^{-4}$**	**Scherzo (-)**
Prostaglandin H2	**17.6**		**1.8**	**$1.3x10^{-3}$**	**PFP (-)**
Prostaglandin I2	13.0	$C_{20}H_{32}O_5$	1.1	$3.3x10^{-1}$	Scherzo (+)
Prostaglandin I2	12.8		1.1	$3.3x10^{-1}$	Scherzo (+)
Prostaglandin I2	13.8		-1.1	$5.0x10^{-1}$	Scherzo (+)
Prostaglandin I2	17.4		1.3	$3.6x10^{-2}$	PFP (+)

Unlike the prostaglandins that are increased in the distal colon, shown in Table 2.2, other prostaglandins were putatively identified but not found to be changing between the regions. These prostaglandins, namely prostaglandin I2 (PGI2), 13,14-dihydro-15-ketoprostaglandin A2, prostaglandin B1 (PGB1), isoprostaglandin F2 alpha (PGF2a), prostaglandin D1 (PGD1), Ketoprostaglandin F1 alpha, and bicyclo-prostaglandin E2 did not have sufficiently low *p*-values and high enough fold changes to be considered as significantly different as shown in Table 2.2. PGI2 and PGF2a are shown to be products of arachidonic metabolism (Figure 2.7) (Wang, B. *et al.*, 2021; Zhang, Y. *et al.*, 2023). PGH2 acts as a precursor for various prostaglandins, such as PGI2, PGA2, and PGF2a (Wang, B. *et al.*, 2021; Zhang, Y. *et al.*, 2023). The lack of significance in this dataset of these other prostaglandins could potentially be due to lower signal-to-noise and therefore higher variabilities in these measured peaks within samples from the same region. An

additional prostaglandin molecule initially found as statistically significant was putatively identified as 15-deoxy-Δ 12,14-prostaglandin J2 (15ΔPGJ2). This prostaglandin was identified at the same retention times as PGA2 on both Scherzo (-) (shown in Figure 2.8) and PFP (-) and results from an in-source loss of water from PGA2, and thus did not correspond to a separate metabolite. This highlights the need to verify final lists of statistically significant metabolites, for artifacts stemming from in-source fragmentation. A similar in-source dehydration was seen in the case of PGA2 and PGH2 and with 8-iso PGA1 and PGE1 from Scherzo (-), where they co-elute at 14.6 minutes and 14.8 minutes, respectively.

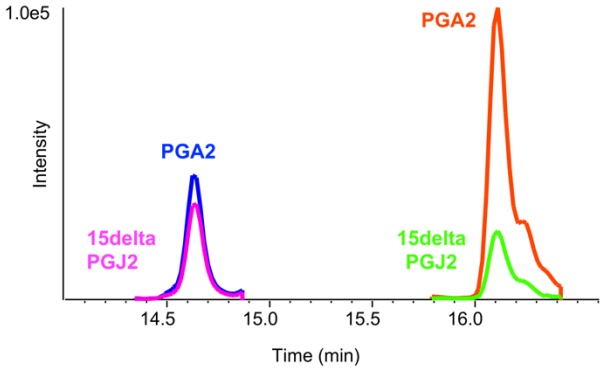

Figure 2.8 Extracted ion chromatograms demonstrating 15delta-PGJ2 as in-source fragment of PGA2 isomers in Scherzo (-) at retention times of 14.6 and 16.1 minutes.

Carnitines are a group of metabolites that have also been shown to be largely implicated in the colon, in which they are have roles in the transport of long-chain fatty acids into the mitochondria for their oxidation (Roscilli *et al.*, 2013; Srinivas *et al.*, 2007). Acylcarnitines are the result of the conjugation of carnitine with fatty acids and linked to energy production required for cell activity. Acylcarnitines are an important group of metabolites to study as they are known biomarkers for metabolic, diabetic, cardiovascular, and neurodegenerative disorders (Dambrova *et al.*, 2022). They have also been shown to play a role in various cancers in which Roscilli *et al*. found that a mixture of three acylcarnitines (carnitine, acetyl-carnitine, and propionyl-carnitine) were found to halt formation of lesions throughout all steps of tumour progession in an induced colon cancer mouse model indicating their promise in cancer therapeutics (Roscilli *et al.*, 2013). As shown in Table 2.3, 34 acylcarnitines have been identified in colon samples with 16 having significantly

higher levels in the distal colon.. Zhao *et* al. also found that various acylcarntines had beneficial actions agains colorectal cancer, but no distinction between proximal or distal colorectal cancer was made (Zhao *et al.*, 2023). The significance of many acylcarnitines being increased in the distal colon could be a potential reason as to why there are better outcomes reported with tumours residing in the distal colon as opposed to the proximal colon.

Table 2.3 All Identified Acylcarnitines in Colon Samples from All Metabolomic Datasets

Metabolite ID	Retention Time (min)	Chemical Formula	Fold Change DC/PC	*p*-value	Column (+/-)
Carnitine	2.0	$C_7H_{15}NO_3$	1.4	$2.6x10^{-2}$	PFP (+)
Carnitine	2.4		1.3	$1.6x10^{-2}$	Scherzo (+)
Acetylcarnitine	**2.5**		**1.6**	**$4.6x10^{-2}$**	**Scherzo (+)**
Acetylcarnitine	2.9	**$C_9H_{17}NO_4$**	1.2	$5.1x10^{-1}$	PFP (+)
Acetylcarnitine	3.8		1.1	$5.0x10^{-1}$	PFP (+)
Propionylcarnitine	2.9		1.8	$1.1x10^{-1}$	Scherzo (+)
Propionylcarnitine	3.5	$C_{10}H_{19}NO_4$	1.6	$6.2x10^{-2}$	Scherzo (+)
Propionylcarnitine	6.4		1.5	$7.9x10^{-2}$	PFP (+)
Butyrylcarnitine	**4.5**		**1.9**	**$2.4x10^{-3}$**	**Scherzo (+)**
Butyrylcarnitine	5.0	**$C_{11}H_{21}NO_4$**	1.4	$1.7x10^{-1}$	Scherzo (+)
Butyrylcarnitine	**8.5**		**1.6**	**$2.3x10^{-2}$**	**PFP (+)**
3-Hydroxybutyrylcarnitine	**2.6**	**$C_{11}H_{21}NO_5$**	**1.5**	**$2.2x10^{-2}$**	**Scherzo (+)**
3-Hydroxybutyrylcarnitine	4.2		1.2	$9.0x10^{-2}$	PFP (+)
2-Methylbutyrylcarnitine	7.3	**$C_{12}H_{23}NO_4$**	1.4	$2.3x10^{-1}$	Scherzo (+)
2-Methylbutyrylcarnitine	**10.3**		**1.8**	**$1.6x10^{-2}$**	**PFP (+)**
3-Hydroxyisovaleroylcarnitine	2.9		1.3	$9.1x10^{-3}$	Scherzo (+)
3-Hydroxyisovaleroylcarnitine	3.5	$C_{12}H_{23}NO_5$	1.0	$7.9x10^{-1}$	Scherzo (+)
3-Hydroxyisovaleroylcarnitine	6.4		1.1	$5.6x10^{-1}$	PFP (+)
Hexanoylcarnitine	**8.9**	**$C_{13}H_{25}NO_4$**	**2.4**	**$2.4x10^{-2}$**	**Scherzo (+)**
Hexanoylcarnitine	**12.6**		**2.0**	**$3.4x10^{-2}$**	**PFP (+)**
Octanoylcarnitine	**11.0**	**$C_{15}H_{29}NO_4$**	**2.7**	**$1.5x10^{-2}$**	**Scherzo (+)**
Octanoylcarnitine	**15.9**		**2.3**	**$1.1x10^{-2}$**	**PFP (+)**
Lauroylcarnitine	**17.7**	**$C_{19}H_{37}NO_4$**	**1.9**	**$1.9x10^{-2}$**	**PFP (+)**
Lauroylcarnitine	13.6		1.7	$2.2x10^{-1}$	Scherzo (+)
Palmitoylcarnitine	16.6	$C_{23}H_{45}NO_4$	3.5	$1.0x10^{-1}$	Scherzo (+)
Palmitoylcarnitine	17.9		4.8	$7.3x10^{-2}$	PFP (+)
3-Hydroxyhexadecanoylcarnitine	**15.3**	**$C_{23}H_{45}NO_5$**	**2.5**	**$1.6x10^{-2}$**	**Scherzo (+)**
3-Hydroxyhexadecanoylcarnitine	**17.8**		**3.0**	**$1.9x10^{-2}$**	**PFP (+)**
Linoleoyl carnitine	**17.8**	**$C_{25}H_{45}NO_4$**	**2.0**	**$1.2x10^{-2}$**	**PFP (+)**
Oleoylcarnitine	**16.8**	**$C_{25}H_{47}NO_4$**	**3.1**	**$3.1x10^{-2}$**	**Scherzo (+)**
Oleoylcarnitine	**17.9**		**2.1**	**$2.2x10^{-2}$**	**PFP (+)**
3-Hydroxyoleylcarnitine	**15.7**	**$C_{25}H_{47}NO_5$**	**2.9**	**$2.5x10^{-3}$**	**Scherzo (+)**
Stearoylcarnitine	17.9	$C_{25}H_{49}NO_4$	5.0	$3.0x10^{-1}$	Scherzo (+)
Stearoylcarnitine	17.9		3.5	$2.0x10^{-1}$	PFP (+)

To help maximize the coverage of identified colon metabolites, a method based on targeted SWATH acquisition was employed. From the initial peak list generated from raw data, a list of statistically significant features was generated, using *p-value* < 0.01 and fold change ≥ |2| as threshold, yielding 981 peaks of interest. This list was filtered after peaks were verified to ensure adequate peak shape and signal/noise ratio. The remaining 713 features were targeted for SWATH acquisitions to potentially gain more putative metabolite IDs with spectral searching of SWATH data. Using this approach, only four new putative metabolites of interest were found, in which 50 metabolites were previously identified from the IDA data. Metabolites involved in tryptophan and arachidonic metabolism pathways that were not previously identified from the original methods used were searched in the set of significantly changing features by exact mass with the purpose of potentially identifying more putative metabolites. Unfortunately, this strategy did not lead to any new identifications of metabolites from these pathways. *N*-formyl kynurenine, 3-hydroxy-kynurenine, 3-hydroxy-anthranilate, quinolinic acid, picolinic acid, 5-hydroxy-tryptophan, *N*-acetylserotonin, 5-hydroxyindole-acetaldehyde, melatonin, 5-hydroxyindole-acetylglycine and 6-methoxy-indoleacetate are molecules that are part of the tryptophan metabolism pathway but were not identified these datasets. Prostaglandin G2, D2, E2, J2, arachidonic acid, and linolenic acid were metabolites from arachidonic metabolism pathway were searched by exact mass as well but not found in these data either.

2.5.2 Untargeted Quantitative Proteomics

Protein digests from colon and fecal samples were used to assess proteome coverage and verify any region-specific differences on the protein level. Pooled samples, one from each sample group (proximal colon, distal colon, proximal feces, distal feces), were first analysed with data-dependent acquisition (IDA) for protein identification purposes and served as an "*ion library*" (database) for quantitative analysis. Individual samples were injected using data-independent acquisition (SWATH) for peptide quantitation. A total of 1103 and 75 **mouse** proteins were quantified in colon and fecal samples, respectively, as shown in supplemental tables 2.12 and 2.13. The number of quantified mouse proteins in feces were much lower than colon, but this was expected due to the main composition of fecal matter being from microorganisms (Cortes *et al.*, 2019). From these results, metaproteomics was performed and the results and challenges are described following the discussion of proteins from colon tissue samples.

2.5.2.1 Protein Level Differences Between Distal and Proximal Regions in Colon Tissue

Proteins quantified in colon samples with *p-values* below 0.01 and *fold changes* of 100% were considered as significant between the distal and proximal regions. Of 1103 quantified proteins, 158 proteins were statistically significant, in which 80 and 78 proteins were shown to be increased in the distal and proximal colon, respectively. A heatmap of these proteins can be seen in Figure 2.9a, showing their relative abundances, and distinct patterns between both portions of the colon. Figure 2.9b also shows the difference in number of proteins that are increased in the distal and proximal colon that are implicated in different biological processes in which "Muscle Contraction" was shown to only be mapped from proteins that are increased in distal colon.

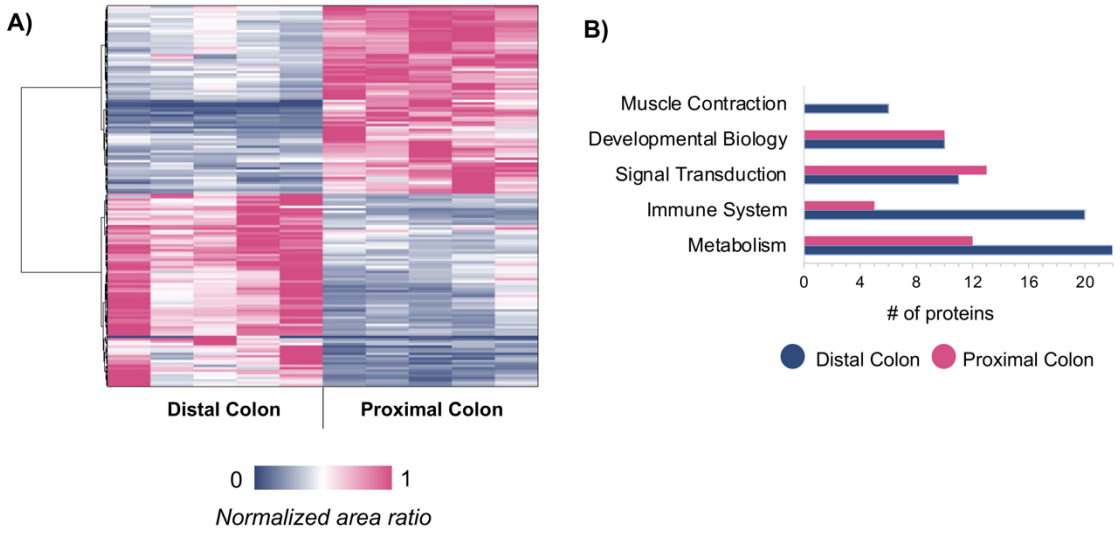

Figure 2.9 a) Heatmap with hierarchical clustering of 158 statistically significant mouse proteins from proximal and distal colon tissue, and b) the number of these proteins increased in each region involved in different pathways.

The online software Reactome was used to perform pathway analysis on these changing proteins (Fabregat *et al.*, 2017). When proteins increased in the distal region were considered, pathways involved in the immune response were enriched. As seen in Table 2.4, sixteen of these proteins are directly implicated in the innate immune system and more specifically, eleven of these are implicated in neutrophil degranulation. Neutrophils, which are a type of leukocyte, are important cells for the elimination of pathogens and invading microbes, although their activation can often

cause extensive inflammation (Lehman et Segal, 2020). These proteins could play a role in chronic inflammation found particularly in intestinal diseases that are localized in the distal colon, such as ulcerative colitis and Hirschsprung's disease (James *et al.*, 2008; Koutroubakis, 2010; Soret *et al.*, 2020). They could also be of interest for inflammatory bowel diseases that are expressed mainly in one region of the colon, using the unaffected region as a potential control. Although proteins involved in axon guidance are found in both regions (Table 2.4), this pathway has more proteins elevated in the distal region, with ten proteins compared to only five in the proximal region. Axon guidance involves an array of different cytoskeletal proteins, such as microtubules and actin filaments that make up the axon growth cone, the area at the tip of an axon that is responsible for detecting environmental cues, demonstrating that neuronal signalling in the gut could be region specific (Dent *et al.*, 2011; Russell et Bashaw, 2018). Proteins involved in keratinization were increased in the proximal colon. This is a pertinent finding as keratins tend to play an important role in the intestine even though their exact mechanisms are not clearly defined. Of the 8 keratin proteins quantified, cytoskeletal keratin type II 8, 18, 19, and 20 (K8, K18, K19, and K20) have been reported to be expressed in the intestines (Corfe *et al.*, 2015; Majumdar *et al.*, 2012; Mun *et al.*, 2022). Keratins are important filament proteins that make up the cytoskeleton allowing the cell to maintain its integrity during stress (Majumdar *et al.*, 2012; Mun *et al.*, 2022). There is growing evidence that keratins and their expression levels, as well as their mutations, correlate with several intestinal diseases such as Crohn's, ulcerative colitis and colorectal cancer, demonstrated by studies showing how mice deficient in K8 develop colonic inflammation similar to IBD (Baribault *et al.*, 1994; Habtezion *et al.*, 2005; Mun *et al.*, 2022). These results demonstrate that keratin proteins are expressed differently within the colon.

Table 2.4 Protein Pathways in Distal and Proximal Colon Regions pertaining to Immune System, Metabolism, Developmental Biology, and Muscle Contraction

	Pathway	Accession #	Protein Name	Fold Change DC/PC
Immune System	Innate: Neutrophil Degranulation	Q61598	Rab GDP dissociation inhibitor beta	3.2*
		P97430	Antileukoproteinase	4.8**
		Q91V92	ATP-citrate synthase	3.9*
		Q9CQI6	Coactosin-like protein	2.1**
		Q8BG32	26S proteasome non-ATPase regulatory	3.1*
		O08709	Peroxiredoxin-6	3**
		P13020	Gelsolin	2.8*
		P07356	Annexin A2	2.8*
		Q60854	Serpin B6	3*
		Q9D154	Leukocyte elastase inhibitor A	2.8*
		Q9Z0L8	Gamma-glutamyl hydrolase	4.4**
		P15379	CD44 antigen	-2.4**
		P09528	Ferritin heavy chain	-7.4**
	Cytokine Signalling: Signalling by Interleukins	P11983	T-complex protein 1 subunit alpha	2.3**
		P10107/P07356	Annexin A1/A2	2.2**
		Q8BG32	26S proteasome non-ATPase regulatory	3.1*
	Adaptive: TCR Signalling/Class I MHC Mediated Antigen Processing and Presentation	P62838	Ubiquitin-conjugating enzyme E2 D2	2.1*
		Q8BG32	26S proteasome non-ATPase regulatory	3.1*
	Cytokine Signalling: Interferon Signalling	Q6NZJ6	Eukaryotic translation initiation factor 4 gamma 1	-2.2**
		P62960	Nuclease-sensitive element-binding protein 1	-2.1**
		P15379	CD44 antigen	-2.4**
Metabolism	Metabolism of Carbohydrates	P21550	Beta-enolase	7.2*
		P45376	Aldose reductase	3.2**
		P16858	Glyceraldehyde-3-phosphate dehydrogenase	2.4**
		Q9JK53	Prolargin	3.1**
		Q62000	Mimecan	2.7*
		Q8R059	UDP-glucose 4-epimerase	2.2*
		P61022	Calcineurin B homologous protein 1	-2.3**
		P15379	CD44 antigen	-2.4**
	Metabolism of Lipids	P45376	Aldose reductase	3.2**
		Q91V92	ATP-citrate synthase	3.9*
		Q9D0K2	Succinyl-CoA:3-ketoacid coenzyme A transferase	2.3**
		Q91V12	Cytosolic acyl coenzyme A thioester hydrolase	2.5*
		Q9DBG5	Perilipin-3	-2.5**
		P55050	Fatty acid-binding protein, intestinal	-11.3**
	Metabolism of Amino Acids and derivatives	P62245	40S ribosomal protein S15a	2*
		P27659/P62918	60S ribosomal protein L3/L8	2.1**
		Q8BG32	26S proteasome non-ATPase regulatory	3*
		P30275	Creatine kinase U-type, mitochondrial	2.9*
		Q9DCM0	Persulfide dioxygenase ETHE1	-2.3**
	Citric Acid Cycle (TCA)	P0615/P16125	L-lactate dehydrogenase A/B chain	2.3**
		Q60932	Voltage-dependent anion-selective channel	2.4*
		P19536/P56391	Cytochrome c oxidase subunit 5B/6B1	-2.2**
		P99028	Cytochrome b-c1 complex subunit 6	-2.3**
		P52503	NADH dehydrogenase iron-sulfur protein 6	-2.3**
Developmental Biology	Axon Guidance	Q922F4	Tubulin beta-6 chain	2.3*
		Q02788	Collagen alpha-2(VI) chain	4.1*
		P62245	40S ribosomal protein S15a	2*
		Q9CVB6/P59999	Actin-related protein 2/3 complex subunit 2/ 4	2.1**
		P62962	Profilin-1	3.3**
		P27659/P62918	60S ribosomal protein L3/L8	2.1**
		Q8BG32	26S proteasome non-ATPase regulatory	3*
		Q99JY9	Actin-related protein 3	2.6*

		Q6NZJ6	Eukaryotic translation initiation factor 4 gamma 1	-2.2**
		Q6IRU5	Clathrin light chain B	-2.4**
		Q62261	Spectrin beta chain, non-erythrocytic 1	-2.2**
		Q9ES28	Rho guanine nucleotide exchange factor 7	-5.1*
		Q6URW6	Myosin-14	-4.1*
	Keratinization	P11679	Keratin, type II cytoskeletal 8	-2*
		Q9DCV7	Keratin, type II cytoskeletal 7	-2.7**
		P19001	Keratin, type I cytoskeletal 19	-2.1**
		Q9D312	Keratin, type I cytoskeletal 20	-7.5**
		P05784	Keratin, type I cytoskeletal 18	-2.9**
Muscle Contraction	Smooth Muscle Contraction	P63268	Actin, gamma-enteric smooth muscle	2.9*
		P47738	Aldehyde dehydrogenase, mitochondrial	3.2**
		P10107/P07356	Annexin A1/A2	2.2**
	Striated Muscle Contraction	P68134	Actin, alpha skeletal muscle	3.8**
		P20801	Troponin C, skeletal muscle	58.2*

p < 0.01*, p < 0.001*

2.5.3 Combining Metabolomic and Proteomic Analyses

Although individual metabolomic and proteomic analyses revealed lots of information regarding metabolites and proteins having regional specificity and clinical significance in colon tissue, a joint pathway analysis combining both types of analyses was performed as well to observe the pathways triggered from a combination of the significant proteins and metabolites. To perform this joint pathway analysis, MetaboAnalyst was used by inputting the 153 and 158 statistically significant metabolites and proteins, respectively. As shown in Figure 2.10, pathways such as pyrimidine metabolism, glycolysis/gluconeogenesis, central carbon metabolism in cancer, and bacterial evasion in epithelial cells were shown to be enriched. Amongst these pathways, pyrimidine metabolism, central carbon metabolism in cancer, cysteine/methionine metabolism, and arginine/proline metabolism were mapped from a combination of metabolites and proteins, whereas glycolysis/gluconeogenesis and bacterial evasion in epithelial cells were only mapped from proteins. A diagram showing the proteins and metabolites involved in pyrimidine metabolism are outlined in Figure 2.11, demonstrating that the metabolites and proteins that are involved are being mapped to each node/branch of the overall pathway.

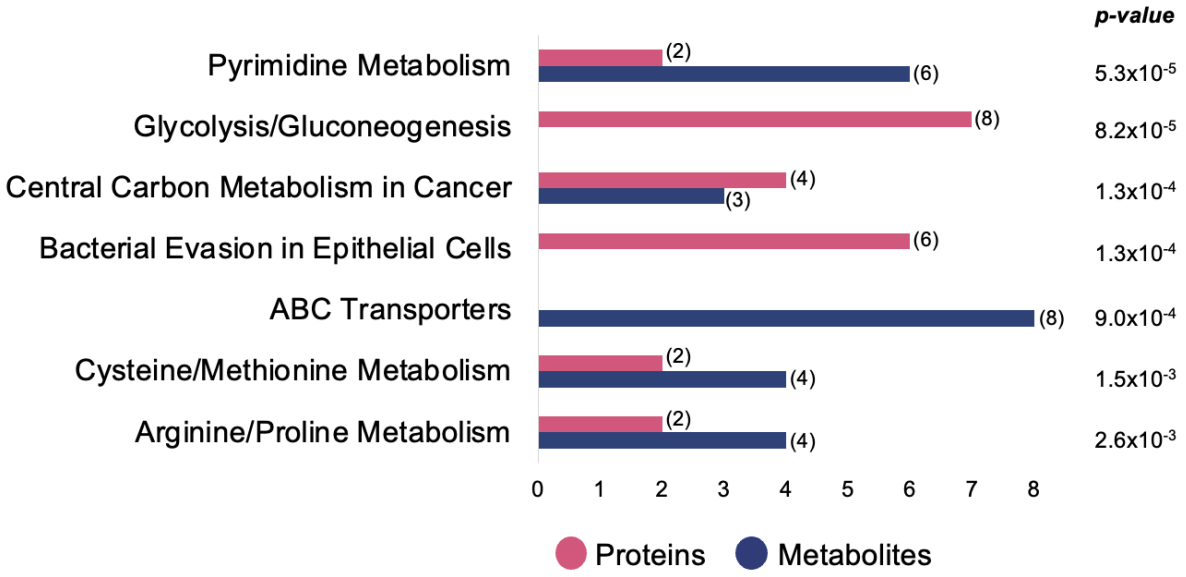

Figure 2.10 Joint pathway analysis of 153 metabolites and 158 proteins significantly changing between distal and proximal colon

Table 2.5 Metabolites and Proteins Mapped to Each Pathway from Joint Pathway Analysis

Pathway	Hits	Metabolites	Proteins (Accession #)
Arginine/Proline Metabolism	6	S-Adenosyl-L-methionine* Creatine Creatinine Sarcosine	P47738* P30275
Cysteine/Methionine Metabolism	6	5'-Methylthioadenosine; S-Adenosyl-L-methionine L-Methionine S-oxide O-phospho-l-serine	P06151* P16125*
ABC Transporters	8	l-Glutamine* l-Histidine* sn-glycerol 3 phosphate l-Phenylalanine* Adenosine Uridine* Deoxyuridine* Deoxyadenosine	
Bacterial Evasion in Epithelial Cells	6	No metabolites	Q80UG5 Q60598 P59999 Q9CVB6 Q9JLQ0 Q6IRU5
Central Carbon Metabolism in Cancer	7	l-Glutamine* Citric Acid l-Phenylalanine* l-Histidine*	P06151* P16125* P17710*
Glycolysis/Gluconeogenesis	7	No metabolites	P17710* P16858 P21550 P16125* P00329 P47738* P06151*
Pyrimidine Metabolism	8	l-Glutamine* Uridine* Thymine Beta-alanine Deoxyuridine* Orotic Acid	Q8VCE6 P23492

Within these mapped pathways, several metabolites and proteins were shown to be overlapping across almost all pathways. Although this is the case with metabolites such as glutamine, histidine, and uridine, each pathway contains some metabolites that are unique to each pathway as seen in Table 2.5. Several proteins also show the same patterns of being mapped to several pathways but when observing bacterial evasion in epithelial cells pathway, it is observed that all proteins in this pathway are unique. Regarding the *bacterial evasion in epithelial cells* pathway, the six

proteins that were mapped back to this pathway interestingly don't overlap much with pathways found from the Reactome protein pathway analysis. The only overlap observed is from the subunit 4 of *actin related protein 2/3 complex,* which mapped to axon guidance from the Reactome pathway analysis, seen in Table 2.4. Additionally, the proteins that mapped to glycolysis/gluconeogenesis correlate with other pathways found from the Reactome pathway analysis. Proteins such as *glyceraldehyde-3-dehydrogenase*, *enolase*, and *lactate dehydrogenase* also involved the metabolism of carbohydrates and the TCA cycle from the Reactome pathway analysis (Table 2.4). This crossover between glycolysis/gluconeogenesis, metabolism of carbohydrates and TCA cycle is due to the fact that glycolysis/gluconeogenesis involves the combination of metabolism of carbohydrates and the TCA cycle (Chandel, 2021). This demonstrates the benefits of using various pathway analysis tools to exploit the different results obtained. As opposed to separating proteins and metabolites based on their different expression levels in the distal/proximal colon as previously performed for the earlier pathway analyses, all statistically significant metabolites and proteins were considered when performing this analysis, as it was shown that proteins and metabolites don't necessarily always follow the same trends in expression. For example, a higher amount of a given metabolite could be the result of a low amount of a given protein and vice versa. This is shown for pyrimidine metabolism in which the metabolites are overall lower in the distal colon region, whereas the proteins quantified in this pathway are overall higher in the distal colon region as shown in Table 2.6. Separating the compounds based on their expression levels would likely lead to skewed results as well as the potential loss of information.

Table 2.6 Significant Colon Proteins and Metabolites from Pyrimidine Metabolism

Compound Type	**Compound ID**	***p*-value**	**Fold Change DC/PC**	**Column (+/-)**
Metabolite	Glutamine	9.0×10^{-3}	1.6	Scherzo (-)
	Uridine	4.0×10^{-3}	-2.1	Scherzo (-)
	Thymine	9.0×10^{-3}	-2.4	Scherzo (+)
	Beta-alanine	1.0×10^{-4}	1.7	PFP (-)
	Deoxyuridine	2.6×10^{-2}	-2.5	PFP (-)
	Orotic acid	1.3×10^{-2}	-2.5	PFP (-)
Protein	5'(3')-deoxyribonucleotidase	2.0×10^{-7}	3.2	Aeris (+)
	Purine nucleoside phosphorylase	3.0×10^{-3}	2.1	Aeris (+)

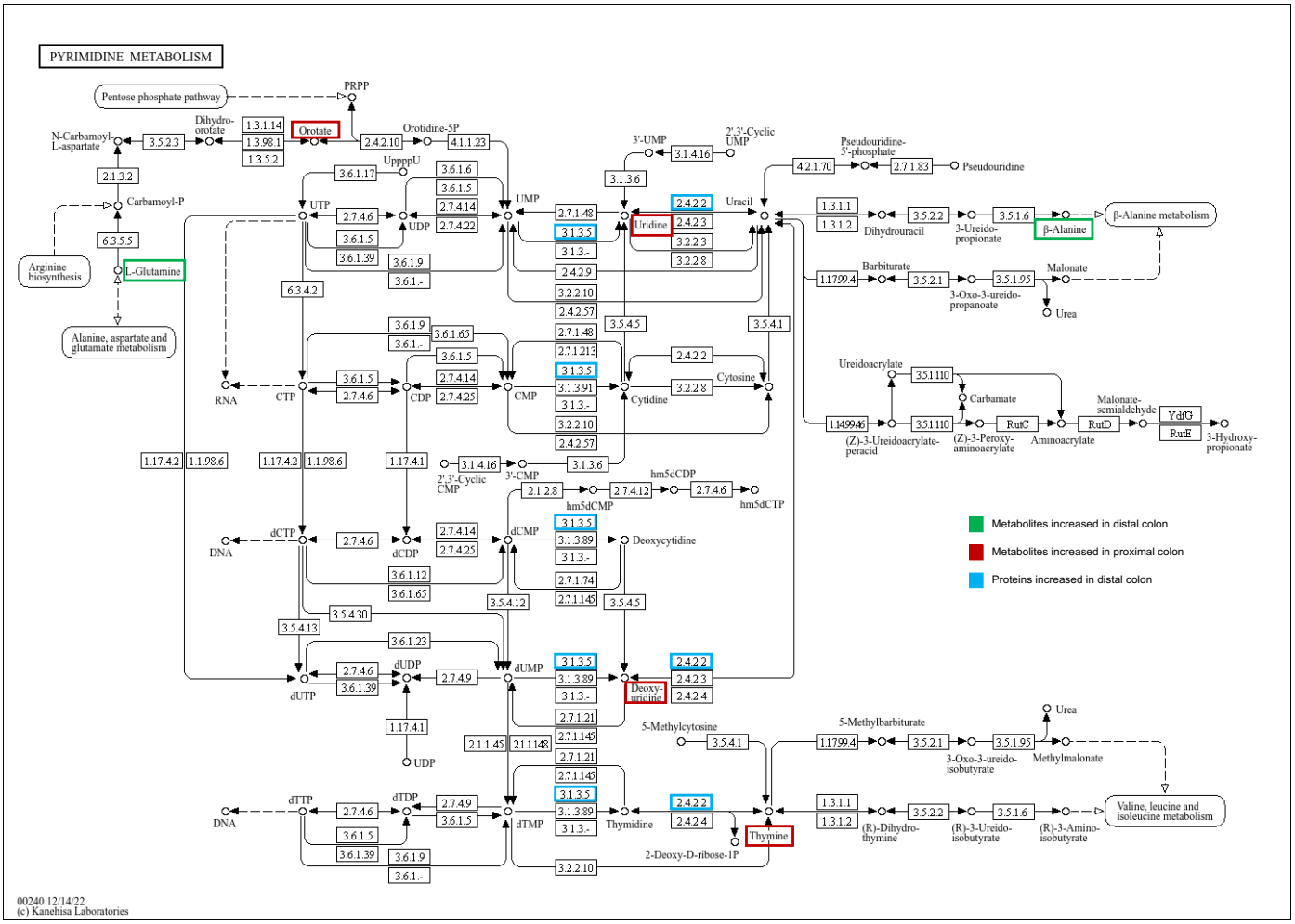

Figure 2.11 Diagram of Pyrimidine Pathway with Significant Proteins and Metabolites from Colon

2.5.4 Metaproteomics of Fecal Samples

As previously mentioned, quantifying mouse proteins in fecal samples was not very successful, due to fecal proteins originating mainly from microorganisms in the gut (Cortes *et al.*, 2019). Therefore, metaproteomics was performed to further study the microbial proteins and the species from which they originated. There are considerable challenges with performing metaproteomics, due to the high complexity of databases including all possible species. The main goal was to find which peptide signals were able to identify unique bacterial species, and thus assess the differences in these species from the two regions of the colon. Being able to identify unique bacterial species present in the respective fecal samples was only possible on the peptide level rather than the protein level. On the protein level, the same protein quantified would often come from multiple bacterial species, complicating any possible conclusions that could be made for the

distribution of bacterial species. This indicates that these bacterial species can only be distinguished by the specific unique peptide sequence of a given protein being quantified. Table 2.7 summarizes the bacterial species being identified with the associated protein and peptides from IDA acquisition. This table exemplifies how many quantified proteins are common across various bacterial species, but the peptides that were used to identify these proteins are unique.

Once peptides of interest were selected and associated to specific bacterial species (Table 2.7), individual samples analysed with SWATH acquisition were used for quantitation purposes. The fact that a peptide was uniquely identified by IDA in the sample from distal feces and not the proximal sample, does not mean that the species was found uniquely in that region, as the SWATH data confirms. From these results, it is evident that these peptides did not show regional specificity. In fact, looking at the heatmap of the resulting peptide intensities throughout the sample set (Figure 2.12), it clearly shows that there are no species clearly distinguishing distal and proximal fecal samples, which is not surprising in the context of a healthy colon without the presence of disease in a specific region.

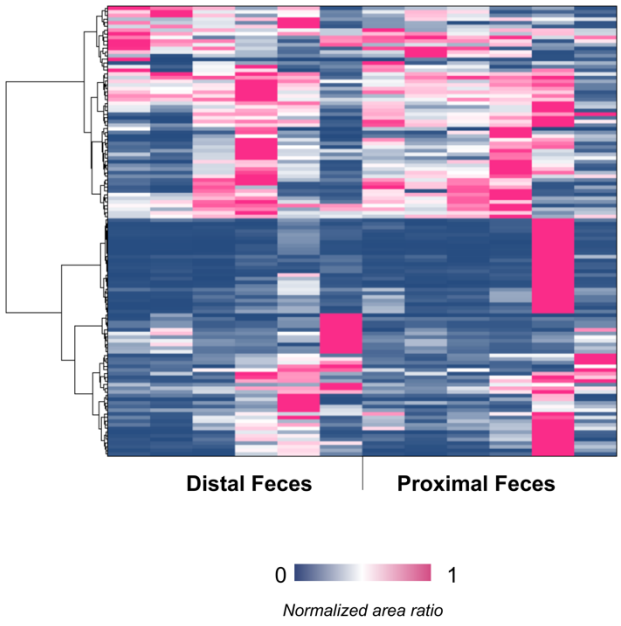

Figure 2.12 Distribution of peptides from bacterial species between distal and proximal fecal samples from SWATH quantitative analysis

The data-dependent approach selects precursors of the highest intensity for MS/MS acquisition, whereas the SWATH approach utilizes varying mass windows and all precursors within the given mass window will get fragmented for MS/MS (Li *et al.*, 2021), therefore SWATH ensures that if a peptide is detectable over a minimal signal-to-noise threshold, it can be quantified in all samples in the dataset. These results stress the fact that IDA data is not quantitative if relying of peptide identification by acquired MS/MS (Barkovits *et al.*, 2020).

Table 2.7 Bacterial Species and their Unique Peptides Identified in Distal and Proximal fecal Samples from IDA data

Species Code	Species	Protein	Peptide	ID from:
AGARV	Agathobacter rectalis	30S ribosomal protein S10	NGSQVSGPVPLPTK	DF/PF
		30S ribosomal protein S9	DIDEYLGLETLK	DF
		50S ribosomal protein L5	IVVNMGVGEAK	DF
		Chaperonin GroEL	DLVEGMQFDR	DF
			TELDLVEGMQFDR	DF
		30S ribosomal protein S19	KGPFADESLLK	PF
			STIFPSFVGH	PF
		30S ribosomal protein S3	ADIDYGFAEADTTYGK	PF
		50S ribosomal protein L15	SGAPRPGFEGGQMPL	PF
		Elongation factor Tu	CDMVDDPELI	PF
			CMPGDNVEMTI	PF
			TVVTGIEMFR	PF
ACET2	Acetivibrio thermocellus	50S ribosomal protein L1	IQNENWFEFDVV	PF
ALISL	Aliivibrio salmonicida	Multifunctional CCA protein	DLTINAIAQSDK	DF
ANAPI	Anaerotignum propionicum	Acryloyl-CoA reductase electron transfer subunit gamma	QAIDGDTAQVGPQIAEK	DF/PF
			VAVNPDGTLNR	PF
BACME	Bacillus megaterium	Sirohydrochlorin ferrochelatase	DLNEIAQLLK	DF/PF
CLOSY	Clostridium symbiosum	Pyruvate, phosphate dikinase	LAVTYPEIAK	DF/PF
			NAQGEDVVAGVR	DF/PF
			SLDQLLHPT	DF/PF
			ASMPGMMDTIL	PF
COREF*/CORGL*	Corynebacterium efficiens*/glutamicum*	NADP-specific glutamate dehydrogenase	NSLTGLPIGGGK	DF
BACLD	Bacillus licheniformis	Elongation factor Tu	LLDYAEAGDNIGALLR	PF
CYTH3	Cytophaga hutchinsonii	50S ribosomal protein L11	SFDFVVK	DF
		50S ribosomal protein L7/L12	DLVDGAPK	PF
			QLEEAGAEVEIK	PF

CLOB8	Clostridium beijerinckii	50S ribosomal protein L5	EQLIFPEIEYDKIDKV	DF/PF
			IVINMGVGEAK	DF/PF
GEOUR	Geobacter uraniireducens	Glycogen synthase	TGGLADVTAALPK	DF/PF
LACE2	Lachnospira eligens	Chaperonin GroEL	IIAEDVEGEALT	DF/PF
			LLIIAEDVEGEAL	PF
			SALQNATSVASTLL	PF
		Elongation factor Tu	ALEDPNSEWGDK	DF/PF
LACP7	Lachnoclostridium phytofermentans	30S ribosomal protein S10	LIDIIAPTQK	DF/PF
		50S ribosomal protein L23	YYDVILKPIVTEK	DF/PF
		ATP synthase subunit alpha	MNLRPEEISSVIK	DF/PF
			AIDSMVPIGR	PF
			SVDTPLQTGIK	PF
		30S ribosomal protein S10	LIDIIAPTQK	DF/PF
		30S ribosomal protein S11	ALQACGIEVTSIK	PF
		50S ribosomal protein L23	YYDVILKPIVTEK	DF/PF
		ATP synthase subunit beta	SIVELGIYPAVDPLESTSR	PF
			VVDLLCPYQK	PF
		Chaperonin GroEL	AAVEEGIIAGGGSAY	PF
			IIAEDIEGEAL	PF
			SFGAPLITNDGVTIAK	PF
			TMQTELDLVEGMQFDR	PF
		Elongation factor Tu	LLDEAQAGDNIGALLR	PF
			NKPHCNIGTI	PF
OCEIH	Oceanobacillus iheyensis	30S ribosomal protein S7	LANEILDASNNTGAAVK	DF/PF
		Ribonuclease HIII	AKTNNAVITAYQSGK	PF
PARD8	Parabacteroides distasonis	50S ribosomal protein L11	GGAANPSPPVGPALGSK	PF
		50S ribosomal protein L7/L12	QLEEAGAEVELK	DF/PF
		Phosphoenolpyruvate carboxykinase (ATP)	VINLDKESEPDIY	DF/PF
			ALVAAGPQL	DF

		Elongation factor Tu	KLLDQGEAGDNVGL	DF
			LLDQGEAGDNVGLLL	DF
			SFDSIDNAPEEK	DF
		50S ribosomal protein L2	GVVMNPVDHPMGGGEGR	DF
RUMCH	Ruminiclostridium cellulolyticum	30S ribosomal protein S9	GGGFTGQAGAIR	DF/PF
			SLDDYFGLETLK	DF/PF
		Elongation factor G	ANPVLLEPIMK	PF
BACFR	Bacteroides fragilis	Phosphoenolpyruvate carboxykinase (ATP)	FDFVVPTELPGVDPK	PF
		50S ribosomal protein L7/L12	DMVDGAPSVVK/TLEEAGAEVELK	DF
CLOPE/CLOP1/CLOPS	Clostridium perfringens	50S ribosomal protein L5	EQLIFPEIEYDKVDKV	DF/PF
			VVINMGVGEAK	DF/PF
		Phosphoglycerate kinase	CDFNVPLK	DF/PF
			MSHISTGGGASLEFLEGK	DF/PF
			STGGGASLEFLEGK	DF/PF
			SLEFLEGK	DF
CLOTE	Clostridium tetani	Triosephosphate isomerase	LVIAYEPIWAIGTGK	DF/PF
CORGL	Corynebacterium glutamicum	NADP-specific glutamate dehydrogenase	FLGFEQIFK	PF
			NSLTGLPIGGGK	DF
ECOLI	Escherichia coli	Uncharacterized ABC transporter ATP-binding protein YcjV	ALYPHMTV	PF
			DFNLEIADK	DF/PF
			MDEPLSNLDAK	DF/PF
			FVGPSGCGK	DF
PORGI*/PORG3*	Porphyromonas gingivalis	Phosphoenolpyruvate carboxykinase (ATP)	SADAFGVLPPVSILTPEQTK	PF
		30S ribosomal protein S14	EMASAGLIPGVK	DF
STRP6/STRP8/STRPQ	Streptococcus pyogenes	Glyceraldehyde-3-phosphate dehydrogenase	AGAANIVPNSTGAAK	DF/PF
			AIGLVIPELNGK	DF/PF
			NIVPNSTGAAK	DF

			TGDQMILDGPHR	DF
SPITD	Spirochaeta thermophila	Pyrophosphate--fructose 6-phosphate 1-phosphotransferase	NTGGFDIIGSGR	DF
BACTN	Bacteroides thetaiotaomicron	30S ribosomal protein S7	ALDNVTPQVEVK	DF
		Phosphoenolpyruvate carboxykinase ATP	ALVAAGPK	DF
			DFVVPTELPGVDPK	DF
			GIIDAILDGSIDK	DF
			VINLDKESEPDI	DF
PROM4	Prochlorococcus marinus	Enolase	VNQIGSLTETL	DF
SELRU	Selenomonas ruminantium	Phosphoenolpyruvate carboxykinase ATP	GVLPPVSILTPEQTK	DF
SHEAM*/SHELP*	Shewanella amazonensis/loihica	50S ribosomal protein L7/L12	ELEEAGAQVEIK	DF
SYNJB	Synechococcus sp.	50S ribosomal protein L3	LGGGRVTTRK	DF
SYNS3	Synechococcus sp.	Ketol-acid reductoisomerase NADP+	ILSDIQDGTFAK	DF
THEP3	Thermoanaerobacter pseudethanolicus	50S ribosomal protein L17	LFDEIAPK	DF
LACDB	Lactobacillus delbrueckii	Phosphoglycerate kinase	IVAALPTIK	DF
FLAJ1	Flavobacterium johnsoniae	30S ribosomal protein S8	VVEIPASNLK	DF
PSEAE	Pseudomonas aeruginosa	30S ribosomal protein S8	SMQDPLADMLTR	PF
FUSNN	Fusobacterium nucleatum subsp. nucleatum	Chaperonin GroEL	EIELEDPFENMGA	PF
			VGAATEVEMK	PF
CORDI	Corynebacterium diphtheriae	50S ribosomal protein L14	IVSLAPEVI	PF
CLOBB	Clostridium botulinum	Chaperone protein DnaK	GIPQIEVTF	PF
			IIGIDLGTTN	PF
			LGGDDFDQK	PF
SYNY3	Synechocystis sp.	Putative nickel insertion protein	VGLGAGSK	PF
LEPBP	Leptospira biflexa serovar Patoc	Elongation factor Tu	AYDQIDNAPEEK	PF
			SVVTGIEMFR	PF

LEUMM*/LEUCK*	Leuconostoc mesenteroides/citreum	Phosphoglycerate kinase	TVVWNGPMGV	PF
LISIN*/LISMO*	Listeria innocua/monocytogenes	30S ribosomal protein S9	GGGYTGQAGAIR	PF
LACLM	Lactococcus lactis subsp. Cremoris	Chaperonin GroEL	TELDVVEGMQFDR	PF
			VGSDGVITIEESK	PF
DEHMC	Dehalococcoides mccartyi	30S ribosomal protein S12	GTLDTAGVANR	PF
DICTD	Dictyoglomus turgidum	Chaperonin GroEL	EIDLEDPFENMGAQLVK	PF
CARHZ	Carboxydothermus hydrogenoformans	Formate--tetrahydrofolate ligase	AINPTPAGEGK	PF
			GGAAGGGYAQVVPMEDINLH	PF
			LILVTAINPTPAGEGK	PF
CELJU	Cellvibrio japonicus	50S ribosomal protein L3	VTVQNLEIVR	PF
CLOAB	Clostridium acetobutylicum	50S ribosomal protein L11	ATPAPPVGPALGQHGV	PF
			MPDLNAASLEAAMSMIAGTAR	PF
			TPPAAVLIK	PF

*Peptide quantified sourced back to two species of the same family

Fecal samples represent a very complex matrix, where there is the potential of high background signal being produced and consequently these background signals could get mistakenly integrated if not properly verified, and therefore this should be considered for future studies. Manual peptide verification can be employed to ensure proper peak integration and more accurate statistical analysis. Although, no major differences in bacterial species were seen when the two regions were compared in these healthy mice, the results from this metaproteomics analysis were able to provide unique peptides for 47 different bacterial species, useful for quantitative analyses in the context of microbiome dysbiosis in subsequent studies.

2.6 Conclusion

Untargeted analyses allowed for extensive metabolome and proteome coverage in colon and fecal samples from healthy mice. Statistical analysis revealed high metabolite and protein differences between the distal and proximal colon regions, and less so on the fecal level, highlighting baseline differences that can be seen between the two regions in healthy subjects. By compiling the metabolites and proteins showing regional specificity within the colon highlights certain molecular pathways of interest in future studies involving various diseases affecting the gut and can help thus further understand mechanisms involved and if distinctive regions are implicated.

Metaproteomics was performed on fecal samples with the goal of characterizing which species can be quantified using this data as well as to verify if certain bacterial species were localized preferentially in one region. Although this proved to be a great challenge, partly due to the complexity of fecal samples, bacterial identification was achieved for 47 species.

Despite the limitations and challenges presented, this study demonstrated the high heterogeneity present within the gut of healthy mice offering a better understanding of the baseline changes expected within the colon prior to the introduction of diseases. This analysis also yielded extensive characterization of the metabolome and proteome in colon and feces that will be useful for subsequent studies involving perturbations in the gut in the context of disease or nutrition.

2.7 Supplemental Tables

Table 2.8 Putative Colon Metabolite Identifications Compiled from Four Untargeted Metabolomic Datasets

Putative ID	Retention Time (min)	Chemical Formula	Found at Mass (*m/z*)	Exact Mass (*m/z*)	Mass Error (ppm)	Column (+/-)
(-)-Homoeriodictyol	14.2	C16H14O6	303.0865	303.0863	-0.6	Scherzo (+)
(-)-N-Acetylneuraminic acid	2.1	C11H19NO9	308.0992	308.0987	-1.6	PFP (-)
(-)-N-Acetylneuraminic acid	5.5	C11H19NO9	310.1147	310.1133	-4.6	Scherzo (+)
(-)-N-Acetylneuraminic acid	5.6	C11H19NO9	308.0995	308.0987	-2.6	Scherzo (-)
(-)-N-Acetylneuraminic acid	1.9	C11H19NO9	310.1136	310.1133	-1.1	PFP (+)
(-)-N-Acetylneuraminic acid	2.1	C11H19NO9	310.1141	310.1133	-2.7	PFP (+)
(-)-Quinic acid	3.4	C7H12O6	191.0561	191.0561	0.1	Scherzo (-)
(-)-Quinic acid	3.6	C7H12O6	191.0567	191.0561	-3.1	Scherzo (-)
(+-)-2-Hydroxyisocaproic acid	9.4	C6H12O3	131.0712	131.0714	1.3	PFP (-)
(+-)-2-Hydroxyisocaproic acid	9.9	C6H12O3	131.0710	131.0714	2.8	PFP (-)
(+-)-2-Hydroxyisocaproic acid	10.1	C6H12O3	131.0714	131.0714	-0.2	Scherzo (-)
(+-)7-epi-Jasmonic acid	9.6	C12H18O3	211.1326	211.1329	1.3	Scherzo (+)
(+-)7-epi-Jasmonic acid	12.3	C12H18O3	211.1328	211.1329	0.3	PFP (+)
(+)2Hydroxy3methylbutyric acid	5.7	C5H10O3	117.0557	117.0557	0.2	PFP (-)
1-(1Z-Hexadecenyl)-sn-glycero-3-phosphocholine	14.4	C24H50NO6P	480.3438	480.3449	2.2	Scherzo (+)
1-beta-D-Arabinofuranosyluracil 5'-monophosphate	2.8	C9H13N2O9P	323.0301	323.0286	-4.7	PFP (-)
1-beta-D-Arabinofuranosyluracil 5'-monophosphate	13.0	C9H13N2O9P	323.0297	323.0286	-3.4	Scherzo (-)
1-beta-D-Arabinofuranosyluracil 5'-monophosphate	2.8	C9H13N2O9P	325.0424	325.0432	2.3	PFP (+)
1-Ethyl-3-piperidinamine	2.0	C7H16N2	129.1385	129.1386	1.0	Scherzo (+)
1-Ethyl-3-piperidinamine	3.3	C7H16N2	129.1386	129.1386	0.2	PFP (+)
1-Methyl-L-histidine	1.9	C7H11N3O2	170.0922	170.0924	1.2	PFP (+)
1-Methyladenosine	2.6	C11H15N5O4	282.1202	282.1197	-1.8	Scherzo (+)
1-Methyladenosine	2.7	C11H15N5O4	282.1199	282.1197	-0.8	PFP (+)
1-Methyladenosine	6.7	C11H15N5O4	282.1206	282.1197	-3.3	Scherzo (+)
1-Methyladenosine	6.8	C11H15N5O4	282.1199	282.1197	-0.8	PFP (+)
1-Methylhistamine	2.3	C6H11N3	126.1021	126.1026	3.7	Scherzo (+)
1-Methyluric acid	7.0	C6H6N4O3	181.0369	181.0367	-1.0	Scherzo (-)
1-Methylxanthine	7.4	C6H6N4O2	167.0563	167.0564	0.3	Scherzo (+)
1-Methylxanthine	7.1	C6H6N4O2	167.0563	167.0564	0.3	PFP (+)
1-Myristoyl-2-hydroxy-sn-glycero-3-phosphoethanolamine	16.1	C19H40NO7P	426.2623	426.2615	-1.8	Scherzo (+)
1-Myristoyl-2-hydroxy-sn-glycero-3-phosphoethanolamine	16.2	C19H40NO7P	424.2472	424.2470	-0.5	Scherzo (-)
1-Myristoyl-sn-glycero-3-phosphocholine	16.6	C22H46NO7P	468.3093	468.3085	-1.8	Scherzo (+)
1-Naphthalenamine	7.8	C10H9N	144.0802	144.0808	4.0	Scherzo (+)
1-Naphthalenamine	9.4	C10H9N	144.0805	144.0808	1.9	PFP (+)
1-Oleoyl-sn-glycero-3-phosphocholine	14.9	C26H52NO7P	522.3562	522.3554	-1.5	Scherzo (+)
1-Oleoyl-sn-glycero-3-phosphoethanolamine	16.3	C23H46NO7P	478.2942	478.2939	-0.6	Scherzo (-)
1-Palmitoyl-2-hydroxy-sn-glycero-3-phosphoethanolamine	15.0	C21H44NO7P	454.2932	454.2928	-0.8	Scherzo (+)

1-Palmitoyl-2-hydroxy-sn-glycero-3-phosphoethanolamine	15.2	C21H44NO7P	452.2779	452.2783	0.8	Scherzo (-)
1-Palmitoyl-2-hydroxy-sn-glycero-3-phosphoethanolamine	17.4	C21H44NO7P	452.2779	452.2783	0.8	Scherzo (-)
1-Pentadecanoyl-sn-glycero-3-phosphocholine	17.6	C23H48NO7P	482.3248	482.3241	-1.4	PFP (+)
1,11-Undecanedicarboxylic acid	15.9	C13H24O4	243.1609	243.1602	-3.0	Scherzo (-)
1,11-Undecanedicarboxylic acid	17.8	C13H24O4	243.1604	243.1602	-0.9	PFP (-)
1,2-Dimethylimidazole	2.7	C5H8N2	97.0760	97.0760	0.2	PFP (+)
1,3-Cyclohexanedicarboxylic acid	9.5	C8H12O4	171.0662	171.0663	0.5	PFP (-)
1,3-Cyclohexanedicarboxylic acid	12.4	C8H12O4	171.0665	171.0663	-1.3	PFP (-)
1,3-Dicyclohexylurea	16.4	C13H24N2O	225.1962	225.1961	-0.3	Scherzo (+)
1,3,5-Benzenetriol	8.5	C6H6O3	127.0386	127.0390	2.9	Scherzo (+)
1,5-Diaminonaphthalene	7.8	C10H10N2	159.0916	159.0917	0.4	Scherzo (+)
1,5-Diaminonaphthalene	9.4	C10H10N2	159.0919	159.0917	-1.4	PFP (+)
1,5-Isoquinolinediol	9.4	C9H7NO2	162.0549	162.0550	0.4	Scherzo (+)
1,5-Isoquinolinediol	10.2	C9H7NO2	162.0551	162.0550	-0.9	PFP (+)
1,5-Isoquinolinediol	12.5	C9H7NO2	162.0549	162.0550	0.4	PFP (+)
10-Formyl-7,8-dihydrofolic acid	9.3	C20H21N7O7	472.1578	472.1575	-0.6	Scherzo (+)
10-Formyl-7,8-dihydrofolic acid	9.4	C20H21N7O7	470.1444	470.1430	-3.0	Scherzo (-)
10-Formyl-7,8-dihydrofolic acid	10.1	C20H21N7O7	470.1453	470.1430	-5.0	PFP (-)
10-Formyl-7,8-dihydrofolic acid	10.1	C20H21N7O7	472.1587	472.1575	-2.5	PFP (+)
10E,12Z-octadecadienoic acid	16.6	C18H32O2	281.2474	281.2475	0.4	Scherzo (+)
11(12)-Epoxy-5Z,8Z,14Z-eicosatrienoic acid	18.0	C20H32O3	319.2282	319.2279	-1.0	PFP (-)
12,13-Dihydroxy-9Z-octadecenoic acid	14.3	C18H34O4	315.2526	315.2530	1.2	Scherzo (+)
12,13-Dihydroxy-9Z-octadecenoic acid	17.1	C18H34O4	315.2534	315.2530	-1.3	Scherzo (+)
12,13-Dihydroxy-9Z-octadecenoic acid	17.9	C18H34O4	313.2380	313.2384	1.4	PFP (-)
12,13-Dihydroxy-9Z-octadecenoic acid	17.9	C18H34O4	315.2522	315.2530	2.5	PFP (+)
12(13)-Epoxy-9Z-octadecenoic acid	17.9	C18H32O3	295.2291	295.2279	-4.2	PFP (-)
12S-Hydroxy-5Z,8E,10E-heptadecatrienoic acid	17.8	C17H28O3	279.1973	279.1966	-2.6	Scherzo (-)
12S-Hydroxy-5Z,8E,10E-heptadecatrienoic acid	17.9	C17H28O3	279.1979	279.1966	-4.8	PFP (-)
13,14-Dihydro-15-ketoprostaglandin A2	15.4	C20H30O4	333.2076	333.2071	-1.4	Scherzo (-)
13,14-Dihydro-15-ketoprostaglandin A2	16.8	C20H30O4	335.2223	335.2217	-1.8	Scherzo (+)
13,14-Dihydro-15-ketoprostaglandin A2	16.8	C20H30O4	333.2080	333.2071	-2.6	Scherzo (-)
15-Deoxy-DELTA12,14-prostaglandin J2	17.1	C20H28O3	315.1969	315.1966	-1.0	Scherzo (-)
17alpha-Nandrolone	17.5	C18H26O2	275.2008	275.2006	-0.9	PFP (+)
1H-Indole-3-propanoic acid	13.6	C11H11NO2	190.0865	190.0863	-1.3	Scherzo (+)
1H-Indole-3-propanoic acid	15.8	C11H11NO2	188.0726	188.0717	-4.8	PFP (-)
1H-Indole-3-propanoic acid	15.8	C11H11NO2	190.0866	190.0863	-1.8	PFP (+)
1H-Indole-3-propanoic acid	16.5	C11H11NO2	190.0858	190.0863	2.4	PFP (+)
1H-Indole-4-carboxaldehyde	7.8	C9H7NO	146.0598	146.0600	1.6	Scherzo (+)
1H-Indole-4-carboxaldehyde	9.6	C9H7NO	146.0598	146.0600	1.6	Scherzo (+)
1H-Indole-4-carboxaldehyde	12.3	C9H7NO	146.0596	146.0600	3.0	Scherzo (+)
1H-Indole-4-carboxaldehyde	10.6	C9H7NO	146.0601	146.0600	-0.4	PFP (+)
2-Amino-1-naphthol	3.9	C10H9NO	160.0747	160.0757	6.2	Scherzo (+)
2-Amino-1-naphthol	9.2	C10H9NO	160.0757	160.0757	-0.1	Scherzo (+)

2-Amino-1-naphthol	6.1	C10H9NO	160.0757	160.0757	-0.1	PFP (+)
2-Amino-1-naphthol	9.9	C10H9NO	160.0758	160.0757	-0.7	PFP (+)
2-Aminoadipic acid	2.6	C6H11NO4	160.0620	160.0615	-2.9	Scherzo (-)
2-Aminocaprylic acid	10.5	C8H17NO2	160.1328	160.1332	2.6	PFP (+)
2-Deoxyguanosine 5-monophosphate	11.4	C10H14N5O7P	346.0564	346.0558	-1.7	Scherzo (-)
2-Deoxyribose 5-phosphate	9.5	C5H11O7P	213.0169	213.0170	0.3	Scherzo (-)
2-Dimethylamino-6-hydroxypurine	5.0	C7H9N5O	180.0874	180.0880	3.3	Scherzo (+)
2-Dimethylamino-6-hydroxypurine	7.4	C7H9N5O	180.0879	180.0880	0.5	Scherzo (+)
2-Dimethylamino-6-hydroxypurine	5.9	C7H9N5O	180.0881	180.0880	-0.6	PFP (+)
2-Dimethylamino-6-hydroxypurine	8.3	C7H9N5O	180.0884	180.0880	-2.3	PFP (+)
2-Hydroxy-3-methoxybenzoic acid	10.0	C8H8O4	167.0356	167.0350	-3.7	Scherzo (-)
2-Hydroxy-3-methoxybenzoic acid	11.6	C8H8O4	167.0348	167.0350	1.1	PFP (-)
2-Hydroxyglutaric acid	4.4	C5H8O5	147.0307	147.0299	-5.4	Scherzo (-)
2-Hydroxyibuprofen	17.3	C13H18O3	221.1187	221.1183	-1.7	PFP (-)
2-Hydroxyoctanoic acid	15.5	C8H16O3	159.1026	159.1027	0.4	PFP (-)
2-Isopropylmalic acid	8.4	C7H12O5	175.0611	175.0612	0.6	PFP (-)
2-Ketohexanoic acid	9.2	C6H10O3	129.0558	129.0557	-0.6	PFP (-)
2-Methoxybenzoic acid	10.1	C8H8O3	151.0401	151.0401	-0.2	PFP (-)
2-Methyl-3-ketovaleric acid	8.3	C6H10O3	129.0558	129.0557	-0.6	PFP (-)
2-Methylbutyryl-L-carnitine	7.3	C12H23NO4	246.1706	246.1700	-2.5	Scherzo (+)
2-Methylbutyryl-L-carnitine	10.3	C12H23NO4	246.1708	246.1700	-3.3	PFP (+)
2-Nitrophenol	13.0	C6H5NO3	138.0201	138.0197	-3.1	Scherzo (-)
2-Phenylacetamide	3.8	C8H9NO	136.0757	136.0757	-0.1	Scherzo (+)
2-Phenylacetamide	3.0	C8H9NO	136.0759	136.0757	-1.5	PFP (+)
2-Piperidinone	6.6	C5H9NO	100.0758	100.0757	-1.1	PFP (+)
2-tert-Butyl-p-quinone	17.1	C10H12O2	165.0909	165.0910	0.7	Scherzo (+)
2,2-Dimethylglutaric acid	10.4	C7H12O4	159.0667	159.0663	-2.6	Scherzo (-)
2,2-Dimethylglutaric acid	11.2	C7H12O4	159.0663	159.0663	-0.1	PFP (-)
2,3-Dihydroxybenzoic acid	8.6	C7H6O4	153.0196	153.0193	-1.8	Scherzo (-)
2,4(3H,5H)-Furandione	2.9	C4H4O3	101.0231	101.0233	2.2	PFP (+)
2,6-Di-tert-butylphenol	18.0	C14H22O	205.1597	205.1598	0.4	PFP (-)
2,6-Dihydroxybenzoic acid	14.1	C7H6O4	153.0195	153.0193	-1.1	PFP (-)
2,7,8-Trimethyl-2-(beta.-carboxyethyl)-6-hydroxychroman	17.4	C15H20O4	263.1293	263.1289	-1.6	PFP (-)
2'-Deoxyadenosine 5'-monophosphate	6.5	C10H14N5O6P	332.0753	332.0755	0.5	Scherzo (+)
2'-Deoxyadenosine 5'-monophosphate	6.5	C10H14N5O6P	330.0608	330.0609	0.3	Scherzo (-)
2'-Deoxycytidine 5'-monophosphate	3.5	C9H14N3O7P	306.0503	306.0497	-2.1	Scherzo (-)
2'-Deoxyinosine	6.2	C10H12N4O4	253.0932	253.0931	-0.3	PFP (+)
2'-O-Methyladenosine	6.2	C11H15N5O4	282.1194	282.1197	1.0	Scherzo (+)
21-Hydroxy-5 beta-pregnane-3,11,20-trione	11.6	C21H30O4	347.2226	347.2217	-2.6	Scherzo (+)
2S-Amino-4E-octadecene-1,3S-diol	14.8	C18H37NO2	300.2906	300.2897	-3.0	Scherzo (+)
2S-Amino-4E-octadecene-1,3S-diol	17.8	C18H37NO2	300.2901	300.2897	-1.3	PFP (+)
3-(2-Ethylhexoxy)propan-1-amine	11.2	C11H25NO	188.2012	188.2009	-1.6	Scherzo (+)
3-(2-Ethylhexoxy)propan-1-amine	17.1	C11H25NO	188.2011	188.2009	-1.1	PFP (+)
3-(2-Hydroxyphenyl)propionic acid	11.0	C9H10O3	165.0564	165.0557	-4.1	Scherzo (-)

3-(2-Hydroxyphenyl)propionic acid	12.4	C9H10O3	165.0561	165.0557	-2.3	PFP (-)
3-Acetamidophenol	9.5	C8H9NO2	152.0705	152.0706	0.7	Scherzo (+)
3-Acetamidophenol	9.7	C8H9NO2	150.0557	150.0561	2.3	PFP (-)
3-Acetamidophenol	9.7	C8H9NO2	152.0705	152.0706	0.7	PFP (+)
3-Acetyl-11-keto-beta-boswellic acid	17.9	C32H48O5	513.3552	513.3575	4.4	PFP (+)
3-alpha-Hydroxy-7-oxo-5beta-cholanic acid	16.4	C24H38O4	391.2844	391.2843	-0.3	Scherzo (+)
3-Cyclohexyl-1,1-dimethylurea	12.8	C9H18N2O	171.1479	171.1492	7.5	Scherzo (+)
3-Cyclohexyl-1,1-dimethylurea	13.9	C9H18N2O	171.1492	171.1492	-0.1	PFP (+)
3-Deoxy-D-glycero-D-galacto-2-nonulosonic acid	5.1	C9H16O9	267.0736	267.0722	-5.4	Scherzo (-)
3-Ethylphenol	11.0	C8H10O	121.0663	121.0659	-3.4	Scherzo (-)
3-Ethylphenol	12.4	C8H10O	121.0657	121.0659	1.6	PFP (-)
3-Furancarboxylic acid, tetrahydro-4-methylene-2-octyl-5-oxo-, (2R,3S)-	17.6	C14H22O4	253.1452	253.1445	-2.6	PFP (-)
3-Furancarboxylic acid, tetrahydro-4-methylene-2-octyl-5-oxo-, (2R,3S)-rel-	15.6	C14H22O4	253.1444	253.1445	0.5	Scherzo (-)
3-Hydroxy-3-methylglutaric acid	3.0	C6H10O5	161.0458	161.0456	-1.6	PFP (-)
3-Hydroxy-3-methylglutaric acid	3.5	C6H10O5	161.0456	161.0456	-0.3	PFP (-)
3-Hydroxy-3-methylglutaric acid	5.2	C6H10O5	161.0459	161.0456	-2.2	Scherzo (-)
3-Hydroxy-4-methoxybenzoic acid	10.0	C8H8O4	169.0495	169.0495	0.2	Scherzo (+)
3-Hydroxy-4-methoxybenzoic acid	11.6	C8H8O4	169.0496	169.0495	-0.4	PFP (+)
3-Hydroxy-4-methoxycinnamic acid	11.5	C10H10O4	195.0652	195.0652	-0.1	Scherzo (+)
3-Hydroxy-4-methoxycinnamic acid	13.9	C10H10O4	193.0509	193.0506	-1.4	PFP (-)
3-Hydroxy-4-methoxycinnamic acid	13.8	C10H10O4	195.0653	195.0652	-0.6	PFP (+)
3-Hydroxybenzaldehyde	10.4	C7H6O2	121.0300	121.0295	-4.1	Scherzo (-)
3-Hydroxybenzaldehyde	11.2	C7H6O2	121.0291	121.0295	3.3	PFP (-)
3-Hydroxybenzoic acid	9.6	C7H6O3	139.0389	139.0390	0.5	Scherzo (+)
3-Hydroxybutyrylcarnitine	2.6	C11H21NO5	248.1499	248.1493	-2.6	Scherzo (+)
3-Hydroxybutyrylcarnitine	4.2	C11H21NO5	248.1497	248.1493	-1.8	PFP (+)
3-Hydroxydodecanoic acid	17.8	C12H24O3	215.1655	215.1653	-1.1	Scherzo (-)
3-Hydroxyglutaric acid	3.9	C5H8O5	147.0301	147.0299	-1.4	Scherzo (-)
3-Hydroxyhexadecanoylcarnitine	15.3	C23H45NO5	416.3379	416.3371	-2.0	Scherzo (+)
3-Hydroxyhexadecanoylcarnitine	17.8	C23H45NO5	416.3374	416.3371	-0.8	PFP (+)
3-Hydroxyisovaleroylcarnitine	2.9	C12H23NO5	262.1646	262.1649	1.1	Scherzo (+)
3-Hydroxyisovaleroylcarnitine	3.5	C12H23NO5	262.1658	262.1649	-3.4	Scherzo (+)
3-Hydroxyisovaleroylcarnitine	6.4	C12H23NO5	262.1653	262.1649	-1.5	PFP (+)
3-Hydroxyoctanoic acid	14.6	C8H16O3	159.1027	159.1027	-0.2	PFP (-)
3-Hydroxyoleylcarnitine	15.7	C25H47NO5	442.3537	442.3527	-2.3	Scherzo (+)
3-Indoleacetic acid	12.5	C10H9NO2	176.0706	176.0706	0.1	Scherzo (+)
3-Indoleacetic acid	14.4	C10H9NO2	176.0711	176.0706	-2.8	PFP (+)
3-Indoleacetic acid	14.4	C10H9NO2	174.0558	174.0561	1.4	PFP (-)
3-Indoleacetic acid	8.4	C10H9NO2	176.0704	176.0706	1.2	PFP (+)
3-Indoleacrylic acid	7.8	C11H9NO2	188.0712	188.0706	-3.1	Scherzo (+)
3-Indoleacrylic acid	12.2	C11H9NO2	188.0706	188.0706	0.1	Scherzo (+)
3-Indoleacrylic acid	9.4	C11H9NO2	188.0710	188.0706	-2.1	PFP (+)
3-Methylindole	7.9	C9H9N	132.0802	132.0808	4.4	Scherzo (+)

3-Methylindole	9.4	C9H9N	132.0804	132.0808	2.9	PFP (+)
3-O-Methylgallic acid	8.8	C8H8O5	183.0300	183.0299	-0.5	Scherzo (-)
3-Oxocholic acid	15.1	C24H38O5	405.2644	405.2647	0.6	Scherzo (-)
3-Oxocholic acid	16.1	C24H38O5	405.2648	405.2647	-0.4	Scherzo (-)
3-Oxocholic acid	17.7	C24H38O5	405.2656	405.2647	-2.3	PFP (-)
3-Phenyllactic acid	11.6	C9H10O3	165.0562	165.0557	-2.9	PFP (-)
3-Phenyllactic acid	11.8	C9H10O3	165.0562	165.0557	-2.9	Scherzo (-)
3,3-Dimethylacrylic acid	1.9	C5H8O2	101.0595	101.0597	2.1	PFP (+)
3,4-Dihydrocoumarin	5.7	C9H8O2	149.0592	149.0597	3.4	Scherzo (+)
3,4-Dihydrocoumarin	11.0	C9H8O2	149.0599	149.0597	-1.3	Scherzo (+)
3,4-Dihydrocoumarin	12.4	C9H8O2	149.0599	149.0597	-1.3	PFP (+)
3,4-Dihydrocoumarin	15.0	C9H8O2	149.0600	149.0597	-1.9	PFP (+)
3,4-Dihydroxy-L-phenylalanine	3.9	C9H11NO4	196.0619	196.0615	-1.9	Scherzo (-)
3,4-Dimethylbenzoic acid	17.1	C9H10O2	151.0750	151.0754	2.4	PFP (+)
3,4,2',4',6'-Pentahydroxychalcone	16.7	C15H12O6	287.0568	287.0561	-2.4	PFP (-)
3,4,2',4',6'-Pentahydroxychalcone	16.6	C15H12O6	289.0706	289.0707	0.2	PFP (+)
3,4'-Dimethoxy-5,7,3'-trihydroxyflavone	14.6	C17H14O7	329.0662	329.0667	1.5	Scherzo (-)
3,4'-Dimethoxy-5,7,3'-trihydroxyflavone	17.9	C17H14O7	329.0668	329.0667	-0.4	PFP (-)
3,5-Dihydroxybenzoic acid	8.6	C7H6O4	153.0196	153.0193	-1.8	PFP (-)
3,5-Dihydroxybenzoic acid	8.5	C7H6O4	155.0337	155.0339	1.2	PFP (+)
3,5-Dimethoxy-4-hydroxycinnamic acid	11.4	C11H12O5	225.0761	225.0758	-1.6	Scherzo (+)
3,5-Dimethoxy-4-hydroxycinnamic acid	11.4	C11H12O5	223.0622	223.0612	-4.5	Scherzo (-)
3,5-Dimethoxy-4-hydroxycinnamic acid	14.2	C11H12O5	223.0617	223.0612	-2.2	PFP (-)
3,5-Dimethoxy-4-hydroxycinnamic acid	14.2	C11H12O5	225.0758	225.0758	-0.2	PFP (+)
3,7,3'-Trihydroxyflavone	12.3	C15H10O5	269.0459	269.0456	-1.3	Scherzo (-)
4-(2-Hydroxyethyl)piperazine-1-ethanesulfonic acid	3.0	C8H18N2O4S	237.0925	237.0915	-4.4	PFP (-)
4-(2-Hydroxyethyl)piperazine-1-ethanesulfonic acid	3.5	C8H18N2O4S	237.0912	237.0915	1.1	PFP (-)
4-(2-Hydroxyethyl)piperazine-1-ethanesulfonic acid	4.4	C8H18N2O4S	237.0920	237.0915	-2.3	Scherzo (-)
4-Ethoxybenzoic acid	14.1	C9H10O3	167.0700	167.0703	1.6	Scherzo (+)
4-Ethoxybenzoic acid	17.6	C9H10O3	167.0704	167.0703	-0.8	Scherzo (+)
4-Ethoxybenzoic acid	16.2	C9H10O3	167.0702	167.0703	0.4	PFP (+)
4-Hydroxy-L-glutamic acid	3.2	C5H9NO5	164.0549	164.0554	2.7	Scherzo (+)
4-Hydroxybenzaldehyde	4.0	C7H6O2	123.0442	123.0441	-1.1	Scherzo (+)
4-Hydroxybenzaldehyde	2.8	C7H6O2	123.0441	123.0441	-0.3	PFP (+)
4-Hydroxybenzaldehyde	3.0	C7H6O2	123.0440	123.0441	0.5	PFP (+)
4-Hydroxybenzaldehyde	10.1	C7H6O2	123.0438	123.0441	2.1	PFP (+)
4-Hydroxybenzoic acid	9.7	C7H6O3	137.0253	137.0244	-6.4	Scherzo (-)
4-Hydroxybenzoic acid	10.2	C7H6O3	139.0388	139.0390	1.2	PFP (+)
4-Hydroxybenzoic acid	10.3	C7H6O3	137.0245	137.0244	-0.6	PFP (-)
4-Hydroxybenzoic acid	14.8	C7H6O3	137.0245	137.0244	-0.6	PFP (-)
4-Hydroxynonenal glutathione	10.7	C19H33N3O8S	464.2076	464.2061	-3.2	Scherzo (+)
4-Hydroxynonenal glutathione	12.8	C19H33N3O8S	464.2065	464.2061	-0.8	PFP (+)
4-Imidazoleacrylic acid	2.4	C6H6N2O2	137.0355	137.0357	1.1	PFP (-)
4-Imidazoleacrylic acid	2.4	C6H6N2O2	139.0500	139.0502	1.4	PFP (+)
4-Pyridoxic acid	4.3	C8H9NO4	182.0464	182.0459	-2.9	Scherzo (-)

4-Pyridoxic acid	6.0	C8H9NO4	182.0461	182.0459	-1.2	PFP (-)
4-Pyridoxic acid	6.6	C8H9NO4	184.0606	184.0604	-0.9	Scherzo (+)
4-Pyridoxic acid	6.7	C8H9NO4	182.0466	182.0459	-4.0	Scherzo (-)
4-Pyridoxic acid	6.0	C8H9NO4	184.0603	184.0604	0.7	PFP (+)
5-(2-Hydroxyethyl)-4-methylthiazole	4.5	C6H9NOS	144.0473	144.0478	3.2	Scherzo (+)
5-(2-Hydroxyethyl)-4-methylthiazole	4.6	C6H9NOS	144.0474	144.0478	2.5	PFP (+)
5-alpha-Pregnan-3alpha-ol-11,20-dione	12.3	C21H32O3	333.2429	333.2424	-1.4	Scherzo (+)
5-Amino-1-beta-D-ribofuranosyl-1H-imidazole-4-carboxamide	3.6	C9H14N4O5	259.1041	259.1037	-1.5	Scherzo (+)
5-Aminovaleric acid	1.9	C5H11NO2	118.0863	118.0863	-0.3	PFP (+)
5-Hydroxy-6E,8Z,11Z,14Z-eicosatetraenoic acid, 1,5-lactone	17.9	C20H30O2	303.2324	303.2319	-1.8	PFP (+)
5-Hydroxyindole-3-acetic acid	10.5	C10H9NO3	192.0657	192.0655	-0.9	Scherzo (+)
5-Hydroxyindole-3-acetic acid	10.5	C10H9NO3	190.0518	190.0510	-4.4	Scherzo (-)
5-Hydroxyindole-3-acetic acid	10.7	C10H9NO3	190.0515	190.0510	-2.8	PFP (-)
5-Hydroxyindole-3-acetic acid	11.3	C10H9NO3	190.0516	190.0510	-3.3	PFP (-)
5-Hydroxyindole-3-acetic acid	11.3	C10H9NO3	192.0660	192.0655	-2.5	PFP (+)
5-Hydroxyindole-3-acetic acid	11.7	C10H9NO3	192.0657	192.0655	-0.9	PFP (+)
5-Hydroxyindoleacetic acid	9.6	C10H9NO3	192.0655	192.0655	0.1	Scherzo (+)
5-Hydroxyindoleacetic acid	10.6	C10H9NO3	192.0660	192.0655	-2.5	PFP (+)
5-Hydroxyisovanillic acid	9.8	C8H8O5	183.0303	183.0299	-2.2	PFP (-)
5-Hydroxylysine	1.9	C6H14N2O3	163.1074	163.1077	2.0	Scherzo (+)
5-Hydroxytryptophol	9.2	C10H11NO2	178.0860	178.0863	1.5	Scherzo (+)
5-Hydroxytryptophol	9.9	C10H11NO2	178.0865	178.0863	-1.3	PFP (+)
5-Isoprostaglandin-F2 alpha VI	13.9	C20H34O5	353.2329	353.2334	1.3	Scherzo (-)
5-Isoprostaglandin-F2 alpha VI	14.4	C20H34O5	353.2336	353.2334	-0.7	Scherzo (-)
5-Isoprostaglandin-F2 alpha VI	17.1	C20H34O5	353.2333	353.2334	0.1	PFP (-)
5-Keto-D-gluconic acid	4.0	C6H10O7	193.0363	193.0354	-4.8	Scherzo (-)
5-Methyltetrahydrofolic acid	7.1	C20H25N7O6	460.1951	460.1939	-2.6	Scherzo (+)
5-Methyltetrahydrofolic acid	7.2	C20H25N7O6	458.1801	458.1794	-1.6	Scherzo (-)
5-Methyltetrahydrofolic acid	8.6	C20H25N7O6	458.1811	458.1794	-3.8	PFP (-)
5-Methyltetrahydrofolic acid	8.6	C20H25N7O6	460.1947	460.1939	-1.7	PFP (+)
5-Thymidylic acid	4.0	C10H15N2O8P	321.0496	321.0493	-0.8	PFP (-)
5'-S-Methyl-5'-thioadenosine	7.5	C11H15N5O3S	298.0972	298.0968	-1.2	Scherzo (+)
5'-S-Methyl-5'-thioadenosine	2.4	C11H15N5O3S	298.0969	298.0968	-0.2	PFP (+)
5'-S-Methyl-5'-thioadenosine	8.7	C11H15N5O3S	298.0974	298.0968	-1.9	PFP (+)
6,7,4'-Trihydroxyisoflavone	15.5	C15H10O5	271.0602	271.0601	-0.4	PFP (+)
7-Keto-3-alpha,12-alpha-dihydroxycholanic acid	13.3	C24H38O5	407.2790	407.2792	0.5	Scherzo (+)
7-Keto-3-alpha,12-alpha-dihydroxycholanic acid	14.6	C24H38O5	407.2788	407.2792	1.0	Scherzo (+)
7-Methylguanine	2.9	C6H7N5O	166.0714	166.0723	5.7	PFP (+)
7-Methylguanine	3.5	C6H7N5O	166.0725	166.0723	-1.0	Scherzo (+)
7-Methylguanosine	7.0	C11H15N5O5	298.1157	298.1146	-3.7	Scherzo (+)
7-Methylguanosine	7.1	C11H15N5O5	298.1151	298.1146	-1.7	PFP (+)
7,8-Dehydropregnenolone	12.3	C21H30O2	315.2326	315.2319	-2.3	Scherzo (+)
7,8-Dihydro-L-Biopterin	3.0	C9H13N5O3	240.1085	240.1091	2.6	PFP (+)

7,8-Dimethoxycoumarin	11.4	C11H10O4	207.0652	207.0652	0.0	Scherzo (+)
7,8-Dimethoxycoumarin	14.2	C11H10O4	207.0655	207.0652	-1.5	PFP (+)
8-Hydroxyquinoline-5-carboxylic acid	10.6	C10H7NO3	188.0357	188.0353	-2.0	PFP (-)
8-Hydroxyquinoline-5-carboxylic acid	11.8	C10H7NO3	188.0361	188.0353	-4.1	PFP (-)
8-Hydroxyquinoline-5-carboxylic acid	17.1	C10H7NO3	188.0356	188.0353	-1.5	Scherzo (-)
8-iso-Prostaglandin A1	14.8	C20H32O4	335.2229	335.2228	-0.4	Scherzo (-)
9-Oxoprosta-5Z,10,12Z,14E-tetraenoic acid	16.1	C20H28O3	317.2119	317.2111	-2.5	Scherzo (+)
9-Oxoprosta-5Z,10,12Z,14E-tetraenoic acid	17.8	C20H28O3	317.2118	317.2111	-2.1	PFP (+)
9,10-Dihydroxy-12Z-octadecenoic acid	16.9	C18H34O4	315.2521	315.2530	2.8	Scherzo (+)
9(10)-Epoxy-12Z-octadecenoic acid	16.9	C18H32O3	297.2429	297.2424	-1.6	Scherzo (+)
Acetyl-L-carnitine	2.5	C9H17NO4	204.1234	204.1230	-1.8	Scherzo (+)
Acetyl-L-carnitine	2.9	C9H17NO4	204.1233	204.1230	-1.3	PFP (+)
Acetyl-L-carnitine	3.8	C9H17NO4	204.1234	204.1230	-1.8	PFP (+)
Acetyl-L-Threonine	2.5	C6H11NO4	160.0619	160.0615	-2.3	PFP (-)
Acetyl-L-Threonine	4.6	C6H11NO4	160.0623	160.0615	-4.8	Scherzo (-)
Acetyl-L-Threonine	4.7	C6H11NO4	162.0759	162.0761	1.1	Scherzo (+)
Acetylcysteine	17.7	C5H9NO3S	162.0227	162.0230	2.1	PFP (-)
Adenine	2.3	C5H5N5	136.0618	136.0618	-0.2	PFP (+)
Adenine	2.5	C5H5N5	136.0613	136.0618	3.5	Scherzo (+)
Adenine	4.0	C5H5N5	136.0618	136.0618	-0.2	PFP (+)
Adenine	4.0	C5H5N5	134.0471	134.0472	0.9	PFP (-)
Adenine	7.1	C5H5N5	136.0620	136.0618	-1.7	PFP (+)
Adenine	7.4	C5H5N5	136.0614	136.0618	2.7	Scherzo (+)
Adenine	7.9	C5H5N5	136.0618	136.0618	-0.2	PFP (+)
Adenosine	4.0	C10H13N5O4	268.1051	268.1040	-4.0	PFP (+)
Adenosine	4.0	C10H13N5O4	266.0906	266.0895	-4.2	PFP (-)
Adenosine	4.1	C10H13N5O4	268.1044	268.1040	-1.4	Scherzo (+)
Adenosine	7.4	C10H13N5O4	268.1037	268.1040	1.2	Scherzo (+)
Adenosine	7.8	C10H13N5O4	268.1041	268.1040	-0.3	PFP (+)
Adenosine 2'-monophosphate	7.4	C10H14N5O7P	348.0702	348.0704	0.5	Scherzo (+)
Adenosine 2'-monophosphate	7.9	C10H14N5O7P	348.0718	348.0704	-4.1	Scherzo (+)
Adenosine 2'-monophosphate	4.9	C10H14N5O7P	348.0706	348.0704	-0.7	PFP (+)
Adenosine 3'-monophosphate	3.4	C10H14N5O7P	346.0569	346.0558	-3.1	PFP (-)
Adenosine 3'-monophosphate	7.5	C10H14N5O7P	346.0563	346.0558	-1.4	Scherzo (-)
Adenosine 3'-monophosphate	3.5	C10H14N5O7P	348.0703	348.0704	0.2	PFP (+)
Adenosine 5-monophosphate	2.4	C10H14N5O7P	346.0571	346.0558	-3.7	PFP (-)
Adenosine 5-monophosphate	2.5	C10H14N5O7P	348.0708	348.0704	-1.3	PFP (+)
Adenosine 5-monophosphate	3.0	C10H14N5O7P	348.0705	348.0704	-0.4	PFP (+)
Adenosine 5-monophosphate	5.1	C10H14N5O7P	348.0711	348.0704	-2.1	Scherzo (+)
Adenosine 5-monophosphate	5.2	C10H14N5O7P	346.0566	346.0558	-2.3	Scherzo (-)
Adenosine 5-monophosphate	7.9	C10H14N5O7P	348.0695	348.0704	2.5	PFP (+)
Adenosine 5-monophosphate	12.8	C10H14N5O7P	348.0710	348.0704	-1.8	PFP (+)
Adenylosuccinic acid	6.8	C14H18N5O11P	462.0687	462.0668	-4.2	PFP (-)
Adenylosuccinic acid	7.4	C14H18N5O11P	462.0683	462.0668	-3.3	PFP (-)
Adenylyl (3'-5')cytidine	6.7	C19H25N8O11P	573.1470	573.1453	-2.9	Scherzo (+)

Adenylyl (3'-5')cytidine	6.8	C19H25N8O11P	571.1317	571.1308	-1.6	Scherzo (-)
Adenylyl (3'-5')cytidine	7.1	C19H25N8O11P	571.1343	571.1308	-6.2	PFP (-)
Adenylyl (3'-5')cytidine	7.1	C19H25N8O11P	573.1462	573.1453	-1.5	PFP (+)
Adipic acid	7.5	C6H10O4	145.0512	145.0506	-3.9	PFP (-)
Alanine	2.9	C3H7NO2	88.0405	88.0404	-1.1	PFP (-)
Allantoin	2.8	C4H6N4O3	157.0366	157.0367	0.7	Scherzo (-)
Allose	2.6	C6H12O6	179.0564	179.0561	-1.6	Scherzo (-)
alpha-D-Galactose 1-phosphate	2.2	C6H13O9P	259.0235	259.0224	-4.1	PFP (-)
alpha-D-Glucose 1,6-bisphosphate	2.6	C6H14O12P2	338.9887	338.9888	0.2	PFP (-)
alpha-L-Glu-L-Tyr	7.6	C14H18N2O6	311.1248	311.1238	-3.3	Scherzo (+)
alpha-L-Glu-L-Tyr	7.3	C14H18N2O6	311.1246	311.1238	-2.7	PFP (+)
Alpha-Linolenic acid	17.9	C18H30O2	279.2324	279.2319	-1.9	PFP (+)
Amino caproic acid	8.3	C6H13NO2	132.1013	132.1019	4.6	PFP (+)
Apigenin 7-glucoside	14.5	C21H20O10	433.1124	433.1129	1.2	PFP (+)
Arabinonic acid	1.9	C5H10O6	165.0408	165.0405	-2.1	PFP (-)
Arabinonic acid	2.8	C5H10O6	165.0409	165.0405	-2.7	Scherzo (-)
Arabinonic acid	3.3	C5H10O6	165.0413	165.0405	-5.1	Scherzo (-)
Arabitol	2.7	C5H12O5	151.0624	151.0612	-7.9	Scherzo (-)
Arginine	2.2	C6H14N4O2	173.1052	173.1044	-4.6	Scherzo (-)
Arginine	2.5	C6H14N4O2	175.1191	175.1190	-0.9	Scherzo (+)
Arginine	1.9	C6H14N4O2	175.1189	175.1190	0.3	PFP (+)
Argininosuccinic acid	1.9	C10H18N4O6	291.1302	291.1299	-1.0	PFP (+)
Argininosuccinic acid	2.4	C10H18N4O6	289.1160	289.1154	-2.2	Scherzo (-)
Argininosuccinic acid	2.5	C10H18N4O6	291.1306	291.1299	-2.4	Scherzo (+)
Arsenic acid	7.1	AsH3O4	140.9175	140.9175	-0.4	Scherzo (-)
Asiatic acid	17.9	C30H48O5	487.3440	487.3429	-2.3	PFP (-)
Asp-Pro	3.1	C9H14N2O5	231.0981	231.0976	-2.4	Scherzo (+)
Asparagine	2.4	C4H8N2O3	131.0468	131.0462	-4.4	Scherzo (-)
Aspartic acid	1.9	C4H7NO4	132.0303	132.0302	-0.5	PFP (-)
Aspartic acid	2.7	C4H7NO4	134.0445	134.0448	2.1	Scherzo (+)
Aspartic acid	2.8	C4H7NO4	132.0310	132.0302	-5.8	Scherzo (-)
Aspartic acid	3.2	C4H7NO4	134.0449	134.0448	-0.9	Scherzo (+)
Azelaic acid	11.9	C9H16O4	189.1125	189.1121	-1.9	Scherzo (+)
Azelaic acid	11.9	C9H16O4	187.0986	187.0976	-5.5	Scherzo (-)
Azelaic acid	14.3	C9H16O4	189.1123	189.1121	-0.8	PFP (+)
Azelaic acid	14.3	C9H16O4	187.0982	187.0976	-3.3	PFP (-)
Baicalin	13.8	C21H18O11	445.0770	445.0776	1.4	Scherzo (-)
Baicalin	13.9	C21H18O11	447.0922	447.0922	0.0	Scherzo (+)
Baicalin	14.7	C21H18O11	445.0783	445.0776	-1.5	PFP (-)
Benzanilide	15.4	C13H11NO	198.0915	198.0913	-0.8	Scherzo (+)
Benzoic acid ethyl ester	15.0	C9H10O2	151.0752	151.0754	1.1	Scherzo (+)
Benzophenone	17.3	C13H10O	183.0807	183.0804	-1.4	Scherzo (+)
Benzophenone	17.8	C13H10O	183.0805	183.0804	-0.3	PFP (+)
Beta-Alanine	2.0	C3H7NO2	88.0403	88.0404	1.1	PFP (-)
beta-L-Fucose 1-phosphate	9.6	C6H13O8P	243.0281	243.0275	-2.3	Scherzo (-)

beta-Muricholic acid	15.3	C24H40O5	407.2798	407.2803	1.2	Scherzo (-)
beta-Nicotinamide adenine dinucleotide	3.0	C21H27N7O14P2	664.1169	664.1164	-0.8	PFP (+)
Betaine	2.5	C5H11NO2	118.0864	118.0863	-1.2	PFP (+)
Bicyclo-prostaglandin E2	15.3	C20H30O4	335.2226	335.2217	-2.7	Scherzo (+)
Biliverdin	14.8	C33H34N4O6	583.2556	583.2551	-0.8	Scherzo (+)
Biotin	9.9	C10H16N2O3S	245.0962	245.0954	-3.1	Scherzo (+)
Blood Group A Trisaccharide	2.7	C20H35NO15	530.2093	530.2080	-2.5	Scherzo (+)
Butein	2.9	C15H12O5	271.0587	271.0612	9.2	PFP (-)
Butyric acid	5.6	C4H8O2	87.0451	87.0452	0.6	PFP (-)
Butyrylcarnitine	4.5	C11H21NO4	232.1550	232.1543	-2.9	Scherzo (+)
Butyrylcarnitine	5.0	C11H21NO4	232.1550	232.1543	-2.9	Scherzo (+)
Butyrylcarnitine	8.5	C11H21NO4	232.1551	232.1543	-3.3	PFP (+)
Caffeic acid	10.1	C9H8O4	179.0360	179.0350	-5.7	Scherzo (-)
Caffeic acid	11.7	C9H8O4	179.0351	179.0350	-0.7	PFP (-)
Capric acid	17.9	C10H20O2	171.1388	171.1391	1.5	PFP (-)
Carbofuran phenol-3-ketone	11.4	C10H10O3	179.0698	179.0703	2.6	PFP (+)
Carnitine	2.0	C7H15NO3	162.1126	162.1125	-0.8	PFP (+)
Carnitine	2.4	C7H15NO3	162.1126	162.1125	-0.8	Scherzo (+)
Carnosine	1.9	C9H14N4O3	227.1142	227.1139	-1.5	PFP (+)
Carnosine	2.5	C9H14N4O3	225.0990	225.0993	1.4	Scherzo (-)
Cholic acid	17.9	C24H40O5	407.2816	407.2803	-3.2	PFP (-)
Chrysoeriol	14.7	C16H12O6	299.0566	299.0561	-1.6	Scherzo (-)
cis-Aconitate	4.3	C6H6O6	173.0096	173.0092	-2.5	PFP (-)
cis-cinnamic acid	5.2	C9H8O2	147.0448	147.0452	2.4	PFP (-)
cis-Jasmone	14.2	C11H16O	165.1275	165.1274	-0.7	Scherzo (+)
Citraconic acid	4.3	C5H6O4	129.0188	129.0193	4.1	PFP (-)
Citric acid	2.4	C6H8O7	191.0203	191.0197	-3.0	PFP (-)
Citric acid	2.9	C6H8O7	191.0198	191.0197	-0.4	Scherzo (-)
Citric acid	3.0	C6H8O7	191.0203	191.0197	-3.0	PFP (-)
Citric acid	5.8	C6H8O7	191.0202	191.0197	-2.5	Scherzo (-)
Citric acid	7.0	C6H8O7	191.0204	191.0197	-3.5	Scherzo (-)
Citric acid	7.4	C6H8O7	193.0339	193.0343	2.0	Scherzo (+)
Citric acid	9.1	C6H8O7	191.0202	191.0197	-2.5	Scherzo (-)
Citrulline	2.5	C6H13N3O3	176.1031	176.1030	-0.7	Scherzo (+)
Citrulline	2.5	C6H13N3O3	174.0891	174.0884	-3.9	Scherzo (-)
Corticosterone	13.4	C21H30O4	347.2209	347.2217	2.3	Scherzo (+)
Corticosterone	14.6	C21H30O4	347.2219	347.2217	-0.6	Scherzo (+)
Corticosterone	14.8	C21H30O4	347.2222	347.2217	-1.5	PFP (+)
Coumarin	3.9	C9H6O2	147.0438	147.0441	1.8	Scherzo (+)
Creatine	2.0	C4H9N3O2	132.0768	132.0768	-0.4	PFP (+)
Creatine	2.5	C4H9N3O2	132.0768	132.0768	-0.4	Scherzo (+)
Creatine phosphate	7.4	C4H10N3O5P	212.0431	212.0431	0.0	Scherzo (+)
Creatinine	1.9	C4H7N3O	114.0660	114.0662	1.7	PFP (+)
Cyclic adenosine diphosphate ribose	3.0	C15H21N5O13P2	540.0529	540.0538	1.7	PFP (-)
Cyclic adenosine diphosphate ribose	5.8	C15H21N5O13P2	540.0538	540.0538	0.1	Scherzo (-)

Cyclic GMP	6.0	C10H12N5O7P	344.0417	344.0402	-4.5	PFP (-)
Cystathionine	2.5	C7H14N2O4S	223.0748	223.0747	-0.4	Scherzo (+)
Cysteine S-sulfate	8.7	C3H7NO5S2	199.9697	199.9693	-2.1	Scherzo (-)
Cysteine-glutathione disulfide	1.9	C13H22N4O8S2	425.0826	425.0806	-4.6	PFP (-)
Cysteine-glutathione disulfide	3.1	C13H22N4O8S2	427.0960	427.0952	-1.9	Scherzo (+)
Cysteine-glutathione disulfide	3.1	C13H22N4O8S2	425.0808	425.0806	-0.4	Scherzo (-)
Cysteine-glutathione disulfide	6.3	C13H22N4O8S2	427.0962	427.0952	-2.4	Scherzo (+)
Cysteine-glutathione disulfide	1.9	C13H22N4O8S2	427.0959	427.0952	-1.7	PFP (+)
Cytidine	2.3	C9H13N3O5	244.0931	244.0928	-1.2	Scherzo (+)
Cytidine	2.6	C9H13N3O5	244.0931	244.0928	-1.2	Scherzo (+)
Cytidine	2.0	C9H13N3O5	244.0929	244.0928	-0.4	PFP (+)
Cytidine 2',3'-cyclic monophosphoric acid	3.6	C9H12N3O7P	306.0489	306.0486	-1.1	Scherzo (+)
Cytidine 2',3'-cyclic monophosphoric acid	3.6	C9H12N3O7P	304.0347	304.0340	-2.3	Scherzo (-)
Cytidine 2',3'-cyclic monophosphoric acid	6.2	C9H12N3O7P	306.0498	306.0486	-4.1	Scherzo (+)
Cytidine 3'-monophosphate	2.0	C9H14N3O8P	322.0461	322.0446	-4.7	PFP (-)
Cytidine 3'-monophosphate	2.8	C9H14N3O8P	322.0450	322.0446	-1.3	Scherzo (-)
Cytidine 3'-monophosphate	3.6	C9H14N3O8P	322.0451	322.0446	-1.6	Scherzo (-)
Cytidine 5'-diphosphate ethanolamine	3.1	C11H20N4O11P2	445.0537	445.0531	-1.3	Scherzo (-)
Cytidine 5'-diphosphocholine	2.9	C14H26N4O11P2	489.1152	489.1146	-1.2	Scherzo (+)
Cytidine 5'-diphosphocholine	3.5	C14H26N4O11P2	489.1145	489.1146	0.2	Scherzo (+)
Cytidine 5'-diphosphocholine	2.9	C14H26N4O11P2	489.1152	489.1146	-1.2	PFP (+)
Cytidine monophosphate	2.0	C9H14N3O8P	324.0598	324.0591	-2.1	PFP (+)
Cytidine monophosphate	2.3	C9H14N3O8P	324.0598	324.0591	-2.1	PFP (+)
Cytidine monophosphate	3.2	C9H14N3O8P	324.0600	324.0591	-2.7	Scherzo (+)
Cytidine monophosphate	3.6	C9H14N3O8P	324.0600	324.0591	-2.7	Scherzo (+)
Cytidine monophosphate	6.6	C9H14N3O8P	324.0603	324.0591	-3.6	Scherzo (+)
Cytidine monophosphate	6.7	C9H14N3O8P	324.0586	324.0591	1.6	Scherzo (+)
Cytidine-5'-monophospho-N-acetylneuraminic acid	6.5	C20H31N4O16P	613.1409	613.1400	-1.5	Scherzo (-)
Cytosine	2.0	C4H5N3O	112.0506	112.0505	-0.5	PFP (+)
Cytosine	3.0	C4H5N3O	112.0503	112.0505	2.1	PFP (+)
Cytosine	7.1	C4H5N3O	112.0509	112.0505	-3.2	PFP (+)
Daidzein	13.1	C15H10O4	253.0514	253.0506	-3.0	Scherzo (-)
Daidzein	13.2	C15H10O4	255.0661	255.0652	-3.6	Scherzo (+)
Daidzein	16.3	C15H10O4	255.0656	255.0652	-1.6	PFP (+)
Daidzein	16.3	C15H10O4	253.0514	253.0506	-3.0	PFP (-)
Daidzein 4'-sulfate	16.3	C15H10O7S	333.0078	333.0075	-1.1	PFP (-)
Daidzin	10.3	C21H20O9	417.1188	417.1180	-1.9	Scherzo (+)
Daidzin	12.9	C21H20O9	417.1189	417.1180	-2.1	PFP (+)
Decamethylcyclopentasiloxane	1.8	C10H30O5Si5	371.1006	371.1012	1.7	Scherzo (+)
Dehydroascorbic acid	2.4	C6H6O6	173.0094	173.0092	-1.4	PFP (-)
Dehydroascorbic acid	2.7	C6H6O6	173.0093	173.0092	-0.8	PFP (-)
Dehydroascorbic acid	4.7	C6H6O6	173.0103	173.0092	-6.6	Scherzo (-)
Delta-Hexanolactone	8.8	C6H10O2	115.0754	115.0754	-0.3	PFP (+)
DELTA17-6-Ketoprostaglandin F1alpha	12.3	C20H32O6	367.2131	367.2126	-1.3	Scherzo (-)
Deoxyadenosine	4.4	C10H13N5O3	252.1096	252.1091	-1.9	Scherzo (+)

Deoxyguanosine	6.2	C10H13N5O4	268.1033	268.1040	2.7	PFP (+)
Deoxyguanosine	6.2	C10H13N5O4	266.0904	266.0895	-3.5	PFP (-)
Deoxyguanosine	6.6	C10H13N5O4	268.1047	268.1040	-2.5	Scherzo (+)
Deoxyguanosine	6.7	C10H13N5O4	266.0904	266.0895	-3.5	Scherzo (-)
Deoxyinosine	6.2	C10H12N4O4	251.0796	251.0786	-4.1	PFP (-)
Deoxyinosine	6.7	C10H12N4O4	251.0795	251.0786	-3.7	Scherzo (-)
Deoxyuridine	4.3	C9H12N2O5	227.0673	227.0674	0.2	PFP (-)
Deoxyuridine	5.3	C9H12N2O5	227.0669	227.0674	2.0	Scherzo (-)
Diethyl phthalate	16.0	C12H14O4	223.0960	223.0965	2.2	Scherzo (+)
Diethyltoluamide	15.2	C12H17NO	192.1380	192.1383	1.5	Scherzo (+)
Dihydrodaidzein	13.0	C15H12O4	257.0810	257.0808	-0.6	Scherzo (+)
Dihydrodaidzein	13.1	C15H12O4	255.0669	255.0663	-2.4	Scherzo (-)
Dihydrodaidzein	15.7	C15H12O4	255.0672	255.0663	-3.6	PFP (-)
Dihydrodaidzein	15.6	C15H12O4	257.0812	257.0808	-1.4	PFP (+)
Dihydrofolic acid	9.7	C19H21N7O6	442.1480	442.1481	0.1	Scherzo (-)
Dihydrofolic acid	11.4	C19H21N7O6	442.1510	442.1481	-6.6	PFP (-)
Dihydroisoferulic acid	13.5	C10H12O4	195.0666	195.0663	-1.6	PFP (-)
Dimethyl arginine	2.0	C8H18N4O2	203.1504	203.1503	-0.7	PFP (+)
Dimethyl arginine	2.4	C8H18N4O2	203.1498	203.1503	2.2	Scherzo (+)
Dimethylaminopurine	4.5	C7H9N5	164.0926	164.0931	2.9	Scherzo (+)
Dimethylaminopurine	6.3	C7H9N5	164.0929	164.0931	1.0	PFP (+)
Dimethylglycine	1.9	C4H9NO2	102.0555	102.0561	5.4	PFP (-)
Dimethylmalonic acid	7.1	C5H8O4	131.0350	131.0350	-0.2	Scherzo (-)
Diosmetin	14.7	C16H12O6	301.0710	301.0707	-1.1	Scherzo (+)
Dodecanedioic acid	14.7	C12H22O4	229.1452	229.1445	-2.9	Scherzo (-)
Dodecanedioic acid	17.5	C12H22O4	229.1451	229.1445	-2.5	PFP (-)
Dodecyl sulfate	17.6	C12H26O4S	265.1484	265.1479	-1.9	PFP (-)
Emodin	15.5	C15H10O5	269.0457	269.0456	-0.6	PFP (-)
Enterolactone	11.7	C18H18O4	299.1281	299.1278	-1.0	Scherzo (+)
Enterolactone	14.3	C18H18O4	299.1283	299.1278	-1.7	Scherzo (+)
Enterolactone	16.5	C18H18O4	299.1282	299.1278	-1.4	PFP (+)
Equol	14.3	C15H14O3	243.1023	243.1016	-3.0	Scherzo (+)
Equol	17.0	C15H14O3	241.0871	241.0870	-0.3	PFP (-)
Equol	17.0	C15H14O3	243.1021	243.1016	-2.2	PFP (+)
Ergothioneine	2.9	C9H15N3O2S	230.0961	230.0958	-1.4	Scherzo (+)
Ergothioneine	7.0	C9H15N3O2S	230.0962	230.0958	-1.8	Scherzo (+)
Ergothioneine	2.5	C9H15N3O2S	230.0966	230.0958	-3.6	PFP (+)
Ergothioneine	8.4	C9H15N3O2S	230.0962	230.0958	-1.8	PFP (+)
Ergothioneine	8.9	C9H15N3O2S	230.0955	230.0958	1.2	PFP (+)
FAD	12.7	C27H33N9O15P2	784.1556	784.1499	-7.3	PFP (-)
FAD	12.8	C27H33N9O15P2	786.1661	786.1644	-2.1	PFP (+)
Flavin Mononucleotide	12.3	C17H21N4O9P	457.1129	457.1119	-2.2	PFP (+)
Flavin Mononucleotide	12.4	C17H21N4O9P	455.0994	455.0973	-4.5	PFP (-)
Flavin Mononucleotide	13.5	C17H21N4O9P	457.1120	457.1119	-0.2	Scherzo (+)
Flavin Mononucleotide	13.9	C17H21N4O9P	455.0974	455.0973	-0.1	Scherzo (-)

Folate	9.8	C19H19N7O6	440.1316	440.1324	1.8	Scherzo (-)
Folate	11.4	C19H19N7O6	440.1347	440.1324	-5.2	PFP (-)
Galactonic acid	2.8	C6H12O7	195.0521	195.0510	-5.5	Scherzo (-)
Galactonic acid	3.3	C6H12O7	195.0522	195.0510	-6.0	Scherzo (-)
Galactonic acid - lactone	3.3	C6H10O6	179.0541	179.0550	5.1	Scherzo (+)
gamma-Glu-Cys	4.4	C8H14N2O5S	251.0699	251.0696	-1.1	Scherzo (+)
gamma-Glutamyglutamic acid	2.0	C10H16N2O7	275.0896	275.0885	-4.1	PFP (-)
gamma-Glutamyglutamic acid	2.9	C10H16N2O7	277.1040	277.1030	-3.5	Scherzo (+)
gamma-Glutamyglutamic acid	2.9	C10H16N2O7	275.0896	275.0885	-4.1	Scherzo (-)
gamma-Glutamyglutamic acid	3.7	C10H16N2O7	277.1038	277.1030	-2.8	Scherzo (+)
gamma-Glutamyglutamic acid	3.8	C10H16N2O7	275.0896	275.0885	-4.1	Scherzo (-)
gamma-Glutamyglutamic acid	2.1	C10H16N2O7	277.1037	277.1030	-2.4	PFP (+)
gamma-Muricholic acid	16.4	C24H40O5	407.2784	407.2803	4.7	Scherzo (-)
Genistein	12.2	C15H10O5	271.0606	271.0601	-1.8	Scherzo (+)
Genistein	14.5	C15H10O5	271.0605	271.0601	-1.5	Scherzo (+)
Genistein	14.5	C15H10O5	269.0460	269.0456	-1.7	Scherzo (-)
Genistein	17.6	C15H10O5	271.0601	271.0601	0.0	PFP (+)
Genistein	17.6	C15H10O5	269.0468	269.0456	-4.6	PFP (-)
Genkwanin	13.3	C16H12O5	283.0620	283.0612	-2.8	Scherzo (-)
Genkwanin	16.6	C16H12O5	283.0606	283.0612	2.1	Scherzo (-)
Genkwanin	16.7	C16H12O5	283.0617	283.0612	-1.8	PFP (-)
Gentisic acid	11.0	C7H6O4	153.0195	153.0193	-1.1	PFP (-)
Gentisic acid	14.7	C7H6O4	153.0200	153.0193	-4.4	Scherzo (-)
Glu-Gly-Arg	2.5	C13H24N6O6	361.1826	361.1830	1.1	Scherzo (+)
Glu-Ile-Arg	6.5	C17H32N6O6	417.2457	417.2456	-0.2	Scherzo (+)
Glu-Leu-Arg	7.7	C17H32N6O6	417.2466	417.2456	-2.4	PFP (+)
Glu-Met	6.8	C10H18N2O5S	279.1014	279.1009	-1.7	Scherzo (+)
Glu-Phe-Arg	7.4	C20H30N6O6	451.2342	451.2300	-9.4	Scherzo (+)
Glu-Ser	3.2	C8H14N2O6	235.0928	235.0925	-1.4	Scherzo (+)
Glu-Val-Phe	11.9	C19H27N3O6	394.1979	394.1973	-1.6	PFP (+)
Glucoheptonic acid	3.3	C7H14O8	225.0623	225.0616	-3.2	Scherzo (-)
Glucosamine 6-phosphate	2.5	C6H14NO8P	258.0385	258.0384	-0.3	Scherzo (-)
Glucosamine-6-phosphate	2.5	C6H14NO8P	260.0527	260.0530	1.1	Scherzo (+)
Glucose 6-Phosphate	2.2	C6H13O9P	261.0378	261.0370	-3.1	PFP (+)
Glucose 6-Phosphate	8.3	C6H13O9P	261.0372	261.0370	-0.8	Scherzo (+)
Glutamate	1.9	C5H9NO4	148.0607	148.0604	-1.8	PFP (+)
Glutamate	1.9	C5H9NO4	146.0461	146.0459	-1.5	PFP (-)
Glutamate	2.6	C5H9NO4	148.0606	148.0604	-1.1	Scherzo (+)
Glutamate	2.6	C5H9NO4	146.0467	146.0459	-5.6	Scherzo (-)
Glutamate	5.0	C5H9NO4	146.0467	146.0459	-5.6	Scherzo (-)
Glutamine	2.5	C5H10N2O3	147.0765	147.0764	-0.5	Scherzo (+)
Glutamine	2.5	C5H10N2O3	145.0618	145.0619	0.5	Scherzo (-)
Glutaric acid	4.7	C5H8O4	131.0347	131.0350	2.1	PFP (-)
Glutaric acid	5.6	C5H8O4	131.0346	131.0350	2.9	PFP (-)
Glutaric acid	6.2	C5H8O4	131.0348	131.0350	1.4	Scherzo (-)

Glutathione	3.8	C10H17N3O6S	306.0775	306.0765	-3.2	Scherzo (-)
Glutathione oxidized	2.1	C20H32N6O12S2	611.1486	611.1447	-6.4	PFP (-)
Glutathione oxidized	2.8	C20H32N6O12S2	613.1601	613.1592	-1.4	PFP (+)
Glutathione oxidized	2.9	C20H32N6O12S2	613.1597	613.1592	-0.8	Scherzo (+)
Glutathione oxidized	2.9	C20H32N6O12S2	611.1449	611.1447	-0.3	Scherzo (-)
Glutathione oxidized	2.9	C20H32N6O12S2	611.1481	611.1447	-5.6	PFP (-)
Glutathione oxidized	3.5	C20H32N6O12S2	611.1406	611.1447	6.7	Scherzo (-)
Glutathione oxidized	5.2	C20H32N6O12S2	613.1612	613.1592	-3.2	Scherzo (+)
Glutathione oxidized	5.3	C20H32N6O12S2	611.1452	611.1447	-0.8	Scherzo (-)
Glutathione, reduced	3.8	C10H17N3O6S	308.0920	308.0911	-3.0	Scherzo (+)
Gly-Leu	4.2	C8H16N2O3	189.1229	189.1234	2.5	Scherzo (+)
Gly-Leu	5.7	C8H16N2O3	189.1237	189.1234	-1.7	PFP (+)
Gly-Phe	6.6	C11H14N2O3	223.1079	223.1077	-0.8	Scherzo (+)
Gly-Phe	7.7	C11H14N2O3	223.1080	223.1077	-1.3	PFP (+)
Gly-Tyr	4.1	C11H14N2O4	239.1035	239.1026	-3.6	Scherzo (+)
Gly-Tyr	4.9	C11H14N2O4	239.1028	239.1026	-0.7	PFP (+)
Glyceraldehyde, 3-(dihydrogen phosphate)	9.5	C3H7O6P	168.9912	168.9908	-2.7	Scherzo (-)
Glyceric acid	1.9	C3H6O4	105.0192	105.0193	1.2	PFP (-)
Glycerol 3-phosphate	6.1	C3H9O6P	171.0072	171.0064	-4.7	Scherzo (-)
Glycerol 3-phosphate	6.5	C3H9O6P	171.0068	171.0064	-2.3	Scherzo (-)
Glycerolphosphate	2.2	C3H9O6P	173.0205	173.0210	2.6	PFP (+)
Glycerolphosphate	6.5	C3H9O6P	173.0206	173.0210	2.0	Scherzo (+)
Glycerolphosphate	9.1	C3H9O6P	171.0066	171.0064	-1.2	Scherzo (-)
Glycerophosphocholine	2.5	C8H20NO6P	258.1108	258.1101	-2.7	PFP (+)
Glycerophosphocholine	2.8	C8H20NO6P	258.1109	258.1101	-3.1	Scherzo (+)
Glycyl-L-leucine	5.6	C8H16N2O3	187.1088	187.1088	0.1	PFP (-)
Guanidinoethyl sulfonate	2.7	C3H9N3O3S	166.0292	166.0292	-0.1	Scherzo (-)
Guanine	2.4	C5H5N5O	152.0556	152.0567	7.2	PFP (+)
Guanine	2.8	C5H5N5O	152.0565	152.0567	1.2	Scherzo (+)
Guanine	3.1	C5H5N5O	150.0412	150.0421	6.2	Scherzo (-)
Guanine	5.0	C5H5N5O	152.0570	152.0567	-2.0	PFP (+)
Guanine	5.4	C5H5N5O	152.0572	152.0567	-3.4	PFP (+)
Guanine	5.4	C5H5N5O	150.0422	150.0421	-0.5	PFP (-)
Guanine	6.6	C5H5N5O	152.0569	152.0567	-1.4	Scherzo (+)
Guanine	7.3	C5H5N5O	152.0568	152.0567	-0.7	PFP (+)
Guanine	8.0	C5H5N5O	152.0570	152.0567	-2.0	PFP (+)
Guanine	8.4	C5H5N5O	152.0564	152.0567	1.9	Scherzo (+)
Guanine	8.5	C5H5N5O	152.0567	152.0567	-0.1	PFP (+)
Guanine	13.1	C5H5N5O	152.0562	152.0567	3.2	Scherzo (+)
Guanine	6.2	C5H5N5O	152.0565	152.0567	1.2	PFP (+)
Guanosine	5.4	C10H13N5O5	284.0996	284.0990	-2.3	PFP (+)
Guanosine	5.4	C10H13N5O5	282.0858	282.0844	-5.0	PFP (-)
Guanosine	6.2	C10H13N5O5	284.1001	284.0990	-4.0	Scherzo (+)
Guanosine	6.3	C10H13N5O5	282.0857	282.0844	-4.6	Scherzo (-)
Guanosine monophosphate	2.5	C10H14N5O8P	364.0650	364.0653	0.8	PFP (+)

Guanosine monophosphate	3.0	C10H14N5O8P	362.0524	362.0507	-4.6	PFP (-)
Guanosine monophosphate	3.1	C10H14N5O8P	364.0659	364.0653	-1.7	PFP (+)
Guanosine monophosphate	3.9	C10H14N5O8P	362.0521	362.0507	-3.8	PFP (-)
Guanosine monophosphate	4.8	C10H14N5O8P	362.0512	362.0507	-1.3	PFP (-)
Guanosine monophosphate	6.6	C10H14N5O8P	364.0656	364.0653	-0.9	PFP (+)
Guanosine monophosphate	6.6	C10H14N5O8P	362.0523	362.0507	-4.4	PFP (-)
Guanosine monophosphate	9.1	C10H14N5O8P	364.0665	364.0653	-3.4	Scherzo (+)
Guanosine monophosphate	9.3	C10H14N5O8P	362.0513	362.0507	-1.6	Scherzo (-)
Guanosine monophosphate	10.0	C10H14N5O8P	364.0658	364.0653	-1.4	Scherzo (+)
Hexadecanedioic acid	18.0	C16H30O4	285.2071	285.2071	0.1	PFP (-)
Hexaethylene glycol	10.0	C12H26O7	283.1759	283.1751	-2.7	PFP (+)
Hexanoyl-L-carnitine	8.9	C13H25NO4	260.1865	260.1856	-3.3	Scherzo (+)
Hexanoyl-L-carnitine	12.6	C13H25NO4	260.1862	260.1856	-2.2	PFP (+)
Hippuric acid	9.5	C9H9NO3	178.0509	178.0510	0.4	PFP (-)
Histidine	1.9	C6H9N3O2	156.0769	156.0768	-1.0	PFP (+)
Histidine	1.9	C6H9N3O2	154.0620	154.0622	1.3	PFP (-)
Histidine	2.1	C6H9N3O2	154.0619	154.0622	1.9	Scherzo (-)
Histidine	2.1	C6H9N3O2	156.0770	156.0768	-1.6	Scherzo (+)
Histidine	2.4	C6H9N3O2	156.0763	156.0768	2.9	PFP (+)
Homoeriodictyol	14.0	C16H14O6	301.0717	301.0718	0.2	Scherzo (-)
Homovanillic acid sulfate	9.9	C9H10O7S	261.0070	261.0075	1.7	PFP (-)
Homovanillic acid sulfate	10.8	C9H10O7S	261.0080	261.0075	-2.1	PFP (-)
Hydroferulic acid	12.7	C10H12O4	195.0668	195.0663	-2.7	PFP (-)
Hydroxybutyric acid	2.9	C4H8O3	103.0399	103.0401	1.6	PFP (-)
Hydroxyphenyllactic acid	8.7	C9H10O4	181.0511	181.0506	-2.6	PFP (-)
Hypoxanthine	4.2	C5H4N4O	137.0458	137.0458	-0.1	Scherzo (+)
Hypoxanthine	5.2	C5H4N4O	137.0455	137.0458	2.1	PFP (+)
Hypoxanthine	6.1	C5H4N4O	137.0448	137.0458	7.2	Scherzo (+)
Hypoxanthine	6.2	C5H4N4O	137.0458	137.0458	-0.1	PFP (+)
Hypoxanthine	6.7	C5H4N4O	137.0454	137.0458	2.8	Scherzo (+)
Hypoxanthine	3.3	C5H4N4O	137.0457	137.0458	0.7	PFP (+)
Ile-Arg	7.8	C12H25N5O3	288.2036	288.2030	-2.0	PFP (+)
Ile-Leu	10.6	C12H24N2O3	245.1862	245.1860	-0.9	PFP (+)
Ile-Pro-Ile	8.4	C17H31N3O4	342.2389	342.2387	-0.5	Scherzo (+)
Ile-Tyr	8.9	C15H22N2O4	295.1657	295.1652	-1.6	PFP (+)
Ile-Val	6.8	C11H22N2O3	231.1699	231.1703	1.8	PFP (+)
Indole	9.4	C8H7N	118.0652	118.0651	-0.6	PFP (+)
Indole-3-lactic acid	12.2	C11H11NO3	206.0811	206.0812	0.3	Scherzo (+)
Indole-3-lactic acid	12.2	C11H11NO3	204.0675	204.0666	-4.3	Scherzo (-)
Indole-3-lactic acid	13.4	C11H11NO3	204.0670	204.0666	-1.9	PFP (-)
Indole-3-lactic acid	13.4	C11H11NO3	206.0811	206.0812	0.3	PFP (+)
Indole-6-carboxaldehyde	12.3	C9H7NO	144.0461	144.0455	-4.2	Scherzo (-)
Indole-6-carboxaldehyde	14.4	C9H7NO	144.0458	144.0455	-2.2	PFP (-)
Indole-6-carboxaldehyde	9.4	C9H7NO	146.0601	146.0600	-0.4	PFP (+)
Indole-6-carboxaldehyde	14.4	C9H7NO	146.0601	146.0600	-0.4	PFP (+)

Indoleacrylic acid	13.4	C11H9NO2	186.0567	186.0561	-3.5	Scherzo (-)
Indoleacrylic acid	16.1	C11H9NO2	186.0561	186.0561	-0.3	PFP (-)
Indoxyl sulfate	10.7	C8H7NO4S	212.0029	212.0023	-2.8	PFP (-)
Inosine	4.3	C10H12N4O5	267.0744	267.0735	-3.4	PFP (-)
Inosine	4.6	C10H12N4O5	269.0888	269.0881	-2.8	PFP (+)
Inosine	5.2	C10H12N4O5	269.0882	269.0881	-0.6	PFP (+)
Inosine	6.1	C10H12N4O5	269.0890	269.0881	-3.5	Scherzo (+)
Inosine	6.3	C10H12N4O5	267.0736	267.0735	-0.4	Scherzo (-)
Inosinic acid	3.0	C10H13N4O8P	347.0398	347.0398	0.1	PFP (-)
Isocitric acid lactone	5.8	C6H6O6	173.0090	173.0092	0.9	Scherzo (-)
Isoferulic acid	16.3	C10H10O4	193.0502	193.0506	2.2	PFP (-)
Isoleucine	3.5	C6H13NO2	132.1016	132.1019	2.3	Scherzo (+)
Isoleucine	3.5	C6H13NO2	130.0877	130.0874	-2.7	Scherzo (-)
Isopentenyladenine	12.6	C10H13N5	204.1240	204.1244	1.8	PFP (+)
Isosteviol	14.8	C20H30O3	317.2123	317.2122	-0.3	Scherzo (-)
Itaconic acid	9.0	C5H6O4	129.0181	129.0193	9.5	Scherzo (-)
Jasmonic acid	11.2	C12H18O3	211.1334	211.1329	-2.5	PFP (+)
Kaempferol	14.7	C15H10O6	285.0409	285.0405	-1.5	Scherzo (-)
Kynurenic acid	9.4	C10H7NO3	190.0497	190.0499	0.9	Scherzo (+)
Kynurenic acid	17.2	C10H7NO3	190.0499	190.0499	-0.2	Scherzo (+)
Kynurenic acid	10.2	C10H7NO3	190.0503	190.0499	-2.3	PFP (+)
Kynurenic acid	10.6	C10H7NO3	190.0501	190.0499	-1.2	PFP (+)
Kynurenic acid	11.8	C10H7NO3	190.0499	190.0499	-0.2	PFP (+)
Kynurenine	5.7	C10H12N2O3	209.0923	209.0921	-1.1	PFP (+)
Kynurenine	5.7	C10H12N2O3	207.0774	207.0775	0.6	PFP (-)
Kynurenine	5.9	C10H12N2O3	209.0917	209.0921	1.8	Scherzo (+)
Lactate	2.1	C3H6O3	89.0248	89.0244	-4.3	PFP (-)
Lauric acid diethanolamide	18.0	C16H33NO3	288.2541	288.2533	-2.7	Scherzo (+)
Lauric acid diethanolamide	17.9	C16H33NO3	288.2536	288.2533	-1.0	PFP (+)
Lauroyl-L-carnitine	13.6	C19H37NO4	344.2800	344.2795	-1.3	Scherzo (+)
Lauroyl-L-carnitine	17.7	C19H37NO4	344.2788	344.2795	2.1	PFP (+)
Leu-Leu	11.2	C12H24N2O3	245.1865	245.1860	-2.2	PFP (+)
Leu-Pro-Arg	6.7	C17H32N6O4	385.2555	385.2558	0.7	PFP (+)
Leu-Val	7.8	C11H22N2O3	231.1708	231.1703	-2.1	PFP (+)
Leucine	2.7	C6H13NO2	130.0873	130.0874	0.4	PFP (-)
Leukotriene E4	15.5	C23H37NO5S	438.2295	438.2320	5.6	Scherzo (-)
Linoleoylcarnitine	17.8	C25H45NO4	424.3422	424.3421	-0.1	PFP (+)
Lumichrome	12.0	C12H10N4O2	243.0880	243.0877	-1.4	Scherzo (+)
Lumichrome	15.1	C12H10N4O2	241.0735	241.0731	-1.7	PFP (-)
Lumichrome	15.1	C12H10N4O2	243.0878	243.0877	-0.6	PFP (+)
Luteolin	17.6	C15H10O6	285.0408	285.0405	-1.2	PFP (-)
Lysine	2.0	C6H14N2O2	147.1129	147.1128	-0.7	Scherzo (+)
Maleic acid	2.0	C4H4O4	115.0035	115.0037	1.6	PFP (-)
Maleic acid	3.0	C4H4O4	115.0037	115.0037	-0.2	PFP (-)
Malic acid	2.0	C4H6O5	133.0146	133.0143	-2.6	PFP (-)

Malic acid	4.5	C4H6O5	133.0150	133.0143	-5.6	Scherzo (-)
Maltol	7.7	C6H6O3	127.0384	127.0390	4.5	PFP (+)
Mandelic acid	9.5	C8H8O3	151.0401	151.0401	-0.2	Scherzo (-)
Matairesinol	11.9	C20H22O6	359.1484	359.1489	1.4	Scherzo (+)
Matairesinol	13.9	C20H22O6	359.1501	359.1489	-3.3	Scherzo (+)
Methionine	2.3	C5H11NO2S	150.0584	150.0583	-0.5	PFP (+)
Methionine	2.8	C5H11NO2S	148.0445	148.0438	-4.9	Scherzo (-)
Methionine	2.9	C5H11NO2S	150.0587	150.0583	-2.5	Scherzo (+)
Methionine	9.2	C5H11NO2S	150.0583	150.0583	0.2	Scherzo (+)
Methionine sulfoxide	2.6	C5H11NO3S	166.0529	166.0532	2.0	Scherzo (+)
Methyl trans-cinnamate	12.7	C10H10O2	163.0752	163.0754	1.0	Scherzo (+)
Methylsuccinic acid	10.5	C5H8O4	131.0358	131.0350	-6.3	Scherzo (-)
Monobutyl phthalate	17.2	C12H14O4	221.0827	221.0819	-3.5	PFP (-)
myo-Inositol-1,2-diphosphate	8.3	C6H14O12P2	338.9885	338.9888	0.8	Scherzo (-)
Myristoleic acid	17.9	C14H26O2	227.2010	227.2006	-1.9	PFP (+)
N-(4-Aminobenzoyl)-L-glutamic acid	6.3	C12H14N2O5	265.0840	265.0830	-3.8	PFP (-)
N-(4-Aminobenzoyl)-L-glutamic acid	7.4	C12H14N2O5	267.0990	267.0976	-5.4	Scherzo (+)
N-(4-Aminobenzoyl)-L-glutamic acid	7.6	C12H14N2O5	265.0843	265.0830	-4.9	Scherzo (-)
N-(4-Aminobenzoyl)-L-glutamic acid	6.3	C12H14N2O5	267.0979	267.0976	-1.3	PFP (+)
N-Acetyl galactosamine	2.7	C8H15NO6	222.0982	222.0972	-4.5	Scherzo (+)
N-Acetyl galactosamine	2.7	C8H15NO6	220.0831	220.0827	-2.0	Scherzo (-)
N-acetyl glutamic acid	2.8	C7H11NO5	190.0710	190.0710	0.0	PFP (+)
N-acetyl glutamic acid	2.8	C7H11NO5	188.0569	188.0565	-2.4	PFP (-)
N-acetyl glutamic acid	3.0	C7H11NO5	188.0567	188.0565	-1.3	PFP (-)
N-acetyl glutamic acid	5.7	C7H11NO5	190.0709	190.0710	0.5	Scherzo (+)
N-acetyl glutamic acid	5.7	C7H11NO5	188.0569	188.0565	-2.4	Scherzo (-)
N-Acetyl-D-glucosamine 6-phosphate	1.9	C8H16NO9P	300.0485	300.0490	1.6	PFP (-)
N-Acetyl-D-glucosamine 6-phosphate	2.3	C8H16NO9P	300.0486	300.0490	1.3	PFP (-)
N-Acetyl-D-glucosamine 6-phosphate	6.6	C8H16NO9P	300.0498	300.0490	-2.7	Scherzo (-)
N-Acetyl-D-glucosamine 6-phosphate	8.6	C8H16NO9P	300.0481	300.0490	3.0	Scherzo (-)
N-Acetyl-D-glucosamine 6-phosphate	9.3	C8H16NO9P	300.0495	300.0490	-1.7	Scherzo (-)
N-Acetyl-D-norleucine	11.1	C8H15NO3	172.0981	172.0979	-1.0	PFP (-)
N-Acetyl-DL-valine	6.6	C7H13NO3	158.0824	158.0823	-0.8	PFP (-)
N-Acetyl-DL-valine	7.2	C7H13NO3	158.0825	158.0823	-1.5	Scherzo (-)
N-Acetyl-DL-valine	7.8	C7H13NO3	158.0823	158.0823	-0.2	PFP (-)
N-Acetyl-DL-valine	8.7	C7H13NO3	158.0828	158.0823	-3.4	Scherzo (-)
N-Acetyl-L-alanine	2.8	C5H9NO3	130.0511	130.0510	-1.0	PFP (-)
N-Acetyl-L-alanine	5.1	C5H9NO3	130.0513	130.0510	-2.5	Scherzo (-)
N-Acetyl-L-alanine	5.7	C5H9NO3	130.0514	130.0510	-3.3	Scherzo (-)
N-Acetyl-L-Aspartate	5.7	C6H9NO5	174.0415	174.0408	-4.0	Scherzo (-)
N-Acetyl-L-Glutamine	4.4	C7H12N2O4	189.0869	189.0870	0.4	Scherzo (+)
N-Acetyl-L-Glutamine	4.5	C7H12N2O4	187.0725	187.0724	-0.4	Scherzo (-)
N-Acetyl-L-Leucine	10.6	C8H15NO3	174.1118	174.1125	3.8	Scherzo (+)
N-Acetyl-L-Leucine	11.1	C8H15NO3	174.1128	174.1125	-1.9	PFP (+)
N-Acetyl-L-methionine	8.1	C7H13NO3S	192.0683	192.0689	3.1	PFP (+)

N-Acetyl-L-Methionine	8.1	C7H13NO3S	190.0548	190.0543	-2.4	PFP (-)
N-Acetyl-L-methionine	9.2	C7H13NO3S	192.0684	192.0689	2.6	Scherzo (+)
N-Acetyl-L-Methionine	9.3	C7H13NO3S	190.0550	190.0543	-3.5	Scherzo (-)
N-Acetyl-L-Phenylalanine	12.0	C11H13NO3	208.0975	208.0968	-3.3	Scherzo (+)
N-Acetyl-L-phenylalanine	12.3	C11H13NO3	206.0828	206.0823	-2.6	PFP (-)
N-Acetyl-L-Phenylalanine	12.4	C11H13NO3	208.0973	208.0968	-2.3	PFP (+)
N-Acetyl-L-tyrosine	9.4	C11H13NO4	222.0779	222.0772	-3.2	PFP (-)
N-Acetylaspartylglutamic acid	7.1	C11H16N2O8	303.0839	303.0834	-1.7	Scherzo (-)
N-Acetylaspartylglutamic acid	7.2	C11H16N2O8	305.0973	305.0979	2.1	Scherzo (+)
N-Alpha-acetyllysine	1.9	C8H16N2O3	189.1242	189.1234	-4.4	PFP (+)
N-Alpha-acetyllysine	2.6	C8H16N2O3	189.1233	189.1234	0.4	Scherzo (+)
N-Formyl-L-methionine	7.3	C6H11NO3S	176.0384	176.0387	1.6	PFP (-)
N-Formyl-L-methionine	9.3	C6H11NO3S	176.0383	176.0387	2.2	Scherzo (-)
N-Glycolylneuraminic acid	2.1	C11H19NO10	324.0939	324.0936	-0.9	PFP (-)
N-Glycolylneuraminic acid	4.9	C11H19NO10	324.0949	324.0936	-3.9	Scherzo (-)
N-Glycolylneuraminic acid	5.2	C11H19NO10	324.0945	324.0936	-2.7	Scherzo (-)
N-Glycolylneuraminic acid	5.3	C11H19NO10	326.1088	326.1082	-1.9	Scherzo (+)
N-Succinyl-5-aminoimidazole-4-carboxamide ribose	6.1	C13H18N4O9	375.1146	375.1147	0.1	PFP (+)
N,N-Dimethylaniline	3.6	C8H11N	122.0966	122.0964	-1.4	Scherzo (+)
N,N-Dimethylaniline	8.2	C8H11N	122.0966	122.0964	-1.4	PFP (+)
N,N-Dimethylguanosine	7.4	C12H17N5O5	312.1311	312.1303	-2.7	Scherzo (+)
N,N-Dimethylguanosine	8.3	C12H17N5O5	312.1312	312.1303	-3.0	PFP (+)
N.epsilon.-Acetyl-L-lysine	2.8	C8H16N2O3	189.1233	189.1234	0.4	Scherzo (+)
N.epsilon.-Acetyl-L-lysine	2.4	C8H16N2O3	189.1236	189.1234	-1.2	PFP (+)
NAD	3.5	C21H27N7O14P2	664.1184	664.1164	-3.0	PFP (+)
NAD	5.9	C21H27N7O14P2	664.1167	664.1164	-0.5	Scherzo (+)
NAD	5.9	C21H27N7O14P2	662.1042	662.1019	-3.5	Scherzo (-)
Nandrolone	14.1	C18H26O2	275.2005	275.2006	0.2	Scherzo (+)
Naringenin	14.2	C15H12O5	273.0762	273.0758	-1.6	Scherzo (+)
Naringenin	17.5	C15H12O5	271.0621	271.0612	-3.3	PFP (-)
Naringenin	17.5	C15H12O5	273.0761	273.0758	-1.3	PFP (+)
Naringenin-4'-O-.beta.-D-glucuronide	14.1	C21H20O11	447.0929	447.0933	0.9	Scherzo (-)
Naringenin-4'-O-.beta.-D-glucuronide	14.7	C21H20O11	447.0949	447.0933	-3.6	PFP (-)
Niacinamide	2.7	C6H6N2O	123.0556	123.0553	-2.5	PFP (+)
Nicotinamide	3.5	C6H6N2O	123.0555	123.0553	-1.7	Scherzo (+)
Nicotinate	2.6	C6H5NO2	124.0395	124.0393	-1.6	PFP (+)
Nicotinate	2.6	C6H5NO2	122.0248	122.0248	-0.4	PFP (-)
Nicotinate	2.9	C6H5NO2	124.0395	124.0393	-1.6	Scherzo (+)
Nicotinate	3.6	C6H5NO2	124.0395	124.0393	-1.6	Scherzo (+)
Nicotinate	3.6	C6H5NO2	122.0254	122.0248	-5.3	Scherzo (-)
Nicotinic acid mononucleotide	8.6	C11H14NO9P	336.0484	336.0479	-1.5	Scherzo (+)
Nutriacholic acid	15.7	C24H38O4	391.2853	391.2843	-2.6	Scherzo (+)
Nutriacholic acid	17.8	C24H38O4	391.2849	391.2843	-1.6	PFP (+)
O-Phospho-L-Serine	6.8	C3H8NO6P	184.0015	184.0017	0.8	Scherzo (-)
O-Phospho-L-Serine	6.9	C3H8NO6P	186.0155	186.0162	3.8	Scherzo (+)

O-phosphoryl-ethanolamine	1.9	C2H8NO4P	140.0117	140.0118	0.9	PFP (-)
O-phosphoryl-ethanolamine	2.5	C2H8NO4P	140.0123	140.0118	-3.4	Scherzo (-)
O-phosphoryl-ethanolamine	2.6	C2H8NO4P	142.0260	142.0264	2.6	Scherzo (+)
Octadecanedioic acid	16.4	C18H34O4	313.2390	313.2384	-1.8	Scherzo (-)
Octanoylcarnitine	11.0	C15H29NO4	288.2175	288.2169	-1.9	Scherzo (+)
Octanoylcarnitine	15.9	C15H29NO4	288.2174	288.2169	-1.6	PFP (+)
Oleoyl-L-carnitine	16.8	C25H47NO4	426.3586	426.3578	-1.9	Scherzo (+)
Oleoyl-L-carnitine	17.9	C25H47NO4	426.3569	426.3578	2.1	PFP (+)
omega-Benzoyloxyphloracetophenone	12.9	C15H12O6	287.0565	287.0561	-1.4	Scherzo (-)
Ophtalmic acid	3.8	C11H19N3O6	290.1351	290.1347	-1.5	Scherzo (+)
Orotic acid	2.9	C5H4N2O4	155.0098	155.0098	0.2	PFP (-)
Oxypurinol	3.5	C5H4N4O2	151.0267	151.0262	-3.6	PFP (-)
Oxypurinol	5.0	C5H4N4O2	151.0273	151.0262	-7.6	Scherzo (-)
p-Acetamidophenyl .beta.-D-glucuronide	9.7	C14H17NO8	326.0877	326.0881	1.3	PFP (-)
p-Acetamidophenyl .beta.-D-glucuronide	10.8	C14H17NO8	328.1028	328.1027	-0.3	Scherzo (+)
p-Acetamidophenyl .beta.-D-glucuronide	11.0	C14H17NO8	326.0879	326.0881	0.7	Scherzo (-)
p-Acetaminobenzoic acid	10.1	C9H9NO3	180.0654	180.0655	0.7	Scherzo (+)
p-Acetaminobenzoic acid	10.2	C9H9NO3	178.0515	178.0510	-3.0	Scherzo (-)
p-Acetaminobenzoic acid	11.7	C9H9NO3	178.0513	178.0510	-1.9	PFP (-)
p-Acetaminobenzoic acid	11.7	C9H9NO3	180.0656	180.0655	-0.4	PFP (+)
p-Hydroxyphenyllactic acid	9.0	C9H10O4	181.0512	181.0506	-3.1	Scherzo (-)
p-tert-Butylcatechol	16.4	C10H14O2	165.0921	165.0921	0.0	PFP (-)
Palmitic acid alkyne	14.9	C16H28O2	253.2160	253.2162	0.8	Scherzo (+)
Palmitoyl sphingomyelin	17.9	C39H79N2O6P	703.5747	703.5749	0.2	PFP (+)
Palmitoylcarnitine	16.6	C23H45NO4	400.3434	400.3421	-3.1	Scherzo (+)
Palmitoylcarnitine	17.9	C23H45NO4	400.3428	400.3421	-1.6	PFP (+)
Pantothenate	6.4	C9H17NO5	220.1182	220.1180	-1.1	PFP (+)
Pantothenate	7.0	C9H17NO5	220.1184	220.1180	-2.0	Scherzo (+)
Pantothenic acid	6.4	C9H17NO5	218.1042	218.1034	-3.7	PFP (-)
Pantothenic acid	7.1	C9H17NO5	218.1044	218.1034	-4.6	Scherzo (-)
Pentaethylene glycol	7.6	C10H22O6	239.1475	239.1489	5.9	Scherzo (+)
Pentaethylene glycol	8.9	C10H22O6	239.1484	239.1489	2.2	PFP (+)
Phe-Asp	4.4	C13H16N2O5	281.1131	281.1132	0.4	Scherzo (+)
Phe-Glu	4.9	C14H18N2O5	295.1287	295.1289	0.5	Scherzo (+)
Phe-Glu	6.5	C14H18N2O5	295.1293	295.1289	-1.5	PFP (+)
Phe-Gly	5.4	C11H14N2O3	223.1080	223.1077	-1.3	Scherzo (+)
Phe-Gly	6.8	C11H14N2O3	223.1079	223.1077	-0.8	PFP (+)
Phe-Leu	12.6	C15H22N2O3	279.1712	279.1703	-3.2	PFP (+)
Phe-Pro	8.6	C14H18N2O3	263.1388	263.1390	0.8	Scherzo (+)
Phe-Val	9.8	C14H20N2O3	265.1544	265.1547	1.0	PFP (+)
Phenaceturic acid	11.2	C10H11NO3	194.0813	194.0812	-0.7	Scherzo (+)
Phenaceturic acid	10.2	C10H11NO3	194.0813	194.0812	-0.7	PFP (+)
Phenyl glucuronide	8.2	C12H14O7	269.0675	269.0667	-3.0	PFP (-)
Phenyl glucuronide	11.0	C12H14O7	269.0667	269.0667	-0.1	Scherzo (-)
Phenylacetaldehyde	3.9	C8H8O	121.0650	121.0648	-1.7	Scherzo (+)

Phenylacetaldehyde	11.0	C8H8O	121.0648	121.0648	-0.1	Scherzo (+)
Phenylacetaldehyde	12.4	C8H8O	121.0649	121.0648	-0.9	PFP (+)
Phenylacetylglycine	10.2	C10H11NO3	192.0670	192.0666	-2.0	PFP (-)
Phenylacetylglycine	11.3	C10H11NO3	192.0674	192.0666	-4.1	Scherzo (-)
Phenylalanine	4.8	C9H11NO2	166.0867	166.0863	-2.6	PFP (+)
Phenylalanine	5.2	C9H11NO2	164.0722	164.0717	-3.0	PFP (-)
Phenylalanine	5.7	C9H11NO2	166.0864	166.0863	-0.8	Scherzo (+)
Phenylalanine	5.8	C9H11NO2	164.0725	164.0717	-4.9	Scherzo (-)
Phenylalanine	9.0	C9H11NO2	166.0859	166.0863	2.2	Scherzo (+)
Phenylalanine	9.1	C9H11NO2	166.0862	166.0863	0.4	Scherzo (+)
Phenylalanine	12.0	C9H11NO2	166.0859	166.0863	2.2	Scherzo (+)
Phenylalanine	12.3	C9H11NO2	166.0862	166.0863	0.4	PFP (+)
Phenylalanine	14.0	C9H11NO2	166.0858	166.0863	2.8	Scherzo (+)
Phenylalanine	9.6	C9H11NO2	166.0859	166.0863	2.2	PFP (+)
Phosphocreatine	7.3	C4H10N3O5P	210.0293	210.0285	-3.7	Scherzo (-)
Phosphorylcholine	2.5	C5H14NO4P	184.0736	184.0733	-1.5	PFP (+)
Phosphorylcholine	2.8	C5H14NO4P	184.0737	184.0733	-2.1	Scherzo (+)
Phthalic anhydride	16.0	C8H4O3	149.0233	149.0233	0.1	Scherzo (+)
Phthalic anhydride	17.2	C8H4O3	149.0233	149.0233	0.1	PFP (+)
Phytosphingosine	14.4	C18H39NO3	318.3007	318.3003	-1.4	Scherzo (+)
Pimelic acid	9.3	C7H12O4	159.0667	159.0663	-2.6	Scherzo (-)
Pimelic acid	10.2	C7H12O4	159.0666	159.0663	-2.0	PFP (-)
Pipecolic acid	2.8	C6H11NO2	130.0861	130.0863	1.2	Scherzo (+)
Pipecolinic acid	2.0	C6H11NO2	130.0862	130.0863	0.5	Scherzo (+)
Pipecolinic acid	2.4	C6H11NO2	130.0860	130.0863	2.0	PFP (+)
Pro-Arg	5.2	C11H21N5O3	272.1709	272.1717	3.0	Scherzo (+)
Pro-Arg	8.1	C11H21N5O3	272.1721	272.1717	-1.4	PFP (+)
Pro-Asp	2.0	C9H14N2O5	231.0974	231.0976	0.6	PFP (+)
Pro-Gly	2.4	C7H12N2O3	173.0920	173.0921	0.4	Scherzo (+)
Pro-Ile	5.0	C11H20N2O3	229.1550	229.1547	-1.4	Scherzo (+)
Pro-Phe	9.6	C14H18N2O3	263.1394	263.1390	-1.4	PFP (+)
Pro-Val	3.5	C10H18N2O3	215.1390	215.1390	0.1	Scherzo (+)
Proline	2.1	C5H9NO2	116.0707	116.0706	-0.8	PFP (+)
Propionylcarnitine	2.9	C10H19NO4	218.1393	218.1387	-2.8	Scherzo (+)
Propionylcarnitine	3.5	C10H19NO4	218.1393	218.1387	-2.8	Scherzo (+)
Propionylcarnitine	6.4	C10H19NO4	218.1391	218.1387	-1.9	PFP (+)
Prostaglandin A1	16.4	C20H32O4	335.2233	335.2228	-1.6	Scherzo (-)
Prostaglandin A2	14.6	C20H30O4	333.2075	333.2071	-1.1	Scherzo (-)
Prostaglandin A2	16.1	C20H30O4	333.2079	333.2071	-2.3	Scherzo (-)
Prostaglandin A2	17.8	C20H30O4	333.2085	333.2071	-4.1	PFP (-)
Prostaglandin B1	15.6	C20H32O4	335.2231	335.2228	-1.0	Scherzo (-)
Prostaglandin D1	17.7	C20H34O5	353.2338	353.2334	-1.3	PFP (-)
Prostaglandin E1	14.8	C20H34O5	353.2338	353.2334	-1.3	Scherzo (-)
Prostaglandin H2	14.6	C20H32O5	351.2180	351.2177	-0.9	Scherzo (-)
Prostaglandin H2	17.6	C20H32O5	351.2195	351.2177	-5.1	PFP (-)

Prostaglandin I2	12.8	C20H32O5	353.2329	353.2323	-1.8	Scherzo (+)
Prostaglandin I2	13.0	C20H32O5	353.2334	353.2323	-3.3	Scherzo (+)
Prostaglandin I2	13.8	C20H32O5	353.2333	353.2323	-3.0	Scherzo (+)
Prostaglandin I2	17.4	C20H32O5	353.2329	353.2323	-1.8	PFP (+)
Purine	4.2	C5H4N4	121.0508	121.0509	0.6	PFP (+)
Purine	4.2	C5H4N4	119.0365	119.0363	-1.5	PFP (-)
Purine	4.6	C5H4N4	121.0509	121.0509	-0.2	Scherzo (+)
Pyridoxal 5-phosphate	6.7	C8H10NO6P	248.0324	248.0319	-2.2	Scherzo (+)
Pyridoxal 5-phosphate	6.7	C8H10NO6P	246.0177	246.0173	-1.6	Scherzo (-)
PyroGlu-Phe	11.8	C14H16N2O4	277.1189	277.1183	-2.2	Scherzo (+)
PyroGlu-Phe	12.2	C14H16N2O4	277.1184	277.1183	-0.4	PFP (+)
PyroGlu-Pro	7.7	C10H14N2O4	227.1026	227.1026	0.1	Scherzo (+)
PyroGlu-Pro	7.0	C10H14N2O4	227.1029	227.1026	-1.2	PFP (+)
PyroGlu-Pro	7.4	C10H14N2O4	227.1026	227.1026	0.1	PFP (+)
PyroGlu-Tyr	9.6	C14H16N2O5	293.1132	293.1132	0.0	Scherzo (+)
Pyroglutamic acid	1.9	C5H7NO3	130.0503	130.0499	-3.3	PFP (+)
Pyroglutamic acid	2.6	C5H7NO3	128.0356	128.0353	-2.2	PFP (-)
Pyroglutamic acid	2.6	C5H7NO3	128.0354	128.0353	-0.6	Scherzo (-)
Pyroglutamic acid	2.6	C5H7NO3	130.0499	130.0499	-0.2	Scherzo (+)
Pyroglutamic acid	2.6	C5H7NO3	130.0493	130.0499	4.4	PFP (+)
Pyroglutamic acid	5.6	C5H7NO3	128.0359	128.0353	-4.5	Scherzo (-)
Pyroglutamic acid	5.6	C5H7NO3	130.0498	130.0499	0.5	Scherzo (+)
Pyroglutamic acid	6.3	C5H7NO3	130.0497	130.0499	1.3	Scherzo (+)
Quinolin-2-ol	10.6	C9H7NO	144.0454	144.0455	0.6	PFP (-)
Quinolin-2-ol	11.3	C9H7NO	144.0451	144.0455	2.7	PFP (-)
Quinolin-3-ol	10.5	C9H7NO	146.0598	146.0600	1.6	Scherzo (+)
Quinolin-3-ol	17.1	C9H7NO	144.0460	144.0455	-3.5	Scherzo (-)
Quinoline-2,8-diol	10.7	C9H7NO2	160.0406	160.0404	-1.2	PFP (-)
Resorcinol	8.6	C6H6O2	109.0289	109.0295	5.5	PFP (-)
Riboflavin	9.6	C17H20N4O6	377.1466	377.1456	-2.8	Scherzo (+)
Riboflavin	9.6	C17H20N4O6	375.1316	375.1310	-1.6	Scherzo (-)
Riboflavin	11.7	C17H20N4O6	377.1467	377.1456	-3.0	PFP (+)
Riboflavin	11.7	C17H20N4O6	375.1331	375.1310	-5.6	PFP (-)
Ribonolactone	6.5	C5H8O5	147.0305	147.0299	-4.1	Scherzo (-)
Ribose 1-phosphate	2.2	C5H11O8P	229.0113	229.0119	2.5	PFP (-)
Ribose 1-phosphate	9.2	C5H11O8P	229.0128	229.0119	-4.0	Scherzo (-)
(5'-Adenosyl)-L-homocysteine	3.5	C14H20N6O5S	385.1301	385.1289	-3.2	Scherzo (+)
Adenosyl-L-methionine	2.5	C15H22N6O5S	399.1452	399.1445	-1.7	Scherzo (+)
Adenosyl-L-methionine	2.3	C15H22N6O5S	399.1450	399.1445	-1.2	PFP (+)
Lactoylglutathione	5.1	C13H21N3O8S	380.1131	380.1122	-2.3	Scherzo (+)
Saccharic acid	5.1	C6H10O8	209.0309	209.0303	-2.9	Scherzo (-)
Sarcosine	2.0	C3H7NO2	90.0551	90.0550	-1.6	PFP (+)
Schaftoside	10.0	C26H28O14	565.1569	565.1552	-3.0	Scherzo (+)
Schaftoside	10.0	C26H28O14	563.1425	563.1406	-3.3	Scherzo (-)
Schaftoside	13.1	C26H28O14	563.1442	563.1406	-6.3	PFP (-)

Schaftoside	13.5	C26H28O14	563.1439	563.1406	-5.8	PFP (-)
Schaftoside	13.1	C26H28O14	565.1560	565.1552	-1.5	PFP (+)
Schaftoside	13.5	C26H28O14	565.1560	565.1552	-1.5	PFP (+)
Sebacic acid	15.4	C10H18O4	201.1137	201.1132	-2.3	PFP (-)
Ser-Leu	4.7	C9H18N2O4	219.1339	219.1339	0.1	PFP (+)
Serotonin	4.1	C10H12N2O	177.1015	177.1022	4.2	Scherzo (+)
sn-Glycerol 3-phosphate	2.2	C3H9O6P	171.0066	171.0064	-1.2	PFP (-)
sn-Glycerol 3-phosphate	9.3	C3H9O6P	173.0210	173.0210	-0.3	Scherzo (+)
sn-Glycerol 3-phosphate	9.4	C3H9O6P	171.0073	171.0064	-5.3	Scherzo (-)
Spermidine	2.2	C7H19N3	146.1649	146.1652	1.8	Scherzo (+)
Spermine	1.9	C10H26N4	203.2232	203.2230	-0.9	Scherzo (+)
Sphinganine	14.3	C18H39NO2	302.3061	302.3054	-2.4	Scherzo (+)
Sphinganine	17.7	C18H39NO2	302.3057	302.3054	-1.1	PFP (+)
Stachydrine	2.9	C7H13NO2	144.1020	144.1019	-0.6	PFP (+)
Stachydrine	3.7	C7H13NO2	144.1019	144.1019	0.1	PFP (+)
Stearidonic acid	16.1	C18H28O2	277.2161	277.2162	0.4	Scherzo (+)
Stearoyl-L-carnitine	17.9	C25H49NO4	428.3744	428.3734	-2.2	Scherzo (+)
Stearoyl-L-carnitine	17.9	C25H49NO4	428.3738	428.3734	-0.8	PFP (+)
Suberic acid	10.7	C8H14O4	173.0825	173.0819	-3.3	Scherzo (-)
Suberic acid	12.5	C8H14O4	173.0821	173.0819	-1.0	PFP (-)
Succinic acid	2.9	C4H6O4	117.0196	117.0193	-2.3	PFP (-)
Syringic acid	10.1	C9H10O5	199.0602	199.0601	-0.5	Scherzo (+)
Syringic acid	10.1	C9H10O5	197.0460	197.0456	-2.3	Scherzo (-)
Syringic acid	12.4	C9H10O5	197.0457	197.0456	-0.8	PFP (-)
Syringic acid	12.4	C9H10O5	199.0605	199.0601	-2.0	PFP (+)
Taurine	1.9	C2H7NO3S	126.0222	126.0219	-2.1	PFP (+)
Taurine	1.9	C2H7NO3S	124.0076	124.0074	-1.7	PFP (-)
Taurine	2.6	C2H7NO3S	126.0218	126.0219	1.1	Scherzo (+)
Taurine	2.6	C2H7NO3S	124.0075	124.0074	-0.9	Scherzo (-)
Taurocholic acid	15.0	C26H45NO7S	514.2873	514.2844	-5.6	PFP (-)
Taurocholic acid	17.7	C26H45NO7S	516.3002	516.2990	-2.4	PFP (+)
Taurodeoxycholic acid	17.2	C26H45NO6S	498.2900	498.2895	-1.0	PFP (-)
Tetradecanedioic acid	16.3	C14H26O4	257.1753	257.1758	2.1	Scherzo (-)
Tetradecanedioic acid	17.9	C14H26O4	257.1759	257.1758	-0.3	PFP (-)
Tetraethylene glycol	6.8	C8H18O5	195.1224	195.1227	1.5	Scherzo (+)
Tetraethylene glycol	7.4	C8H18O5	195.1228	195.1227	-0.5	PFP (+)
Thiamine	2.2	C12H16N4OS	263.0979	263.0972	-2.6	Scherzo (-)
Thiamine	2.6	C12H16N4OS	265.1123	265.1118	-2.0	PFP (+)
Thiamine monophosphate	2.4	C12H17N4O4PS	345.0790	345.0781	-2.6	PFP (+)
Thiamine pyrophosphate	3.5	C12H18N4O7P2S	425.0451	425.0444	-1.6	Scherzo (+)
Threonic acid	1.9	C4H8O5	135.0300	135.0299	-0.7	PFP (-)
Threonic acid	2.9	C4H8O5	135.0302	135.0299	-2.2	Scherzo (-)
Threonic acid	3.4	C4H8O5	135.0307	135.0299	-5.9	Scherzo (-)
Threonine	2.5	C4H9NO3	120.0655	120.0655	0.2	Scherzo (+)
Threonine	4.6	C4H9NO3	120.0653	120.0655	1.8	Scherzo (+)

Thromboxane B2	16.8	C20H34O6	369.2289	369.2283	-1.7	PFP (-)
Thromboxane B2	17.4	C20H34O6	369.2285	369.2283	-0.7	PFP (-)
Thymidine	6.7	C10H14N2O5	243.0976	243.0976	-0.2	PFP (+)
Thymidine	6.7	C10H14N2O5	241.0825	241.0830	2.1	PFP (-)
Thymidine	7.0	C10H14N2O5	243.0979	243.0976	-1.4	Scherzo (+)
Thymidine	7.1	C10H14N2O5	241.0839	241.0830	-3.7	Scherzo (-)
Thymine	4.0	C5H6N2O2	127.0501	127.0502	0.8	PFP (+)
Thymine	4.0	C5H6N2O2	125.0360	125.0357	-2.8	PFP (-)
Thymine	5.3	C5H6N2O2	127.0499	127.0502	2.4	Scherzo (+)
Thymine	5.4	C5H6N2O2	125.0363	125.0357	-5.2	Scherzo (-)
Thymine	6.2	C5H6N2O2	127.0505	127.0502	-2.4	Scherzo (+)
Thymine	6.7	C5H6N2O2	127.0500	127.0502	1.6	PFP (+)
Thymine	7.0	C5H6N2O2	127.0503	127.0502	-0.8	Scherzo (+)
trans-2-Hydroxycinnamic acid	3.0	C9H8O3	165.0541	165.0546	3.2	Scherzo (+)
trans-2-Hydroxycinnamic acid	3.9	C9H8O3	165.0548	165.0546	-1.1	Scherzo (+)
trans-2-Hydroxycinnamic acid	11.2	C9H8O3	163.0407	163.0401	-3.9	Scherzo (-)
trans-2-Hydroxycinnamic acid	13.2	C9H8O3	163.0400	163.0401	0.4	PFP (-)
trans-2-Hydroxycinnamic acid	3.0	C9H8O3	165.0550	165.0546	-2.3	PFP (+)
trans-Ferulic acid	11.5	C10H10O4	193.0507	193.0506	-0.4	Scherzo (-)
trans-Traumatic acid	16.3	C12H20O4	227.1288	227.1289	0.4	PFP (-)
trans-Traumatic acid	17.0	C12H20O4	227.1291	227.1289	-1.0	PFP (-)
Tri(3-chloropropyl) phosphate	16.5	C9H18Cl3O4P	327.0084	327.0081	-0.9	Scherzo (+)
Tri(3-chloropropyl) phosphate	17.8	C9H18Cl3O4P	327.0077	327.0081	1.3	PFP (+)
Tributylamine	16.2	C12H27N	186.2216	186.2216	0.2	PFP (+)
Tricin	14.6	C17H14O7	331.0818	331.0812	-1.7	Scherzo (+)
Trigonelline	2.8	C7H7NO2	138.0549	138.0550	0.4	Scherzo (+)
Trihydroxycholestanoic acid	17.7	C27H46O5	449.3259	449.3273	3.0	Scherzo (-)
Trp-Glu	8.9	C16H19N3O5	334.1378	334.1398	5.8	PFP (+)
Tryptophan	7.8	C11H12N2O2	205.0971	205.0972	0.2	Scherzo (+)
Tryptophan	7.9	C11H12N2O2	203.0830	203.0826	-2.0	Scherzo (-)
Tryptophan	9.3	C11H12N2O2	203.0825	203.0826	0.5	PFP (-)
Tryptophan	9.4	C11H12N2O2	205.0978	205.0972	-3.2	PFP (+)
Tryptophol	12.5	C10H11NO	162.0908	162.0913	3.3	Scherzo (+)
Tyr-Gly	3.6	C11H14N2O4	239.1018	239.1026	3.5	Scherzo (+)
Tyr-Gly	3.9	C11H14N2O4	239.1028	239.1026	-0.7	PFP (+)
Tyr-Leu	10.2	C15H22N2O4	295.1661	295.1652	-2.9	PFP (+)
Tyrosine	3.0	C9H11NO3	182.0807	182.0812	2.6	Scherzo (+)
Tyrosine	3.0	C9H11NO3	182.0816	182.0812	-2.4	PFP (+)
Tyrosine	3.3	C9H11NO3	180.0669	180.0666	-1.6	PFP (-)
Tyrosine	3.6	C9H11NO3	182.0815	182.0812	-1.8	PFP (+)
Tyrosine	3.7	C9H11NO3	180.0665	180.0666	0.7	PFP (-)
Tyrosine	3.9	C9H11NO3	182.0811	182.0812	0.4	Scherzo (+)
Tyrosine	3.9	C9H11NO3	180.0668	180.0666	-1.0	Scherzo (-)
Undecanedioic acid	14.1	C11H20O4	215.1302	215.1289	-6.1	Scherzo (-)
Undecanedioic acid	16.9	C11H20O4	215.1296	215.1289	-3.3	PFP (-)

Uracil	2.4	C4H4N2O2	113.0346	113.0346	-0.4	PFP (+)
Uracil	2.5	C4H4N2O2	111.0201	111.0200	-0.9	PFP (-)
Uracil	5.9	C4H4N2O2	113.0343	113.0346	2.2	PFP (+)
Urate	2.6	C5H4N4O3	167.0215	167.0211	-2.6	PFP (-)
Urate	2.8	C5H4N4O3	169.0357	169.0356	-0.5	PFP (+)
Urate	4.1	C5H4N4O3	169.0357	169.0356	-0.5	Scherzo (+)
Urate	4.2	C5H4N4O3	167.0219	167.0211	-5.0	Scherzo (-)
Uridine	2.6	C9H12N2O6	243.0634	243.0623	-4.7	PFP (-)
Uridine	2.8	C9H12N2O6	245.0771	245.0768	-1.2	PFP (+)
Uridine	3.0	C9H12N2O6	243.0633	243.0623	-4.3	PFP (-)
Uridine	3.8	C9H12N2O6	245.0768	245.0768	0.0	Scherzo (+)
Uridine	3.9	C9H12N2O6	243.0630	243.0623	-3.0	Scherzo (-)
Uridine	4.3	C9H12N2O6	243.0622	243.0623	0.2	Scherzo (-)
Uridine 5'-monophosphate	10.4	C9H13N2O9P	325.0439	325.0432	-2.3	Scherzo (+)
Urobilin	11.0	C33H42N4O6	591.3178	591.3177	-0.2	Scherzo (+)
Urobilin	17.0	C33H42N4O6	591.3182	591.3177	-0.8	PFP (+)
Urocanate	2.5	C6H6N2O2	139.0503	139.0502	-0.7	Scherzo (+)
Val-Leu	7.2	C11H22N2O3	231.1703	231.1703	0.1	PFP (+)
Val-Leu	8.6	C11H22N2O3	231.1703	231.1703	0.1	PFP (+)
Val-Val	4.1	C10H20N2O3	217.1549	217.1547	-1.1	PFP (+)
Vitamin C	2.0	C6H8O6	175.0252	175.0248	-2.2	PFP (-)
Vitamin C	3.4	C6H8O6	177.0397	177.0394	-1.9	Scherzo (+)
Vitamin C	3.5	C6H8O6	175.0257	175.0248	-5.1	Scherzo (-)
Xanthine	3.6	C5H4N4O2	153.0409	153.0407	-1.3	PFP (+)
Xanthine	4.5	C5H4N4O2	153.0408	153.0407	-0.7	Scherzo (+)
Xanthine	6.5	C5H4N4O2	153.0411	153.0407	-2.6	PFP (+)
Xanthine	7.0	C5H4N4O2	153.0406	153.0407	0.7	Scherzo (+)
Xanthosine	6.5	C10H12N4O6	283.0687	283.0684	-1.0	Scherzo (-)
Xanthosine	6.5	C10H12N4O6	285.0837	285.0830	-2.6	PFP (+)
Xanthosine	6.8	C10H12N4O6	285.0836	285.0830	-2.2	PFP (+)
Xanthosine	6.8	C10H12N4O6	283.0690	283.0684	-2.1	PFP (-)
Xanthosine	7.0	C10H12N4O6	285.0838	285.0830	-2.9	Scherzo (+)
Xanthosine	7.1	C10H12N4O6	283.0694	283.0684	-3.5	Scherzo (-)
Xanthurenic acid	10.7	C10H7NO4	204.0307	204.0302	-2.3	PFP (-)
Xanthurenic acid	12.2	C10H7NO4	204.0308	204.0302	-2.8	PFP (-)
Xylose	3.7	C5H10O5	149.0455	149.0456	0.3	Scherzo (-)

Table 2.9 Putative Fecal Metabolite Identifications Compiled from Four Untargeted Metabolomic Datasets

Putative ID	Retention Time (min)	Chemical Formula	Found at Mass (*m/z*)	Exact Mass (*m/z*)	Mass Error (ppm)	Column (+/-)
alpha-Hydroxybutyric acid	2.9	C4H8O3	103.0399	103.0401	1.6	PFP (-)
alpha-L-Glu-L-Tyr	4.5	C14H18N2O6	311.1261	311.1238	-7.5	Scherzo (+)
alpha-L-Glu-L-Tyr	7.6	C14H18N2O6	311.1255	311.1238	-5.6	Scherzo (+)
alpha-L-Glu-L-Tyr	5.8	C14H18N2O6	311.1253	311.1238	-4.9	PFP (+)
alpha-L-Glu-L-Tyr	7.3	C14H18N2O6	311.1246	311.1238	-2.7	PFP (+)
alpha,alpha'-Trehalose 6-phosphate	9.6	C12H23O14P	421.0747	421.0753	1.4	Scherzo (-)
beta-Nicotinamide adenine dinucleotide	5.9	C21H27N7O14P2	664.1158	664.1164	0.9	Scherzo (+)
gamma-Muricholic acid	17.4	C24H40O5	407.2803	407.2803	0.0	PFP (-)
gamma-Muricholic acid	15.3	C24H40O5	407.2810	407.2803	-1.7	Scherzo (-)
gamma-Muricholic acid	15.7	C24H40O5	407.2803	407.2803	0.0	Scherzo (-)
gamma-Nonalactone	12.1	C9H16O2	157.1228	157.1223	-3.1	Scherzo (+)
omega-Benzoyloxyphloracetophenone	15.7	C15H12O6	287.0563	287.0561	-0.7	PFP (-)
omega-Benzoyloxyphloracetophenone	12.9	C15H12O6	287.0564	287.0561	-1.0	Scherzo (-)
(-)-Catechin	10.6	C15H14O6	289.0713	289.0718	1.6	PFP (-)
(-)-Catechin	9.3	C15H14O6	289.0731	289.0718	-4.6	Scherzo (-)
(-)-Homoeriodictyol	14.2	C16H14O6	303.0874	303.0863	-3.6	Scherzo (+)
(-)-Hydroxycitric acid lactone	2.4	C6H6O7	189.0045	189.0041	-2.2	PFP (-)
(-)-N-Acetylneuraminic acid	2.1	C11H19NO9	308.1000	308.0987	-4.2	PFP (-)
(-)-N-Acetylneuraminic acid	5.6	C11H19NO9	308.1000	308.0987	-4.2	Scherzo (-)
(-)-N-Acetylneuraminic acid	5.6	C11H19NO9	310.1143	310.1133	-3.4	Scherzo (+)
(-)-N-Acetylneuraminic acid	6.3	C11H19NO9	310.1154	310.1133	-6.9	Scherzo (+)
(-)-N-Acetylneuraminic acid	1.9	C11H19NO9	310.1150	310.1133	-5.6	PFP (+)
(-)-N-Acetylneuraminic acid	2.1	C11H19NO9	310.1146	310.1133	-4.3	PFP (+)
(-)-Quinic acid	1.9	C7H12O6	191.0565	191.0561	-2.0	PFP (-)
(-)-Quinic acid	3.6	C7H12O6	191.0569	191.0561	-4.1	Scherzo (-)
(-)-Quinic acid	3.6	C7H12O6	193.0706	193.0707	0.3	Scherzo (+)
(+-)-2-Hydroxyisocaproic acid	9.4	C6H12O3	131.0711	131.0714	2.1	PFP (-)
(+-)-2-Hydroxyisocaproic acid	10.1	C6H12O3	131.0715	131.0714	-1.0	Scherzo (-)
(+-)7-epi-Jasmonic acid	9.6	C12H18O3	211.1333	211.1329	-2.0	Scherzo (+)
(+-)7-epi-Jasmonic acid	10.3	C12H18O3	211.1333	211.1329	-2.0	Scherzo (+)
(+-)7-epi-Jasmonic acid	11.2	C12H18O3	211.1333	211.1329	-2.0	PFP (+)
(+-)7-epi-Jasmonic acid	12.3	C12H18O3	211.1325	211.1329	1.8	PFP (+)
(+)-2-Hydroxyisocaproic acid	9.9	C6H12O3	131.0714	131.0714	-0.2	PFP (-)
Butyrylcarnitine	4.5	C11H21NO4	232.1550	232.1543	-2.9	Scherzo (+)
Butyrylcarnitine	5.0	C11H21NO4	232.1564	232.1543	-8.9	Scherzo (+)
Butyrylcarnitine	8.5	C11H21NO4	232.1551	232.1543	-3.3	PFP (+)

(+)-2-Hydroxy-3-methylbutyric acid	5.7	C5H10O3	117.0557	117.0557	0.2	PFP (-)
Lactate	2.1	C3H6O3	89.0245	89.0244	-0.9	PFP (-)
1-beta-D-Arabinofuranosyluracil 5'-monophosphate	2.5	C9H13N2O9P	323.0291	323.0286	-1.6	PFP (-)
1-beta-D-Arabinofuranosyluracil 5'-monophosphate	13.0	C9H13N2O9P	323.0288	323.0286	-0.7	Scherzo (-)
1-(10Z-Heptadecenoyl)-sn-glycero-3-phospho-(1'-rac-glycerol)	17.8	C23H45O9P	495.2735	495.2729	-1.3	PFP (-)
1-(1Z-Octadecenyl)-sn-glycero-3-phosphocholine	12.7	C26H54NO6P	508.3745	508.3762	3.2	Scherzo (+)
1-Ethyl-3-piperidinamine	3.4	C7H16N2	129.1385	129.1386	1.0	Scherzo (+)
1-Ethyl-3-piperidinamine	5.5	C7H16N2	129.1389	129.1386	-2.1	PFP (+)
1-Hexadecanoyl-2-octadecadienoyl-sn-glycero-3-phosphocholine	15.6	C42H80NO8P	758.5673	758.5694	2.8	Scherzo (+)
1-Methyladenosine	2.6	C11H15N5O4	282.1202	282.1197	-1.8	Scherzo (+)
1-Methyladenosine	6.7	C11H15N5O4	282.1185	282.1197	4.2	Scherzo (+)
1-Methyladenosine	6.8	C11H15N5O4	282.1197	282.1197	-0.1	PFP (+)
1-Methyluric acid	7.0	C6H6N4O3	181.0373	181.0367	-3.3	Scherzo (-)
1-Methyluric acid	6.9	C6H6N4O3	183.0513	183.0513	-0.2	Scherzo (+)
1-Methylxanthine	7.4	C6H6N4O2	167.0569	167.0564	-3.3	Scherzo (+)
1-Methylxanthine	7.1	C6H6N4O2	167.0565	167.0564	-0.9	PFP (+)
1-Myristoyl-2-hydroxy-sn-glycero-3-phosphoethanolamine	16.2	C19H40NO7P	424.2482	424.2470	-2.9	Scherzo (-)
1-Myristoyl-2-hydroxy-sn-glycero-3-phosphoethanolamine	15.3	C19H40NO7P	426.2631	426.2615	-3.7	Scherzo (+)
1-Myristoyl-2-hydroxy-sn-glycero-3-phosphoethanolamine	16.1	C19H40NO7P	426.2623	426.2615	-1.8	Scherzo (+)
1-Myristoyl-sn-glycero-3-phosphocholine	16.6	C22H46NO7P	468.3097	468.3085	-2.6	Scherzo (+)
1-Oleoyl-2-myristoyl-sn-glycero-3-phosphocholine	15.7	C40H78NO8P	732.5532	732.5538	0.8	Scherzo (+)
1-Oleoyl-sn-glycero-3-phosphocholine	14.4	C26H52NO7P	522.3559	522.3554	-0.9	Scherzo (+)
1-Oleoyl-sn-glycero-3-phosphocholine	18.0	C26H52NO7P	522.3523	522.3554	6.0	PFP (+)
1-Oleoyl-sn-glycero-3-phosphoethanolamine	16.3	C23H46NO7P	478.2942	478.2939	-0.6	Scherzo (-)
1-Palmitoyl-2-hydroxy-sn-glycero-3-phospho-(1'-rac-glycerol)	17.5	C22H45O9P	483.2751	483.2729	-4.7	Scherzo (-)
1-Palmitoyl-2-hydroxy-sn-glycero-3-phosphoethanolamine	15.2	C21H44NO7P	452.2798	452.2783	-3.4	Scherzo (-)
1-Palmitoyl-2-hydroxy-sn-glycero-3-phosphoethanolamine	17.4	C21H44NO7P	452.2781	452.2783	0.4	Scherzo (-)

1-Palmitoyl-2-hydroxy-sn-glycero-3-phosphoethanolamine	15.0	C21H44NO7P	454.2933	454.2928	-1.1	Scherzo (+)
1-Stearoyl-2-hydroxy-sn-glycero-3-phosphate	15.3	C21H43O7P	437.2675	437.2674	-0.3	Scherzo (-)
1-Stearoyl-2-hydroxy-sn-glycero-3-phosphate	17.3	C21H43O7P	437.2675	437.2674	-0.3	Scherzo (-)
1,11-Undecanedicarboxylic acid	17.8	C13H24O4	243.1599	243.1602	1.2	PFP (-)
1,11-Undecanedicarboxylic acid	15.9	C13H24O4	243.1606	243.1602	-1.7	Scherzo (-)
1,2-Benzenedicarboxylic acid	10.4	C8H6O4	165.0197	165.0193	-2.2	PFP (-)
1,2-dioleoyl-sn-glycero-3-phosphatidylcholine	15.7	C44H84NO8P	786.6001	786.6007	0.8	Scherzo (+)
1,2-Dipentadecanoyl-sn-glycero-3-phosphocholine	15.6	C38H76NO8P	706.5374	706.5381	1.0	Scherzo (+)
1,2,3-Benzenetriol	7.7	C6H6O3	127.0387	127.0390	2.1	PFP (+)
1,3-Cyclohexanedicarboxylic acid	9.5	C8H12O4	171.0664	171.0663	-0.7	PFP (-)
1,3-Cyclohexanedicarboxylic acid	12.4	C8H12O4	171.0662	171.0663	0.5	PFP (-)
1,3-Cyclohexanedicarboxylic acid	9.0	C8H12O4	171.0663	171.0663	-0.1	Scherzo (-)
1,3-Dicyclohexylurea	16.4	C13H24N2O	225.1961	225.1961	0.2	Scherzo (+)
1,5-Diaminonaphthalene	7.8	C10H10N2	159.0920	159.0917	-2.1	Scherzo (+)
1,5-Diaminonaphthalene	9.4	C10H10N2	159.0918	159.0917	-0.8	PFP (+)
1,5-Isoquinolinediol	4.8	C9H7NO2	160.0405	160.0404	-0.6	PFP (-)
1,5-Isoquinolinediol	10.1	C9H7NO2	160.0397	160.0404	4.4	PFP (-)
1,5-Isoquinolinediol	7.0	C9H7NO2	160.0413	160.0404	-5.6	Scherzo (-)
1,5-Isoquinolinediol	9.4	C9H7NO2	160.0411	160.0404	-4.4	Scherzo (-)
1,5-Isoquinolinediol	7.0	C9H7NO2	162.0552	162.0550	-1.5	Scherzo (+)
1,5-Isoquinolinediol	9.4	C9H7NO2	162.0553	162.0550	-2.1	Scherzo (+)
1,5-Isoquinolinediol	4.8	C9H7NO2	162.0550	162.0550	-0.2	PFP (+)
1,5-Isoquinolinediol	10.2	C9H7NO2	162.0552	162.0550	-1.5	PFP (+)
1,5-Isoquinolinediol	12.5	C9H7NO2	162.0554	162.0550	-2.7	PFP (+)
10-Formyl-7,8-dihydrofolic acid	10.1	C20H21N7O7	470.1450	470.1430	-4.3	PFP (-)
10-Formyl-7,8-dihydrofolic acid	9.4	C20H21N7O7	470.1447	470.1430	-3.7	Scherzo (-)
10-Formyl-7,8-dihydrofolic acid	9.3	C20H21N7O7	472.1591	472.1575	-3.3	Scherzo (+)
10-Formyl-7,8-dihydrofolic acid	10.1	C20H21N7O7	472.1575	472.1575	0.0	PFP (+)
10E,12Z-octadecadienoic acid	16.6	C18H32O2	281.2484	281.2475	-3.2	Scherzo (+)
10E,12Z-octadecadienoic acid	17.8	C18H32O2	281.2482	281.2475	-2.5	PFP (+)
11.alpha.-Hydroxyprogesterone	11.5	C21H30O3	331.2273	331.2268	-1.6	Scherzo (+)
12,13-Dihydroxy-9Z-octadecenoic acid	17.9	C18H34O4	313.2378	313.2384	2.0	PFP (-)
12,13-Dihydroxy-9Z-octadecenoic acid	14.3	C18H34O4	315.2530	315.2530	0.0	Scherzo (+)
12,13-Dihydroxy-9Z-octadecenoic acid	17.1	C18H34O4	315.2541	315.2530	-3.5	Scherzo (+)
12(13)-Epoxy-9Z-octadecenoic acid	17.4	C18H32O3	297.2434	297.2424	-3.3	Scherzo (+)

16-Hydroxyhexadecanoic acid	18.0	C16H32O3	271.2285	271.2279	-2.3	PFP (-)
16.alpha.-Hydroxypregnenolone	15.8	C21H32O3	333.2426	333.2424	-0.5	Scherzo (+)
16.alpha.-Hydroxypregnenolone	15.3	C21H32O3	333.2431	333.2424	-2.0	PFP (+)
17.alpha.-Nandrolone	17.5	C18H26O2	275.2003	275.2006	0.9	PFP (+)
1H-Indole-3-propanoic acid	13.6	C11H11NO2	190.0867	190.0863	-2.3	Scherzo (+)
1H-Indole-3-propanoic acid	15.8	C11H11NO2	190.0868	190.0863	-2.8	PFP (+)
1H-Indole-3-propanoic acid	16.5	C11H11NO2	190.0866	190.0863	-1.8	PFP (+)
1H-Indole-4-carboxaldehyde	7.8	C9H7NO	146.0598	146.0600	1.6	Scherzo (+)
1H-Indole-4-carboxaldehyde	12.3	C9H7NO	146.0598	146.0600	1.6	Scherzo (+)
1H-Indole-4-carboxaldehyde	9.4	C9H7NO	146.0595	146.0600	3.7	PFP (+)
1H-Indole-4-carboxaldehyde	14.4	C9H7NO	146.0601	146.0600	-0.4	PFP (+)
2-(N-Morpholino)ethanesulfonic acid	4.0	C6H13NO4S	194.0499	194.0493	-3.3	PFP (-)
2-(N-Morpholino)ethanesulfonic acid	4.8	C6H13NO4S	194.0501	194.0493	-4.4	PFP (-)
2-(N-Morpholino)ethanesulfonic acid	6.5	C6H13NO4S	194.0496	194.0493	-1.8	Scherzo (-)
2-Acetylpyrazine	2.3	C6H6N2O	123.0553	123.0553	-0.1	Scherzo (+)
2-Acetylpyrazine	2.0	C6H6N2O	123.0555	123.0553	-1.7	PFP (+)
2-Amino-1-naphthol	6.1	C10H9NO	160.0755	160.0757	1.2	PFP (+)
2-Dimethylamino-6-hydroxypurine	5.0	C7H9N5O	180.0882	180.0880	-1.2	Scherzo (+)
2-Dimethylamino-6-hydroxypurine	7.4	C7H9N5O	180.0874	180.0880	3.3	Scherzo (+)
2-Dimethylamino-6-hydroxypurine	5.9	C7H9N5O	180.0883	180.0880	-1.7	PFP (+)
2-Hydroxy-3-methoxybenzoic acid	11.6	C8H8O4	167.0351	167.0350	-0.7	PFP (-)
2-Hydroxy-3-methoxybenzoic acid	10.0	C8H8O4	167.0361	167.0350	-6.7	Scherzo (-)
2-Hydroxyibuprofen	17.3	C13H18O3	221.1187	221.1183	-1.7	PFP (-)
2-Isopropylmalic acid	8.4	C7H12O5	175.0613	175.0612	-0.6	PFP (-)
2-Isopropylmalic acid	10.2	C7H12O5	175.0618	175.0612	-3.4	Scherzo (-)
2-Keto-3-deoxyoctonic acid	1.9	C8H14O8	237.0623	237.0616	-3.0	PFP (-)
2-Keto-3-deoxyoctonic acid	4.6	C8H14O8	237.0625	237.0616	-3.8	Scherzo (-)
2-Keto-3-deoxyoctonic acid	5.2	C8H14O8	237.0624	237.0616	-3.4	Scherzo (-)
2-Ketohexanoic acid	8.3	C6H10O3	129.0551	129.0557	4.8	PFP (-)
2-Methoxybenzoic acid	10.1	C8H8O3	151.0403	151.0401	-1.5	PFP (-)
2-Methoxycinnamic acid	11.4	C10H10O3	177.0560	177.0557	-1.6	PFP (-)
2-Methyl-1,4-benzoquinone	14.3	C7H6O2	123.0442	123.0441	-1.1	Scherzo (+)
2-Methyl-1,4-benzoquinone	17.0	C7H6O2	123.0437	123.0441	2.9	PFP (+)
2-Methyl-3-ketovaleric acid	9.2	C6H10O3	129.0556	129.0557	0.9	PFP (-)
2-Methyl-3-ketovaleric acid	16.8	C6H10O3	129.0561	129.0557	-2.9	Scherzo (-)
2-Methylbutyryl-L-carnitine	7.3	C12H23NO4	246.1699	246.1700	0.3	Scherzo (+)
2-Methylbutyryl-L-carnitine	10.3	C12H23NO4	246.1708	246.1700	-3.3	PFP (+)
2-Methylquinolin-8-ol	12.2	C10H9NO	160.0760	160.0757	-1.9	Scherzo (+)
2-Oleoyl-1-palmitoyl-sn-glycero-3-phosphocholine	15.6	C42H82NO8P	760.5844	760.5851	0.9	Scherzo (+)

2-Phenylacetamide	3.8	C8H9NO	136.0759	136.0757	-1.5	Scherzo (+)
2-Phenylacetamide	3.0	C8H9NO	136.0757	136.0757	-0.1	PFP (+)
2-Phenylbutyric acid	10.5	C10H12O2	165.0912	165.0910	-1.2	Scherzo (+)
2-Piperidinone	6.6	C5H9NO	100.0757	100.0757	-0.1	PFP (+)
2,2-Dimethylglutaric acid	11.2	C7H12O4	159.0661	159.0663	1.1	PFP (-)
2,2-Dimethylglutaric acid	10.4	C7H12O4	159.0666	159.0663	-2.0	Scherzo (-)
2,3-Dihydroxy-4-methoxybenzoic acid	8.8	C8H8O5	183.0296	183.0299	1.6	Scherzo (-)
2,3-Dihydroxybenzoic acid	8.6	C7H6O4	153.0194	153.0193	-0.5	Scherzo (-)
2,3,5-Trimethylpyrazine	11.2	C7H10N2	123.0917	123.0917	-0.2	PFP (+)
2,4-Dimethylphenol	12.4	C8H10O	121.0659	121.0659	-0.1	PFP (-)
2,4(3H,5H)-Furandione	2.9	C4H4O3	101.0233	101.0233	0.2	PFP (+)
2,6-Dihydroxybenzoic acid	14.1	C7H6O4	153.0203	153.0193	-6.3	PFP (-)
2,6-Dimethoxyphenol	10.1	C8H10O3	155.0706	155.0703	-2.1	Scherzo (+)
2,6-Dimethoxyphenol	12.4	C8H10O3	155.0696	155.0703	4.3	PFP (+)
2,6-Xylidine	8.2	C8H11N	122.0960	122.0964	3.5	PFP (+)
2'-Deoxyadenosine	4.7	C10H13N5O3	252.1086	252.1091	2.1	PFP (+)
2'-Deoxycytidine	2.4	C9H13N3O4	228.0979	228.0979	-0.1	Scherzo (+)
2'-Deoxycytidine	2.3	C9H13N3O4	228.0973	228.0979	2.5	PFP (+)
2'-Deoxyinosine	6.7	C10H12N4O4	253.0943	253.0931	-4.6	Scherzo (+)
2'-Deoxyinosine	6.2	C10H12N4O4	253.0936	253.0931	-1.9	PFP (+)
2'-O-Methyladenosine	6.2	C11H15N5O4	282.1204	282.1197	-2.6	Scherzo (+)
2S-Amino-4E-octadecene-1,3S-diol	14.8	C18H37NO2	300.2910	300.2897	-4.3	Scherzo (+)
2S-Amino-4E-octadecene-1,3S-diol	17.8	C18H37NO2	300.2894	300.2897	1.0	PFP (+)
3-(2-Ethylhexoxy)propan-1-amine	11.2	C11H25NO	188.2014	188.2009	-2.7	Scherzo (+)
3-(2-Ethylhexoxy)propan-1-amine	17.1	C11H25NO	188.2010	188.2009	-0.6	PFP (+)
3-(2-Hydroxyphenyl)propionic acid	12.4	C9H10O3	165.0561	165.0557	-2.3	PFP (-)
3-(2-Hydroxyphenyl)propionic acid	11.0	C9H10O3	165.0567	165.0557	-5.9	Scherzo (-)
3-(4-Hydroxyphenyl)propionic acid	10.5	C9H10O3	165.0565	165.0557	-4.7	Scherzo (-)
3-Acetamidophenol	9.7	C8H9NO2	150.0557	150.0561	2.3	PFP (-)
3-Acetamidophenol	9.5	C8H9NO2	152.0701	152.0706	3.4	Scherzo (+)
3-Acetamidophenol	9.7	C8H9NO2	152.0702	152.0706	2.7	PFP (+)
3-Acetoxypyridine	2.8	C7H7NO2	138.0543	138.0550	4.8	Scherzo (+)
3-Aminobenzoic acid	6.6	C7H7NO2	138.0545	138.0550	3.3	PFP (+)
3-Aminohexanoic acid	2.7	C6H13NO2	130.0873	130.0874	0.4	PFP (-)
3-Aminopentanoic acid	2.0	C5H11NO2	116.0719	116.0717	-1.7	PFP (-)
3-Coumaric acid	11.3	C9H8O3	165.0543	165.0546	1.9	Scherzo (+)
3-Cyclohexyl-1,1-dimethylurea	12.8	C9H18N2O	171.1491	171.1492	0.5	Scherzo (+)
3-Cyclohexyl-1,1-dimethylurea	13.9	C9H18N2O	171.1492	171.1492	-0.1	PFP (+)
3-Dehydroshikimic acid	6.1	C7H8O5	171.0304	171.0299	-2.9	Scherzo (-)
3-Ethylphenol	11.0	C8H10O	121.0664	121.0659	-4.2	Scherzo (-)

3-Hydroxy-3-methylglutaric acid	3.0	C6H10O5	161.0459	161.0456	-2.2	PFP (-)
3-Hydroxy-3-methylglutaric acid	3.5	C6H10O5	161.0459	161.0456	-2.2	PFP (-)
3-Hydroxy-3-methylglutaric acid	5.2	C6H10O5	161.0460	161.0456	-2.8	Scherzo (-)
3-Hydroxy-4-methoxybenzaldehyde	8.8	C8H8O3	151.0407	151.0401	-4.2	PFP (-)
3-Hydroxy-4-methoxybenzaldehyde	10.5	C8H8O3	151.0407	151.0401	-4.2	Scherzo (-)
3-Hydroxy-4-methoxybenzaldehyde	10.8	C8H8O3	153.0548	153.0546	-1.2	Scherzo (+)
3-Hydroxy-4-methoxybenzoic acid	10.0	C8H8O4	169.0496	169.0495	-0.4	Scherzo (+)
3-Hydroxy-4-methoxybenzoic acid	11.6	C8H8O4	169.0495	169.0495	0.2	PFP (+)
3-Hydroxy-4-methoxycinnamic acid	13.1	C10H10O4	193.0512	193.0506	-3.0	PFP (-)
3-Hydroxy-4-methoxycinnamic acid	14.7	C10H10O4	193.0504	193.0506	1.2	PFP (-)
3-Hydroxy-4-methoxycinnamic acid	16.3	C10H10O4	193.0501	193.0506	2.7	PFP (-)
3-Hydroxy-4-methoxycinnamic acid	14.0	C10H10O4	193.0509	193.0506	-1.4	Scherzo (-)
3-Hydroxy-4-methoxycinnamic acid	11.5	C10H10O4	195.0657	195.0652	-2.6	Scherzo (+)
3-Hydroxy-4-methoxycinnamic acid	13.8	C10H10O4	195.0655	195.0652	-1.6	PFP (+)
3-Hydroxyanthranilic acid	4.3	C7H7NO3	152.0351	152.0353	1.4	Scherzo (-)
3-Hydroxybenzaldehyde	10.1	C7H6O2	121.0292	121.0295	2.5	PFP (-)
3-Hydroxybenzaldehyde	11.2	C7H6O2	121.0294	121.0295	0.8	PFP (-)
3-Hydroxybenzaldehyde	10.4	C7H6O2	121.0304	121.0295	-7.4	Scherzo (-)
3-Hydroxybenzoic acid	9.7	C7H6O3	137.0240	137.0244	3.1	Scherzo (-)
3-Hydroxybutyrylcarnitine	4.2	C11H21NO5	248.1488	248.1493	1.8	PFP (+)
3-Hydroxyoleylcarnitine	17.7	C25H47NO5	442.3525	442.3527	0.5	PFP (+)
3-Hydroxypicolinic acid	2.9	C6H5NO3	138.0196	138.0197	0.5	PFP (-)
3-Hydroxypicolinic acid	7.0	C6H5NO3	138.0198	138.0197	-0.9	Scherzo (-)
3-Indoleacetic acid	14.4	C10H9NO2	176.0710	176.0706	-2.2	PFP (+)
3-Indoleacetic acid	12.5	C10H9NO2	174.0561	174.0561	-0.3	Scherzo (-)
3-Indoleacetic acid	10.8	C10H9NO2	176.0708	176.0706	-1.1	Scherzo (+)
3-Indoleacetic acid	12.5	C10H9NO2	176.0709	176.0706	-1.6	Scherzo (+)
3-Indoleacrylic acid	7.8	C11H9NO2	188.0713	188.0706	-3.7	Scherzo (+)
3-Indoleacrylic acid	10.0	C11H9NO2	188.0709	188.0706	-1.5	Scherzo (+)
3-Indoleacrylic acid	12.2	C11H9NO2	188.0710	188.0706	-2.1	Scherzo (+)
3-Indoleacrylic acid	13.0	C11H9NO2	188.0701	188.0706	2.7	Scherzo (+)
3-Indoleacrylic acid	9.4	C11H9NO2	188.0710	188.0706	-2.1	PFP (+)
3-Indoleacrylic acid	10.7	C11H9NO2	188.0706	188.0706	0.1	PFP (+)
3-Indolepropionic acid	15.8	C11H11NO2	188.0724	188.0717	-3.7	PFP (-)
3-Methyladipic acid	9.3	C7H12O4	159.0667	159.0663	-2.6	Scherzo (-)
3-Methylindole	7.9	C9H9N	132.0808	132.0808	-0.2	Scherzo (+)
3-Methylindole	9.4	C9H9N	132.0806	132.0808	1.4	PFP (+)
3-O-Methylgallic acid	9.8	C8H8O5	183.0302	183.0299	-1.6	PFP (-)
3-Oxocholic acid	17.7	C24H38O5	405.2663	405.2647	-4.1	PFP (-)
3-Oxocholic acid	14.5	C24H38O5	405.2652	405.2647	-1.4	Scherzo (-)

3-Oxocholic acid	15.1	C24H38O5	405.2663	405.2647	-4.1	Scherzo (-)
3-Oxocholic acid	16.1	C24H38O5	405.2656	405.2647	-2.3	Scherzo (-)
3-tert-Butylphenol	14.7	C10H14O	149.0971	149.0972	0.6	PFP (-)
3-tert-Butylphenol	13.8	C10H14O	149.0979	149.0972	-4.8	Scherzo (-)
3-Ureidopropionic acid	3.5	C4H8N2O3	131.0455	131.0462	5.5	Scherzo (-)
3,3-Dimethylacrylic acid	1.9	C5H8O2	101.0599	101.0597	-1.9	PFP (+)
3,4-Dihydro-6-hydroxy-.alpha.,2,5,7,8-pentamethyl-2H-1-benzopyran-2-pentanoic acid	17.1	C19H28O4	321.2069	321.2060	-2.7	Scherzo (+)
3,4-Dihydrocoumarin	5.7	C9H8O2	149.0595	149.0597	1.4	Scherzo (+)
3,4-Dihydrocoumarin	11.0	C9H8O2	149.0601	149.0597	-2.6	Scherzo (+)
3,4-Dihydrocoumarin	5.2	C9H8O2	149.0589	149.0597	5.4	PFP (+)
3,4-Dihydrocoumarin	12.4	C9H8O2	149.0600	149.0597	-1.9	PFP (+)
3,4-Dihydroxy-L-phenylalanine	3.9	C9H11NO4	196.0619	196.0615	-1.9	Scherzo (-)
3,4-Dihydroxyacetophenone	9.5	C8H8O3	151.0407	151.0401	-4.2	Scherzo (-)
3,4-Dihydroxybenzoic acid	8.6	C7H6O4	155.0338	155.0339	0.6	Scherzo (+)
3,4-Dimethylbenzoic acid	12.6	C9H10O2	151.0755	151.0754	-0.9	Scherzo (+)
3,4,2',4',6'-Pentahydroxychalcone	16.7	C15H12O6	287.0562	287.0561	-0.3	PFP (-)
3,4,2',4',6'-Pentahydroxychalcone	16.6	C15H12O6	289.0711	289.0707	-1.5	PFP (+)
3,4'-Dimethoxy-5,7,3'-trihydroxyflavone	17.9	C17H14O7	329.0673	329.0667	-1.9	PFP (-)
3,4'-Dimethoxy-5,7,3'-trihydroxyflavone	14.6	C17H14O7	329.0680	329.0667	-4.0	Scherzo (-)
3,5-Dihydroxybenzoic acid	8.6	C7H6O4	153.0195	153.0193	-1.1	PFP (-)
3,5-Dihydroxybenzoic acid	8.5	C7H6O4	155.0337	155.0339	1.2	PFP (+)
3,5-Dimethoxy-4-hydroxycinnamic acid	14.2	C11H12O5	223.0616	223.0612	-1.8	PFP (-)
3,5-Dimethoxy-4-hydroxycinnamic acid	11.4	C11H12O5	223.0624	223.0612	-5.4	Scherzo (-)
3,5-Dimethoxy-4-hydroxycinnamic acid	11.4	C11H12O5	225.0763	225.0758	-2.4	Scherzo (+)
3,5-Dimethoxy-4-hydroxycinnamic acid	14.2	C11H12O5	225.0762	225.0758	-2.0	PFP (+)
3,6,4'-Trihydroxyflavone	12.3	C15H10O5	269.0467	269.0456	-4.3	Scherzo (-)
3alpha-Hydroxy-7-oxo-5beta-cholanic acid	14.6	C24H38O4	391.2835	391.2843	2.0	Scherzo (+)
3alpha-Hydroxy-7-oxo-5beta-cholanic acid	15.1	C24H38O4	391.2844	391.2843	-0.3	Scherzo (+)
3alpha-Hydroxy-7-oxo-5beta-cholanic acid	16.4	C24H38O4	391.2845	391.2843	-0.5	Scherzo (+)
3',4',5,7-Tetrahydroxy-3-methoxyflavone	14.8	C16H12O7	317.0662	317.0656	-2.0	Scherzo (+)
4-Aminobenzoic acid	8.0	C7H7NO2	138.0548	138.0550	1.2	Scherzo (+)
4-Ethoxybenzoic acid	14.1	C9H10O3	167.0704	167.0703	-0.8	Scherzo (+)
4-Ethoxybenzoic acid	17.6	C9H10O3	167.0705	167.0703	-1.4	Scherzo (+)
4-Guanidinobutanoic acid	2.3	C5H11N3O2	146.0924	146.0924	0.0	Scherzo (+)
4-Hydroxy-L-glutamic acid	3.2	C5H9NO5	164.0558	164.0554	-2.7	Scherzo (+)
4-Hydroxybenzaldehyde	4.0	C7H6O2	123.0444	123.0441	-2.8	Scherzo (+)
4-Hydroxybenzaldehyde	3.0	C7H6O2	123.0444	123.0441	-2.8	PFP (+)
4-Hydroxybenzoic acid	10.3	C7H6O3	137.0246	137.0244	-1.3	PFP (-)

4-Hydroxybenzoic acid	14.8	C7H6O3	137.0244	137.0244	0.1	PFP (-)
4-Hydroxybenzoic acid	10.2	C7H6O3	139.0386	139.0390	2.7	PFP (+)
4-Hydroxybenzoic acid	9.6	C7H6O3	139.0389	139.0390	0.5	Scherzo (+)
4-Hydroxyisophthalic acid	9.2	C8H6O5	181.0141	181.0143	0.8	PFP (-)
4-Hydroxyisophthalic acid	14.1	C8H6O5	181.0144	181.0143	-0.8	PFP (-)
4-Hydroxyquinoline-2-carbaldehyde	11.3	C10H7NO2	172.0405	172.0404	-0.6	PFP (-)
4-Imidazoleacrylic acid	2.5	C6H6N2O2	139.0502	139.0502	0.0	Scherzo (+)
4-Imidazoleacrylic acid	2.4	C6H6N2O2	139.0500	139.0502	1.4	PFP (+)
4-Methylquinolin-2-ol	13.4	C10H9NO	158.0609	158.0611	1.5	PFP (-)
4-Pyridoxic acid	4.7	C8H9NO4	182.0460	182.0459	-0.7	PFP (-)
4-Pyridoxic acid	6.0	C8H9NO4	182.0463	182.0459	-2.3	PFP (-)
4-Pyridoxic acid	4.3	C8H9NO4	182.0469	182.0459	-5.6	Scherzo (-)
4-Pyridoxic acid	6.7	C8H9NO4	182.0465	182.0459	-3.4	Scherzo (-)
4-Pyridoxic acid	6.6	C8H9NO4	184.0607	184.0604	-1.5	Scherzo (+)
4-Pyridoxic acid	6.0	C8H9NO4	184.0608	184.0604	-2.0	PFP (+)
5-(2-Hydroxyethyl)-4-methylthiazole	4.5	C6H9NOS	144.0477	144.0478	0.4	Scherzo (+)
5-(2-Hydroxyethyl)-4-methylthiazole	2.5	C6H9NOS	144.0475	144.0478	1.8	PFP (+)
5-(2-Hydroxyethyl)-4-methylthiazole	4.6	C6H9NOS	144.0473	144.0478	3.2	PFP (+)
5-Amino-1-naphthol	3.9	C10H9NO	160.0753	160.0757	2.4	Scherzo (+)
5-Aminovaleric acid	1.9	C5H11NO2	118.0864	118.0863	-1.2	PFP (+)
5-Hydroxyindole	10.2	C8H7NO	134.0602	134.0600	-1.2	PFP (+)
5-Hydroxyindole-3-acetic acid	10.7	C10H9NO3	190.0502	190.0510	4.1	PFP (-)
5-Hydroxyindole-3-acetic acid	11.3	C10H9NO3	190.0517	190.0510	-3.8	PFP (-)
5-Hydroxyindole-3-acetic acid	10.5	C10H9NO3	192.0660	192.0655	-2.5	Scherzo (+)
5-Hydroxyindole-3-acetic acid	10.6	C10H9NO3	192.0658	192.0655	-1.5	PFP (+)
5-Hydroxyindole-3-acetic acid	11.3	C10H9NO3	192.0660	192.0655	-2.5	PFP (+)
5-Hydroxyindole-3-acetic acid	11.7	C10H9NO3	192.0656	192.0655	-0.4	PFP (+)
5-Hydroxyindoleacetic acid	9.6	C10H9NO3	192.0659	192.0655	-2.0	Scherzo (+)
5-Hydroxyisovanillic acid	9.9	C8H8O5	183.0305	183.0299	-3.3	PFP (-)
5-Hydroxytryptophol	9.9	C10H11NO2	178.0858	178.0863	2.6	PFP (+)
5-Keto-D-gluconic acid	1.9	C6H10O7	193.0351	193.0354	1.5	PFP (-)
5-Keto-D-gluconic acid	4.0	C6H10O7	193.0361	193.0354	-3.7	Scherzo (-)
5-Methyl-2'-deoxycytidine	2.9	C10H15N3O4	242.1130	242.1135	2.2	PFP (+)
5-Methyl-5,6-Dihydrouracil	4.5	C5H8N2O2	129.0660	129.0659	-1.2	Scherzo (+)
5-Thymidylic acid	4.0	C10H15N2O8P	321.0499	321.0493	-1.8	PFP (-)
5-Thymidylic acid	4.7	C10H15N2O8P	321.0498	321.0493	-1.5	PFP (-)
5,7,3',4',5'-Pentahydroxyflavone	16.9	C15H10O7	301.0355	301.0354	-0.4	PFP (-)
5.alpha.-Pregnan-3.alpha.,17-diol-20-one 3-sulfate	15.6	C21H34O6S	413.2002	413.2003	0.3	PFP (-)

5.alpha.-Pregnan-3.alpha.,17-diol-20-one 3-sulfate	16.6	C21H34O6S	413.2001	413.2003	0.6	PFP (-)
5'-S-Methyl-5'-thioadenosine	7.5	C11H15N5O3S	298.0976	298.0968	-2.5	Scherzo (+)
6-Dimethylaminopurine	6.3	C7H9N5	164.0930	164.0931	0.4	PFP (+)
6-Dimethylaminopurine	4.5	C7H9N5	164.0928	164.0931	1.6	Scherzo (+)
6-Hydroxynicotinic acid	6.9	C6H5NO3	140.0340	140.0342	1.6	Scherzo (+)
6-Methyladenine	3.4	C6H7N5	150.0772	150.0774	1.5	PFP (+)
6-Methyladenine	7.3	C6H7N5	150.0766	150.0774	5.5	PFP (+)
6-Methyladenine	6.9	C6H7N5	150.0773	150.0774	0.8	Scherzo (+)
6,7,4'-Trihydroxyisoflavone	12.2	C15H10O5	271.0600	271.0601	0.4	Scherzo (+)
6,7,4'-Trihydroxyisoflavone	15.5	C15H10O5	271.0603	271.0601	-0.7	PFP (+)
6alpha-Mannobiose	2.6	C12H22O11	341.1103	341.1089	-4.0	Scherzo (-)
6''-O-Acetylgenistin	12.4	C23H22O11	475.1261	475.1235	-5.5	Scherzo (+)
6''-O-Acetylgenistin	12.8	C23H22O11	475.1252	475.1235	-3.6	Scherzo (+)
7-Hydroxy-3-(4-methoxyphenyl)coumarin	15.3	C16H12O4	267.0667	267.0663	-1.6	Scherzo (-)
7-Hydroxy-4-(methoxymethyl)coumarin	12.7	C11H10O4	207.0646	207.0652	2.8	PFP (+)
7-Hydroxy-4-(methoxymethyl)coumarin	16.7	C11H10O4	207.0647	207.0652	2.4	PFP (+)
7-Hydroxy-4'-methoxyflavone	15.3	C16H12O4	269.0813	269.0808	-1.7	Scherzo (+)
7-Keto-3.alpha.,12-.alpha.-dihydroxycholanic acid	13.3	C24H38O5	407.2798	407.2792	-1.5	Scherzo (+)
7-Keto-3.alpha.,12-.alpha.-dihydroxycholanic acid	14.1	C24H38O5	407.2796	407.2792	-1.0	Scherzo (+)
7-Keto-3.alpha.,12-.alpha.-dihydroxycholanic acid	14.6	C24H38O5	407.2803	407.2792	-2.7	Scherzo (+)
7-Methylguanine	2.8	C6H7N5O	164.0583	164.0578	-3.2	PFP (-)
7-Methylguanine	2.9	C6H7N5O	166.0720	166.0723	2.0	PFP (+)
7-Methylguanine	3.5	C6H7N5O	166.0727	166.0723	-2.2	Scherzo (+)
7-Methylguanosine	7.1	C11H15N5O5	298.1157	298.1146	-3.7	PFP (+)
7,8-Dehydropregnenolone	12.3	C21H30O2	315.2325	315.2319	-2.0	Scherzo (+)
7,8-Dehydropregnenolone	12.9	C21H30O2	315.2312	315.2319	2.1	Scherzo (+)
7,8-Dehydropregnenolone	15.3	C21H30O2	315.2321	315.2319	-0.8	PFP (+)
7,8-Dimethoxycoumarin	11.4	C11H10O4	207.0656	207.0652	-2.0	Scherzo (+)
7,8-Dimethoxycoumarin	14.2	C11H10O4	207.0652	207.0652	0.0	PFP (+)
7,8,4'-Trihydroxyisoflavone	11.4	C15H10O5	271.0604	271.0601	-1.1	Scherzo (+)
8-Hydroxyquinoline-2-carbaldehyde	10.5	C10H7NO2	172.0409	172.0404	-2.9	Scherzo (-)
8-Hydroxyquinoline-5-carboxylic acid	10.6	C10H7NO3	188.0357	188.0353	-2.0	PFP (-)
8-Hydroxyquinoline-5-carboxylic acid	11.8	C10H7NO3	188.0355	188.0353	-1.0	PFP (-)
8-Hydroxyquinoline-5-carboxylic acid	17.1	C10H7NO3	188.0358	188.0353	-2.6	Scherzo (-)
9,10-Dihydroxy-12Z-octadecenoic acid	16.9	C18H34O4	315.2545	315.2530	-4.8	Scherzo (+)
9,10-Dihydroxy-12Z-octadecenoic acid	17.9	C18H34O4	315.2539	315.2530	-2.9	PFP (+)

9(10)-Epoxy-12Z-octadecenoic acid	14.3	C18H32O3	297.2435	297.2424	-3.6	Scherzo (+)
9(10)-Epoxy-12Z-octadecenoic acid	15.7	C18H32O3	297.2425	297.2424	-0.3	Scherzo (+)
9(10)-Epoxy-12Z-octadecenoic acid	16.9	C18H32O3	297.2437	297.2424	-4.3	Scherzo (+)
9(10)-Epoxy-12Z-octadecenoic acid	17.9	C18H32O3	297.2433	297.2424	-3.0	PFP (+)
Acetyl-L-carnitine	2.5	C9H17NO4	204.1235	204.1230	-2.3	Scherzo (+)
Acetyl-L-carnitine	2.6	C9H17NO4	204.1235	204.1230	-2.3	Scherzo (+)
Acetyl-L-carnitine	3.8	C9H17NO4	204.1236	204.1230	-2.8	PFP (+)
Acetyl-L-Threonine	2.5	C6H11NO4	160.0619	160.0615	-2.3	PFP (-)
Acetyl-L-Threonine	4.6	C6H11NO4	160.0621	160.0615	-3.6	Scherzo (-)
Acetyl-L-Threonine	4.7	C6H11NO4	162.0761	162.0761	-0.1	Scherzo (+)
Acetylcysteine	14.2	C5H9NO3S	162.0226	162.0230	2.7	PFP (-)
Acetylcysteine	17.7	C5H9NO3S	162.0227	162.0230	2.1	PFP (-)
Acetylglycine	2.3	C4H7NO3	116.0355	116.0353	-1.6	PFP (-)
Adenine	2.3	C5H5N5	134.0473	134.0472	-0.6	PFP (-)
Adenine	4.0	C5H5N5	134.0473	134.0472	-0.6	PFP (-)
Adenine	2.3	C5H5N5	136.0620	136.0618	-1.7	PFP (+)
Adenine	4.0	C5H5N5	136.0615	136.0618	2.0	PFP (+)
Adenine	4.7	C5H5N5	136.0618	136.0618	-0.2	PFP (+)
Adenine	2.5	C5H5N5	136.0622	136.0618	-3.2	Scherzo (+)
Adenine	4.5	C5H5N5	136.0615	136.0618	2.0	Scherzo (+)
Adenosine	4.0	C10H13N5O4	266.0892	266.0895	1.1	PFP (-)
Adenosine	2.4	C10H13N5O4	268.1037	268.1040	1.2	PFP (+)
Adenosine	4.0	C10H13N5O4	268.1049	268.1040	-3.2	PFP (+)
Adenosine	4.1	C10H13N5O4	268.1054	268.1040	-5.1	Scherzo (+)
Adenosine 5-monophosphate	5.2	C10H14N5O7P	346.0567	346.0558	-2.6	Scherzo (-)
Adenosine 5-monophosphate	5.1	C10H14N5O7P	348.0710	348.0704	-1.8	Scherzo (+)
Adenylyl(3'-5')cytidine	7.1	C19H25N8O11P	571.1327	571.1308	-3.4	PFP (-)
Adenylyl(3'-5')cytidine	6.8	C19H25N8O11P	571.1324	571.1308	-2.9	Scherzo (-)
Adenylyl(3'-5')cytidine	6.7	C19H25N8O11P	573.1456	573.1453	-0.5	Scherzo (+)
Adenylyl(3'-5')cytidine	7.1	C19H25N8O11P	573.1455	573.1453	-0.3	PFP (+)
Adipic acid	7.5	C6H10O4	145.0511	145.0506	-3.2	PFP (-)
Agmatine	2.2	C5H14N4	131.1291	131.1291	0.2	Scherzo (+)
Ala-Ile	3.6	C9H18N2O3	203.1389	203.1390	0.6	Scherzo (+)
Ala-Ile-Arg	2.9	C15H30N6O4	359.2396	359.2401	1.5	PFP (+)
Ala-Ile-Lys	2.2	C15H30N4O4	331.2340	331.2340	-0.1	Scherzo (+)
Ala-Leu	4.0	C9H18N2O3	203.1396	203.1390	-2.9	Scherzo (+)
Ala-Leu	5.4	C9H18N2O3	203.1401	203.1390	-5.3	PFP (+)
Ala-Met	2.8	C8H16N2O3S	221.0956	221.0954	-0.7	PFP (+)
Ala-Phe	6.6	C12H16N2O3	237.1245	237.1234	-4.8	Scherzo (+)
Ala-Phe	8.0	C12H16N2O3	237.1235	237.1234	-0.5	PFP (+)

Ala-Ser	2.2	C6H12N2O4	177.0866	177.0870	2.1	Scherzo (+)
Ala-Thr	2.2	C7H14N2O4	191.1033	191.1026	-3.5	Scherzo (+)
Ala-Tyr	4.0	C12H16N2O4	253.1191	253.1183	-3.2	Scherzo (+)
Ala-Val	2.6	C8H16N2O3	189.1237	189.1234	-1.7	Scherzo (+)
Ala-Val	2.4	C8H16N2O3	189.1240	189.1234	-3.3	PFP (+)
Ala-Val-Arg	3.2	C14H28N6O4	345.2241	345.2245	1.1	PFP (+)
Albizziin	3.8	C4H9N3O3	146.0573	146.0571	-1.3	Scherzo (-)
Alpha-D-Glucose	1.9	C6H12O6	179.0559	179.0561	1.2	PFP (-)
Alpha-Linolenic acid	17.9	C18H30O2	279.2327	279.2319	-3.0	PFP (+)
Alpha-Linolenic acid	14.3	C18H30O2	279.2324	279.2319	-1.9	Scherzo (+)
Alpha-Linolenic acid	15.6	C18H30O2	279.2321	279.2319	-0.9	Scherzo (+)
Alpha-Linolenic acid	16.9	C18H30O2	279.2330	279.2319	-4.1	Scherzo (+)
Amino caproic acid	5.7	C6H13NO2	132.1020	132.1019	-0.7	PFP (+)
Aminocaproic acid	3.5	C6H13NO2	130.0880	130.0874	-5.0	Scherzo (-)
Apigenin 7-glucoside	14.5	C21H20O10	431.0999	431.0984	-3.5	PFP (-)
Apigenin 7-glucoside	11.3	C21H20O10	431.0997	431.0984	-3.1	Scherzo (-)
Apigenin 7-glucoside	11.3	C21H20O10	433.1143	433.1129	-3.2	Scherzo (+)
Apigenin 7-glucoside	14.5	C21H20O10	433.1131	433.1129	-0.4	PFP (+)
Apiin	10.9	C26H28O14	565.1570	565.1552	-3.2	Scherzo (+)
Arg-Ile	4.0	C12H25N5O3	288.2034	288.2030	-1.3	PFP (+)
Arg-Phe	6.5	C15H23N5O3	322.1872	322.1874	0.5	PFP (+)
Arg-Tyr	2.6	C15H23N5O4	338.1821	338.1823	0.5	Scherzo (+)
Arg-Tyr	4.0	C15H23N5O4	338.1825	338.1823	-0.7	PFP (+)
Argininosuccinic acid	2.5	C10H18N4O6	291.1309	291.1299	-3.4	Scherzo (+)
Asiatic acid	17.6	C30H48O5	487.3425	487.3429	0.8	Scherzo (-)
Asn-Ile-Arg	2.4	C16H31N7O5	402.2471	402.2459	-2.9	Scherzo (+)
Asn-Ile-Lys	2.2	C16H31N5O5	374.2415	374.2398	-4.5	Scherzo (+)
Asn-Ile-Lys	2.3	C16H31N5O5	374.2411	374.2398	-3.5	PFP (+)
Asn-Phe	6.5	C13H17N3O4	280.1303	280.1292	-4.0	Scherzo (+)
Asn-Phe	7.5	C13H17N3O4	280.1301	280.1292	-3.3	PFP (+)
Asn-Phe-Lys	3.9	C19H29N5O5	408.2237	408.2242	1.1	PFP (+)
Asn-Tyr	4.0	C13H17N3O5	296.1241	296.1241	0.0	Scherzo (+)
Asn-Tyr	5.0	C13H17N3O5	296.1241	296.1241	0.0	PFP (+)
Asp-Ile-Arg	3.5	C16H30N6O6	403.2309	403.2300	-2.3	Scherzo (+)
Asp-Ile-Arg	3.5	C16H30N6O6	403.2305	403.2300	-1.3	PFP (+)
Asp-Ile-Arg	4.2	C16H30N6O6	403.2304	403.2300	-1.1	PFP (+)
Asp-Ile-Lys	2.5	C16H30N4O6	375.2251	375.2238	-3.4	Scherzo (+)
Asp-Ile-Lys	2.4	C16H30N4O6	375.2250	375.2238	-3.2	PFP (+)
Asp-Leu	5.2	C10H18N2O5	247.1294	247.1289	-2.2	Scherzo (+)
Asp-Leu	5.7	C10H18N2O5	247.1293	247.1289	-1.8	Scherzo (+)

Asp-Leu	4.7	C10H18N2O5	247.1297	247.1289	-3.4	PFP (+)
Asp-Leu	5.7	C10H18N2O5	247.1297	247.1289	-3.4	PFP (+)
Asp-Pro	3.1	C9H14N2O5	231.0981	231.0976	-2.4	Scherzo (+)
Asp-Pro	2.4	C9H14N2O5	231.0982	231.0976	-2.8	PFP (+)
Asp-Tyr	6.0	C13H16N2O6	297.1090	297.1081	-3.0	Scherzo (+)
Asp-Tyr	5.6	C13H16N2O6	297.1090	297.1081	-3.0	PFP (+)
Asparagine	2.4	C4H8N2O3	131.0467	131.0462	-3.7	Scherzo (-)
Aspartic acid	2.7	C4H7NO4	134.0454	134.0448	-4.6	Scherzo (+)
Aspartic acid	3.2	C4H7NO4	134.0449	134.0448	-0.9	Scherzo (+)
Azelaic acid	14.3	C9H16O4	187.0981	187.0976	-2.8	PFP (-)
Azelaic acid	14.3	C9H16O4	189.1119	189.1121	1.3	PFP (+)
Azelaic acid	11.9	C9H16O4	187.0986	187.0976	-5.5	Scherzo (-)
Azelaic acid	11.9	C9H16O4	189.1132	189.1121	-5.6	Scherzo (+)
B6 pyridoxine	2.5	C8H11NO3	170.0812	170.0812	-0.2	PFP (+)
B6 pyridoxine	2.4	C8H11NO3	170.0809	170.0812	1.6	Scherzo (+)
Baicalin	13.9	C21H18O11	447.0934	447.0922	-2.7	Scherzo (+)
Benzoic acid ethyl ester	15.0	C9H10O2	151.0761	151.0754	-4.9	Scherzo (+)
Benzoic acid ethyl ester	16.6	C9H10O2	151.0752	151.0754	1.1	PFP (+)
Benzophenone	17.3	C13H10O	183.0803	183.0804	0.8	Scherzo (+)
Beta-N-Acetylglucosamine	2.7	C8H15NO6	220.0828	220.0827	-0.6	Scherzo (-)
Betaine	2.5	C5H11NO2	118.0865	118.0863	-2.0	PFP (+)
Biliverdin	14.8	C33H34N4O6	583.2568	583.2551	-2.9	Scherzo (+)
Biliverdin	17.7	C33H34N4O6	583.2546	583.2551	0.9	PFP (+)
Biocytin	8.2	C16H28N4O4S	373.1917	373.1904	-3.5	PFP (+)
Biotin	9.9	C10H16N2O3S	245.0962	245.0954	-3.1	Scherzo (+)
Butyric acid	5.6	C4H8O2	87.0453	87.0452	-1.7	PFP (-)
Caffeic acid	11.7	C9H8O4	179.0352	179.0350	-1.2	PFP (-)
Caffeic acid	10.1	C9H8O4	179.0365	179.0350	-8.5	Scherzo (-)
Caffeic acid	10.1	C9H8O4	181.0498	181.0495	-1.4	Scherzo (+)
Capric acid	17.9	C10H20O2	171.1389	171.1391	0.9	PFP (-)
Carbofuran phenol-3-ketone	11.4	C10H10O3	179.0698	179.0703	2.6	PFP (+)
Chenodeoxycholic acid	16.8	C24H40O4	391.2853	391.2854	0.2	Scherzo (-)
Chenodeoxycholic acid	17.8	C24H40O4	391.2852	391.2854	0.5	Scherzo (-)
Cholic acid	17.9	C24H40O5	407.2814	407.2803	-2.7	PFP (-)
Cholic acid	16.4	C24H40O5	407.2817	407.2803	-3.4	Scherzo (-)
Chrysoeriol	14.7	C16H12O6	299.0567	299.0561	-2.0	Scherzo (-)
Chrysoeriol	14.7	C16H12O6	301.0712	301.0707	-1.8	Scherzo (+)
cis-Jasmone	14.2	C11H16O	165.1275	165.1274	-0.7	Scherzo (+)
Citraconic acid	2.3	C5H6O4	129.0189	129.0193	3.3	PFP (-)
Citraconic acid	4.4	C5H6O4	129.0198	129.0193	-3.6	Scherzo (-)

Citraconic acid	4.5	C5H6O4	131.0337	131.0339	1.5	Scherzo (+)
Citric acid	2.4	C6H8O7	191.0203	191.0197	-3.0	PFP (-)
Citric acid	3.0	C6H8O7	191.0201	191.0197	-1.9	PFP (-)
Citric acid	2.9	C6H8O7	191.0202	191.0197	-2.5	Scherzo (-)
Citric acid	4.8	C6H8O7	191.0206	191.0197	-4.6	Scherzo (-)
Citrulline	1.9	C6H13N3O3	174.0889	174.0884	-2.8	PFP (-)
Citrulline	1.9	C6H13N3O3	176.1028	176.1030	1.0	PFP (+)
Citrulline	2.5	C6H13N3O3	174.0893	174.0884	-5.1	Scherzo (-)
Citrulline	2.5	C6H13N3O3	176.1035	176.1030	-3.0	Scherzo (+)
Coproporphyrin I	17.2	C36H38N4O8	655.2761	655.2762	0.2	Scherzo (+)
Corticosterone	14.8	C21H30O4	347.2219	347.2217	-0.6	PFP (+)
Corticosterone	11.6	C21H30O4	347.2224	347.2217	-2.0	Scherzo (+)
Cortisol	16.9	C21H30O5	363.2169	363.2166	-0.8	PFP (+)
Cortisol	14.4	C21H30O5	363.2175	363.2166	-2.5	Scherzo (+)
Creatine	2.0	C4H9N3O2	132.0771	132.0768	-2.6	PFP (+)
Creatine	2.5	C4H9N3O2	132.0771	132.0768	-2.6	Scherzo (+)
Creatinine	1.9	C4H7N3O	114.0663	114.0662	-1.0	PFP (+)
Cuminaldehyde	11.8	C10H12O	149.0958	149.0961	1.9	PFP (+)
Cyclic adenosine diphosphate ribose	3.0	C15H21N5O13P2	540.0552	540.0538	-2.5	PFP (-)
Cyclic adenosine diphosphate ribose	5.8	C15H21N5O13P2	540.0537	540.0538	0.3	Scherzo (-)
Cytidine	2.3	C9H13N3O5	244.0937	244.0928	-3.7	Scherzo (+)
Cytidine	2.0	C9H13N3O5	244.0935	244.0928	-2.9	PFP (+)
Cytidine-5'-monophospho-N-acetylneuraminic acid	6.5	C20H31N4O16P	613.1416	613.1400	-2.6	Scherzo (-)
Cytosine	2.0	C4H5N3O	112.0506	112.0505	-0.5	PFP (+)
Cytosine	7.1	C4H5N3O	112.0506	112.0505	-0.5	PFP (+)
(-)-Citramalic acid	5.6	C5H8O5	147.0301	147.0299	-1.4	Scherzo (-)
Arabinonic acid	1.9	C5H10O6	165.0412	165.0405	-4.5	PFP (-)
Arabinonic acid	2.8	C5H10O6	165.0414	165.0405	-5.7	Scherzo (-)
Arabitol	2.7	C5H12O5	151.0621	151.0612	-6.0	Scherzo (-)
Aspartic acid	1.9	C4H7NO4	132.0301	132.0302	1.0	PFP (-)
Aspartic acid	2.8	C4H7NO4	132.0309	132.0302	-5.1	Scherzo (-)
erythro-Sphinganine	15.2	C18H39NO2	302.3061	302.3054	-2.4	Scherzo (+)
Fructose 1,6-bisphosphate	3.3	C6H14O12P2	338.9892	338.9888	-1.2	Scherzo (-)
Gluconic acid	3.3	C6H12O7	195.0517	195.0510	-3.4	Scherzo (-)
Gluconic acid, .delta.-lactone	3.3	C6H10O6	179.0550	179.0550	0.1	Scherzo (+)
Glucosamine, 6-sulfate	2.5	C6H13NO8S	258.0302	258.0289	-5.0	Scherzo (-)
Glucose	2.6	C6H12O6	179.0567	179.0561	-3.3	Scherzo (-)
myo-Inositol-4-phosphate	8.6	C6H13O9P	259.0228	259.0224	-1.4	Scherzo (-)
Pipecolinic acid	2.0	C6H11NO2	130.0864	130.0863	-1.1	Scherzo (+)

Pipecolinic acid	2.8	C6H11NO2	130.0861	130.0863	1.2	Scherzo (+)
Pipecolinic acid	2.4	C6H11NO2	130.0861	130.0863	1.2	PFP (+)
Pyroglutamic acid	2.6	C5H7NO3	128.0355	128.0353	-1.4	PFP (-)
Pyroglutamic acid	2.6	C5H7NO3	128.0357	128.0353	-3.0	Scherzo (-)
Pyroglutamic acid	5.6	C5H7NO3	128.0360	128.0353	-5.3	Scherzo (-)
Quinovose	2.8	C6H12O5	163.0615	163.0612	-1.8	Scherzo (-)
Saccharic acid	5.1	C6H10O8	209.0311	209.0303	-3.9	Scherzo (-)
Xylose	1.9	C5H10O5	149.0451	149.0456	3.0	PFP (-)
Xylose	3.7	C5H10O5	149.0462	149.0456	-4.4	Scherzo (-)
Daidzein	16.3	C15H10O4	253.0510	253.0506	-1.5	PFP (-)
Daidzein	16.3	C15H10O4	255.0658	255.0652	-2.4	PFP (+)
Daidzein	13.1	C15H10O4	253.0512	253.0506	-2.3	Scherzo (-)
Daidzein	13.2	C15H10O4	255.0664	255.0652	-4.7	Scherzo (+)
Daidzein 4'-sulfate	16.3	C15H10O7S	333.0076	333.0075	-0.5	PFP (-)
Daidzin	10.3	C21H20O9	417.1199	417.1180	-4.5	Scherzo (+)
Daidzin	12.9	C21H20O9	417.1190	417.1180	-2.4	PFP (+)
Datiscin	14.4	C27H30O15	593.1541	593.1512	-4.9	PFP (-)
Deoxyadenosine	4.4	C10H13N5O3	252.1101	252.1091	-3.9	Scherzo (+)
Deoxyadenosine monophosphate	6.5	C10H14N5O6P	330.0621	330.0609	-3.6	Scherzo (-)
Deoxyadenosine monophosphate	6.5	C10H14N5O6P	332.0754	332.0755	0.2	Scherzo (+)
Deoxycytidine	2.5	C9H13N3O4	226.0838	226.0833	-2.1	Scherzo (-)
Deoxyguanosine	6.2	C10H13N5O4	266.0904	266.0895	-3.5	PFP (-)
Deoxyguanosine	6.2	C10H13N5O4	268.1047	268.1040	-2.5	PFP (+)
Deoxyguanosine	6.7	C10H13N5O4	266.0908	266.0895	-5.0	Scherzo (-)
Deoxyguanosine	6.6	C10H13N5O4	268.1051	268.1040	-4.0	Scherzo (+)
Deoxyinosine	6.2	C10H12N4O4	251.0795	251.0786	-3.7	PFP (-)
Deoxyinosine	6.7	C10H12N4O4	251.0798	251.0786	-4.9	Scherzo (-)
Deoxyuridine	4.3	C9H12N2O5	227.0679	227.0674	-2.4	PFP (-)
Deoxyuridine	5.3	C9H12N2O5	227.0683	227.0674	-4.2	Scherzo (-)
Deoxyuridine	5.2	C9H12N2O5	229.0821	229.0819	-0.9	Scherzo (+)
Diethyl phthalate	16.0	C12H14O4	223.0963	223.0965	0.9	Scherzo (+)
Diethyltoluamide	15.2	C12H17NO	192.1378	192.1383	2.6	Scherzo (+)
Dihydrodaidzein	15.7	C15H12O4	255.0668	255.0663	-2.0	PFP (-)
Dihydrodaidzein	13.1	C15H12O4	255.0670	255.0663	-2.8	Scherzo (-)
Dihydrodaidzein	13.0	C15H12O4	257.0817	257.0808	-3.3	Scherzo (+)
Dihydrodaidzein	15.6	C15H12O4	257.0814	257.0808	-2.2	PFP (+)
Dihydroisoferulic acid	13.5	C10H12O4	195.0666	195.0663	-1.6	PFP (-)
Dihydroisoferulic acid	11.4	C10H12O4	195.0664	195.0663	-0.6	Scherzo (-)
Dimethyl arginine	2.0	C8H18N4O2	203.1501	203.1503	0.7	PFP (+)
Dimethyl arginine	2.4	C8H18N4O2	203.1505	203.1503	-1.2	Scherzo (+)

Diosmetin	12.3	C16H12O6	301.0720	301.0707	-4.5	Scherzo (+)
Diosmetin	15.7	C16H12O6	301.0699	301.0707	2.5	PFP (+)
3-Phenyllactic acid	11.6	C9H10O3	165.0563	165.0557	-3.5	PFP (-)
3-Phenyllactic acid	10.9	C9H10O3	167.0706	167.0703	-2.0	Scherzo (+)
Arginine	2.2	C6H14N4O2	175.1193	175.1190	-2.0	Scherzo (+)
Arginine	2.0	C6H14N4O2	175.1192	175.1190	-1.4	PFP (+)
Indole-3-lactic acid	13.4	C11H11NO3	204.0671	204.0666	-2.4	PFP (-)
Indole-3-lactic acid	12.2	C11H11NO3	204.0677	204.0666	-5.3	Scherzo (-)
Indole-3-lactic acid	12.2	C11H11NO3	206.0817	206.0812	-2.6	Scherzo (+)
Indole-3-lactic acid	13.4	C11H11NO3	206.0813	206.0812	-0.6	PFP (+)
Isocitric acid lactone	2.4	C6H6O6	173.0095	173.0092	-2.0	PFP (-)
Isocitric acid lactone	2.7	C6H6O6	173.0094	173.0092	-1.4	PFP (-)
Leu-Val	6.8	C11H22N2O3	229.1564	229.1558	-2.7	PFP (-)
Leu-Val	7.8	C11H22N2O3	229.1564	229.1558	-2.7	PFP (-)
Leu-Val	4.3	C11H22N2O3	229.1564	229.1558	-2.7	Scherzo (-)
Leu-Val	5.1	C11H22N2O3	229.1564	229.1558	-2.7	Scherzo (-)
Leu-Val	6.1	C11H22N2O3	231.1697	231.1703	2.7	Scherzo (+)
Leu-Val	7.8	C11H22N2O3	231.1710	231.1703	-2.9	PFP (+)
Malic acid	2.0	C4H6O5	133.0145	133.0143	-1.9	PFP (-)
Malic acid	4.5	C4H6O5	133.0148	133.0143	-4.1	Scherzo (-)
Phenylalanine	12.0	C9H11NO2	166.0859	166.0863	2.2	Scherzo (+)
Phenylalanine	13.7	C9H11NO2	166.0862	166.0863	0.4	PFP (+)
Dodecanedioic acid	17.5	C12H22O4	229.1450	229.1445	-2.1	PFP (-)
Dodecanedioic acid	14.7	C12H22O4	229.1456	229.1445	-4.7	Scherzo (-)
Dodecanedioic acid	14.7	C12H22O4	231.1594	231.1591	-1.3	Scherzo (+)
Dodecyl sulfate	17.6	C12H26O4S	265.1482	265.1479	-1.1	PFP (-)
Emodin	14.4	C15H10O5	269.0461	269.0456	-2.0	PFP (-)
Emodin	15.5	C15H10O5	269.0462	269.0456	-2.4	PFP (-)
Enterolactone	11.7	C18H18O4	299.1286	299.1278	-2.7	Scherzo (+)
Enterolactone	12.6	C18H18O4	299.1283	299.1278	-1.7	Scherzo (+)
Enterolactone	14.3	C18H18O4	299.1287	299.1278	-3.0	Scherzo (+)
Enterolactone	14.2	C18H18O4	299.1279	299.1278	-0.4	PFP (+)
Enterolactone	15.4	C18H18O4	299.1287	299.1278	-3.0	PFP (+)
Enterolactone	16.5	C18H18O4	299.1283	299.1278	-1.7	PFP (+)
Equol	17.0	C15H14O3	241.0874	241.0870	-1.6	PFP (-)
Equol	14.3	C15H14O3	243.1026	243.1016	-4.2	Scherzo (+)
Equol	17.0	C15H14O3	243.1022	243.1016	-2.6	PFP (+)
Ethoxyquin	11.6	C14H19NO	218.1544	218.1539	-2.1	Scherzo (+)
Ethylmalonic acid	5.6	C5H8O4	131.0350	131.0350	-0.2	PFP (-)
Ethylmalonic acid	7.1	C5H8O4	131.0349	131.0350	0.6	Scherzo (-)

FAD	12.7	C27H33N9O15P2	784.1515	784.1499	-2.1	PFP (-)
Ferulic acid ethyl ester	15.0	C12H14O4	223.0970	223.0965	-2.3	Scherzo (+)
Ferulic acid ethyl ester	17.5	C12H14O4	223.0960	223.0965	2.2	PFP (+)
Ferulic acid methyl ester	16.5	C11H12O4	207.0668	207.0663	-2.5	PFP (-)
Ferulic acid methyl ester	13.8	C11H12O4	209.0805	209.0808	1.6	PFP (+)
Flavin Mononucleotide	12.4	C17H21N4O9P	455.0971	455.0973	0.5	PFP (-)
Flavin Mononucleotide	12.3	C17H21N4O9P	457.1111	457.1119	1.7	PFP (+)
Folate	11.4	C19H19N7O6	440.1318	440.1324	1.4	PFP (-)
Folate	11.4	C19H19N7O6	442.1476	442.1470	-1.4	PFP (+)
Folate	9.8	C19H19N7O6	440.1339	440.1324	-3.4	Scherzo (-)
Fumaric acid	2.0	C4H4O4	115.0035	115.0037	1.6	PFP (-)
Galactonic acid	1.9	C6H12O7	195.0518	195.0510	-3.9	PFP (-)
Galactonic acid	2.8	C6H12O7	195.0522	195.0510	-6.0	Scherzo (-)
Galactonic acid	3.3	C6H12O7	197.0652	197.0656	1.9	Scherzo (+)
Genistein	17.6	C15H10O5	269.0458	269.0456	-0.9	PFP (-)
Genistein	14.4	C15H10O5	271.0597	271.0601	1.5	PFP (+)
Genistein	17.6	C15H10O5	271.0604	271.0601	-1.1	PFP (+)
Genistein	13.2	C15H10O5	269.0467	269.0456	-4.3	Scherzo (-)
Genistein	14.5	C15H10O5	269.0466	269.0456	-3.9	Scherzo (-)
Genistein	14.5	C15H10O5	271.0607	271.0601	-2.2	Scherzo (+)
Genkwanin	16.7	C16H12O5	283.0618	283.0612	-2.1	PFP (-)
Genkwanin	13.3	C16H12O5	283.0615	283.0612	-1.1	Scherzo (-)
Genkwanin	16.6	C16H12O5	283.0623	283.0612	-3.9	Scherzo (-)
Gentisic acid	11.0	C7H6O4	153.0195	153.0193	-1.1	PFP (-)
Gentisic acid	14.7	C7H6O4	153.0200	153.0193	-4.4	Scherzo (-)
Gln-Leu-Arg	2.4	C17H33N7O5	416.2615	416.2616	0.2	Scherzo (+)
Glu-Gly-Arg	2.5	C13H24N6O6	361.1821	361.1830	2.5	Scherzo (+)
Glu-Ile-Arg	2.4	C17H32N6O6	417.2466	417.2456	-2.4	Scherzo (+)
Glu-Ile-Arg	6.5	C17H32N6O6	417.2454	417.2456	0.5	Scherzo (+)
Glu-Ile-Arg	3.2	C17H32N6O6	417.2465	417.2456	-2.1	PFP (+)
Glu-Ile-Arg	7.7	C17H32N6O6	417.2458	417.2456	-0.5	PFP (+)
Glu-Ile-Lys	2.2	C17H32N4O6	389.2413	389.2395	-4.7	Scherzo (+)
Glu-Ile-Lys	2.4	C17H32N4O6	389.2409	389.2395	-3.7	PFP (+)
Glu-Phe	7.0	C14H18N2O5	295.1303	295.1289	-4.9	Scherzo (+)
Glu-Phe	8.5	C14H18N2O5	295.1301	295.1289	-4.2	PFP (+)
Glu-Val	2.8	C10H18N2O5	247.1293	247.1289	-1.8	Scherzo (+)
Glu-Val	2.5	C10H18N2O5	247.1290	247.1289	-0.6	PFP (+)
Glucoheptonic acid	3.3	C7H14O8	225.0615	225.0616	0.4	Scherzo (-)
Glucosaminic acid	2.4	C6H13NO6	194.0667	194.0670	1.6	Scherzo (-)
Glucose 1-phosphate	2.2	C6H13O9P	259.0218	259.0224	2.5	PFP (-)

Glutamine	2.5	C5H10N2O3	147.0769	147.0764	-3.3	Scherzo (+)
Glutaric acid	4.7	C5H8O4	131.0351	131.0350	-0.9	PFP (-)
Glutaric acid	6.2	C5H8O4	131.0350	131.0350	-0.2	Scherzo (-)
Gly-Ile	4.7	C8H16N2O3	189.1234	189.1234	-0.2	PFP (+)
Gly-Ile-Arg	3.1	C14H28N6O4	345.2235	345.2245	2.8	PFP (+)
Gly-Leu	4.2	C8H16N2O3	189.1239	189.1234	-2.8	Scherzo (+)
Gly-Leu	5.7	C8H16N2O3	189.1241	189.1234	-3.9	PFP (+)
Gly-Leu-Arg	2.4	C14H28N6O4	345.2258	345.2245	-3.8	Scherzo (+)
Gly-Leu-Lys	2.2	C14H28N4O4	317.2183	317.2183	0.1	Scherzo (+)
Gly-Lys	2.0	C8H17N3O3	204.1344	204.1343	-0.6	Scherzo (+)
Gly-Met	2.8	C7H14N2O3S	207.0799	207.0798	-0.5	Scherzo (+)
Gly-Met	3.5	C7H14N2O3S	207.0804	207.0798	-2.9	Scherzo (+)
Gly-Met	2.8	C7H14N2O3S	207.0802	207.0798	-2.0	PFP (+)
Gly-Phe	6.6	C11H14N2O3	223.1084	223.1077	-3.0	Scherzo (+)
Gly-Phe	7.7	C11H14N2O3	223.1084	223.1077	-3.0	PFP (+)
Gly-Tyr	4.1	C11H14N2O4	239.1034	239.1026	-3.2	Scherzo (+)
Gly-Tyr	4.9	C11H14N2O4	239.1033	239.1026	-2.8	PFP (+)
Glyceric acid	1.9	C3H6O4	105.0194	105.0193	-0.7	PFP (-)
Glycerolphosphate	6.5	C3H9O6P	171.0071	171.0064	-4.1	Scherzo (-)
Glycerophosphocholine	2.5	C8H20NO6P	258.1104	258.1101	-1.2	PFP (+)
Glycerophosphocholine	2.8	C8H20NO6P	258.1111	258.1101	-3.9	Scherzo (+)
Glycyl-L-leucine	4.6	C8H16N2O3	187.1093	187.1088	-2.6	PFP (-)
Glycyl-L-leucine	5.6	C8H16N2O3	187.1093	187.1088	-2.6	PFP (-)
Glycyl-L-leucine	3.9	C8H16N2O3	187.1091	187.1088	-1.5	Scherzo (-)
Guanine	2.3	C5H5N5O	150.0421	150.0421	0.2	PFP (-)
Guanine	5.4	C5H5N5O	150.0416	150.0421	3.5	PFP (-)
Guanine	2.4	C5H5N5O	152.0567	152.0567	-0.1	PFP (+)
Guanine	5.0	C5H5N5O	152.0572	152.0567	-3.4	PFP (+)
Guanine	5.4	C5H5N5O	152.0572	152.0567	-3.4	PFP (+)
Guanine	6.2	C5H5N5O	152.0570	152.0567	-2.0	PFP (+)
Guanine	7.3	C5H5N5O	152.0566	152.0567	0.6	PFP (+)
Guanine	8.7	C5H5N5O	152.0567	152.0567	-0.1	PFP (+)
Guanine	3.1	C5H5N5O	150.0427	150.0421	-3.8	Scherzo (-)
Guanine	2.8	C5H5N5O	152.0569	152.0567	-1.4	Scherzo (+)
Guanine	6.6	C5H5N5O	152.0572	152.0567	-3.4	Scherzo (+)
Guanosine	5.4	C10H13N5O5	282.0852	282.0844	-2.9	PFP (-)
Guanosine	5.4	C10H13N5O5	284.0999	284.0990	-3.3	PFP (+)
Guanosine	6.3	C10H13N5O5	282.0858	282.0844	-5.0	Scherzo (-)
Guanosine	6.2	C10H13N5O5	284.1004	284.0990	-5.1	Scherzo (+)
Hematoporphyrin IX	16.5	C34H38N4O6	597.2743	597.2719	-4.1	PFP (-)

Heptadecasphinganine	14.4	C17H37NO2	288.2898	288.2897	-0.3	Scherzo (+)
Hexadecanedioic acid	18.0	C16H30O4	285.2075	285.2071	-1.3	PFP (-)
Hexanoyl-L-carnitine	8.9	C13H25NO4	260.1866	260.1856	-3.7	Scherzo (+)
Hexanoyl-L-carnitine	12.6	C13H25NO4	260.1856	260.1856	0.2	PFP (+)
Hippuric acid	9.5	C9H9NO3	178.0508	178.0510	1.0	PFP (-)
His-Ile	2.4	C12H20N4O3	269.1619	269.1608	-4.0	Scherzo (+)
His-Ile	2.8	C12H20N4O3	269.1618	269.1608	-3.6	PFP (+)
His-Lys	2.4	C12H21N5O3	284.1712	284.1717	1.8	PFP (+)
His-Phe	3.5	C15H18N4O3	303.1474	303.1452	-7.4	Scherzo (+)
His-Phe	4.8	C15H18N4O3	303.1461	303.1452	-3.1	PFP (+)
His-Pro	2.1	C11H16N4O3	253.1297	253.1295	-0.7	Scherzo (+)
His-Pro	1.9	C11H16N4O3	253.1300	253.1295	-1.9	PFP (+)
His-Trp	5.5	C17H19N5O3	342.1578	342.1561	-5.1	Scherzo (+)
His-Trp	8.4	C17H19N5O3	342.1575	342.1561	-4.2	PFP (+)
His-Tyr	2.4	C15H18N4O4	319.1420	319.1401	-6.0	Scherzo (+)
His-Tyr	3.0	C15H18N4O4	319.1387	319.1401	4.3	PFP (+)
His-Val	2.1	C11H18N4O3	255.1445	255.1452	2.6	Scherzo (+)
His-Val	1.9	C11H18N4O3	255.1459	255.1452	-2.9	PFP (+)
Histidine	7.6	C6H9N3O2	156.0763	156.0768	2.9	PFP (+)
Histidine	2.1	C6H9N3O2	154.0625	154.0622	-1.9	Scherzo (-)
Histidine	2.1	C6H9N3O2	156.0763	156.0768	2.9	Scherzo (+)
Homovanillic acid	10.4	C9H10O4	181.0509	181.0506	-1.5	Scherzo (-)
Hydroferulic acid	12.7	C10H12O4	195.0668	195.0663	-2.7	PFP (-)
Hydroferulic acid	10.8	C10H12O4	195.0673	195.0663	-5.2	Scherzo (-)
Hydroxyphenylacetic acid	10.0	C8H8O3	153.0548	153.0546	-1.2	PFP (+)
Hydroxyphenyllactic acid	8.7	C9H10O4	181.0514	181.0506	-4.3	PFP (-)
Hydroxyphenyllactic acid	9.0	C9H10O4	181.0514	181.0506	-4.3	Scherzo (-)
Hypoxanthine	3.3	C5H4N4O	137.0459	137.0458	-0.8	PFP (+)
Hypoxanthine	5.2	C5H4N4O	137.0453	137.0458	3.6	PFP (+)
Hypoxanthine	6.2	C5H4N4O	137.0459	137.0458	-0.8	PFP (+)
Hypoxanthine	4.2	C5H4N4O	137.0461	137.0458	-2.3	Scherzo (+)
Hypoxanthine	6.1	C5H4N4O	137.0460	137.0458	-1.5	Scherzo (+)
Hypoxanthine	6.7	C5H4N4O	137.0460	137.0458	-1.5	Scherzo (+)
Ile-Ala	2.7	C9H18N2O3	203.1394	203.1390	-1.9	Scherzo (+)
Ile-Ala	2.9	C9H18N2O3	203.1395	203.1390	-2.4	PFP (+)
Ile-Arg	2.2	C12H25N5O3	288.2041	288.2030	-3.7	Scherzo (+)
Ile-Arg	2.5	C12H25N5O3	288.2038	288.2030	-2.7	Scherzo (+)
Ile-Arg	2.4	C12H25N5O3	288.2043	288.2030	-4.4	PFP (+)
Ile-Arg	7.8	C12H25N5O3	288.2028	288.2030	0.8	PFP (+)
Ile-Asp	3.1	C10H18N2O5	247.1300	247.1289	-4.7	Scherzo (+)

Ile-Asp	3.5	C10H18N2O5	247.1275	247.1289	5.5	Scherzo (+)
Ile-Glu	2.8	C11H20N2O5	261.1452	261.1445	-2.7	Scherzo (+)
Ile-Glu	3.5	C11H20N2O5	261.1454	261.1445	-3.4	Scherzo (+)
Ile-Glu	2.9	C11H20N2O5	261.1451	261.1445	-2.3	PFP (+)
Ile-Gly	3.5	C8H16N2O3	189.1238	189.1234	-2.3	Scherzo (+)
Ile-His	2.0	C12H20N4O3	269.1605	269.1608	1.2	PFP (+)
Ile-His	7.0	C12H20N4O3	269.1596	269.1608	4.5	PFP (+)
Ile-Ile-Arg	3.5	C18H36N6O4	401.2871	401.2871	0.0	Scherzo (+)
Ile-Ile-Arg	6.4	C18H36N6O4	401.2884	401.2871	-3.3	PFP (+)
Ile-Ile-Arg	7.0	C18H36N6O4	401.2872	401.2871	-0.3	PFP (+)
Ile-Ile-Arg	7.8	C18H36N6O4	401.2867	401.2871	0.9	PFP (+)
Ile-Leu	6.9	C12H24N2O3	245.1867	245.1860	-3.0	Scherzo (+)
Ile-Leu	7.3	C12H24N2O3	245.1870	245.1860	-4.2	Scherzo (+)
Ile-Leu	9.8	C12H24N2O3	245.1866	245.1860	-2.6	PFP (+)
Ile-Leu	10.6	C12H24N2O3	245.1865	245.1860	-2.2	PFP (+)
Ile-Leu-Lys	3.5	C18H36N4O4	373.2813	373.2809	-1.0	Scherzo (+)
Ile-Leu-Lys	10.0	C18H36N4O4	373.2809	373.2809	0.1	PFP (+)
Ile-Lys	2.3	C12H25N3O3	260.1975	260.1969	-2.4	Scherzo (+)
Ile-Lys	1.9	C12H25N3O3	260.1973	260.1969	-1.7	PFP (+)
Ile-Lys	6.3	C12H25N3O3	260.1971	260.1969	-0.9	PFP (+)
Ile-Lys	6.9	C12H25N3O3	260.1972	260.1969	-1.3	PFP (+)
Ile-Met	6.3	C11H22N2O3S	263.1436	263.1424	-4.6	Scherzo (+)
Ile-Met	6.7	C11H22N2O3S	263.1433	263.1424	-3.5	Scherzo (+)
Ile-Met	8.4	C11H22N2O3S	263.1436	263.1424	-4.6	PFP (+)
Ile-Met	9.1	C11H22N2O3S	263.1430	263.1424	-2.3	PFP (+)
Ile-Phe	8.3	C15H22N2O3	279.1711	279.1703	-2.8	Scherzo (+)
Ile-Phe	8.7	C15H22N2O3	279.1685	279.1703	6.5	Scherzo (+)
Ile-Phe	12.1	C15H22N2O3	279.1710	279.1703	-2.4	PFP (+)
Ile-Pro	6.6	C11H20N2O3	229.1551	229.1547	-1.9	Scherzo (+)
Ile-Pro-Ile	8.1	C17H31N3O4	342.2387	342.2387	0.1	Scherzo (+)
Ile-Pro-Ile	8.4	C17H31N3O4	342.2400	342.2387	-3.7	Scherzo (+)
Ile-Pro-Ile	12.2	C17H31N3O4	342.2396	342.2387	-2.5	PFP (+)
Ile-Pro-Ile	12.8	C17H31N3O4	342.2390	342.2387	-0.8	PFP (+)
Ile-Ser	2.6	C9H18N2O4	219.1341	219.1339	-0.8	Scherzo (+)
Ile-Ser	2.4	C9H18N2O4	219.1340	219.1339	-0.3	PFP (+)
Ile-Thr	2.6	C10H20N2O4	233.1501	233.1496	-2.2	Scherzo (+)
Ile-Thr	2.5	C10H20N2O4	233.1503	233.1496	-3.1	PFP (+)
Ile-Trp	12.9	C17H23N3O3	318.1819	318.1812	-2.1	PFP (+)
Ile-Tyr	8.9	C15H22N2O4	295.1663	295.1652	-3.6	PFP (+)
Ile-Tyr	9.3	C15H22N2O4	295.1658	295.1652	-1.9	PFP (+)

Ile-Val	4.3	C11H22N2O3	231.1711	231.1703	-3.4	Scherzo (+)
Ile-Val	6.8	C11H22N2O3	231.1710	231.1703	-2.9	PFP (+)
Ile-Val-Arg	4.3	C17H34N6O4	387.2717	387.2714	-0.7	PFP (+)
Ile-Val-Lys	7.0	C17H34N4O4	359.2658	359.2653	-1.4	PFP (+)
Indole	9.4	C8H7N	118.0650	118.0651	1.1	PFP (+)
Indole-2-carboxylic acid	13.9	C9H7NO2	160.0398	160.0404	3.7	PFP (-)
Indole-3-carboxylic acid	12.1	C9H7NO2	160.0410	160.0404	-3.7	Scherzo (-)
Indole-6-carboxaldehyde	11.8	C9H7NO	144.0453	144.0455	1.3	PFP (-)
Indole-6-carboxaldehyde	14.4	C9H7NO	144.0460	144.0455	-3.5	PFP (-)
Indole-6-carboxaldehyde	12.3	C9H7NO	144.0460	144.0455	-3.5	Scherzo (-)
Indoleacrylic acid	16.1	C11H9NO2	186.0558	186.0561	1.3	PFP (-)
Indoleacrylic acid	13.4	C11H9NO2	186.0564	186.0561	-1.9	Scherzo (-)
Indoxyl sulfate	10.7	C8H7NO4S	212.0020	212.0023	1.4	PFP (-)
Inosine	4.3	C10H12N4O5	267.0738	267.0735	-1.2	PFP (-)
Inosine	5.2	C10H12N4O5	267.0745	267.0735	-3.8	PFP (-)
Inosine	4.6	C10H12N4O5	269.0884	269.0881	-1.3	PFP (+)
Inosine	5.2	C10H12N4O5	269.0889	269.0881	-3.2	PFP (+)
Inosine	6.3	C10H12N4O5	267.0750	267.0735	-5.7	Scherzo (-)
Inosine	6.1	C10H12N4O5	269.0891	269.0881	-3.9	Scherzo (+)
Isopentenyladenine	9.2	C10H13N5	204.1248	204.1244	-2.1	Scherzo (+)
Isopentenyladenine	12.6	C10H13N5	204.1244	204.1244	-0.1	PFP (+)
Isosakuranetin	15.9	C16H14O5	285.0776	285.0769	-2.6	Scherzo (-)
Jasmonic acid	12.0	C12H18O3	211.1329	211.1329	-0.1	PFP (+)
Kaempferol	17.6	C15H10O6	287.0551	287.0550	-0.3	PFP (+)
Kaempferol	14.7	C15H10O6	285.0402	285.0405	0.9	Scherzo (-)
Kaempferol	14.7	C15H10O6	287.0556	287.0550	-2.1	Scherzo (+)
Kaempferol-7-O-neohesperidoside	14.4	C27H30O15	595.1668	595.1658	-1.8	PFP (+)
Kynurenic acid	9.4	C10H7NO3	190.0505	190.0499	-3.3	Scherzo (+)
Kynurenic acid	17.2	C10H7NO3	190.0504	190.0499	-2.8	Scherzo (+)
Kynurenic acid	10.2	C10H7NO3	190.0501	190.0499	-1.2	PFP (+)
Kynurenic acid	10.6	C10H7NO3	190.0498	190.0499	0.4	PFP (+)
Kynurenic acid	11.8	C10H7NO3	190.0500	190.0499	-0.7	PFP (+)
Kynurenic acid	12.5	C10H7NO3	190.0501	190.0499	-1.2	PFP (+)
gamma-Glutamyglutamic acid	2.0	C10H16N2O7	275.0888	275.0885	-1.2	PFP (-)
gamma-Glutamyglutamic acid	2.4	C10H16N2O7	275.0895	275.0885	-3.7	Scherzo (-)
gamma-Glutamyglutamic acid	3.8	C10H16N2O7	275.0899	275.0885	-5.2	Scherzo (-)
gamma-Glutamyglutamic acid	3.7	C10H16N2O7	277.1045	277.1030	-5.3	Scherzo (+)
2-Hydroxyglutaric acid	2.4	C5H8O5	147.0302	147.0299	-2.0	PFP (-)
2-Hydroxyglutaric acid	4.4	C5H8O5	147.0304	147.0299	-3.4	Scherzo (-)
3-Phenyllactic acid	11.8	C9H10O3	165.0564	165.0557	-4.1	Scherzo (-)

Alanynorleucine	4.3	C9H18N2O3	203.1392	203.1390	-0.9	PFP (+)
Arginine	2.2	C6H14N4O2	173.1051	173.1044	-4.0	Scherzo (-)
Arginine	1.8	C6H14N4O2	175.1189	175.1190	0.3	Scherzo (+)
Aspartyphenylalanine	8.1	C13H16N2O5	279.0994	279.0987	-2.7	PFP (-)
Aspartyphenylalanine	8.1	C13H16N2O5	281.1142	281.1132	-3.6	PFP (+)
Aspartyphenylalanine	7.6	C13H16N2O5	279.0999	279.0987	-4.5	Scherzo (-)
Aspartyphenylalanine	7.6	C13H16N2O5	281.1144	281.1132	-4.3	Scherzo (+)
Carnitine	2.0	C7H15NO3	162.1122	162.1125	1.7	PFP (+)
Carnitine	2.4	C7H15NO3	162.1127	162.1125	-1.4	Scherzo (+)
Citrulline	2.5	C6H13N3O3	176.1031	176.1030	-0.7	Scherzo (+)
Cysteic acid	7.5	C3H7NO5S	167.9978	167.9972	-3.5	Scherzo (-)
Cysteine S-sulfate	2.2	C3H7NO5S2	199.9691	199.9693	1.0	PFP (-)
Cysteine S-sulfate	9.6	C3H7NO5S2	199.9697	199.9693	-2.1	Scherzo (-)
Cysteine S-sulfate	9.7	C3H7NO5S2	201.9840	201.9838	-0.8	Scherzo (+)
Cysteine-glutathione disulfide	3.1	C13H22N4O8S2	425.0804	425.0806	0.5	Scherzo (-)
Cysteine-glutathione disulfide	3.1	C13H22N4O8S2	427.0955	427.0952	-0.7	Scherzo (+)
Cystine	2.4	C6H12N2O4S2	239.0170	239.0166	-1.8	Scherzo (-)
Cystine	2.4	C6H12N2O4S2	241.0319	241.0311	-3.2	Scherzo (+)
Glutamate	1.9	C5H9NO4	146.0465	146.0459	-4.2	PFP (-)
Glutamate	1.9	C5H9NO4	148.0610	148.0604	-3.8	PFP (+)
Glutamate	2.6	C5H9NO4	146.0465	146.0459	-4.2	Scherzo (-)
Glutamate	2.6	C5H9NO4	148.0600	148.0604	2.9	Scherzo (+)
Glutamine	2.5	C5H10N2O3	145.0623	145.0619	-3.0	Scherzo (-)
Histidine	1.9	C6H9N3O2	156.0765	156.0768	1.6	PFP (+)
Isoleucine	3.7	C6H13NO2	130.0878	130.0874	-3.5	Scherzo (-)
Isoleucine	3.5	C6H13NO2	132.1021	132.1019	-1.4	Scherzo (+)
Lysine	2.1	C6H14N2O2	145.0985	145.0983	-1.7	Scherzo (-)
Lysine	2.0	C6H14N2O2	147.1132	147.1128	-2.7	Scherzo (+)
Methionine	2.1	C5H11NO2S	148.0440	148.0438	-1.6	PFP (-)
Methionine	8.1	C5H11NO2S	148.0436	148.0438	1.1	PFP (-)
Methionine	2.3	C5H11NO2S	150.0587	150.0583	-2.5	PFP (+)
Methionine	8.1	C5H11NO2S	150.0580	150.0583	2.2	PFP (+)
Methionine	2.8	C5H11NO2S	148.0444	148.0438	-4.3	Scherzo (-)
Methionine	2.9	C5H11NO2S	150.0587	150.0583	-2.5	Scherzo (+)
Methionine	9.2	C5H11NO2S	150.0592	150.0583	-5.8	Scherzo (+)
Methionine sulfoxide	1.9	C5H11NO3S	166.0534	166.0532	-1.0	PFP (+)
Methionine sulfoxide	2.6	C5H11NO3S	164.0389	164.0387	-1.3	Scherzo (-)
Methionine sulfoxide	2.6	C5H11NO3S	166.0536	166.0532	-2.2	Scherzo (+)
Phenylalanine	5.2	C9H11NO2	164.0724	164.0717	-4.3	PFP (-)
Phenylalanine	11.1	C9H11NO2	164.0718	164.0717	-0.6	PFP (-)

Phenylalanine	5.2	C9H11NO2	166.0868	166.0863	-3.3	PFP (+)
Phenylalanine	7.7	C9H11NO2	166.0866	166.0863	-2.0	PFP (+)
Phenylalanine	11.5	C9H11NO2	166.0864	166.0863	-0.8	PFP (+)
Phenylalanine	5.8	C9H11NO2	164.0724	164.0717	-4.3	Scherzo (-)
Phenylalanine	5.7	C9H11NO2	166.0867	166.0863	-2.6	Scherzo (+)
Pipecolic acid	2.6	C6H11NO2	130.0863	130.0863	-0.3	PFP (+)
Proline	2.1	C5H9NO2	116.0705	116.0706	0.9	PFP (+)
Propionylcarnitine	2.9	C10H19NO4	218.1386	218.1387	0.4	Scherzo (+)
Propionylcarnitine	6.4	C10H19NO4	218.1383	218.1387	1.7	PFP (+)
Saccharopine	2.5	C11H20N2O6	277.1403	277.1394	-3.2	Scherzo (+)
Threonine	2.5	C4H9NO3	120.0659	120.0655	-3.2	Scherzo (+)
Tryptophan	9.3	C11H12N2O2	203.0834	203.0826	-3.9	PFP (-)
Tryptophan	13.6	C11H12N2O2	203.0826	203.0826	0.0	PFP (-)
Tryptophan	9.4	C11H12N2O2	205.0976	205.0972	-2.2	PFP (+)
Tryptophan	7.9	C11H12N2O2	203.0832	203.0826	-3.0	Scherzo (-)
Tryptophan	7.8	C11H12N2O2	205.0978	205.0972	-3.2	Scherzo (+)
Tyrosine	3.3	C9H11NO3	180.0673	180.0666	-3.8	PFP (-)
Tyrosine	3.0	C9H11NO3	182.0819	182.0812	-4.0	PFP (+)
Tyrosine	3.6	C9H11NO3	182.0816	182.0812	-2.4	PFP (+)
Tyrosine	3.9	C9H11NO3	180.0672	180.0666	-3.2	Scherzo (-)
Tyrosine	3.0	C9H11NO3	182.0815	182.0812	-1.8	Scherzo (+)
Tyrosine	3.9	C9H11NO3	182.0818	182.0812	-3.5	Scherzo (+)
Tyrosine	11.2	C9H11NO3	182.0808	182.0812	2.0	Scherzo (+)
Tyrosine	7.0	C9H11NO3	182.0815	182.0812	-1.8	PFP (+)
Lauroyl-L-carnitine	13.6	C19H37NO4	344.2808	344.2795	-3.7	Scherzo (+)
Leu-Gln-Arg	3.5	C17H33N7O5	416.2609	416.2616	1.7	PFP (+)
Leu-Gln-Arg	15.9	C17H33N7O5	416.2635	416.2616	-4.6	PFP (+)
Leu-Gly-Lys	2.5	C14H28N4O4	317.2198	317.2183	-4.6	PFP (+)
Leu-Ile-Lys	6.9	C18H36N4O4	373.2807	373.2809	0.6	PFP (+)
Leu-Leu	11.2	C12H24N2O3	245.1866	245.1860	-2.6	PFP (+)
Leu-Leu	14.1	C12H24N2O3	245.1865	245.1860	-2.2	PFP (+)
Leu-Leu-Lys	6.2	C18H36N4O4	373.2819	373.2809	-2.6	PFP (+)
Leu-Phe	12.6	C15H22N2O3	279.1708	279.1703	-1.7	PFP (+)
Leu-Val-Lys	2.3	C17H34N4O4	359.2639	359.2653	3.8	Scherzo (+)
Luteolin	17.6	C15H10O6	285.0404	285.0405	0.2	PFP (-)
Lys-Leu	3.1	C12H25N3O3	260.1976	260.1969	-2.8	PFP (+)
Lys-Lys	2.8	C12H26N4O3	275.2089	275.2078	-4.1	PFP (+)
Lys-Trp	5.3	C17H24N4O3	333.1921	333.1921	0.1	Scherzo (+)
Lys-Trp	8.9	C17H24N4O3	333.1909	333.1921	3.7	PFP (+)
m-cresol	10.1	C7H8O	107.0499	107.0502	3.2	PFP (-)

Malonic acid	2.3	C3H4O4	103.0036	103.0037	0.8	PFP (-)
Maltotetraose	2.7	C24H42O21	665.2180	665.2146	-5.1	Scherzo (-)
Maltotriose	2.7	C18H32O16	503.1639	503.1618	-4.3	Scherzo (-)
Matairesinol	11.9	C20H22O6	359.1496	359.1489	-1.9	Scherzo (+)
Matairesinol	13.9	C20H22O6	359.1503	359.1489	-3.8	Scherzo (+)
Matairesinol	15.2	C20H22O6	359.1501	359.1489	-3.3	PFP (+)
Met-Ile	10.0	C11H22N2O3S	261.1283	261.1278	-1.8	PFP (-)
Met-Leu	7.1	C11H22N2O3S	263.1416	263.1424	3.0	Scherzo (+)
Met-Leu	10.0	C11H22N2O3S	263.1420	263.1424	1.5	PFP (+)
Met-Val	6.4	C10H20N2O3S	249.1274	249.1267	-2.6	PFP (+)
Methyl trans-cinnamate	12.0	C10H10O2	163.0748	163.0754	3.4	Scherzo (+)
Methyl trans-cinnamate	12.7	C10H10O2	163.0753	163.0754	0.4	Scherzo (+)
Mucic acid	1.9	C6H10O8	209.0302	209.0303	0.4	PFP (-)
Mucic acid	4.1	C6H10O8	209.0313	209.0303	-4.8	Scherzo (-)
Myristoleic acid	17.9	C14H26O2	227.2004	227.2006	0.7	PFP (+)
N-(4-Aminobenzoyl)-L-glutamic acid	6.3	C12H14N2O5	267.0977	267.0976	-0.6	PFP (+)
N-acetyl glutamic acid	2.8	C7H11NO5	188.0571	188.0565	-3.5	PFP (-)
N-acetyl glutamic acid	3.0	C7H11NO5	188.0566	188.0565	-0.8	PFP (-)
N-acetyl glutamic acid	5.7	C7H11NO5	188.0573	188.0565	-4.5	Scherzo (-)
N-acetyl glutamic acid	5.7	C7H11NO5	190.0708	190.0710	1.1	Scherzo (+)
N-acetyl Mannosamine	1.9	C8H15NO6	222.0971	222.0972	0.5	PFP (+)
N-acetyl Mannosamine	2.7	C8H15NO6	222.0981	222.0972	-4.0	Scherzo (+)
N-Acetyl-D-galactosamine 4-sulfate	2.3	C8H15NO9S	300.0401	300.0395	-2.1	PFP (-)
N-Acetyl-D-glucosamine 6-phosphate	9.3	C8H16NO9P	300.0499	300.0490	-3.0	Scherzo (-)
N-Acetyl-D-lactosamine	2.6	C14H25NO11	384.1506	384.1500	-1.5	Scherzo (+)
N-Acetyl-D-norleucine	11.1	C8H15NO3	172.0981	172.0979	-1.0	PFP (-)
N-Acetyl-D-norleucine	10.6	C8H15NO3	172.0986	172.0979	-4.0	Scherzo (-)
N-Acetyl-D-norleucine	12.6	C8H15NO3	172.0987	172.0979	-4.5	Scherzo (-)
N-Acetyl-DL-valine	6.6	C7H13NO3	158.0824	158.0823	-0.8	PFP (-)
N-Acetyl-DL-valine	7.8	C7H13NO3	158.0824	158.0823	-0.8	PFP (-)
N-Acetyl-DL-valine	7.2	C7H13NO3	158.0827	158.0823	-2.7	Scherzo (-)
N-Acetyl-DL-valine	8.7	C7H13NO3	158.0828	158.0823	-3.4	Scherzo (-)
N-Acetyl-DL-valine	10.7	C7H13NO3	158.0829	158.0823	-4.0	Scherzo (-)
N-Acetyl-L-alanine	5.1	C5H9NO3	130.0513	130.0510	-2.5	Scherzo (-)
N-Acetyl-L-alanine	7.5	C5H9NO3	130.0519	130.0510	-7.2	Scherzo (-)
N-Acetyl-L-alanine	5.0	C5H9NO3	132.0647	132.0655	6.2	Scherzo (+)
N-Acetyl-L-Aspartate	5.7	C6H9NO5	174.0411	174.0408	-1.7	Scherzo (-)
N-Acetyl-L-Glutamine	4.5	C7H12N2O4	187.0730	187.0724	-3.0	Scherzo (-)
N-Acetyl-L-Glutamine	4.4	C7H12N2O4	189.0871	189.0870	-0.6	Scherzo (+)
N-Acetyl-L-Leucine	10.2	C8H15NO3	172.0981	172.0979	-1.0	PFP (-)

N-Acetyl-L-Leucine	10.5	C8H15NO3	174.1123	174.1125	1.0	PFP (+)
N-Acetyl-L-Leucine	11.1	C8H15NO3	174.1125	174.1125	-0.2	PFP (+)
N-Acetyl-L-Leucine	10.6	C8H15NO3	174.1124	174.1125	0.4	Scherzo (+)
N-Acetyl-L-Methionine	7.6	C7H13NO3S	190.0547	190.0543	-1.9	PFP (-)
N-Acetyl-L-Methionine	8.1	C7H13NO3S	190.0548	190.0543	-2.4	PFP (-)
N-Acetyl-L-methionine	8.1	C7H13NO3S	192.0683	192.0689	3.1	PFP (+)
N-Acetyl-L-Methionine	9.3	C7H13NO3S	190.0550	190.0543	-3.5	Scherzo (-)
N-Acetyl-L-methionine	9.2	C7H13NO3S	192.0685	192.0689	2.0	Scherzo (+)
N-Acetyl-L-phenylalanine	12.3	C11H13NO3	206.0821	206.0823	0.8	PFP (-)
N-Acetyl-L-Phenylalanine	12.4	C11H13NO3	208.0971	208.0968	-1.3	PFP (+)
N-Acetyl-L-phenylalanine	12.0	C11H13NO3	206.0820	206.0823	1.3	Scherzo (-)
N-Acetyl-L-Phenylalanine	15.9	C11H13NO3	206.0819	206.0823	1.8	Scherzo (-)
N-Acetyl-L-Phenylalanine	12.0	C11H13NO3	208.0974	208.0968	-2.8	Scherzo (+)
N-Acetyl-L-tyrosine	9.4	C11H13NO4	222.0775	222.0772	-1.4	PFP (-)
N-Acetyl-L-tyrosine	9.3	C11H13NO4	224.0928	224.0917	-4.8	PFP (+)
N-Acetylglucosaminylasparagine	2.4	C12H21N3O8	336.1410	336.1401	-2.6	Scherzo (+)
N-Acetylglutamic acid	2.8	C7H11NO5	190.0709	190.0710	0.5	PFP (+)
N-Acetylhistamine	2.2	C7H11N3O	154.0974	154.0975	0.6	Scherzo (+)
N-Acetylhistamine	2.3	C7H11N3O	154.0973	154.0975	1.2	PFP (+)
N-Acetylputrescine	2.2	C6H14N2O	131.1180	131.1179	-0.8	Scherzo (+)
N-Caffeoyl-O-methyltyramine	15.7	C18H19NO4	312.1251	312.1241	-3.1	PFP (-)
N-Carboxyethyl-.gamma.-aminobutyric acid	2.3	C7H13NO4	176.0921	176.0917	-2.1	Scherzo (+)
N-Desmethyltramadol	17.4	C15H23NO2	250.1780	250.1802	8.6	PFP (+)
N-Formyl-L-methionine	7.3	C6H11NO3S	176.0389	176.0387	-1.2	PFP (-)
N-Formyl-L-methionine	9.3	C6H11NO3S	176.0385	176.0387	1.1	Scherzo (-)
N-Glycolylneuraminic acid	5.2	C11H19NO10	324.0945	324.0936	-2.7	Scherzo (-)
N-Glycolylneuraminic acid	5.3	C11H19NO10	326.1092	326.1082	-3.2	Scherzo (+)
N,N-Bis(2-hydroxyethyl)glycine	2.6	C6H13NO4	164.0915	164.0917	1.4	Scherzo (+)
N,N-Dimethylguanosine	7.4	C12H17N5O5	312.1318	312.1303	-5.0	Scherzo (+)
N.alpha.-Acetyl-L-lysine	2.4	C8H16N2O3	187.1089	187.1088	-0.4	Scherzo (-)
N.alpha.-Acetyl-L-lysine	1.9	C8H16N2O3	189.1238	189.1234	-2.3	PFP (+)
N.epsilon.-Acetyl-L-lysine	2.8	C8H16N2O3	189.1230	189.1234	2.0	Scherzo (+)
N6-Methyladenine	2.3	C6H7N5	150.0774	150.0774	0.1	Scherzo (+)
NAD	3.0	C21H27N7O14P2	664.1155	664.1164	1.4	PFP (+)
NAD	5.9	C21H27N7O14P2	662.1061	662.1019	-6.4	Scherzo (-)
Naringenin	17.6	C15H12O5	271.0615	271.0612	-1.1	PFP (-)
Naringenin	14.2	C15H12O5	273.0770	273.0758	-4.6	Scherzo (+)
Naringenin	17.5	C15H12O5	273.0762	273.0758	-1.6	PFP (+)
Nicotinate	2.6	C6H5NO2	122.0249	122.0248	-1.2	PFP (-)

Nicotinate	2.6	C6H5NO2	124.0395	124.0393	-1.6	PFP (+)
Nicotinate	3.6	C6H5NO2	122.0253	122.0248	-4.5	Scherzo (-)
Nicotinate	2.9	C6H5NO2	124.0394	124.0393	-0.8	Scherzo (+)
Nicotinate	3.6	C6H5NO2	124.0396	124.0393	-2.4	Scherzo (+)
Nutriacholic acid	17.8	C24H38O4	391.2852	391.2843	-2.3	PFP (+)
Nutriacholic acid	13.6	C24H38O4	391.2858	391.2843	-3.9	Scherzo (+)
Nutriacholic acid	15.7	C24H38O4	391.2857	391.2843	-3.6	Scherzo (+)
Octadecanedioic acid	15.7	C18H34O4	313.2394	313.2384	-3.1	Scherzo (-)
Octanoylcarnitine	15.9	C15H29NO4	288.2167	288.2169	0.8	PFP (+)
Oleoyl-L-carnitine	16.8	C25H47NO4	426.3589	426.3578	-2.6	Scherzo (+)
Ornithine	2.5	C5H12N2O2	131.0828	131.0826	-1.5	Scherzo (-)
Orotic acid	14.5	C5H4N2O4	155.0096	155.0098	1.5	Scherzo (-)
Oxypurinol	3.5	C5H4N4O2	151.0268	151.0262	-4.3	PFP (-)
Oxypurinol	5.0	C5H4N4O2	151.0272	151.0262	-7.0	Scherzo (-)
p-tert-Butylcatechol	16.4	C10H14O2	165.0920	165.0921	0.6	PFP (-)
p-tert-Butylcatechol	14.7	C10H14O2	165.0922	165.0921	-0.6	Scherzo (-)
Palmitic acid alkyne	14.9	C16H28O2	253.2170	253.2162	-3.1	Scherzo (+)
Palmitoylcarnitine	16.6	C23H45NO4	400.3434	400.3421	-3.1	Scherzo (+)
Palmitoylcarnitine	17.9	C23H45NO4	400.3430	400.3421	-2.1	PFP (+)
Pantothenate	6.4	C9H17NO5	218.1034	218.1034	0.0	PFP (-)
Pantothenate	6.4	C9H17NO5	220.1183	220.1180	-1.6	PFP (+)
Pantothenate	7.0	C9H17NO5	220.1184	220.1180	-2.0	Scherzo (+)
Pantothenic acid	7.1	C9H17NO5	218.1045	218.1034	-5.0	Scherzo (-)
Phe-Ala	4.5	C12H16N2O3	237.1240	237.1234	-2.7	Scherzo (+)
Phe-Ala	6.6	C12H16N2O3	237.1239	237.1234	-2.2	PFP (+)
Phe-Arg	4.4	C15H23N5O3	322.1867	322.1874	2.1	PFP (+)
Phe-Asn	4.0	C13H17N3O4	280.1294	280.1292	-0.8	PFP (+)
Phe-Asp	4.4	C13H16N2O5	281.1144	281.1132	-4.3	Scherzo (+)
Phe-Asp	5.4	C13H16N2O5	281.1141	281.1132	-3.2	PFP (+)
Phe-Asp	7.3	C13H16N2O5	281.1122	281.1132	3.6	PFP (+)
Phe-Asp-Lys	4.4	C19H28N4O6	409.2083	409.2082	-0.3	PFP (+)
Phe-Gln	5.1	C14H19N3O4	294.1452	294.1448	-1.3	PFP (+)
Phe-Glu	4.9	C14H18N2O5	295.1303	295.1289	-4.9	Scherzo (+)
Phe-Glu	6.5	C14H18N2O5	295.1300	295.1289	-3.9	PFP (+)
Phe-Gly	5.4	C11H14N2O3	223.1083	223.1077	-2.6	Scherzo (+)
Phe-Gly	6.8	C11H14N2O3	223.1083	223.1077	-2.6	PFP (+)
Phe-Ile-Lys	8.2	C21H34N4O4	407.2641	407.2653	2.9	PFP (+)
Phe-Met	7.7	C14H20N2O3S	297.1283	297.1267	-5.3	Scherzo (+)
Phe-Met	11.0	C14H20N2O3S	297.1275	297.1267	-2.6	PFP (+)
Phe-Phe	9.0	C18H20N2O3	313.1558	313.1547	-3.6	Scherzo (+)

Phe-Phe	13.5	C18H20N2O3	313.1554	313.1547	-2.3	PFP (+)
Phe-Pro	8.6	C14H18N2O3	263.1398	263.1390	-3.0	Scherzo (+)
Phe-Pro	11.7	C14H18N2O3	263.1395	263.1390	-1.8	PFP (+)
Phe-Ser	4.4	C12H16N2O4	253.1186	253.1183	-1.3	PFP (+)
Phe-Thr	3.7	C13H18N2O4	267.1350	267.1339	-4.0	Scherzo (+)
Phe-Thr	5.0	C13H18N2O4	267.1347	267.1339	-2.9	PFP (+)
Phe-Trp	9.4	C20H21N3O3	352.1673	352.1656	-4.9	Scherzo (+)
Phe-Tyr	7.7	C18H20N2O4	329.1512	329.1496	-4.9	Scherzo (+)
Phe-Tyr	10.9	C18H20N2O4	329.1508	329.1496	-3.7	PFP (+)
Phe-Val	6.9	C14H20N2O3	265.1556	265.1547	-3.5	Scherzo (+)
Phe-Val	9.8	C14H20N2O3	265.1552	265.1547	-2.0	PFP (+)
Phe-Val-Lys	6.5	C20H32N4O4	393.2501	393.2496	-1.2	PFP (+)
Phenylacetaldehyde	11.6	C8H8O	119.0500	119.0502	2.0	PFP (-)
Phenylacetaldehyde	12.4	C8H8O	119.0497	119.0502	4.5	PFP (-)
Phenylacetaldehyde	13.2	C8H8O	119.0499	119.0502	2.9	PFP (-)
Phenylacetaldehyde	3.9	C8H8O	121.0650	121.0648	-1.7	Scherzo (+)
Phenylacetaldehyde	11.0	C8H8O	121.0650	121.0648	-1.7	Scherzo (+)
Phenylacetaldehyde	11.8	C8H8O	121.0646	121.0648	1.6	Scherzo (+)
Phenylacetaldehyde	11.6	C8H8O	121.0649	121.0648	-0.9	PFP (+)
Phenylacetaldehyde	12.4	C8H8O	121.0648	121.0648	-0.1	PFP (+)
Phenylacetylglycine	11.3	C10H11NO3	192.0671	192.0666	-2.5	Scherzo (-)
Phloroglucinolcarboxylic acid	11.1	C7H6O5	169.0133	169.0143	5.6	PFP (-)
Phosphorylcholine	2.4	C5H14NO4P	184.0731	184.0733	1.2	PFP (+)
Phosphorylcholine	2.8	C5H14NO4P	184.0734	184.0733	-0.4	Scherzo (+)
Phthalic anhydride	16.0	C8H4O3	149.0238	149.0233	-3.2	Scherzo (+)
Phthalic anhydride	17.7	C8H4O3	149.0241	149.0233	-5.2	PFP (+)
Phytosphingosine	14.4	C18H39NO3	318.3015	318.3003	-3.9	Scherzo (+)
Pro-Ala	2.3	C8H14N2O3	187.1081	187.1077	-2.0	Scherzo (+)
Pro-Ala	2.0	C8H14N2O3	187.1077	187.1077	0.1	PFP (+)
Pro-Arg	2.4	C11H21N5O3	272.1724	272.1717	-2.5	PFP (+)
Pro-Leu	4.3	C11H20N2O3	229.1553	229.1547	-2.7	Scherzo (+)
Pro-Leu	5.0	C11H20N2O3	229.1552	229.1547	-2.3	Scherzo (+)
Pro-Lys-Arg	16.3	C17H33N7O4	400.2685	400.2667	-4.5	PFP (+)
Pro-Phe	9.6	C14H18N2O3	263.1399	263.1390	-3.3	PFP (+)
Pro-Thr	1.9	C9H16N2O4	217.1182	217.1183	0.4	PFP (+)
Pro-Trp	11.4	C16H19N3O3	302.1495	302.1499	1.4	PFP (+)
Pro-Tyr	6.5	C14H18N2O4	279.1339	279.1339	0.1	PFP (+)
Pro-Val	3.2	C10H18N2O3	215.1392	215.1390	-0.8	PFP (+)
Pro-Val	4.3	C10H18N2O3	215.1385	215.1390	2.4	PFP (+)
Pygenic acid C	16.7	C30H48O6	503.3375	503.3378	0.6	Scherzo (-)

PyroGlu-Met	8.3	C10H16N2O4S	261.0902	261.0904	0.6	PFP (+)
PyroGlu-Phe	7.1	C14H16N2O4	277.1193	277.1183	-3.7	Scherzo (+)
PyroGlu-Phe	11.8	C14H16N2O4	277.1195	277.1183	-4.4	Scherzo (+)
PyroGlu-Phe	8.5	C14H16N2O4	277.1189	277.1183	-2.2	PFP (+)
PyroGlu-Pro	3.6	C10H14N2O4	227.1030	227.1026	-1.6	Scherzo (+)
PyroGlu-Pro	7.7	C10H14N2O4	227.1030	227.1026	-1.6	Scherzo (+)
PyroGlu-Pro	7.4	C10H14N2O4	227.1025	227.1026	0.6	PFP (+)
PyroGlu-Tyr	9.6	C14H16N2O5	293.1138	293.1132	-2.0	Scherzo (+)
PyroGlu-Tyr	5.8	C14H16N2O5	293.1127	293.1132	1.7	PFP (+)
PyroGlu-Tyr	9.5	C14H16N2O5	293.1131	293.1132	0.3	PFP (+)
PyroGlu-Val	2.6	C10H16N2O4	229.1184	229.1183	-0.5	PFP (+)
Pyroglutamic acid	1.9	C5H7NO3	130.0506	130.0499	-5.6	PFP (+)
Pyroglutamic acid	2.6	C5H7NO3	130.0500	130.0499	-1.0	PFP (+)
Pyroglutamic acid	2.6	C5H7NO3	130.0494	130.0499	3.6	Scherzo (+)
Pyroglutamic acid	5.6	C5H7NO3	130.0500	130.0499	-1.0	Scherzo (+)
Quinaldic acid	11.3	C10H7NO2	174.0546	174.0550	2.1	PFP (+)
Quinaldic acid	10.5	C10H7NO2	174.0547	174.0550	1.5	Scherzo (+)
Quinolin-2-ol	6.7	C9H7NO	144.0451	144.0455	2.7	PFP (-)
Quinolin-2-ol	10.6	C9H7NO	144.0455	144.0455	-0.1	PFP (-)
Quinolin-2-ol	11.3	C9H7NO	144.0450	144.0455	3.4	PFP (-)
Quinolin-2-ol	17.1	C9H7NO	144.0460	144.0455	-3.5	Scherzo (-)
Quinolin-3-ol	9.6	C9H7NO	144.0461	144.0455	-4.2	Scherzo (-)
Quinolin-3-ol	6.7	C9H7NO	146.0598	146.0600	1.6	PFP (+)
Quinoline-2,4-diol	7.0	C9H7NO2	160.0401	160.0404	1.9	PFP (-)
Quinoline-2,4-diol	11.4	C9H7NO2	160.0405	160.0404	-0.6	Scherzo (-)
Quinoline-2,4-diol	11.4	C9H7NO2	162.0551	162.0550	-0.9	Scherzo (+)
Quinoline-2,4-diol	13.9	C9H7NO2	162.0547	162.0550	1.6	PFP (+)
Quinoline-2,8-diol	8.2	C9H7NO2	162.0550	162.0550	-0.2	PFP (+)
Resorcinol	8.6	C6H6O2	109.0294	109.0295	0.9	PFP (-)
Resveratrol	15.5	C14H12O3	227.0723	227.0714	-4.1	PFP (-)
Riboflavin	11.7	C17H20N4O6	375.1321	375.1310	-2.9	PFP (-)
Riboflavin	11.7	C17H20N4O6	377.1462	377.1456	-1.7	PFP (+)
Riboflavin	9.6	C17H20N4O6	375.1315	375.1310	-1.3	Scherzo (-)
Riboflavin	9.6	C17H20N4O6	377.1468	377.1456	-3.3	Scherzo (+)
S-Adenosyl-L-methionine	2.3	C15H22N6O5S	399.1443	399.1445	0.6	PFP (+)
Sabinene	16.9	C10H16	137.1318	137.1325	5.0	Scherzo (+)
Sarcosine	2.0	C3H7NO2	90.0552	90.0550	-2.7	PFP (+)
Schaftoside	13.1	C26H28O14	563.1442	563.1406	-6.3	PFP (-)
Schaftoside	13.5	C26H28O14	563.1440	563.1406	-6.0	PFP (-)
Schaftoside	10.0	C26H28O14	563.1435	563.1406	-5.1	Scherzo (-)

Schaftoside	10.0	C26H28O14	565.1576	565.1552	-4.3	Scherzo (+)
Schaftoside	13.1	C26H28O14	565.1558	565.1552	-1.1	PFP (+)
Schaftoside	13.5	C26H28O14	565.1562	565.1552	-1.8	PFP (+)
Sebacic acid	15.4	C10H18O4	201.1135	201.1132	-1.3	PFP (-)
Sebacic acid	12.8	C10H18O4	201.1139	201.1132	-3.3	Scherzo (-)
Ser-Glu	2.3	C8H14N2O6	235.0932	235.0925	-3.1	Scherzo (+)
Ser-Ile	3.9	C9H18N2O4	219.1335	219.1339	2.0	PFP (+)
Ser-Leu	3.8	C9H18N2O4	219.1341	219.1339	-0.8	Scherzo (+)
Ser-Leu	4.7	C9H18N2O4	219.1343	219.1339	-1.7	PFP (+)
Ser-Leu-Lys	2.2	C15H30N4O5	347.2300	347.2289	-3.2	Scherzo (+)
Ser-Leu-Lys	2.4	C15H30N4O5	347.2286	347.2289	0.9	PFP (+)
Ser-Lys	2.0	C9H19N3O4	234.1452	234.1448	-1.6	Scherzo (+)
Ser-Met	2.8	C8H16N2O4S	237.0912	237.0904	-3.5	Scherzo (+)
Ser-Met	2.6	C8H16N2O4S	237.0915	237.0904	-4.8	PFP (+)
Ser-Pro	1.9	C8H14N2O4	203.1025	203.1026	0.6	PFP (+)
Ser-Thr	2.2	C7H14N2O5	207.0979	207.0976	-1.7	Scherzo (+)
Ser-Tyr	4.1	C12H16N2O5	269.1133	269.1132	-0.4	Scherzo (+)
Ser-Val	2.6	C8H16N2O4	205.1184	205.1183	-0.6	Scherzo (+)
Ser-Val	2.3	C8H16N2O4	205.1188	205.1183	-2.5	PFP (+)
Serotonin	6.1	C10H12N2O	177.1018	177.1022	2.5	PFP (+)
Sorbitol	2.6	C6H14O6	181.0717	181.0718	0.3	Scherzo (-)
Spermidine	2.1	C7H19N3	146.1652	146.1652	-0.2	Scherzo (+)
Spermidine	3.4	C7H19N3	146.1654	146.1652	-1.6	Scherzo (+)
Sphinganine	17.7	C18H39NO2	302.3061	302.3054	-2.4	PFP (+)
Sphinganine	14.3	C18H39NO2	302.3066	302.3054	-4.1	Scherzo (+)
Stachydrine	2.9	C7H13NO2	144.1020	144.1019	-0.6	PFP (+)
Stachydrine	3.7	C7H13NO2	144.1021	144.1019	-1.3	PFP (+)
Stearidonic acid	16.6	C18H28O2	277.2161	277.2162	0.4	Scherzo (+)
Stearoyl-L-carnitine	17.9	C25H49NO4	428.3742	428.3734	-1.8	Scherzo (+)
Suberic acid	12.5	C8H14O4	173.0820	173.0819	-0.4	PFP (-)
Suberic acid	10.6	C8H14O4	173.0826	173.0819	-3.9	Scherzo (-)
Succinic acid	2.9	C4H6O4	117.0195	117.0193	-1.5	PFP (-)
Syringaldehyde	15.7	C9H10O4	183.0650	183.0652	1.0	PFP (+)
Syringic acid	12.4	C9H10O5	197.0460	197.0456	-2.3	PFP (-)
Syringic acid	13.0	C9H10O5	197.0463	197.0456	-3.8	PFP (-)
Syringic acid	10.1	C9H10O5	197.0462	197.0456	-3.3	Scherzo (-)
Syringic acid	10.1	C9H10O5	199.0606	199.0601	-2.5	Scherzo (+)
Syringic acid	12.4	C9H10O5	199.0605	199.0601	-2.0	PFP (+)
Taurine	1.9	C2H7NO3S	124.0075	124.0074	-0.9	PFP (-)
Taurine	2.6	C2H7NO3S	124.0078	124.0074	-3.3	Scherzo (-)

Taurine	2.6	C2H7NO3S	126.0217	126.0219	1.9	Scherzo (+)
Taurochenodeoxycholic acid	17.2	C26H45NO6S	498.2883	498.2895	2.4	PFP (-)
Taurocholic acid	15.0	C26H45NO7S	514.2865	514.2844	-4.1	PFP (-)
Taurocholic acid	17.8	C26H45NO7S	514.2864	514.2844	-3.9	PFP (-)
Tetradecanedioic acid	17.9	C14H26O4	257.1757	257.1758	0.5	PFP (-)
Tetradecanedioic acid	16.3	C14H26O4	257.1751	257.1758	2.8	Scherzo (-)
Thiamine	2.6	C12H16N4OS	265.1127	265.1118	-3.5	PFP (+)
Thiamine	2.2	C12H16N4OS	263.0979	263.0972	-2.6	Scherzo (-)
Thiamine	2.1	C12H16N4OS	265.1127	265.1118	-3.5	Scherzo (+)
Thiamine monophosphate	2.4	C12H17N4O4PS	345.0783	345.0781	-0.6	PFP (+)
Thr-Ile-Lys	2.2	C16H32N4O5	361.2455	361.2446	-2.6	Scherzo (+)
Thr-Leu	3.8	C10H20N2O4	233.1494	233.1496	0.8	Scherzo (+)
Thr-Leu	4.1	C10H20N2O4	233.1505	233.1496	-3.9	Scherzo (+)
Thr-Leu	4.6	C10H20N2O4	233.1500	233.1496	-1.8	PFP (+)
Thr-Leu	5.7	C10H20N2O4	233.1503	233.1496	-3.1	PFP (+)
Thr-Lys	2.0	C10H21N3O4	248.1606	248.1605	-0.5	Scherzo (+)
Thr-Met	3.4	C9H18N2O4S	251.1072	251.1060	-4.7	Scherzo (+)
Thr-Met	2.9	C9H18N2O4S	251.1073	251.1060	-5.1	PFP (+)
Thr-Phe	6.8	C13H18N2O4	267.1351	267.1339	-4.4	Scherzo (+)
Thr-Thr	2.2	C8H16N2O5	221.1133	221.1132	-0.5	Scherzo (+)
Thr-Tyr	4.2	C13H18N2O5	283.1299	283.1289	-3.7	Scherzo (+)
Thr-Tyr	4.4	C13H18N2O5	283.1299	283.1289	-3.7	Scherzo (+)
Thr-Tyr	5.3	C13H18N2O5	283.1293	283.1289	-1.6	PFP (+)
Threonic acid	1.9	C4H8O5	135.0300	135.0299	-0.7	PFP (-)
Threonic acid	2.9	C4H8O5	135.0306	135.0299	-5.2	Scherzo (-)
Threonic acid	3.4	C4H8O5	135.0303	135.0299	-3.0	Scherzo (-)
Threonine	4.6	C4H9NO3	120.0653	120.0655	1.8	Scherzo (+)
Thymidine	6.7	C10H14N2O5	241.0836	241.0830	-2.5	PFP (-)
Thymidine	6.7	C10H14N2O5	243.0980	243.0976	-1.9	PFP (+)
Thymidine	7.1	C10H14N2O5	241.0834	241.0830	-1.7	Scherzo (-)
Thymidine	7.0	C10H14N2O5	243.0982	243.0976	-2.7	Scherzo (+)
Thymine	4.0	C5H6N2O2	125.0361	125.0357	-3.6	PFP (-)
Thymine	4.0	C5H6N2O2	127.0501	127.0502	0.8	PFP (+)
Thymine	6.7	C5H6N2O2	127.0503	127.0502	-0.8	PFP (+)
Thymine	5.4	C5H6N2O2	125.0359	125.0357	-2.0	Scherzo (-)
Thymine	5.3	C5H6N2O2	127.0501	127.0502	0.8	Scherzo (+)
Thymine	6.2	C5H6N2O2	127.0496	127.0502	4.7	Scherzo (+)
Thymine	7.0	C5H6N2O2	127.0506	127.0502	-3.1	Scherzo (+)
trans-2-Hydroxycinnamic acid	3.3	C9H8O3	163.0406	163.0401	-3.3	PFP (-)
trans-2-Hydroxycinnamic acid	13.2	C9H8O3	163.0403	163.0401	-1.4	PFP (-)

trans-2-Hydroxycinnamic acid	11.2	C9H8O3	163.0407	163.0401	-3.9	Scherzo (-)
trans-2-Hydroxycinnamic acid	3.0	C9H8O3	165.0548	165.0546	-1.1	Scherzo (+)
trans-2-Hydroxycinnamic acid	3.9	C9H8O3	165.0549	165.0546	-1.7	Scherzo (+)
trans-2-Hydroxycinnamic acid	3.0	C9H8O3	165.0549	165.0546	-1.7	PFP (+)
trans-2-Hydroxycinnamic acid	7.2	C9H8O3	165.0548	165.0546	-1.1	PFP (+)
trans-3-Coumaric acid	13.2	C9H8O3	165.0545	165.0546	0.7	PFP (+)
trans-Cinnamic acid	5.2	C9H8O2	147.0451	147.0452	0.3	PFP (-)
trans-Cinnamic acid	11.8	C9H8O2	149.0597	149.0597	0.1	Scherzo (+)
trans-Cinnamic acid	15.0	C9H8O2	149.0601	149.0597	-2.6	PFP (+)
trans-Ferulic acid	13.9	C10H10O4	193.0514	193.0506	-4.0	PFP (-)
trans-Ferulic acid	11.5	C10H10O4	193.0514	193.0506	-4.0	Scherzo (-)
trans-Ferulic acid	10.8	C10H10O4	195.0648	195.0652	2.0	Scherzo (+)
trans-Traumatic acid	17.0	C12H20O4	227.1291	227.1289	-1.0	PFP (-)
trans-Traumatic acid	14.2	C12H20O4	227.1297	227.1289	-3.6	Scherzo (-)
Tri(3-chloropropyl) phosphate	16.5	C9H18Cl3O4P	327.0090	327.0081	-2.7	Scherzo (+)
Tricin	14.6	C17H14O7	331.0822	331.0812	-2.9	Scherzo (+)
Tricin	17.9	C17H14O7	331.0816	331.0812	-1.1	PFP (+)
Trigonelline	3.1	C7H7NO2	138.0550	138.0550	-0.3	Scherzo (+)
Trp-Asn	6.2	C15H18N4O4	319.1412	319.1401	-3.5	Scherzo (+)
Trp-Asn	7.2	C15H18N4O4	319.1411	319.1401	-3.2	PFP (+)
Trp-Gln	8.0	C16H20N4O4	333.1565	333.1557	-2.3	PFP (+)
Trp-Glu	7.1	C16H19N3O5	334.1417	334.1398	-5.8	Scherzo (+)
Trp-Glu	8.9	C16H19N3O5	334.1405	334.1398	-2.2	PFP (+)
Trp-Ile	9.1	C17H23N3O3	318.1828	318.1812	-5.0	Scherzo (+)
Trp-Ile	13.7	C17H23N3O3	318.1823	318.1812	-3.4	PFP (+)
Trp-Phe	14.5	C20H21N3O3	352.1664	352.1656	-2.4	PFP (+)
Trp-Trp	9.9	C22H22N4O3	391.1776	391.1765	-2.9	Scherzo (+)
Trp-Trp	14.9	C22H22N4O3	391.1769	391.1765	-1.1	PFP (+)
Trp-Tyr	8.6	C20H21N3O4	368.1613	368.1605	-2.2	Scherzo (+)
Tyr-Ala	3.6	C12H16N2O4	253.1187	253.1183	-1.7	PFP (+)
Tyr-Asn	2.7	C13H17N3O5	296.1249	296.1241	-2.7	Scherzo (+)
Tyr-Asn	2.4	C13H17N3O5	296.1242	296.1241	-0.3	PFP (+)
Tyr-Gln	2.9	C14H19N3O5	310.1405	310.1398	-2.4	PFP (+)
Tyr-Glu	3.8	C14H18N2O6	311.1239	311.1238	-0.4	PFP (+)
Tyr-Gly	3.6	C11H14N2O4	239.1033	239.1026	-2.8	Scherzo (+)
Tyr-Gly	3.9	C11H14N2O4	239.1028	239.1026	-0.7	PFP (+)
Tyr-Ile-Lys	5.8	C21H34N4O5	423.2604	423.2602	-0.5	PFP (+)
Tyr-Ile-Lys	6.4	C21H34N4O5	423.2594	423.2602	1.9	PFP (+)
Tyr-Leu	10.2	C15H22N2O4	295.1661	295.1652	-2.9	PFP (+)
Tyr-Met	6.8	C14H20N2O4S	313.1231	313.1217	-4.6	Scherzo (+)

Tyr-Met	8.3	C14H20N2O4S	313.1231	313.1217	-4.6	PFP (+)
Tyr-Phe	8.2	C18H20N2O4	329.1504	329.1496	-2.5	Scherzo (+)
Tyr-Phe	11.5	C18H20N2O4	329.1504	329.1496	-2.5	PFP (+)
Tyr-Pro	6.9	C14H18N2O4	279.1350	279.1339	-3.8	Scherzo (+)
Tyr-Pro	7.8	C14H18N2O4	279.1346	279.1339	-2.4	PFP (+)
Tyr-Ser	3.4	C12H16N2O5	269.1137	269.1132	-1.9	Scherzo (+)
Tyr-Thr	2.8	C13H18N2O5	283.1304	283.1289	-5.5	Scherzo (+)
Tyr-Thr	3.5	C13H18N2O5	283.1299	283.1289	-3.7	Scherzo (+)
Tyr-Thr	2.8	C13H18N2O5	283.1316	283.1289	-9.7	PFP (+)
Tyr-Tyr	7.0	C18H20N2O5	345.1462	345.1445	-4.9	Scherzo (+)
Tyr-Tyr	8.9	C18H20N2O5	345.1458	345.1445	-3.8	PFP (+)
Tyr-Val	5.1	C14H20N2O4	281.1507	281.1496	-4.0	Scherzo (+)
Tyr-Val-Lys	3.6	C20H32N4O5	409.2449	409.2446	-0.9	PFP (+)
Undecanedioic acid	16.9	C11H20O4	215.1296	215.1289	-3.3	PFP (-)
Undecanedioic acid	14.1	C11H20O4	215.1300	215.1289	-5.2	Scherzo (-)
Uracil	2.5	C4H4N2O2	111.0201	111.0200	-0.9	PFP (-)
Uracil	2.4	C4H4N2O2	113.0347	113.0346	-1.3	PFP (+)
Urate	2.6	C5H4N4O3	167.0216	167.0211	-3.2	PFP (-)
Urate	2.8	C5H4N4O3	169.0353	169.0356	1.9	PFP (+)
Urate	4.2	C5H4N4O3	167.0218	167.0211	-4.4	Scherzo (-)
Urate	4.1	C5H4N4O3	169.0358	169.0356	-1.1	Scherzo (+)
Ureidosuccinic acid	4.5	C5H8N2O5	175.0365	175.0361	-2.6	Scherzo (-)
Uridine	2.6	C9H12N2O6	243.0627	243.0623	-1.8	PFP (-)
Uridine	3.0	C9H12N2O6	243.0630	243.0623	-3.0	PFP (-)
Uridine	2.8	C9H12N2O6	245.0777	245.0768	-3.6	PFP (+)
Uridine	3.9	C9H12N2O6	243.0630	243.0623	-3.0	Scherzo (-)
Uridine	4.3	C9H12N2O6	243.0633	243.0623	-4.3	Scherzo (-)
Uridine	3.8	C9H12N2O6	245.0764	245.0768	1.7	Scherzo (+)
Uridine diphosphate glucose	3.1	C15H24N2O17P2	565.0486	565.0478	-1.5	PFP (-)
Urobilin	11.0	C33H42N4O6	591.3195	591.3177	-3.0	Scherzo (+)
Urobilin	17.0	C33H42N4O6	591.3186	591.3177	-1.5	PFP (+)
Val-Arg	2.2	C11H23N5O3	274.1876	274.1874	-0.8	Scherzo (+)
Val-Arg	1.9	C11H23N5O3	274.1875	274.1874	-0.5	PFP (+)
Val-Asp	2.5	C9H16N2O5	233.1141	233.1132	-3.9	Scherzo (+)
Val-Asp	2.0	C9H16N2O5	233.1134	233.1132	-0.9	PFP (+)
Val-Glu	2.5	C10H18N2O5	247.1301	247.1289	-5.1	Scherzo (+)
Val-Ile	5.0	C11H22N2O3	231.1711	231.1703	-3.4	Scherzo (+)
Val-Leu	4.8	C11H22N2O3	231.1707	231.1703	-1.6	Scherzo (+)
Val-Leu	7.2	C11H22N2O3	231.1710	231.1703	-2.9	PFP (+)
Val-Leu	8.6	C11H22N2O3	231.1712	231.1703	-3.8	PFP (+)

Val-Leu	12.3	C11H22N2O3	231.1706	231.1703	-1.2	PFP (+)
Val-Leu-Lys	3.0	C17H34N4O4	359.2662	359.2653	-2.6	PFP (+)
Val-Leu-Lys	3.7	C17H34N4O4	359.2641	359.2653	3.3	PFP (+)
Val-Phe	7.5	C14H20N2O3	265.1557	265.1547	-3.9	Scherzo (+)
Val-Phe	10.5	C14H20N2O3	265.1553	265.1547	-2.4	PFP (+)
Val-Thr	1.9	C9H18N2O4	219.1341	219.1339	-0.8	PFP (+)
Val-Trp	8.2	C16H21N3O3	304.1671	304.1656	-5.0	Scherzo (+)
Val-Trp	11.8	C16H21N3O3	304.1663	304.1656	-2.4	PFP (+)
Val-Tyr	5.5	C14H20N2O4	281.1507	281.1496	-4.0	Scherzo (+)
Val-Tyr	7.0	C14H20N2O4	281.1505	281.1496	-3.3	PFP (+)
Val-Val	2.9	C10H20N2O3	217.1555	217.1547	-3.8	Scherzo (+)
Val-Val	3.5	C10H20N2O3	217.1554	217.1547	-3.4	Scherzo (+)
Val-Val	4.1	C10H20N2O3	217.1555	217.1547	-3.8	PFP (+)
Xanthine	3.6	C5H4N4O2	153.0410	153.0407	-2.0	PFP (+)
Xanthine	4.5	C5H4N4O2	153.0412	153.0407	-3.3	Scherzo (+)
Xanthine	7.0	C5H4N4O2	153.0408	153.0407	-0.7	Scherzo (+)
Xanthine	6.5	C5H4N4O2	153.0404	153.0407	2.0	PFP (+)
Xanthosine	6.8	C10H12N4O6	283.0695	283.0684	-3.9	PFP (-)
Xanthosine	6.8	C10H12N4O6	285.0836	285.0830	-2.2	PFP (+)
Xanthosine	7.1	C10H12N4O6	283.0683	283.0684	0.4	Scherzo (-)
Xanthosine	7.0	C10H12N4O6	285.0838	285.0830	-2.9	Scherzo (+)
Xanthurenic acid	12.2	C10H7NO4	204.0305	204.0302	-1.3	PFP (-)
Xanthurenic acid	12.8	C10H7NO4	206.0450	206.0448	-1.1	Scherzo (+)
Xanthurenic acid	15.3	C10H7NO4	206.0449	206.0448	-0.6	Scherzo (+)
Xanthurenic acid	16.9	C10H7NO4	206.0456	206.0448	-4.0	Scherzo (+)
Xanthurenic acid	10.1	C10H7NO4	206.0457	206.0448	-4.5	PFP (+)
Xanthurenic acid	12.3	C10H7NO4	206.0450	206.0448	-1.1	PFP (+)

Table 2.10 Statistically Significant Colon Metabolites

Metabolite ID	Retention Time (min)	Chemical Formula	Fold Change DC/PC	*p*-value	Column (+/-)
2-Amino-1-naphthol	3.9	C10H9NO	-37.0	0.017	Scherzo (+)
2-Amino-1-naphthol	6.1	C10H9NO	-31.9	0.015	PFP (+)
Serotonin	4.1	C10H12N2O	-23.7	0.016	Scherzo (+)
2-Dimethylamino-6-hydroxypurine	5.9	C7H9N5O	-9.7	0.046	PFP (+)
gamma-Glu-Cys	4.4	C8H14N2O5S	-6.5	0.042	Scherzo (+)
Deoxyadenosine	4.4	C10H13N5O3	-5.7	0.015	Scherzo (+)
2'-O-Methyladenosine	6.2	C11H15N5O4	-4.9	0.043	Scherzo (+)
Xanthurenic acid	10.7	C10H7NO4	-4.5	0.005	PFP (-)
Cysteine-glutathione disulfide	6.3	C13H22N4O8S2	-4.0	0.005	Scherzo (+)
Kynurenine	5.9	C10H12N2O3	-3.9	0.032	Scherzo (+)
Kynurenine	5.7	C10H12N2O3	-3.8	0.025	PFP (+)
1H-Indole-4-carboxaldehyde	9.6	C9H7NO	-3.8	0.012	Scherzo (+)
5-Hydroxyindole-3-acetic acid	10.7	C10H9NO3	-3.7	0.001	PFP (-)
Quinoline-2,8-diol	10.7	C9H7NO2	-3.7	0.003	PFP (-)
Adenosine	4.1	C10H13N5O4	-3.6	0.028	Scherzo (+)
Nicotinate	2.6	C6H5NO2	-3.6	0.000	PFP (-)
5-Hydroxyindoleacetic acid	9.6	C10H9NO3	-3.5	0.010	Scherzo (+)
Nicotinate	3.6	C6H5NO2	-3.4	0.001	Scherzo (-)
1H-Indole-4-carboxaldehyde	10.6	C9H7NO	-3.3	0.006	PFP (+)
5-Hydroxyindoleacetic acid	10.6	C10H9NO3	-3.3	0.005	PFP (+)
Cytidine 5'-diphosphocholine	2.9	C14H26N4O11P2	-3.2	0.010	PFP (+)
Kynurenine	5.7	C10H12N2O3	-3.2	0.026	PFP (-)
Nicotinate	3.6	C6H5NO2	-3.2	0.000	Scherzo (+)
Nicotinate	2.6	C6H5NO2	-2.9	0.001	PFP (+)
Quinolin-2-ol	10.6	C9H7NO	-2.8	0.007	PFP (-)
Glutathione oxidized	3.5	C20H32N6O12S2	-2.5	0.025	Scherzo (-)
Deoxyuridine	4.3	C9H12N2O5	-2.5	0.026	PFP (-)
Orotic acid	2.9	C5H4N2O4	-2.5	0.013	PFP (-)
Glycerol 3-phosphate	6.1	C3H9O6P	-2.4	0.011	Scherzo (-)
Thymine	6.2	C5H6N2O2	-2.4	0.009	Scherzo (+)
Cytidine 5'-diphosphocholine	3.5	C14H26N4O11P2	-2.3	0.012	Scherzo (+)
N-Acetyl galactosamine	2.7	C8H15NO6	-2.2	0.015	Scherzo (+)
Pro-Ile	5.0	C11H20N2O3	-2.2	0.014	Scherzo (+)
Uridine	3.9	C9H12N2O6	-2.1	0.004	Scherzo (-)
Cytidine 5'-diphosphocholine	2.9	C14H26N4O11P2	-2.1	0.005	Scherzo (+)
alpha-L-Glu-L-Tyr	7.6	C14H18N2O6	-2.1	0.005	Scherzo (+)
Phenylalanine	9.6	C9H11NO2	-2.0	0.009	PFP (+)

gamma-Glutamyglutamic acid	2.9	C10H16N2O7	-2.0	0.007	Scherzo (-)
Glu-Met	6.8	C10H18N2O5S	-2.0	0.046	Scherzo (+)
Phenylalanine	9.0	C9H11NO2	-2.0	0.011	Scherzo (+)
O-Phospho-L-Serine	6.9	C3H8NO6P	-2.0	0.009	Scherzo (+)
gamma-Glutamyglutamic acid	2.9	C10H16N2O7	-1.9	0.006	Scherzo (+)
alpha-L-Glu-L-Tyr	7.3	C14H18N2O6	-1.9	0.028	PFP (+)
Cysteine-glutathione disulfide	3.1	C13H22N4O8S2	-1.9	0.031	Scherzo (+)
Glycerolphosphate	6.5	C3H9O6P	-1.9	0.043	Scherzo (+)
Glu-Ser	3.2	C8H14N2O6	-1.9	0.002	Scherzo (+)
gamma-Glutamyglutamic acid	3.8	C10H16N2O7	-1.9	0.000	Scherzo (-)
Amino caproic acid	8.3	C6H13NO2	-1.8	0.041	PFP (+)
Gly-Tyr	4.9	C11H14N2O4	-1.8	0.012	PFP (+)
gamma-Glutamyglutamic acid	2.1	C10H16N2O7	-1.8	0.008	PFP (+)
gamma-Glutamyglutamic acid	3.7	C10H16N2O7	-1.7	0.003	Scherzo (+)
Phenylalanine	9.1	C9H11NO2	-1.7	0.017	Scherzo (+)
Glyceric acid	1.9	C3H6O4	-1.6	0.005	PFP (-)
N-Acetyl-L-methionine	9.2	C7H13NO3S	-1.6	0.041	Scherzo (+)
N,N-Dimethylguanosine	8.3	C12H17N5O5	-1.5	0.025	PFP (+)
2-Dimethylamino-6-hydroxypurine	8.3	C7H9N5O	-1.5	0.028	PFP (+)
N.epsilon.-Acetyl-L-lysine	2.4	C8H16N2O3	-1.5	0.003	PFP (+)
NAD	5.9	C21H27N7O14P2	-1.5	0.047	Scherzo (+)
Prostaglandin E1	14.8	C20H34O5	1.5	0.028	Scherzo (-)
Pimelic acid	10.2	C7H12O4	1.5	0.024	PFP (-)
Threonic acid	1.9	C4H8O5	1.5	0.007	PFP (-)
3-Hydroxybenzaldehyde	11.2	C7H6O2	1.5	0.012	PFP (-)
3-Hydroxyoctanoic acid	14.6	C8H16O3	1.5	0.010	PFP (-)
O-phosphoryl-ethanolamine	2.5	C2H8NO4P	1.5	0.040	Scherzo (-)
3-Hydroxybutyrylcarnitine	2.6	C11H21NO5	1.5	0.022	Scherzo (+)
cis-Aconitate	4.3	C6H6O6	1.5	0.040	PFP (-)
N-(4-Aminobenzoyl)-L-glutamic acid	7.4	C12H14N2O5	1.6	0.020	Scherzo (+)
N-Acetyl-D-glucosamine 6-phosphate	8.6	C8H16NO9P	1.6	0.007	Scherzo (-)
Sarcosine	2.0	C3H7NO2	1.6	0.007	PFP (+)
Butyrylcarnitine	8.5	C11H21NO4	1.6	0.023	PFP (+)
Glutathione oxidized	5.3	C20H32N6O12S2	1.6	0.006	Scherzo (-)
Glutamine	2.5	C5H10N2O3	1.6	0.009	Scherzo (-)
Creatine	2.5	C4H9N3O2	1.6	0.000	Scherzo (+)
Adipic acid	7.5	C6H10O4	1.6	0.005	PFP (-)
Acetyl-L-carnitine	2.5	C9H17NO4	1.6	0.046	Scherzo (+)
Acetyl-L-carnitine	2.5	C9H17NO4	1.6	0.046	Scherzo (+)
Prostaglandin A1	16.4	C20H32O4	1.6	0.011	Scherzo (-)

Creatine	2.0	C4H9N3O2	1.6	0.006	PFP (+)
Dihydrofolic acid	11.4	C19H21N7O6	1.7	0.007	PFP (-)
4-Hydroxynonenal glutathione	12.8	C19H33N3O8S	1.7	0.019	PFP (+)
Azelaic acid	11.9	C9H16O4	1.7	0.035	Scherzo (+)
Beta-Alanine	2.0	C3H7NO2	1.7	0.000	PFP (-)
Citric acid	7.0	C6H8O7	1.7	0.009	Scherzo (-)
Suberic acid	12.5	C8H14O4	1.7	0.010	PFP (-)
Pimelic acid	9.3	C7H12O4	1.7	0.009	Scherzo (-)
Arsenic acid	7.1	AsH3O4	1.8	0.018	Scherzo (-)
2-Methylbutyryl-L-carnitine	10.3	C12H23NO4	1.8	0.016	PFP (+)
8-iso-Prostaglandin A1	14.8	C20H32O4	1.8	0.002	Scherzo (-)
Prostaglandin H2	17.6	C20H32O5	1.8	0.001	PFP (-)
Histidine	1.9	C6H9N3O2	1.8	0.039	PFP (-)
N,N-Dimethylaniline	3.6	C8H11N	1.8	0.006	Scherzo (+)
Allantoin	2.8	C4H6N4O3	1.8	0.007	Scherzo (-)
Biliverdin	14.8	C33H34N4O6	1.8	0.004	Scherzo (+)
Azelaic acid	14.3	C9H16O4	1.8	0.030	PFP (-)
Suberic acid	10.7	C8H14O4	1.9	0.004	Scherzo (-)
Ergothioneine	2.9	C9H15N3O2S	1.9	0.046	Scherzo (+)
Glutathione oxidized	2.8	C20H32N6O12S2	1.9	0.009	PFP (+)
Azelaic acid	14.3	C9H16O4	1.9	0.040	PFP (+)
Butyrylcarnitine	4.5	C11H21NO4	1.9	0.002	Scherzo (+)
Azelaic acid	11.9	C9H16O4	1.9	0.033	Scherzo (-)
Creatinine	1.9	C4H7N3O	1.9	0.003	PFP (+)
Glutathione oxidized	2.9	C20H32N6O12S2	1.9	0.007	PFP (-)
Lauroyl-L-carnitine	17.7	C19H37NO4	1.9	0.019	PFP (+)
Glu-Phe-Arg	7.4	C20H30N6O6	1.9	0.020	Scherzo (+)
Urate	2.6	C5H4N4O3	1.9	0.002	PFP (-)
Tetraethylene glycol	6.8	C8H18O5	1.9	0.010	Scherzo (+)
Hexanoyl-L-carnitine	12.6	C13H25NO4	2.0	0.034	PFP (+)
N-(4-Aminobenzoyl)-L-glutamic acid	7.6	C12H14N2O5	2.0	0.022	Scherzo (-)
Linoleoylcarnitine	17.8	C25H45NO4	2.0	0.012	PFP (+)
Glutathione oxidized	2.1	C20H32N6O12S2	2.0	0.019	PFP (-)
Urate	4.2	C5H4N4O3	2.0	0.001	Scherzo (-)
9-Oxoprosta-5Z,10,12Z,14E-tetraenoic acid	17.8	C20H28O3	2.0	0.000	PFP (+)
Methionine sulfoxide	2.6	C5H11NO3S	2.1	0.000	Scherzo (+)
1-Myristoyl-2-hydroxy-sn-glycero-3-phosphoethanolamine	16.1	C19H40NO7P	2.1	0.037	Scherzo (+)
Oleoyl-L-carnitine	17.9	C25H47NO4	2.1	0.022	PFP (+)
Prostaglandin A2	17.8	C20H30O4	2.1	0.000	PFP (-)

N-Acetyl-L-Glutamine	4.5	C7H12N2O4	2.2	0.015	Scherzo (-)
Prostaglandin H2	14.6	C20H32O5	2.2	0.001	Scherzo (-)
1-Myristoyl-2-hydroxy-sn-glycero-3-phosphoethanolamine	16.2	C19H40NO7P	2.3	0.036	Scherzo (-)
Urate	4.1	C5H4N4O3	2.3	0.003	Scherzo (+)
Prostaglandin A2	14.6	C20H30O4	2.3	0.001	Scherzo (-)
N-Acetyl-D-glucosamine 6-phosphate	1.9	C8H16NO9P	2.3	0.020	PFP (-)
Pyridoxal 5-phosphate	6.7	C8H10NO6P	2.3	0.007	Scherzo (+)
Adenosyl-L-methionine	2.5	C15H22N6O5S	2.3	0.034	Scherzo (+)
Ergothioneine	2.5	C9H15N3O2S	2.3	0.020	PFP (+)
Dodecyl sulfate	17.6	C12H26O4S	2.3	0.033	PFP (-)
Homovanillic acid sulfate	9.9	C9H10O7S	2.3	0.009	PFP (-)
Octanoylcarnitine	15.9	C15H29NO4	2.3	0.011	PFP (+)
Threonic acid	2.9	C4H8O5	2.4	0.005	Scherzo (-)
Hexanoyl-L-carnitine	8.9	C13H25NO4	2.4	0.024	Scherzo (+)
3-Hydroxyhexadecanoylcarnitine	15.3	C23H45NO5	2.5	0.016	Scherzo (+)
4-Hydroxybenzaldehyde	2.8	C7H6O2	2.5	0.008	PFP (+)
2-Deoxyribose 5-phosphate	9.5	C5H11O7P	2.5	0.037	Scherzo (-)
Urate	2.8	C5H4N4O3	2.6	0.003	PFP (+)
1-Myristoyl-sn-glycero-3-phosphocholine	16.6	C22H46NO7P	2.6	0.027	Scherzo (+)
Octanoylcarnitine	11.0	C15H29NO4	2.7	0.015	Scherzo (+)
Prostaglandin A2	16.1	C20H30O4	2.7	0.000	Scherzo (-)
9-Oxoprosta-5Z,10,12Z,14E-tetraenoic acid	16.1	C20H28O3	2.8	0.006	Scherzo (+)
Nicotinamide	3.5	C6H6N2O	2.8	0.010	Scherzo (+)
3-Hydroxyoleylcarnitine	15.7	C25H47NO5	2.9	0.003	Scherzo (+)
1-Oleoyl-sn-glycero-3-phosphocholine	14.9	C26H52NO7P	3.0	0.041	Scherzo (+)
3-Hydroxyhexadecanoylcarnitine	17.8	C23H45NO5	3.0	0.019	PFP (+)
Niacinamide	2.7	C6H6N2O	3.0	0.005	PFP (+)
N-Acetylaspartylglutamic acid	7.2	C11H16N2O8	3.0	0.007	Scherzo (+)
5'-S-Methyl-5'-thioadenosine	2.4	C11H15N5O3S	3.1	0.004	PFP (+)
Oleoyl-L-carnitine	16.8	C25H47NO4	3.1	0.031	Scherzo (+)
Isosteviol	14.8	C20H30O3	3.2	0.000	Scherzo (-)
2-Piperidinone	6.6	C5H9NO	3.2	0.033	PFP (+)
3,3-Dimethylacrylic acid	1.9	C5H8O2	3.4	0.016	PFP (+)
trans-2-Hydroxycinnamic acid	3.0	C9H8O3	3.4	0.042	Scherzo (+)
N-Acetyl-DL-valine	6.6	C7H13NO3	4.1	0.024	PFP (-)
1-Palmitoyl-2-hydroxy-sn-glycero-3-phosphoethanolamine	17.4	C21H44NO7P	4.2	0.004	Scherzo (-)
Glutaric acid	4.7	C5H8O4	4.4	0.004	PFP (-)
Glutathione oxidized	2.9	C20H32N6O12S2	4.4	0.013	Scherzo (-)

N-Acetyl-DL-valine	7.2	C7H13NO3	4.6	0.017	Scherzo (-)
Glutathione oxidized	2.9	C20H32N6O12S2	5.3	0.041	Scherzo (+)
Glutaric acid	6.2	C5H8O4	5.4	0.004	Scherzo (-)
1-Oleoyl-sn-glycero-3-phosphoethanolamine	16.3	C23H46NO7P	8.5	0.000	Scherzo (-)
1-Palmitoyl-2-hydroxy-sn-glycero-3-phosphoethanolamine	15.2	C21H44NO7P	9.5	0.001	Scherzo (-)
Adenosyl-L-methionine	2.3	C15H22N6O5S	13.8	0.008	PFP (+)
1,2-Dimethylimidazole	2.7	C5H8N2	16.5	0.006	PFP (+)

Table 2.11 Statistically Significant Fecal Metabolites

Metabolite ID	Retention Time (min)	Chemical Formula	Fold Change DF/PF	*p*-value	Column (+/-)
alpha-Hydroxybutyric acid	2.9	C4H8O3	-1.9	0.012	PFP (-)
Guanine	8.7	C5H5N5O	-3.2	0.017	PFP (+)
Guanine (in-source fragment)	6.2	C5H5N5O	-2.1	0.006	PFP (+)
Acetylcysteine	17.7	C5H9NO3S	-1.9	0.018	PFP (-)
Fructose 1,6-bisphosphate	3.3	C6H14O12P2	8.7	0.042	Scherzo (-)
N.alpha.-Acetyl-L-lysine	1.9	C8H16N2O3	1.7	0.017	PFP (+)
Uridine	4.3	C9H12N2O6	-2.2	0.033	Scherzo (-)
2'-Deoxycytidine	2.4	C9H13N3O4	-1.9	0.045	Scherzo (+)
Pro-Thr	1.9	C9H16N2O4	1.7	0.002	PFP (+)
Quinoline-2,4-diol	11.4	C9H7NO2	2.1	0.020	Scherzo (+)
Deoxyguanosine	6.2	C10H13N5O4	-2.5	0.028	PFP (-)
Deoxyguanosine	6.7	C10H13N5O4	-2.5	0.045	Scherzo (-)
Deoxyguanosine	6.2	C10H13N5O4	-2.1	0.006	PFP (+)
p-tert-Butylcatechol	16.4	C10H14O2	-1.5	0.007	PFP (-)
Undecanedioic acid	16.9	C11H20O4	-1.7	0.002	PFP (-)
Val-Leu	12.3	C11H22N2O3	2.7	0.008	PFP (+)
2-Hydroxyibuprofen	17.3	C13H18O3	-1.6	0.001	PFP (-)
2-Amino-4E-octadecene-1,3S-diol	17.8	C14H20N2O3	1.9	0.036	PFP (+)
Leu-Gln-Arg	3.5	C17H33N7O5	-2.2	0.012	PFP (+)
Cytidine-5'-monophospho-N-acetylneuraminic acid	6.5	C20H31N4O16P	-2.1	0.035	Scherzo (-)
Stearoyl-L-carnitine	17.9	C25H49NO4	2.3	0.001	Scherzo (+)
1-Oleoyl-sn-glycero-3-phosphocholine	14.4	C26H52NO7P	-8.9	0.009	Scherzo (+)
Coproporphyrin I	17.2	C36H38N4O8	1.7	0.033	Scherzo (+)

Table 2.12 Complete List of Quantified Mouse Proteins in Colon Samples

Accession Number	Gene ID	Protein Name	Fold Change DC/PC	*p*-value
P13595	NCAM1_MOUSE	Neural cell adhesion molecule 1	**-81.0**	0.8711
Q8R2Y2	MUC18_MOUSE	Cell surface glycoprotein MUC18	**-70.4**	0.1244
Q9CQN3	TOM6_MOUSE	Mitochondrial import receptor subunit TOM6 homolog	**-34.4**	0.2753
P49312	ROA1_MOUSE	Heterogeneous nuclear ribonucleoprotein A1	**-27.0**	0.9462
P97816	S100G_MOUSE	Protein S100-G	**-12.9**	0.0003*
P55050	FABPI_MOUSE	Fatty acid-binding protein, intestinal	**-11.3**	0.0001*
Q99JX3	GORS2_MOUSE	Golgi reassembly-stacking protein 2	**-8.5**	0.1841
Q9QZM0	UBQL2_MOUSE	Ubiquilin-2	**-7.7**	0.9121
Q9D312	K1C20_MOUSE	Keratin, type I cytoskeletal 20	**-7.5**	0.0000*
P09528	FRIH_MOUSE	Ferritin heavy chain	**-7.4**	0.0013*
P13634	CAH1_MOUSE	Carbonic anhydrase 1	**-6.8**	0.0001*
Q9D816	CP255_MOUSE	Cytochrome P450 2C55	**-6.5**	0.1040
Q9ES28	ARHG7_MOUSE	Rho guanine nucleotide exchange factor 7	**-5.1**	0.0088*
Q9D279	MISP_MOUSE	Mitotic interactor and substrate of PLK1	**-4.2**	0.0001*
Q8VI24	SATB2_MOUSE	DNA-binding protein SATB2	**-4.1**	0.0035*
Q91VR5	DDX1_MOUSE	ATP-dependent RNA helicase DDX1	**-4.1**	0.0211*
Q6URW6	MYH14_MOUSE	Myosin-14	**-4.1**	0.0072*
P29391	FRIL1_MOUSE	Ferritin light chain 1	**-4.1**	0.0000*
P07146	TRY2_MOUSE	Anionic trypsin-2	**-4.1**	0.0708
P20065	TYB4_MOUSE	Thymosin beta-4	**-4.0**	0.0007*
P59242	CING_MOUSE	Cingulin	**-4.0**	0.0029*
P55095	GLUC_MOUSE	Glucagon	**-3.8**	0.0001*
P54869	HMCS2_MOUSE	Hydroxymethylglutaryl-CoA synthase, mitochondrial	**-3.8**	0.0245*
Q9JIX8	ACINU_MOUSE	Apoptotic chromatin condensation inducer in the nucleus	**-3.8**	0.0044*
Q99P86	RETNB_MOUSE	Resistin-like beta	**-3.7**	0.0821
P16014	SCG1_MOUSE	Secretogranin-1	**-3.7**	0.0011*
Q8BK30	NDUV3_MOUSE	NADH dehydrogenase [ubiquinone] flavoprotein 3, mitochondrial	**-3.6**	0.0612
Q99K30	ES8L2_MOUSE	Epidermal growth factor receptor kinase substrate 8-like protein 2	**-3.6**	0.0005*
Q99K28	ARFG2_MOUSE	ADP-ribosylation factor GTPase-activating protein 2	**-3.3**	0.008*
Q60598	SRC8_MOUSE	Src substrate cortactin	**-3.2**	0.0005*
Q8CHP5	PYM1_MOUSE	Partner of Y14 and mago	**-3.2**	0.0591
Q91WK0	LRRF2_MOUSE	Leucine-rich repeat flightless-interacting protein 2	**-3.2**	0.0143*
Q80Z19	MUC2_MOUSE	Mucin-2	**-3.1**	0.0003*
E9Q7G0	NUMA1_MOUSE	Nuclear mitotic apparatus protein 1	**-3.1**	0.0026*
Q62393	TPD52_MOUSE	Tumor protein D52	**-3.0**	0.0001*
Q91VW5	GOGA4_MOUSE	Golgin subfamily A member 4	**-3.0**	0.3107
Q8VDM6	HNRL1_MOUSE	Heterogeneous nuclear ribonucleoprotein U-like protein 1	**-3.0**	0.0013*

P05784	K1C18_MOUSE	Keratin, type I cytoskeletal 18	**-2.9**	0.0002*
Q8BI84	TGO1_MOUSE	Melanoma inhibitory activity protein 3	**-2.9**	0.0003*
P63054	PCP4_MOUSE	Purkinje cell protein 4	**-2.8**	0.0125*
P97450	ATP5J_MOUSE	ATP synthase-coupling factor 6, mitochondrial	**-2.8**	0.0117*
P21447	MDR1A_MOUSE	Multidrug resistance protein 1A	**-2.8**	0.1481
Q99PL5	RRBP1_MOUSE	Ribosome-binding protein 1	**-2.8**	0.0000*
Q62093	SRSF2_MOUSE	Serine/arginine-rich splicing factor 2	**-2.8**	0.0569
Q99KN9	EPN4_MOUSE	Clathrin interactor 1	**-2.8**	0.0019*
Q9D1L0	CHCH2_MOUSE	Coiled-coil-helix-coiled-coil-helix domain-containing protein 2	**-2.8**	0.0000*
Q9DCV7	K2C7_MOUSE	Keratin, type II cytoskeletal 7	**-2.7**	0.0000*
Q9D7S9	CHMP5_MOUSE	Charged multivesicular body protein 5	**-2.7**	0.1603
Q91WG0	EST2C_MOUSE	Acylcarnitine hydrolase	**-2.7**	0.0277*
Q64133	AOFA_MOUSE	Amine oxidase [flavin-containing] A	**-2.7**	0.7291
Q4VAA2	CDV3_MOUSE	Protein CDV3	**-2.6**	0.0012*
Q80W00	PP1RA_MOUSE	Serine/threonine-protein phosphatase 1 regulatory subunit 10	**-2.6**	0.0019*
O35459	ECH1_MOUSE	Delta(3,5)-Delta(2,4)-dienoyl-CoA isomerase, mitochondrial	**-2.6**	0.2093
P47212	GALA_MOUSE	Galanin peptides	**-2.6**	0.0000*
P53564	CUX1_MOUSE	Homeobox protein cut-like 1	**-2.5**	0.4866
O08784	TCOF_MOUSE	Treacle protein	**-2.5**	0.2537
P09541	MYL4_MOUSE	Myosin light chain 4	**-2.5**	0.0011*
Q9DBG5	PLIN3_MOUSE	Perilipin-3	**-2.5**	0.0003*
Q6PDG5	SMRC2_MOUSE	SWI/SNF complex subunit SMARCC2	**-2.5**	0.0035*
O88312	AGR2_MOUSE	Anterior gradient protein 2 homolog	**-2.5**	0.0033*
Q9D8Y0	EFHD2_MOUSE	EF-hand domain-containing protein D2	**-2.5**	0.0000*
Q99NB9	SF3B1_MOUSE	Splicing factor 3B subunit 1	**-2.4**	0.0713
Q921F2	TADBP_MOUSE	TAR DNA-binding protein 43	**-2.4**	0.1046
O70400	PDLI1_MOUSE	PDZ and LIM domain protein 1	**-2.4**	0.0001*
Q80VJ2	SRA1_MOUSE	Steroid receptor RNA activator 1	**-2.4**	0.0037*
P15379	CD44_MOUSE	CD44 antigen	**-2.4**	0.0000*
Q6IRU5	CLCB_MOUSE	Clathrin light chain B	**-2.4**	0.0001*
P14733	LMNB1_MOUSE	Lamin-B1	**-2.4**	0.0000*
Q91WQ9	CALL4_MOUSE	Calmodulin-like protein 4	**-2.4**	0.0006*
P12787	COX5A_MOUSE	Cytochrome c oxidase subunit 5A, mitochondrial	**-2.4**	0.0391*
Q9DCL8	IPP2_MOUSE	Protein phosphatase inhibitor 2	**-2.4**	0.5311
P51125	ICAL_MOUSE	Calpastatin	**-2.4**	0.0172*
Q80X50	UBP2L_MOUSE	Ubiquitin-associated protein 2-like	**-2.3**	0.0194*
Q8BL66	EEA1_MOUSE	Early endosome antigen 1	**-2.3**	0.0307*
Q61699	HS105_MOUSE	Heat shock protein 105 kDa	**-2.3**	0.0259*
Q9DCM0	ETHE1_MOUSE	Persulfide dioxygenase ETHE1, mitochondrial	**-2.3**	0.0002*
P55012	S12A2_MOUSE	Solute carrier family 12 member 2	**-2.3**	0.0005*

Q9JLQ0	CD2AP_MOUSE	CD2-associated protein	**-2.3**	0.0000*
Q921M4	GOGA2_MOUSE	Golgin subfamily A member 2	**-2.3**	0.0369*
P61022	CHP1_MOUSE	Calcineurin B homologous protein 1	**-2.3**	0.0013*
P52503	NDUS6_MOUSE	NADH dehydrogenase [ubiquinone] iron-sulfur protein 6, mitochondrial	**-2.3**	0.0003*
Q9QXS1	PLEC_MOUSE	Plectin	**-2.3**	0.0007*
P57016	LAD1_MOUSE	Ladinin-1	**-2.3**	0.0003*
O08663	MAP2_MOUSE	Methionine aminopeptidase 2	**-2.3**	0.0018*
P21107	TPM3_MOUSE	Tropomyosin alpha-3 chain	**-2.3**	0.0039*
E9Q7P9	CDHR2_MOUSE	Cadherin-related family member 2	**-2.3**	0.0001*
Q8VDJ3	VIGLN_MOUSE	Vigilin	**-2.3**	0.1032
P99028	QCR6_MOUSE	Cytochrome b-c1 complex subunit 6, mitochondrial	**-2.3**	0.0001*
Q8BL97	SRSF7_MOUSE	Serine/arginine-rich splicing factor 7	**-2.3**	0.1334
Q62261	SPTB2_MOUSE	Spectrin beta chain, non-erythrocytic 1	**-2.2**	0.0003*
Q99K01	PDXD1_MOUSE	Pyridoxal-dependent decarboxylase domain-containing protein 1	**-2.2**	0.0112*
Q9ERS2	NDUAD_MOUSE	NADH dehydrogenase [ubiquinone] 1 alpha subcomplex subunit 13	**-2.2**	0.5463
Q61792	LASP1_MOUSE	LIM and SH3 domain protein 1	**-2.2**	0.0000*
Q02819	NUCB1_MOUSE	Nucleobindin-1	**-2.2**	0.0002*
P31428	DPEP1_MOUSE	Dipeptidase 1	**-2.2**	0.017*
P43276	H15_MOUSE	Histone H1.5	**-2.2**	0.0487
Q9Z2I0	LETM1_MOUSE	LETM1 and EF-hand domain-containing protein 1, mitochondrial	**-2.2**	0.0009*
Q61189	ICLN_MOUSE	Methylosome subunit pICln	**-2.2**	0.1117
Q99LT0	DPY30_MOUSE	Protein dpy-30 homolog	**-2.2**	0.0006*
Q9Z1D1	EIF3G_MOUSE	Eukaryotic translation initiation factor 3 subunit G	**-2.2**	0.0036*
Q922Q8	LRC59_MOUSE	Leucine-rich repeat-containing protein 59	**-2.2**	0.0184*
P19536	COX5B_MOUSE	Cytochrome c oxidase subunit 5B, mitochondrial	**-2.2**	0.0001*
P56391	CX6B1_MOUSE	Cytochrome c oxidase subunit 6B1	**-2.2**	0.0000*
Q8VEK3	HNRPU_MOUSE	Heterogeneous nuclear ribonucleoprotein U	**-2.2**	0.5473
Q6NZJ6	IF4G1_MOUSE	Eukaryotic translation initiation factor 4 gamma 1	**-2.2**	0.0002*
P70441	NHRF1_MOUSE	Na(+)/H(+) exchange regulatory cofactor NHE-RF1	**-2.1**	0.0001*
Q91VM9	IPYR2_MOUSE	Inorganic pyrophosphatase 2, mitochondrial	**-2.1**	0.0141*
P19001	K1C19_MOUSE	Keratin, type I cytoskeletal 19	**-2.1**	0.0003*
Q8R4U7	LUZP1_MOUSE	Leucine zipper protein 1	**-2.1**	0.0001*
Q6P9R2	OXSR1_MOUSE	Serine/threonine-protein kinase OSR1	**-2.1**	0.0005*
Q91WJ8	FUBP1_MOUSE	Far upstream element-binding protein 1	**-2.1**	0.0000*
Q91V76	CK054_MOUSE	Ester hydrolase C11orf54 homolog	**-2.1**	0.0076*
Q9WVA2	TIM8A_MOUSE	Mitochondrial import inner membrane translocase subunit Tim8 A	**-2.1**	0.0000*
P62960	YBOX1_MOUSE	Nuclease-sensitive element-binding protein 1	**-2.1**	0.0001*
P26645	MARCS_MOUSE	Myristoylated alanine-rich C-kinase substrate	**-2.1**	0.5655
Q08331	CALB2_MOUSE	Calretinin	**-2.0**	0.0001*
Q9JMD0	ZN207_MOUSE	BUB3-interacting and GLEBS motif-containing protein ZNF207	**-2.0**	0.0011*

Q9D1J3	SARNP_MOUSE	SAP domain-containing ribonucleoprotein	**-2.0**	0.3141
Q61595	KTN1_MOUSE	Kinectin	**-2.0**	0.1282
Q9D8X2	CC124_MOUSE	Coiled-coil domain-containing protein 124	**-2.0**	0.5056
Q9ERG0	LIMA1_MOUSE	LIM domain and actin-binding protein 1	**-2.0**	0.0007*
P11679	K2C8_MOUSE	Keratin, type II cytoskeletal 8	**-2.0**	0.0059*
P84089	ERH_MOUSE	Enhancer of rudimentary homolog	**-2.0**	0.0338*
Q64213	SF01_MOUSE	Splicing factor 1	**-2.0**	0.0000*
Q9CRB6	TPPP3_MOUSE	Tubulin polymerization-promoting protein family member 3	**-2.0**	0.0000*
P62077	TIM8B_MOUSE	Mitochondrial import inner membrane translocase subunit Tim8 B	**-2.0**	0.0028*
P30999	CTND1_MOUSE	Catenin delta-1	**-2.0**	0.4077
P81117	NUCB2_MOUSE	Nucleobindin-2	**-2.0**	0.0001*
Q3UHX2	HAP28_MOUSE	28 kDa heat- and acid-stable phosphoprotein	**-2.0**	0.0001*
Q61191	HCFC1_MOUSE	Host cell factor 1	**-2.0**	0.0009*
Q148V7	RELCH_MOUSE	LisH domain and HEAT repeat-containing protein KIAA1468	**-2.0**	0.0001*
Q99L45	IF2B_MOUSE	Eukaryotic translation initiation factor 2 subunit 2	**-2.0**	0.0485
P03995	GFAP_MOUSE	Glial fibrillary acidic protein	**-2.0**	0.0053*
P16546	SPTN1_MOUSE	Spectrin alpha chain, non-erythrocytic 1	**-2.0**	0.0039*
P22005	PENK_MOUSE	Proenkephalin-A	**-2.0**	0.1620
P29341	PABP1_MOUSE	Polyadenylate-binding protein 1	**-2.0**	0.0468*
Q8BRN9	C2D1B_MOUSE	Coiled-coil and C2 domain-containing protein 1B	**-2.0**	0.0348*
Q8R317	UBQL1_MOUSE	Ubiquilin-1	**-2.0**	0.0017*
Q9CR68	UCRI_MOUSE	Cytochrome b-c1 complex subunit Rieske, mitochondrial	**-2.0**	0.2298
Q64433	CH10_MOUSE	10 kDa heat shock protein, mitochondrial	**-2.0**	0.0004*
P45878	FKBP2_MOUSE	Peptidyl-prolyl cis-trans isomerase FKBP2	**-2.0**	0.0001*
Q05D44	IF2P_MOUSE	Eukaryotic translation initiation factor 5B	**-1.9**	0.013*
Q9Z204	HNRPC_MOUSE	Heterogeneous nuclear ribonucleoproteins C1/C2	**-1.9**	0.1149
Q6PDM2	SRSF1_MOUSE	Serine/arginine-rich splicing factor 1	**-1.9**	0.0194*
Q9CQX8	RT36_MOUSE	28S ribosomal protein S36, mitochondrial	**-1.9**	0.0033*
P17225	PTBP1_MOUSE	Polypyrimidine tract-binding protein 1	**-1.9**	0.0056*
Q61074	PPM1G_MOUSE	Protein phosphatase 1G	**-1.9**	0.0222*
O70475	UGDH_MOUSE	UDP-glucose 6-dehydrogenase	**-1.9**	0.3092
Q8CGC7	SYEP_MOUSE	Bifunctional glutamate/proline--tRNA ligase	**-1.9**	0.0803
Q9EQS3	MYCBP_MOUSE	C-Myc-binding protein	**-1.9**	0.0004*
Q921H9	COA7_MOUSE	Cytochrome c oxidase assembly factor 7	**-1.9**	0.0186*
Q61316	HSP74_MOUSE	Heat shock 70 kDa protein 4	**-1.9**	0.0004*
Q9D8S9	BOLA1_MOUSE	BolA-like protein 1	**-1.9**	0.0042*
Q03517	SCG2_MOUSE	Secretogranin-2	**-1.9**	0.0003*
O55111	DSG2_MOUSE	Desmoglein-2	**-1.9**	0.9939
P97864	CASP7_MOUSE	Caspase-7	**-1.9**	0.0714
P61961	UFM1_MOUSE	Ubiquitin-fold modifier 1	**-1.9**	0.0044*

Q3THE2	ML12B_MOUSE	Myosin regulatory light chain 12B	**-1.9**	0.0001*
Q8K183	PDXK_MOUSE	Pyridoxal kinase	**-1.9**	0.5131
P0DP28	CALM3_MOUSE	sp|P0DP28|CALM3_MOUSE	**-1.9**	0.0811
Q6PGH2	JUPI2_MOUSE	Hematological and neurological expressed 1-like protein	**-1.9**	0.3907
Q3U0V1	FUBP2_MOUSE	Far upstream element-binding protein 2	**-1.9**	0.0022*
Q60997	DMBT1_MOUSE	Deleted in malignant brain tumors 1 protein	**-1.9**	0.0342*
Q62446	FKBP3_MOUSE	Peptidyl-prolyl cis-trans isomerase FKBP3	**-1.9**	0.0001*
P97855	G3BP1_MOUSE	Ras GTPase-activating protein-binding protein 1	**-1.9**	0.8099
Q61545	EWS_MOUSE	RNA-binding protein EWS	**-1.9**	0.0001*
Q8BGD8	COA6_MOUSE	Cytochrome c oxidase assembly factor 6 homolog	**-1.9**	0.1729
Q8BMD8	SCMC1_MOUSE	Calcium-binding mitochondrial carrier protein SCaMC-1	**-1.9**	0.6141
Q9WVE8	PACN2_MOUSE	Protein kinase C and casein kinase substrate in neurons protein 2	**-1.9**	0.0095*
P08228	SODC_MOUSE	Superoxide dismutase [Cu-Zn]	**-1.9**	0.0019*
Q8VHC3	SELM_MOUSE	Selenoprotein M	**-1.9**	0.0018*
P68372	TBB4B_MOUSE	Tubulin beta-4B chain	**-1.9**	0.0203*
Q9ESP1	SDF2L_MOUSE	Stromal cell-derived factor 2-like protein 1	**-1.8**	0.8618
P46656	ADX_MOUSE	Adrenodoxin, mitochondrial	**-1.8**	0.0002*
Q8VDD5	MYH9_MOUSE	Myosin-9	**-1.8**	0.1794
Q9CR98	F136A_MOUSE	Protein FAM136A	**-1.8**	0.0000*
Q91W90	TXND5_MOUSE	Thioredoxin domain-containing protein 5	**-1.8**	0.0002*
Q9QY76	VAPB_MOUSE	Vesicle-associated membrane protein-associated protein B	**-1.8**	0.0127*
P62075	TIM13_MOUSE	Mitochondrial import inner membrane translocase subunit Tim13	**-1.8**	0.0002*
Q6NVF9	CPSF6_MOUSE	Cleavage and polyadenylation specificity factor subunit 6	**-1.8**	0.0000*
Q99K48	NONO_MOUSE	Non-POU domain-containing octamer-binding protein	**-1.8**	0.6999
O08795	GLU2B_MOUSE	Glucosidase 2 subunit beta	**-1.8**	0.0001*
Q9CQH7	BT3L4_MOUSE	Transcription factor BTF3 homolog 4	**-1.8**	0.0107*
Q62523	ZYX_MOUSE	Zyxin	**-1.8**	0.2770
P23116	EIF3A_MOUSE	Eukaryotic translation initiation factor 3 subunit A	**-1.8**	0.3563
P56959	FUS_MOUSE	RNA-binding protein FUS	**-1.8**	0.0015*
Q9JKR6	HYOU1_MOUSE	Hypoxia up-regulated protein 1	**-1.8**	0.0007*
Q921W0	CHM1A_MOUSE	Charged multivesicular body protein 1a	**-1.8**	0.0000*
Q9ER00	STX12_MOUSE	Syntaxin-12	**-1.8**	0.0002*
P48428	TBCA_MOUSE	Tubulin-specific chaperone A	**-1.8**	0.0056*
Q9CYA0	CREL2_MOUSE	Cysteine-rich with EGF-like domain protein 2	**-1.8**	0.3031
P62983	RS27A_MOUSE	Ubiquitin-40S ribosomal protein S27a	**-1.8**	0.9725
Q9CRB9	MIC19_MOUSE	MICOS complex subunit Mic19	**-1.8**	0.003*
P55937	GOGA3_MOUSE	Golgin subfamily A member 3	**-1.8**	0.2261
F6ZDS4	TPR_MOUSE	Nucleoprotein TPR	**-1.8**	0.0019*
Q9CQL7	MOFA1_MOUSE	MORF4 family-associated protein 1	**-1.8**	0.6181
Q9Z1Z0	USO1_MOUSE	General vesicular transport factor p115	**-1.8**	0.2603

Q6NZB0	DNJC8_MOUSE	DnaJ homolog subfamily C member 8	**-1.8**	0.0000*
Q8K3C3	LZIC_MOUSE	Protein LZIC	**-1.8**	0.0051*
Q8BGD9	IF4B_MOUSE	Eukaryotic translation initiation factor 4B	**-1.8**	0.0097*
Q61207	SAP_MOUSE	Prosaposin	**-1.8**	0.0109*
Q6P542	ABCF1_MOUSE	ATP-binding cassette sub-family F member 1	**-1.8**	0.0015*
Q9Z2Q5	RM40_MOUSE	39S ribosomal protein L40, mitochondrial	**-1.8**	0.008*
Q64442	DHSO_MOUSE	Sorbitol dehydrogenase	**-1.8**	0.016*
Q9DB15	RM12_MOUSE	39S ribosomal protein L12, mitochondrial	**-1.8**	0.0015*
Q9CWS0	DDAH1_MOUSE	N(G),N(G)-dimethylarginine dimethylaminohydrolase 1	**-1.8**	0.0042*
Q9Z1X4	ILF3_MOUSE	Interleukin enhancer-binding factor 3	**-1.8**	0.1819
Q9Z0F7	SYUG_MOUSE	Gamma-synuclein	**-1.8**	0.0023*
Q9D855	QCR7_MOUSE	Cytochrome b-c1 complex subunit 7	**-1.7**	0.0356*
Q80Y14	GLRX5_MOUSE	Glutaredoxin-related protein 5, mitochondrial	**-1.7**	0.0001*
P09405	NUCL_MOUSE	Nucleolin	**-1.7**	0.0067*
Q8K310	MATR3_MOUSE	Matrin-3	**-1.7**	0.9197
Q8VIJ6	SFPQ_MOUSE	Splicing factor, proline- and glutamine-rich	**-1.7**	0.2983
E9Q557	DESP_MOUSE	Desmoplakin	**-1.7**	0.0776
Q9CQN7	RM41_MOUSE	39S ribosomal protein L41, mitochondrial	**-1.7**	0.0876
Q8BU85	MSRB3_MOUSE	Methionine-R-sulfoxide reductase B3, mitochondrial	**-1.7**	0.4329
P61979	HNRPK_MOUSE	Heterogeneous nuclear ribonucleoprotein K	**-1.7**	0.1405
Q62241	RU1C_MOUSE	U1 small nuclear ribonucleoprotein C	**-1.7**	0.6463
Q8K5B2	MCFD2_MOUSE	Multiple coagulation factor deficiency protein 2 homolog	**-1.7**	0.0223*
P29452	CASP1_MOUSE	Caspase-1	**-1.7**	0.0421*
Q9R100	CAD17_MOUSE	Cadherin-17	**-1.7**	0.0009*
P97352	S10AD_MOUSE	Protein S100-A13	**-1.7**	0.0008*
P31786	ACBP_MOUSE	Acyl-CoA-binding protein	**-1.7**	0.0006*
Q66JS6	EI3JB_MOUSE	Eukaryotic translation initiation factor 3 subunit J-B	**-1.7**	0.0000*
P27546	MAP4_MOUSE	Microtubule-associated protein 4	**-1.7**	0.0024*
Q62318	TIF1B_MOUSE	Transcription intermediary factor 1-beta	**-1.7**	0.6349
Q9CR21	ACPM_MOUSE	Acyl carrier protein, mitochondrial	**-1.7**	0.0002*
O55023	IMPA1_MOUSE	Inositol monophosphatase 1	**-1.7**	0.0215*
Q8BUV3	GEPH_MOUSE	Gephyrin	**-1.7**	0.0014*
Q9ERR7	SEP15_MOUSE	Selenoprotein F	**-1.7**	0.6905
Q9CQU0	TXD12_MOUSE	Thioredoxin domain-containing protein 12	**-1.7**	0.0025*
P26231	CTNA1_MOUSE	Catenin alpha-1	**-1.7**	0.0208*
Q69ZS7	HBS1L_MOUSE	HBS1-like protein	**-1.6**	0.009*
O35143	ATIF1_MOUSE	ATPase inhibitor, mitochondrial	**-1.6**	0.0017*
P62311	LSM3_MOUSE	U6 snRNA-associated Sm-like protein LSm3	**-1.6**	0.7105
O70318	E41L2_MOUSE	Band 4.1-like protein 2	**-1.6**	0.0003*
O08583	THOC4_MOUSE	THO complex subunit 4	**-1.6**	0.1290

Q9CQZ1	HSBP1_MOUSE	Heat shock factor-binding protein 1	**-1.6**	0.0002*
P21619	LMNB2_MOUSE	Lamin-B2	**-1.6**	0.2382
P54728	RD23B_MOUSE	UV excision repair protein RAD23 homolog B	**-1.6**	0.0315*
Q9JKB3	YBOX3_MOUSE	Y-box-binding protein 3	**-1.6**	0.0690
Q9D6J6	NDUV2_MOUSE	NADH dehydrogenase [ubiquinone] flavoprotein 2, mitochondrial	**-1.6**	0.0126*
O55022	PGRC1_MOUSE	Membrane-associated progesterone receptor component 1	**-1.6**	0.0046*
Q9WVK4	EHD1_MOUSE	EH domain-containing protein 1	**-1.6**	0.0174*
P12367	KAP2_MOUSE	cAMP-dependent protein kinase type II-alpha regulatory subunit	**-1.6**	0.0874
O08539	BIN1_MOUSE	Myc box-dependent-interacting protein 1	**-1.6**	0.3005
Q9QYR6	MAP1A_MOUSE	Microtubule-associated protein 1A	**-1.6**	0.6640
Q80WW9	DDRGK_MOUSE	DDRGK domain-containing protein 1	**-1.6**	0.0004*
Q9WUK2	IF4H_MOUSE	Eukaryotic translation initiation factor 4H	**-1.6**	0.2464
Q9EQK5	MVP_MOUSE	Major vault protein	**-1.6**	0.0191*
O70251	EF1B_MOUSE	Elongation factor 1-beta	**-1.6**	0.0922
Q9EQU5	SET_MOUSE	Protein SET	**-1.6**	0.0346*
Q9D6S7	RRFM_MOUSE	Ribosome-recycling factor, mitochondrial	**-1.6**	0.3841
P97792	CXAR_MOUSE	Coxsackievirus and adenovirus receptor homolog	**-1.6**	0.9575
Q9QXV0	PCSK1_MOUSE	ProSAAS	**-1.6**	0.0346*
P39447	ZO1_MOUSE	Tight junction protein ZO-1	**-1.6**	0.6687
O08585	CLCA_MOUSE	Clathrin light chain A	**-1.6**	0.0025*
P31230	AIMP1_MOUSE	Aminoacyl tRNA synthase complex-interacting multifunctional protein 1	**-1.6**	0.5640
P62073	TIM10_MOUSE	Mitochondrial import inner membrane translocase subunit Tim10	**-1.6**	0.003*
Q9D1L9	LTOR5_MOUSE	Ragulator complex protein LAMTOR5	**-1.6**	0.5383
P60824	CIRBP_MOUSE	Cold-inducible RNA-binding protein	**-1.6**	0.9134
P70670	NACAM_MOUSE	Nascent polypeptide-associated complex subunit alpha, muscle-specific form	**-1.6**	0.0022*
Q99J99	THTM_MOUSE	3-mercaptopyruvate sulfurtransferase	**-1.6**	0.0242*
Q9CXZ1	NDUS4_MOUSE	NADH dehydrogenase [ubiquinone] iron-sulfur protein 4, mitochondrial	**-1.6**	0.0038*
Q60865	CAPR1_MOUSE	Caprin-1	**-1.6**	0.0910
P17563	SBP1_MOUSE	Selenium-binding protein 1	**-1.6**	0.0443*
Q3UMT1	PP12C_MOUSE	Protein phosphatase 1 regulatory subunit 12C	**-1.6**	0.0006*
P14211	CALR_MOUSE	Calreticulin	**-1.6**	0.0907
Q9CYZ2	TPD54_MOUSE	Tumor protein D54	**-1.6**	0.0075*
Q9WU28	PFD5_MOUSE	Prefoldin subunit 5	**-1.6**	0.0001*
Q8R3Q6	CCD58_MOUSE	Coiled-coil domain-containing protein 58	**-1.6**	0.0148*
P01887	B2MG_MOUSE	Beta-2-microglobulin	**-1.6**	0.0048*
P26883	FKB1A_MOUSE	Peptidyl-prolyl cis-trans isomerase FKBP1A	**-1.6**	0.8677
P26369	U2AF2_MOUSE	Splicing factor U2AF 65 kDa subunit	**-1.6**	0.0128*
Q9QZ23	NFU1_MOUSE	NFU1 iron-sulfur cluster scaffold homolog, mitochondrial	**-1.6**	0.3980
O88952	LIN7C_MOUSE	Protein lin-7 homolog C	**-1.6**	0.0001*

P70333	HNRH2_MOUSE	Heterogeneous nuclear ribonucleoprotein H2	**-1.6**	0.8185
O88696	CLPP_MOUSE	ATP-dependent Clp protease proteolytic subunit, mitochondrial	**-1.6**	0.2446
Q64012	RALY_MOUSE	RNA-binding protein Raly	**-1.6**	0.7938
Q9CQE8	RTRAF_MOUSE	UPF0568 protein C14orf166 homolog	**-1.6**	0.0032*
Q8CCH2	NHLC3_MOUSE	NHL repeat-containing protein 3	**-1.6**	0.3497
P05201	AATC_MOUSE	Aspartate aminotransferase, cytoplasmic	**-1.5**	0.6850
P84104	SRSF3_MOUSE	Serine/arginine-rich splicing factor 3	**-1.5**	0.9251
Q6P6L0	FIL1L_MOUSE	Filamin A-interacting protein 1-like	**-1.5**	0.3911
Q8VE37	RCC1_MOUSE	Regulator of chromosome condensation	**-1.5**	0.2936
Q8BP92	RCN2_MOUSE	Reticulocalbin-2	**-1.5**	0.0113*
P29595	NEDD8_MOUSE	NEDD8	**-1.5**	0.0144*
Q9D8B3	CHM4B_MOUSE	Charged multivesicular body protein 4b	**-1.5**	0.0023*
P99027	RLA2_MOUSE	60S acidic ribosomal protein P2	**-1.5**	0.4194
P61458	PHS_MOUSE	Pterin-4-alpha-carbinolamine dehydratase	**-1.5**	0.1540
Q9CPU0	LGUL_MOUSE	Lactoylglutathione lyase	**-1.5**	0.0073*
P47968	RPIA_MOUSE	Ribose-5-phosphate isomerase	**-1.5**	0.1785
Q9WTR5	CAD13_MOUSE	Cadherin-13	**-1.5**	0.0137*
Q61112	CAB45_MOUSE	45 kDa calcium-binding protein	**-1.5**	0.6108
P97300	NPTN_MOUSE	Neuroplastin	**-1.5**	0.0001*
P62627	DLRB1_MOUSE	Dynein light chain roadblock-type 1	**-1.5**	0.1841
Q91YE8	SYNP2_MOUSE	Synaptopodin-2	**-1.5**	0.8018
P32020	NLTP_MOUSE	Non-specific lipid-transfer protein	**-1.5**	0.1208
Q99KJ8	DCTN2_MOUSE	Dynactin subunit 2	**-1.5**	0.0012*
Q9CXI5	MANF_MOUSE	Mesencephalic astrocyte-derived neurotrophic factor	**-1.5**	0.0005*
Q9CR00	PSMD9_MOUSE	26S proteasome non-ATPase regulatory subunit 9	**-1.5**	0.6917
Q9CPQ1	COX6C_MOUSE	Cytochrome c oxidase subunit 6C	**-1.5**	0.0195*
Q62418	DBNL_MOUSE	Drebrin-like protein	**-1.5**	0.0894
Q8R0F8	FAHD1_MOUSE	Acylpyruvase FAHD1, mitochondrial	**-1.5**	0.0131*
Q9QX47	SON_MOUSE	Protein SON	**-1.5**	0.1792
Q8BQ47	CNPY4_MOUSE	Protein canopy homolog 4	**-1.5**	0.0878
Q07797	LG3BP_MOUSE	Galectin-3-binding protein	**-1.5**	0.4307
Q63810	CANB1_MOUSE	Calcineurin subunit B type 1	**-1.5**	0.7866
P61759	PFD3_MOUSE	Prefoldin subunit 3	**-1.5**	0.0257*
Q9DAU1	CNPY3_MOUSE	Protein canopy homolog 3	**-1.5**	0.2672
P19783	COX41_MOUSE	Cytochrome c oxidase subunit 4 isoform 1, mitochondrial	**-1.5**	0.1145
P57776	EF1D_MOUSE	Elongation factor 1-delta	**-1.5**	0.0141*
Q80X90	FLNB_MOUSE	Filamin-B	**-1.5**	0.1927
Q8CI51	PDLI5_MOUSE	PDZ and LIM domain protein 5	**-1.5**	0.9289
Q8BTM8	FLNA_MOUSE	Filamin-A	**-1.5**	0.6068
Q91YQ5	RPN1_MOUSE	Dolichyl-diphosphooligosaccharide--protein glycosyltransferase subunit 1	**-1.5**	0.7415

Q3TIV5	ZC3HF_MOUSE	Zinc finger CCCH domain-containing protein 15	**-1.5**	0.0005*
P34152	FAK1_MOUSE	Focal adhesion kinase 1	**-1.5**	0.9445
O08749	DLDH_MOUSE	Dihydrolipoyl dehydrogenase, mitochondrial	**-1.5**	0.0285*
Q3UPL0	SC31A_MOUSE	Protein transport protein Sec31A	**-1.5**	0.0194*
P51859	HDGF_MOUSE	Hepatoma-derived growth factor	**-1.5**	0.0012*
Q9DBP5	KCY_MOUSE	UMP-CMP kinase	**-1.5**	0.0242*
P63254	CRIP1_MOUSE	Cysteine-rich protein 1	**-1.5**	0.0519
Q3U9G9	LBR_MOUSE	Lamin-B receptor	**-1.5**	0.0086*
Q62468	VILI_MOUSE	Villin-1	**-1.5**	0.8871
Q9JL35	HMGN5_MOUSE	High mobility group nucleosome-binding domain-containing protein 5	**-1.5**	0.1551
Q9CQ10	CHMP3_MOUSE	Charged multivesicular body protein 3	**-1.5**	0.0204*
Q61768	KINH_MOUSE	Kinesin-1 heavy chain	**-1.5**	0.0058*
Q64152	BTF3_MOUSE	Transcription factor BTF3	**-1.5**	0.1049
P19467	MUC13_MOUSE	Mucin-13	**-1.5**	0.5582
Q9D3D9	ATPD_MOUSE	ATP synthase subunit delta, mitochondrial	**-1.5**	0.0161*
Q8K4L3	SVIL_MOUSE	Supervillin	**-1.5**	0.6101
P35564	CALX_MOUSE	Calnexin	**-1.5**	0.9180
Q61937	NPM_MOUSE	Nucleophosmin	**-1.5**	0.0268*
Q9WTQ5	AKA12_MOUSE	A-kinase anchor protein 12	**-1.5**	0.0004*
O70209	PDLI3_MOUSE	PDZ and LIM domain protein 3	**-1.5**	0.9406
Q9NYQ2	HAOX2_MOUSE	Hydroxyacid oxidase 2	**-1.5**	0.7671
Q9JMG7	HDGR3_MOUSE	Hepatoma-derived growth factor-related protein 3	**-1.4**	0.3034
P27773	PDIA3_MOUSE	Protein disulfide-isomerase A3	**-1.4**	0.9353
Q99JF8	PSIP1_MOUSE	PC4 and SFRS1-interacting protein	**-1.4**	0.2057
Q9CZG9	PDZ11_MOUSE	PDZ domain-containing protein 11	**-1.4**	0.5940
Q99LY9	NDUS5_MOUSE	NADH dehydrogenase [ubiquinone] iron-sulfur protein 5	**-1.4**	0.1366
Q64299	CCN3_MOUSE	Protein NOV homolog	**-1.4**	0.022*
P57759	ERP29_MOUSE	Endoplasmic reticulum resident protein 29	-1.4	0.7954
Q8CBW3	ABI1_MOUSE	Abl interactor 1	-1.4	0.0842
O09044	SNP23_MOUSE	Synaptosomal-associated protein 23	-1.4	0.0031*
Q6IRU2	TPM4_MOUSE	Tropomyosin alpha-4 chain	-1.4	0.0192*
Q99020	ROAA_MOUSE	Heterogeneous nuclear ribonucleoprotein A/B	-1.4	0.0056*
Q60829	PPR1B_MOUSE	Protein phosphatase 1 regulatory subunit 1B	-1.4	0.0578
Q9D0A3	ARPIN_MOUSE	Arpin	-1.4	0.1232
Q9CQ45	NENF_MOUSE	Neudesin	-1.4	0.4056
Q63850	NUP62_MOUSE	Nuclear pore glycoprotein p62	-1.4	0.0085*
Q61029	LAP2B_MOUSE	Lamina-associated polypeptide 2, isoforms beta/delta/epsilon/gamma	-1.4	0.0032*
O70591	PFD2_MOUSE	Prefoldin subunit 2	-1.4	0.0429*
Q810Q5	NMES1_MOUSE	Normal mucosa of esophagus-specific gene 1 protein	-1.4	0.5831
Q9DBJ3	BI2L1_MOUSE	Brain-specific angiogenesis inhibitor 1-associated protein 2-like protein 1	-1.4	0.5891

O35226	PSMD4_MOUSE	26S proteasome non-ATPase regulatory subunit 4	-1.4	0.5366
Q8R0W0	EPIPL_MOUSE	Epiplakin	-1.4	0.0697
Q9CQQ8	LSM7_MOUSE	U6 snRNA-associated Sm-like protein LSm7	-1.4	0.0004*
Q62165	DAG1_MOUSE	Dystroglycan	-1.4	0.4224
P54726	RD23A_MOUSE	UV excision repair protein RAD23 homolog A	-1.4	0.3363
P97371	PSME1_MOUSE	Proteasome activator complex subunit 1	-1.4	0.2722
P20029	BIP_MOUSE	78 kDa glucose-regulated protein	-1.4	0.0115*
P10639	THIO_MOUSE	Thioredoxin	-1.4	0.0162*
Q9CWM4	PFD1_MOUSE	Prefoldin subunit 1	-1.4	0.7532
P56812	PDCD5_MOUSE	Programmed cell death protein 5	-1.4	0.4328
P29758	OAT_MOUSE	Ornithine aminotransferase, mitochondrial	-1.4	0.0264*
P08122	CO4A2_MOUSE	Collagen alpha-2(IV) chain	-1.4	0.8406
Q9Z1R2	BAG6_MOUSE	Large proline-rich protein BAG6	-1.4	0.1618
Q9JHJ0	TMOD3_MOUSE	Tropomodulin-3	-1.4	0.0481*
P62858	RS28_MOUSE	40S ribosomal protein S28	-1.4	0.0005*
Q9JLV1	BAG3_MOUSE	BAG family molecular chaperone regulator 3	-1.4	0.1657
P02463	CO4A1_MOUSE	Collagen alpha-1(IV) chain	-1.4	0.5855
Q9CZ44	NSF1C_MOUSE	NSFL1 cofactor p47	-1.4	0.6085
P62748	HPCL1_MOUSE	Hippocalcin-like protein 1	-1.4	0.6453
P43277	H13_MOUSE	Histone H1.3	-1.4	0.2229
O08579	EMD_MOUSE	Emerin	-1.4	0.2371
P56565	S10A1_MOUSE	Protein S100-A1	-1.4	0.0549
Q3V0K9	PLSI_MOUSE	Plastin-1	-1.4	0.0494
Q80YX1	TENA_MOUSE	Tenascin	-1.4	0.1616
Q02248	CTNB1_MOUSE	Catenin beta-1	-1.4	0.2880
Q9CQ89	CUTA_MOUSE	Protein CutA	-1.4	0.0011*
Q03958	PFD6_MOUSE	Prefoldin subunit 6	-1.4	0.0201*
O35887	CALU_MOUSE	Calumenin	-1.4	0.0171*
Q91XA2	GOLM1_MOUSE	Golgi membrane protein 1	-1.4	0.2521
Q9WV32	ARC1B_MOUSE	Actin-related protein 2/3 complex subunit 1B	-1.4	0.1138
Q99L47	F10A1_MOUSE	Hsc70-interacting protein	-1.4	0.4360
P38647	GRP75_MOUSE	Stress-70 protein, mitochondrial	-1.4	0.038*
Q8CAQ8	MIC60_MOUSE	MICOS complex subunit Mic60	-1.4	0.0503
Q7TQD2	TPPP_MOUSE	Tubulin polymerization-promoting protein	-1.4	0.0059*
O35658	C1QBP_MOUSE	Complement component 1 Q subcomponent-binding protein, mitochondrial	-1.4	0.0279*
P54227	STMN1_MOUSE	Stathmin	-1.4	0.0644
Q6ZWM4	LSM8_MOUSE	U6 snRNA-associated Sm-like protein LSm8	-1.4	0.0302*
O08997	ATOX1_MOUSE	Copper transport protein ATOX1	-1.4	0.0076*
Q60902	EP15R_MOUSE	Epidermal growth factor receptor substrate 15-like 1	-1.4	0.0013*
P63038	CH60_MOUSE	60 kDa heat shock protein, mitochondrial	-1.4	0.2790

P21460	CYTC_MOUSE	Cystatin-C	-1.4	0.7071
P30681	HMGB2_MOUSE	High mobility group protein B2	-1.4	0.0196*
Q8R081	HNRPL_MOUSE	Heterogeneous nuclear ribonucleoprotein L	-1.4	0.5185
Q9QXT0	CNPY2_MOUSE	Protein canopy homolog 2	-1.4	0.001*
P56376	ACYP1_MOUSE	Acylphosphatase-1	-1.4	0.035*
Q78ZA7	NP1L4_MOUSE	Nucleosome assembly protein 1-like 4	-1.4	0.7664
Q9DBR7	MYPT1_MOUSE	Protein phosphatase 1 regulatory subunit 12A	-1.4	0.5935
Q9CY58	PAIRB_MOUSE	Plasminogen activator inhibitor 1 RNA-binding protein	-1.4	0.0208*
O35381	AN32A_MOUSE	Acidic leucine-rich nuclear phosphoprotein 32 family member A	-1.4	0.0733
Q60864	STIP1_MOUSE	Stress-induced-phosphoprotein 1	-1.4	0.0169*
Q8VH51	RBM39_MOUSE	RNA-binding protein 39	-1.4	0.2614
O89086	RBM3_MOUSE	RNA-binding protein 3	-1.4	0.6745
Q8BG95	MYPT2_MOUSE	Protein phosphatase 1 regulatory subunit 12B	-1.4	0.0694
Q9CR41	HYPK_MOUSE	Huntingtin-interacting protein K	-1.4	0.6662
P34022	RANG_MOUSE	Ran-specific GTPase-activating protein	-1.4	0.4402
Q9DCW4	ETFB_MOUSE	Electron transfer flavoprotein subunit beta	-1.4	0.4880
P70372	ELAV1_MOUSE	ELAV-like protein 1	-1.4	0.5620
Q9ERE7	MESD_MOUSE	LDLR chaperone MESD	-1.4	0.0000*
Q8BJU0	SGTA_MOUSE	Small glutamine-rich tetratricopeptide repeat-containing protein alpha	-1.4	0.4306
Q9EPB4	ASC_MOUSE	Apoptosis-associated speck-like protein containing a CARD	-1.4	0.0044*
Q9WV55	VAPA_MOUSE	Vesicle-associated membrane protein-associated protein A	-1.4	0.3401
Q9D1K2	VATF_MOUSE	V-type proton ATPase subunit F	-1.4	0.8437
P07724	ALBU_MOUSE	Serum albumin	-1.4	0.2209
Q8R3G9	TSN8_MOUSE	Tetraspanin-8	-1.4	0.6048
Q99LP6	GRPE1_MOUSE	GrpE protein homolog 1, mitochondrial	-1.4	0.2485
Q9DBG9	TX1B3_MOUSE	Tax1-binding protein 3	-1.3	0.4945
O54941	SMCE1_MOUSE	SWI/SNF-related matrix-associated actin-dependent regulator of chromatin subfamily E member 1	-1.3	0.4419
P48771	CX7A2_MOUSE	Cytochrome c oxidase subunit 7A2, mitochondrial	-1.3	0.0407*
Q8BMF4	ODP2_MOUSE	Dihydrolipoyllysine-residue acetyltransferase component of pyruvate dehydrogenase complex, mitochondrial	-1.3	0.6639
Q61581	IBP7_MOUSE	Insulin-like growth factor-binding protein 7	-1.3	0.2542
P47941	CRKL_MOUSE	Crk-like protein	-1.3	0.4695
O09159	MA2B1_MOUSE	Lysosomal alpha-mannosidase	-1.3	0.5075
Q99KC8	VMA5A_MOUSE	von Willebrand factor A domain-containing protein 5A	-1.3	0.6962
P50543	S10AB_MOUSE	Protein S100-A11	-1.3	0.2778
Q6PDN3	MYLK_MOUSE	Myosin light chain kinase, smooth muscle	-1.3	0.2397
O70439	STX7_MOUSE	Syntaxin-7	-1.3	0.1832
Q9CQM5	TXD17_MOUSE	Thioredoxin domain-containing protein 17	-1.3	0.4929
Q922Y1	UBXN1_MOUSE	UBX domain-containing protein 1	-1.3	0.0516

Q8BKZ9	ODPX_MOUSE	Pyruvate dehydrogenase protein X component, mitochondrial	-1.3	0.031*
Q7TPW1	NEXN_MOUSE	Nexilin	-1.3	0.4183
Q78JW9	UBFD1_MOUSE	Ubiquitin domain-containing protein UBFD1	-1.3	0.8338
P58771	TPM1_MOUSE	Tropomyosin alpha-1 chain	-1.3	0.1323
P10711	TCEA1_MOUSE	Transcription elongation factor A protein 1	-1.3	0.0052*
Q03265	ATPA_MOUSE	ATP synthase subunit alpha, mitochondrial	-1.3	0.9476
P60867	RS20_MOUSE	40S ribosomal protein S20	-1.3	0.6138
P01897	HA1L_MOUSE	H-2 class I histocompatibility antigen, L-D alpha chain	-1.3	0.0323*
O54879	HMGB3_MOUSE	High mobility group protein B3	-1.3	0.8910
P97493	THIOM_MOUSE	Thioredoxin, mitochondrial	-1.3	0.3207
P62192	PRS4_MOUSE	26S protease regulatory subunit 4	-1.3	0.8944
Q9WTX5	SKP1_MOUSE	S-phase kinase-associated protein 1	-1.3	0.4547
P18572	BASI_MOUSE	Basigin	-1.3	0.0549
P63158	HMGB1_MOUSE	High mobility group protein B1	-1.3	0.0014*
P09103	PDIA1_MOUSE	Protein disulfide-isomerase	-1.3	0.0259*
P11627	L1CAM_MOUSE	Neural cell adhesion molecule L1	-1.3	0.0562
Q60668	HNRPD_MOUSE	Heterogeneous nuclear ribonucleoprotein D0	-1.3	0.6350
P08003	PDIA4_MOUSE	Protein disulfide-isomerase A4	-1.3	0.1370
Q05BC3	EMAL1_MOUSE	Echinoderm microtubule-associated protein-like 1	-1.3	0.9851
P62774	MTPN_MOUSE	Myotrophin	-1.3	0.8122
Q8K4G1	LTBP4_MOUSE	Latent-transforming growth factor beta-binding protein 4	-1.3	0.4485
Q62048	PEA15_MOUSE	Astrocytic phosphoprotein PEA-15	-1.3	0.0596
P47955	RLA1_MOUSE	60S acidic ribosomal protein P1	-1.3	0.1581
P23198	CBX3_MOUSE	Chromobox protein homolog 3	-1.3	0.2139
P97822	AN32E_MOUSE	Acidic leucine-rich nuclear phosphoprotein 32 family member E	-1.3	0.9885
P97805	FAM3D_MOUSE	Protein FAM3D	-1.3	0.4771
P48024	EIF1_MOUSE	Eukaryotic translation initiation factor 1	-1.3	0.7583
P60335	PCBP1_MOUSE	Poly(rC)-binding protein 1	-1.3	0.8477
Q9D281	NXP20_MOUSE	Protein Noxp20	-1.3	0.5827
P32261	ANT3_MOUSE	Antithrombin-III	-1.3	0.1325
P07309	TTHY_MOUSE	Transthyretin	-1.3	0.7651
P55302	AMRP_MOUSE	Alpha-2-macroglobulin receptor-associated protein	-1.3	0.3499
Q05186	RCN1_MOUSE	Reticulocalbin-1	-1.3	0.1123
P24549	AL1A1_MOUSE	Retinal dehydrogenase 1	-1.3	0.7185
Q8BJW6	EIF2A_MOUSE	Eukaryotic translation initiation factor 2A	-1.3	0.7835
Q9D1I5	MCEE_MOUSE	Methylmalonyl-CoA epimerase, mitochondrial	-1.3	0.5342
P32648	VIP_MOUSE	VIP peptides	-1.3	0.8533
Q9DCX2	ATP5H_MOUSE	ATP synthase subunit d, mitochondrial	-1.3	0.1936
P11438	LAMP1_MOUSE	Lysosome-associated membrane glycoprotein 1	-1.2	0.6630
Q9D7P6	ISCU_MOUSE	Iron-sulfur cluster assembly enzyme ISCU, mitochondrial	-1.2	0.0054*

P16045	LEG1_MOUSE	Galectin-1	-1.2	0.9251
O88569	ROA2_MOUSE	Heterogeneous nuclear ribonucleoproteins A2/B1	-1.2	0.3856
O35215	DOPD_MOUSE	D-dopachrome decarboxylase	-1.2	0.6834
P00493	HPRT_MOUSE	Hypoxanthine-guanine phosphoribosyltransferase	-1.2	0.7951
P63323	RS12_MOUSE	40S ribosomal protein S12	-1.2	0.0087*
Q5EBG8	CA050_MOUSE	Uncharacterized protein C1orf50 homolog	-1.2	0.2458
P58774	TPM2_MOUSE	Tropomyosin beta chain	-1.2	0.0987
P35278	RAB5C_MOUSE	Ras-related protein Rab-5C	-1.2	0.7916
Q9CQK7	RWDD1_MOUSE	RWD domain-containing protein 1	-1.2	0.0087*
Q7TQG1	PKHA6_MOUSE	Pleckstrin homology domain-containing family A member 6	-1.2	0.7595
Q9DCB8	ISCA2_MOUSE	Iron-sulfur cluster assembly 2 homolog, mitochondrial	-1.2	0.1137
Q91WD9	SEGN_MOUSE	Secretagogin	-1.2	0.3691
Q60749	KHDR1_MOUSE	KH domain-containing, RNA-binding, signal transduction-associated protein 1	-1.2	0.2098
P63242	IF5A1_MOUSE	Eukaryotic translation initiation factor 5A-1	-1.2	0.6526
Q9DCT8	CRIP2_MOUSE	Cysteine-rich protein 2	-1.2	0.2515
P48678	LMNA_MOUSE	Prelamin-A/C	-1.2	0.5449
Q9D0E1	HNRPM_MOUSE	Heterogeneous nuclear ribonucleoprotein M	-1.2	0.8987
Q9D2G2	ODO2_MOUSE	Dihydrolipoyllysine-residue succinyltransferase component of 2-oxoglutarate dehydrogenase complex, mitochondrial	-1.2	0.2694
Q93092	TALDO_MOUSE	Transaldolase	-1.2	0.7161
Q99LC5	ETFA_MOUSE	Electron transfer flavoprotein subunit alpha, mitochondrial	-1.2	0.5495
O08638	MYH11_MOUSE	Myosin-11	-1.2	0.7055
Q5XJY5	COPD_MOUSE	Coatomer subunit delta	-1.2	0.9921
Q9CQE5	RGS10_MOUSE	Regulator of G-protein signaling 10	-1.2	0.4703
Q8BH64	EHD2_MOUSE	EH domain-containing protein 2	-1.2	0.8029
O70570	PIGR_MOUSE	Polymeric immunoglobulin receptor	-1.2	0.9420
Q9WU78	PDC6I_MOUSE	Programmed cell death 6-interacting protein	-1.2	0.6603
Q06185	ATP5I_MOUSE	ATP synthase subunit e, mitochondrial	-1.2	0.5964
Q9Z0U1	ZO2_MOUSE	Tight junction protein ZO-2	-1.2	0.9698
P63163	RSMN_MOUSE	Small nuclear ribonucleoprotein-associated protein N	-1.2	0.7952
Q78IK2	USMG5_MOUSE	Up-regulated during skeletal muscle growth protein 5	-1.2	0.9256
O35685	NUDC_MOUSE	Nuclear migration protein nudC	-1.2	0.4157
Q9DBJ1	PGAM1_MOUSE	Phosphoglycerate mutase 1	-1.2	0.4018
O55135	IF6_MOUSE	Eukaryotic translation initiation factor 6	-1.2	0.7399
P09803	CADH1_MOUSE	Cadherin-1	-1.2	0.3392
P20152	VIME_MOUSE	Vimentin	-1.2	0.1808
Q9CQR2	RS21_MOUSE	40S ribosomal protein S21	-1.2	0.3934
Q8BH97	RCN3_MOUSE	Reticulocalbin-3	-1.2	0.3656
P21614	VTDB_MOUSE	Vitamin D-binding protein	-1.2	0.7214

Q9CY50	SSRA_MOUSE	Translocon-associated protein subunit alpha	-1.2	0.1270
P06728	APOA4_MOUSE	Apolipoprotein A-IV	-1.2	0.8529
Q9JMA1	UBP14_MOUSE	Ubiquitin carboxyl-terminal hydrolase 14	-1.2	0.4826
Q9CY02	AHSP_MOUSE	Alpha-hemoglobin-stabilizing protein	-1.2	0.8255
Q9Z2I8	SUCB2_MOUSE	Succinate--CoA ligase [GDP-forming] subunit beta, mitochondrial	-1.2	0.8799
Q925B0	PAWR_MOUSE	PRKC apoptosis WT1 regulator protein	-1.2	0.3812
P14206	RSSA_MOUSE	40S ribosomal protein SA	-1.2	0.2888
O54734	OST48_MOUSE	Dolichyl-diphosphooligosaccharide--protein glycosyltransferase 48 kDa subunit	-1.2	0.8371
Q91YN9	BAG2_MOUSE	BAG family molecular chaperone regulator 2	-1.2	0.7357
P62320	SMD3_MOUSE	Small nuclear ribonucleoprotein Sm D3	-1.2	0.4094
Q9CPT4	MYDGF_MOUSE	Myeloid-derived growth factor	-1.2	0.8323
P62862	RS30_MOUSE	40S ribosomal protein S30	-1.2	0.1284
Q9CR16	PPID_MOUSE	Peptidyl-prolyl cis-trans isomerase D	-1.2	0.6670
P49962	SRP09_MOUSE	Signal recognition particle 9 kDa protein	-1.2	0.7354
Q91VW3	SH3L3_MOUSE	SH3 domain-binding glutamic acid-rich-like protein 3	-1.2	0.8029
Q9CQ19	MYL9_MOUSE	Myosin regulatory light polypeptide 9	-1.2	0.9167
Q99MD9	NASP_MOUSE	Nuclear autoantigenic sperm protein	-1.1	0.5906
Q8BMK4	CKAP4_MOUSE	Cytoskeleton-associated protein 4	-1.1	0.7966
Q9QYJ0	DNJA2_MOUSE	DnaJ homolog subfamily A member 2	-1.1	0.9974
P56480	ATPB_MOUSE	ATP synthase subunit beta, mitochondrial	-1.1	0.8938
P70296	PEBP1_MOUSE	Phosphatidylethanolamine-binding protein 1	-1.1	0.8705
Q60605	MYL6_MOUSE	Myosin light polypeptide 6	-1.1	0.9409
P56395	CYB5_MOUSE	Cytochrome b5	-1.1	0.9548
Q9CQM9	GLRX3_MOUSE	Glutaredoxin-3	-1.1	0.6913
P14873	MAP1B_MOUSE	Microtubule-associated protein 1B	-1.1	0.5638
Q9JKB1	UCHL3_MOUSE	Ubiquitin carboxyl-terminal hydrolase isozyme L3	-1.1	0.5040
O88492	PLIN4_MOUSE	Perilipin-4	1.1	0.8072
Q9D8E6	RL4_MOUSE	60S ribosomal protein L4	1.1	0.3381
P35700	PRDX1_MOUSE	Peroxiredoxin-1	1.1	0.9649
Q9Z2W0	DNPEP_MOUSE	Aspartyl aminopeptidase	1.1	0.9140
Q9Z0J0	NPC2_MOUSE	Epididymal secretory protein E1	1.1	0.2594
Q9D7M1	GID8_MOUSE	Glucose-induced degradation protein 8 homolog	1.2	0.9389
Q00623	APOA1_MOUSE	Apolipoprotein A-I	1.2	0.5396
P20108	PRDX3_MOUSE	Thioredoxin-dependent peroxide reductase, mitochondrial	1.2	0.3929
P17751	TPIS_MOUSE	Triosephosphate isomerase	1.2	0.6175
P46638	RB11B_MOUSE	Ras-related protein Rab-11B	1.2	0.6803
Q99JI1	MSTN1_MOUSE	Musculoskeletal embryonic nuclear protein 1	1.2	0.2261
P23506	PIMT_MOUSE	Protein-L-isoaspartate(D-aspartate) O-methyltransferase	1.2	0.7920
P97315	CSRP1_MOUSE	Cysteine and glycine-rich protein 1	1.2	0.8949

Q9EST5	AN32B_MOUSE	Acidic leucine-rich nuclear phosphoprotein 32 family member B	1.2	0.9799
Q9DCS9	NDUBA_MOUSE	NADH dehydrogenase [ubiquinone] 1 beta subcomplex subunit 10	1.2	0.5223
P14069	S10A6_MOUSE	Protein S100-A6	1.2	0.4944
Q61171	PRDX2_MOUSE	Peroxiredoxin-2	1.2	0.0527
P46935	NEDD4_MOUSE	E3 ubiquitin-protein ligase NEDD4	1.2	0.7752
Q99PT1	GDIR1_MOUSE	Rho GDP-dissociation inhibitor 1	1.2	0.7711
Q99LX0	PARK7_MOUSE	Protein DJ-1	1.2	0.4826
Q9D1Q6	ERP44_MOUSE	Endoplasmic reticulum resident protein 44	1.2	0.0066*
Q9CQ92	FIS1_MOUSE	Mitochondrial fission 1 protein	1.2	0.5954
P07214	SPRC_MOUSE	SPARC	1.2	0.9385
Q60631	GRB2_MOUSE	Growth factor receptor-bound protein 2	1.2	0.5292
Q9CPY7	AMPL_MOUSE	Cytosol aminopeptidase	1.2	0.9545
P35385	HSPB7_MOUSE	Heat shock protein beta-7	1.2	0.2867
Q8BG05	ROA3_MOUSE	Heterogeneous nuclear ribonucleoprotein A3	1.2	0.5977
Q8BWT1	THIM_MOUSE	3-ketoacyl-CoA thiolase, mitochondrial	1.2	0.9559
P26039	TLN1_MOUSE	Talin-1	1.2	0.8777
O08677	KNG1_MOUSE	Kininogen-1	1.2	0.9080
P62137	PP1A_MOUSE	Serine/threonine-protein phosphatase PP1-alpha catalytic subunit	1.2	0.6380
P17182	ENOA_MOUSE	Alpha-enolase	1.2	0.2158
Q63918	CAVN2_MOUSE	Serum deprivation-response protein	1.2	0.2967
P98078	DAB2_MOUSE	Disabled homolog 2	1.2	0.2248
P11031	TCP4_MOUSE	Activated RNA polymerase II transcriptional coactivator p15	1.2	0.4558
P62309	RUXG_MOUSE	Small nuclear ribonucleoprotein G	1.2	0.8696
P70460	VASP_MOUSE	Vasodilator-stimulated phosphoprotein	1.2	0.5925
P18242	CATD_MOUSE	Cathepsin D	1.2	0.0616
Q61206	PA1B2_MOUSE	Platelet-activating factor acetylhydrolase IB subunit beta	1.2	0.1052
P62889	RL30_MOUSE	60S ribosomal protein L30	1.2	0.8767
Q9D172	GAL3A_MOUSE	ES1 protein homolog, mitochondrial	1.2	0.9564
P17742	PPIA_MOUSE	Peptidyl-prolyl cis-trans isomerase A	1.2	0.0538
P28656	NP1L1_MOUSE	Nucleosome assembly protein 1-like 1	1.2	0.9128
P16110	LEG3_MOUSE	Galectin-3	1.2	0.2948
Q8K0C9	GMDS_MOUSE	GDP-mannose 4,6 dehydratase	1.2	0.8202
P15331	PERI_MOUSE	Peripherin	1.2	0.9283
Q70IV5	SYNEM_MOUSE	Synemin	1.2	0.8723
P67778	PHB_MOUSE	Prohibitin	1.2	0.2814
Q62425	NDUA4_MOUSE	Cytochrome c oxidase subunit NDUFA4	1.2	0.1410
P70271	PDLI4_MOUSE	PDZ and LIM domain protein 4	1.2	0.8497
P70349	HINT1_MOUSE	Histidine triad nucleotide-binding protein 1	1.2	0.2609
Q9CPW4	ARPC5_MOUSE	Actin-related protein 2/3 complex subunit 5	1.2	0.4986
Q3URD3	SLMAP_MOUSE	Sarcolemmal membrane-associated protein	1.2	0.1692

P61089	UBE2N_MOUSE	Ubiquitin-conjugating enzyme E2 N	1.2	0.1288
Q9Z2M7	PMM2_MOUSE	Phosphomannomutase 2	1.2	0.7323
P53994	RAB2A_MOUSE	Ras-related protein Rab-2A	1.2	0.2276
P70663	SPRL1_MOUSE	SPARC-like protein 1	1.2	0.8605
Q4KML4	ABRAL_MOUSE	Costars family protein ABRACL	1.2	0.8630
Q9Z2X1	HNRPF_MOUSE	Heterogeneous nuclear ribonucleoprotein F	1.3	0.7046
Q91ZJ5	UGPA_MOUSE	UTP--glucose-1-phosphate uridylyltransferase	1.3	0.1095
Q60972	RBBP4_MOUSE	Histone-binding protein RBBP4	1.3	0.0101*
Q9DCJ5	NDUA8_MOUSE	NADH dehydrogenase [ubiquinone] 1 alpha subcomplex subunit 8	1.3	0.8922
Q9ESY9	GILT_MOUSE	Gamma-interferon-inducible lysosomal thiol reductase	1.3	0.1838
Q9DCT2	NDUS3_MOUSE	NADH dehydrogenase [ubiquinone] iron-sulfur protein 3, mitochondrial	1.3	0.1372
P34884	MIF_MOUSE	Macrophage migration inhibitory factor	1.3	0.0759
P80317	TCPZ_MOUSE	T-complex protein 1 subunit zeta	1.3	0.3555
O08807	PRDX4_MOUSE	Peroxiredoxin-4	1.3	0.2470
P99029	PRDX5_MOUSE	Peroxiredoxin-5, mitochondrial	1.3	0.1520
Q9WTP6	KAD2_MOUSE	Adenylate kinase 2, mitochondrial	1.3	0.5934
P29699	FETUA_MOUSE	Alpha-2-HS-glycoprotein	1.3	0.3079
Q9Z0X1	AIFM1_MOUSE	Apoptosis-inducing factor 1, mitochondrial	1.3	0.0877
Q8QZT1	THIL_MOUSE	Acetyl-CoA acetyltransferase, mitochondrial	1.3	0.0950
P62270	RS18_MOUSE	40S ribosomal protein S18	1.3	0.2514
Q91VI7	RINI_MOUSE	Ribonuclease inhibitor	1.3	0.0419*
Q922R8	PDIA6_MOUSE	Protein disulfide-isomerase A6	1.3	0.0670
Q05793	PGBM_MOUSE	Basement membrane-specific heparan sulfate proteoglycan core protein	1.3	0.8694
Q62422	OSTF1_MOUSE	Osteoclast-stimulating factor 1	1.3	0.4510
P63028	TCTP_MOUSE	Translationally-controlled tumor protein	1.3	0.7827
P62264	RS14_MOUSE	40S ribosomal protein S14	1.3	0.2437
P24369	PPIB_MOUSE	Peptidyl-prolyl cis-trans isomerase B	1.3	0.0693
Q62219	TGFI1_MOUSE	Transforming growth factor beta-1-induced transcript 1 protein	1.3	0.4267
Q9D1D4	TMEDA_MOUSE	Transmembrane emp24 domain-containing protein 10	1.3	0.7751
Q99JW5	EPCAM_MOUSE	Epithelial cell adhesion molecule	1.3	0.1021
Q6WVG3	KCD12_MOUSE	BTB/POZ domain-containing protein KCTD12	1.3	0.0082*
Q9D8S4	ORN_MOUSE	Oligoribonuclease, mitochondrial	1.3	0.8872
Q62356	FSTL1_MOUSE	Follistatin-related protein 1	1.3	0.4155
P08553	NFM_MOUSE	Neurofilament medium polypeptide	1.3	0.9746
P57780	ACTN4_MOUSE	Alpha-actinin-4	1.3	0.9317
O54962	BAF_MOUSE	Barrier-to-autointegration factor	1.3	0.0527
P04117	FABP4_MOUSE	Fatty acid-binding protein, adipocyte	1.3	0.2109
Q9CZ13	QCR1_MOUSE	Cytochrome b-c1 complex subunit 1, mitochondrial	1.3	0.9953
P63017	HSP7C_MOUSE	Heat shock cognate 71 kDa protein	1.3	0.0541
P97927	LAMA4_MOUSE	Laminin subunit alpha-4	1.3	0.8016

P30412	PPIC_MOUSE	Peptidyl-prolyl cis-trans isomerase C	1.3	0.5472
Q8BFW7	LPP_MOUSE	Lipoma-preferred partner homolog	1.3	0.4747
P02469	LAMB1_MOUSE	Laminin subunit beta-1	1.3	0.2609
P62897	CYC_MOUSE	Cytochrome c, somatic	1.3	0.8221
Q64727	VINC_MOUSE	Vinculin	1.3	0.0026*
Q3UTJ2	SRBS2_MOUSE	Sorbin and SH3 domain-containing protein 2	1.3	0.3199
Q8K2B3	SDHA_MOUSE	Succinate dehydrogenase [ubiquinone] flavoprotein subunit, mitochondrial	1.3	0.8654
Q9D7M8	RPB4_MOUSE	DNA-directed RNA polymerase II subunit RPB4	1.3	0.4041
Q08093	CNN2_MOUSE	Calponin-2	1.3	0.1716
Q9D0S9	HINT2_MOUSE	Histidine triad nucleotide-binding protein 2, mitochondrial	1.3	0.3542
P26041	MOES_MOUSE	Moesin	1.3	0.6000
Q64010	CRK_MOUSE	Adapter molecule crk	1.3	0.7364
Q9CQQ7	AT5F1_MOUSE	ATP synthase F(0) complex subunit B1, mitochondrial	1.4	0.2069
P97461	RS5_MOUSE	40S ribosomal protein S5	1.4	0.7885
P58044	IDI1_MOUSE	Isopentenyl-diphosphate Delta-isomerase 1	1.4	0.1222
P08249	MDHM_MOUSE	Malate dehydrogenase, mitochondrial	1.4	0.0614
Q7TMK9	HNRPQ_MOUSE	Heterogeneous nuclear ribonucleoprotein Q	1.4	0.8965
Q9WVA4	TAGL2_MOUSE	Transgelin-2	1.4	0.6543
Q8VC28	AK1CD_MOUSE	Aldo-keto reductase family 1 member C13	1.4	0.9440
P01837	IGKC_MOUSE	Ig kappa chain C region	1.4	0.2521
O54724	CAVN1_MOUSE	Polymerase I and transcript release factor	1.4	0.0427*
Q01853	TERA_MOUSE	Transitional endoplasmic reticulum ATPase	1.4	0.005*
P17047	LAMP2_MOUSE	Lysosome-associated membrane glycoprotein 2	1.4	0.6796
Q60648	SAP3_MOUSE	Ganglioside GM2 activator	1.4	0.0264*
Q8BH95	ECHM_MOUSE	Enoyl-CoA hydratase, mitochondrial	1.4	0.2961
Q60994	ADIPO_MOUSE	Adiponectin	1.4	0.1424
P63276	RS17_MOUSE	40S ribosomal protein S17	1.4	0.5889
P62141	PP1B_MOUSE	Serine/threonine-protein phosphatase PP1-beta catalytic subunit	1.4	0.1507
P26638	SYSC_MOUSE	Serine--tRNA ligase, cytoplasmic	1.4	0.0717
Q8BHC0	LYVE1_MOUSE	Lymphatic vessel endothelial hyaluronic acid receptor 1	1.4	0.3477
O70456	1433S_MOUSE	14-3-3 protein sigma	1.4	0.1305
Q9CXW4	RL11_MOUSE	60S ribosomal protein L11	1.4	0.0500
Q3UM45	PP1R7_MOUSE	Protein phosphatase 1 regulatory subunit 7	1.4	0.4307
O09164	SODE_MOUSE	Extracellular superoxide dismutase [Cu-Zn]	1.4	0.1509
P35279	RAB6A_MOUSE	Ras-related protein Rab-6A	1.4	0.9732
Q8K3J1	NDUS8_MOUSE	NADH dehydrogenase [ubiquinone] iron-sulfur protein 8, mitochondrial	1.4	0.6083
P35979	RL12_MOUSE	60S ribosomal protein L12	1.4	0.0812
P63330	PP2AA_MOUSE	Serine/threonine-protein phosphatase 2A catalytic subunit alpha isoform	1.4	0.3680
P56399	UBP5_MOUSE	Ubiquitin carboxyl-terminal hydrolase 5	1.4	0.0588
Q9D7Z6	CLCA1_MOUSE	Calcium-activated chloride channel regulator 1	1.4	0.0625

Q76MZ3	2AAA_MOUSE	Serine/threonine-protein phosphatase 2A 65 kDa regulatory subunit A alpha isoform	1.4	0.1205
Q9CZX8	RS19_MOUSE	40S ribosomal protein S19	1.4	0.1834
Q3TTY5	K22E_MOUSE	Keratin, type II cytoskeletal 2 epidermal	1.4	0.2208
Q3THW5	H2AV_MOUSE	Histone H2A.V	1.4	0.1335
P47962	RL5_MOUSE	60S ribosomal protein L5	1.4	0.5587
Q9D1A2	CNDP2_MOUSE	Cytosolic non-specific dipeptidase	1.4	0.8093
Q9JJU8	SH3L1_MOUSE	SH3 domain-binding glutamic acid-rich-like protein	1.4	0.003*
Q9QXS6	DREB_MOUSE	Drebrin	1.4	0.7499
P11276	FINC_MOUSE	Fibronectin	1.4	0.3941
P97807	FUMH_MOUSE	Fumarate hydratase, mitochondrial	1.4	0.0523
Q61233	PLSL_MOUSE	Plastin-2	1.4	0.0778
Q921I1	TRFE_MOUSE	Serotransferrin	1.4	0.8916
Q9Z0M6	CD97_MOUSE	CD97 antigen	1.4	0.1485
Q921U8	SMTN_MOUSE	Smoothelin	1.4	0.0308*
Q9D967	MGDP1_MOUSE	Magnesium-dependent phosphatase 1	1.4	0.2777
P09055	ITB1_MOUSE	Integrin beta-1	1.4	0.1655
P62082	RS7_MOUSE	40S ribosomal protein S7	1.4	0.0076*
P08113	ENPL_MOUSE	Endoplasmin	1.4	0.4721
Q62465	VAT1_MOUSE	Synaptic vesicle membrane protein VAT-1 homolog	1.4	0.2884
Q9DAW9	CNN3_MOUSE	Calponin-3	1.4	0.5553
P62855	RS26_MOUSE	40S ribosomal protein S26	1.4	0.0003*
P62259	1433E_MOUSE	14-3-3 protein epsilon	1.4	0.0088*
O88456	CPNS1_MOUSE	Calpain small subunit 1	1.4	0.0034*
Q8CGP2	H2B1P_MOUSE	Histone H2B type 1-P	1.4	0.5368
Q9CQ60	6PGL_MOUSE	6-phosphogluconolactonase	1.4	0.0006*
P42125	ECI1_MOUSE	Enoyl-CoA delta isomerase 1, mitochondrial	1.4	0.9596
P01831	THY1_MOUSE	Thy-1 membrane glycoprotein	1.4	0.1433
Q9CQ62	DECR_MOUSE	2,4-dienoyl-CoA reductase, mitochondrial	1.4	0.5282
Q9D0F9	PGM1_MOUSE	Phosphoglucomutase-1	**1.4**	0.9155
P97447	FHL1_MOUSE	Four and a half LIM domains protein 1	**1.4**	0.0541
Q9ET54	PALLD_MOUSE	Palladin	**1.4**	0.2233
P97351	RS3A_MOUSE	40S ribosomal protein S3a	**1.4**	0.0175*
P18760	COF1_MOUSE	Cofilin-1	**1.5**	0.9629
P54775	PRS6B_MOUSE	26S protease regulatory subunit 6B	**1.5**	0.1493
Q99K41	EMIL1_MOUSE	EMILIN-1	**1.5**	0.6418
Q99J77	SIAS_MOUSE	Sialic acid synthase	**1.5**	0.0554
Q6P069	SORCN_MOUSE	Sorcin	**1.5**	0.0274*
P12970	RL7A_MOUSE	60S ribosomal protein L7a	**1.5**	0.7572
P50247	SAHH_MOUSE	Adenosylhomocysteinase	**1.5**	0.0503

P50518	VATE1_MOUSE	V-type proton ATPase subunit E 1	**1.5**	0.9336
P51150	RAB7A_MOUSE	Ras-related protein Rab-7a	**1.5**	0.0498
P23953	EST1C_MOUSE	Carboxylesterase 1C	**1.5**	0.0199*
Q99KF1	TMED9_MOUSE	Transmembrane emp24 domain-containing protein 9	**1.5**	0.6173
P68037	UB2L3_MOUSE	Ubiquitin-conjugating enzyme E2 L3	**1.5**	0.3984
P62754	RS6_MOUSE	40S ribosomal protein S6	**1.5**	0.0236*
Q99LF4	RTCB_MOUSE	tRNA-splicing ligase RtcB homolog	**1.5**	0.9456
P61358	RL27_MOUSE	60S ribosomal protein L27	**1.5**	0.3692
Q99KI0	ACON_MOUSE	Aconitate hydratase, mitochondrial	**1.5**	0.0358*
Q9JKF1	IQGA1_MOUSE	Ras GTPase-activating-like protein IQGAP1	**1.5**	0.7695
P63321	RALA_MOUSE	Ras-related protein Ral-A	**1.5**	0.5289
P58252	EF2_MOUSE	Elongation factor 2	**1.5**	0.9358
P62900	RL31_MOUSE	60S ribosomal protein L31	**1.5**	0.2530
P68369	TBA1A_MOUSE	Tubulin alpha-1A chain	**1.5**	0.3357
Q91WQ3	SYYC_MOUSE	Tyrosine--tRNA ligase, cytoplasmic	**1.5**	0.9430
P08121	CO3A1_MOUSE	Collagen alpha-1(III) chain	**1.5**	0.7411
Q9Z2U1	PSA5_MOUSE	Proteasome subunit alpha type-5	**1.5**	0.9163
P61255	RL26_MOUSE	60S ribosomal protein L26	**1.5**	0.0114*
Q3TJD7	PDLI7_MOUSE	PDZ and LIM domain protein 7	**1.5**	0.3047
P62334	PRS10_MOUSE	26S protease regulatory subunit 10B	**1.5**	0.0161*
Q9R0Q7	TEBP_MOUSE	Prostaglandin E synthase 3	**1.5**	0.0058*
P47911	RL6_MOUSE	60S ribosomal protein L6	**1.5**	0.0169*
P70195	PSB7_MOUSE	Proteasome subunit beta type-7	**1.5**	0.5072
P62843	RS15_MOUSE	40S ribosomal protein S15	**1.5**	0.1550
Q9QUI0	RHOA_MOUSE	Transforming protein RhoA	**1.5**	0.5857
Q9CX86	ROA0_MOUSE	Heterogeneous nuclear ribonucleoprotein A0	**1.5**	0.9007
P40142	TKT_MOUSE	Transketolase	**1.5**	0.4940
P62751	RL23A_MOUSE	60S ribosomal protein L23a	**1.5**	0.5059
P17918	PCNA_MOUSE	Proliferating cell nuclear antigen	**1.5**	0.0339*
Q9DBH5	LMAN2_MOUSE	Vesicular integral-membrane protein VIP36	**1.5**	0.4778
P00920	CAH2_MOUSE	Carbonic anhydrase 2	**1.5**	0.4955
P47963	RL13_MOUSE	60S ribosomal protein L13	**1.5**	0.0201*
Q60692	PSB6_MOUSE	Proteasome subunit beta type-6	**1.5**	0.7910
P60766	CDC42_MOUSE	Cell division control protein 42 homolog	**1.5**	0.6210
P80316	TCPE_MOUSE	T-complex protein 1 subunit epsilon	**1.5**	0.0017*
P62908	RS3_MOUSE	40S ribosomal protein S3	**1.5**	0.0811
P62301	RS13_MOUSE	40S ribosomal protein S13	**1.5**	0.0472*
P68254	1433T_MOUSE	14-3-3 protein theta	**1.5**	0.0141*
P67984	RL22_MOUSE	60S ribosomal protein L22	**1.5**	0.0195*
Q9Z2U0	PSA7_MOUSE	Proteasome subunit alpha type-7	**1.5**	0.9372

P08207	S10AA_MOUSE	Protein S100-A10	**1.5**	0.3383
Q6ZWX6	IF2A_MOUSE	Eukaryotic translation initiation factor 2 subunit 1	**1.5**	0.002*
P48036	ANXA5_MOUSE	Annexin A5	**1.5**	0.0044*
P14131	RS16_MOUSE	40S ribosomal protein S16	**1.6**	0.0291*
Q62417	SRBS1_MOUSE	Sorbin and SH3 domain-containing protein 1	**1.6**	0.2628
Q04447	KCRB_MOUSE	Creatine kinase B-type	**1.6**	0.014*
P63101	1433Z_MOUSE	14-3-3 protein zeta/delta	**1.6**	0.0066*
P35980	RL18_MOUSE	60S ribosomal protein L18	**1.6**	0.7700
O08553	DPYL2_MOUSE	Dihydropyrimidinase-related protein 2	**1.6**	0.2031
P10126	EF1A1_MOUSE	Elongation factor 1-alpha 1	**1.6**	0.4514
P30416	FKBP4_MOUSE	Peptidyl-prolyl cis-trans isomerase FKBP4	**1.6**	0.9994
Q9JII6	AK1A1_MOUSE	Alcohol dehydrogenase [NADP(+)]	**1.6**	0.001*
Q8BHN3	GANAB_MOUSE	Neutral alpha-glucosidase AB	**1.6**	0.0219*
P62196	PRS8_MOUSE	26S protease regulatory subunit 8	**1.6**	0.0039*
Q9CZS1	AL1B1_MOUSE	Aldehyde dehydrogenase X, mitochondrial	**1.6**	0.7456
P53026	RL10A_MOUSE	60S ribosomal protein L10a	**1.6**	0.1815
P22599	A1AT2_MOUSE	Alpha-1-antitrypsin 1-2	**1.6**	0.4236
Q08091	CNN1_MOUSE	Calponin-1	**1.6**	0.0143*
Q61543	GSLG1_MOUSE	Golgi apparatus protein 1	**1.6**	0.0675
Q9CPV4	GLOD4_MOUSE	Glyoxalase domain-containing protein 4	**1.6**	0.2073
Q61555	FBN2_MOUSE	Fibrillin-2	**1.6**	0.8652
Q91YR1	TWF1_MOUSE	Twinfilin-1	**1.6**	0.1169
Q9EQP2	EHD4_MOUSE	EH domain-containing protein 4	**1.6**	0.3073
P51410	RL9_MOUSE	60S ribosomal protein L9	**1.6**	0.5458
Q8K419	LEG4_MOUSE	Galectin-4	**1.6**	0.0484*
Q8CHP8	PGP_MOUSE	Glycerol-3-phosphate phosphatase	**1.6**	0.0408*
P02468	LAMC1_MOUSE	Laminin subunit gamma-1	**1.6**	0.0094*
Q62186	SSRD_MOUSE	Translocon-associated protein subunit delta	**1.6**	0.4076
Q9DBC7	KAP0_MOUSE	cAMP-dependent protein kinase type I-alpha regulatory subunit	**1.6**	0.0086*
P63325	RS10_MOUSE	40S ribosomal protein S10	**1.6**	0.6137
P11352	GPX1_MOUSE	Glutathione peroxidase 1	**1.6**	0.027*
P10518	HEM2_MOUSE	Delta-aminolevulinic acid dehydratase	**1.6**	0.5958
P42208	SEPT2_MOUSE	Septin-2	**1.6**	0.0014*
Q9CQA3	SDHB_MOUSE	Succinate dehydrogenase [ubiquinone] iron-sulfur subunit, mitochondrial	**1.6**	0.0122*
P62880	GBB2_MOUSE	Guanine nucleotide-binding protein G(I)/G(S)/G(T) subunit beta-2	**1.6**	0.0671
P97372	PSME2_MOUSE	Proteasome activator complex subunit 2	**1.6**	0.0382*
P47791	GSHR_MOUSE	Glutathione reductase, mitochondrial	**1.6**	0.5202
P70695	F16P2_MOUSE	Fructose-1,6-bisphosphatase isozyme 2	**1.6**	0.0770
Q62376	RU17_MOUSE	U1 small nuclear ribonucleoprotein 70 kDa	**1.6**	0.7400
Q9JKA5	GPA33_MOUSE	Cell surface A33 antigen	**1.6**	0.1758

P15947	KLK1_MOUSE	Kallikrein-1	**1.6**	0.2057
Q9Z1N5	DX39B_MOUSE	Spliceosome RNA helicase Ddx39b	**1.6**	0.1256
Q61425	HCDH_MOUSE	Hydroxyacyl-coenzyme A dehydrogenase, mitochondrial	**1.6**	0.2392
P62869	ELOB_MOUSE	Elongin-B	**1.6**	0.0259*
P09671	SODM_MOUSE	Superoxide dismutase [Mn], mitochondrial	**1.6**	0.0063*
Q9CR57	RL14_MOUSE	60S ribosomal protein L14	**1.6**	0.5721
Q9CZY3	UB2V1_MOUSE	Ubiquitin-conjugating enzyme E2 variant 1	**1.6**	0.0003*
Q91X72	HEMO_MOUSE	Hemopexin	**1.6**	0.1122
P62849	RS24_MOUSE	40S ribosomal protein S24	**1.6**	0.8915
P45591	COF2_MOUSE	Cofilin-2	**1.7**	0.0089*
Q923D2	BLVRB_MOUSE	Flavin reductase (NADPH)	**1.7**	0.1716
Q9CWK8	SNX2_MOUSE	Sorting nexin-2	**1.7**	0.0464*
Q920A5	RISC_MOUSE	Retinoid-inducible serine carboxypeptidase	**1.7**	0.6705
Q9WVJ3	CBPQ_MOUSE	Carboxypeptidase Q	**1.7**	0.3180
P09411	PGK1_MOUSE	Phosphoglycerate kinase 1	**1.7**	0.0005*
Q9WVH9	FBLN5_MOUSE	Fibulin-5	**1.7**	0.0789
P52196	THTR_MOUSE	Thiosulfate sulfurtransferase	**1.7**	0.7020
P27601	GNA13_MOUSE	Guanine nucleotide-binding protein subunit alpha-13	**1.7**	0.8643
P21981	TGM2_MOUSE	Protein-glutamine gamma-glutamyltransferase 2	**1.7**	0.9557
P14094	AT1B1_MOUSE	Sodium/potassium-transporting ATPase subunit beta-1	**1.7**	0.8264
P50580	PA2G4_MOUSE	Proliferation-associated protein 2G4	**1.7**	0.0002*
P97384	ANX11_MOUSE	Annexin A11	**1.7**	0.0266*
Q62059	CSPG2_MOUSE	Versican core protein	**1.7**	0.0028*
O88207	CO5A1_MOUSE	Collagen alpha-1(V) chain	**1.7**	0.2657
Q9JHU9	INO1_MOUSE	Inositol-3-phosphate synthase 1	**1.7**	0.0053*
Q9D051	ODPB_MOUSE	Pyruvate dehydrogenase E1 component subunit beta, mitochondrial	**1.7**	0.1987
Q9D898	ARP5L_MOUSE	Actin-related protein 2/3 complex subunit 5-like protein	**1.7**	0.0028*
Q9CWJ9	PUR9_MOUSE	Bifunctional purine biosynthesis protein PURH	**1.7**	0.0471*
Q8CDN6	TXNL1_MOUSE	Thioredoxin-like protein 1	**1.7**	0.2986
P14602	HSPB1_MOUSE	Heat shock protein beta-1	**1.7**	0.0107*
P99026	PSB4_MOUSE	Proteasome subunit beta type-4	**1.7**	0.0981
P10922	H10_MOUSE	Histone H1.0	**1.7**	0.9881
O88322	NID2_MOUSE	Nidogen-2	**1.7**	0.0497
Q9WUM4	COR1C_MOUSE	Coronin-1C	**1.7**	0.0048*
Q9R1P1	PSB3_MOUSE	Proteasome subunit beta type-3	**1.7**	0.7645
P07759	SPA3K_MOUSE	Serine protease inhibitor A3K	**1.7**	0.0164*
Q9WUG6	INSL5_MOUSE	Insulin-like peptide INSL5	**1.7**	0.0019*
P47757	CAPZB_MOUSE	F-actin-capping protein subunit beta	**1.7**	0.0064*
P26443	DHE3_MOUSE	Glutamate dehydrogenase 1, mitochondrial	**1.7**	0.0457*
P62827	RAN_MOUSE	GTP-binding nuclear protein Ran	**1.7**	0.1793

Q9D6R2	IDH3A_MOUSE	Isocitrate dehydrogenase [NAD] subunit alpha, mitochondrial	**1.7**	0.0294*
Q9Z0S1	BPNT1_MOUSE	3'(2'),5'-bisphosphate nucleotidase 1	**1.7**	0.5375
P11688	ITA5_MOUSE	Integrin alpha-5	**1.7**	0.0009*
Q99JY0	ECHB_MOUSE	Trifunctional enzyme subunit beta, mitochondrial	**1.7**	0.0062*
Q9JJI8	RL38_MOUSE	60S ribosomal protein L38	**1.7**	0.9126
P10493	NID1_MOUSE	Nidogen-1	**1.7**	0.8971
P58021	TM9S2_MOUSE	Transmembrane 9 superfamily member 2	**1.7**	0.5797
P51174	ACADL_MOUSE	Long-chain specific acyl-CoA dehydrogenase, mitochondrial	**1.7**	0.0642
P70168	IMB1_MOUSE	Importin subunit beta-1	**1.7**	0.1841
P26043	RADI_MOUSE	Radixin	**1.7**	0.2100
O70423	AOC3_MOUSE	Membrane primary amine oxidase	**1.7**	0.8594
P48758	CBR1_MOUSE	Carbonyl reductase [NADPH] 1	**1.7**	0.0311*
O88685	PRS6A_MOUSE	26S protease regulatory subunit 6A	**1.7**	0.1039
P37804	TAGL_MOUSE	Transgelin	**1.7**	0.0051*
Q9QZZ6	DERM_MOUSE	Dermatopontin	**1.7**	0.2343
P08030	APT_MOUSE	Adenine phosphoribosyltransferase	**1.7**	0.0212*
O08756	HCD2_MOUSE	3-hydroxyacyl-CoA dehydrogenase type-2	**1.7**	0.0104*
Q8BFY6	PEF1_MOUSE	Peflin	**1.7**	0.0055*
Q8BMS1	ECHA_MOUSE	Trifunctional enzyme subunit alpha, mitochondrial	**1.7**	0.0913
P61982	1433G_MOUSE	14-3-3 protein gamma	**1.7**	0.0023*
Q62188	DPYL3_MOUSE	Dihydropyrimidinase-related protein 3	**1.8**	0.0175*
P01027	CO3_MOUSE	Complement C3	**1.8**	0.0701
O35955	PSB10_MOUSE	Proteasome subunit beta type-10	**1.8**	0.5139
P43024	CX6A1_MOUSE	Cytochrome c oxidase subunit 6A1, mitochondrial	**1.8**	0.0989
P62242	RS8_MOUSE	40S ribosomal protein S8	**1.8**	0.0052*
P82198	BGH3_MOUSE	Transforming growth factor-beta-induced protein ig-h3	**1.8**	0.0000*
Q01768	NDKB_MOUSE	Nucleoside diphosphate kinase B	**1.8**	0.0214*
Q9DB20	ATPO_MOUSE	ATP synthase subunit O, mitochondrial	**1.8**	0.0117*
P42932	TCPQ_MOUSE	T-complex protein 1 subunit theta	**1.8**	0.0109*
P32921	SYWC_MOUSE	Tryptophan--tRNA ligase, cytoplasmic	**1.8**	0.0225*
Q6ZWY3	RS27L_MOUSE	40S ribosomal protein S27-like	**1.8**	0.0021*
P15532	NDKA_MOUSE	Nucleoside diphosphate kinase A	**1.8**	0.0305*
P12815	PDCD6_MOUSE	Programmed cell death protein 6	**1.8**	0.3874
Q6ZWN5	RS9_MOUSE	40S ribosomal protein S9	**1.8**	0.0479*
P68510	1433F_MOUSE	14-3-3 protein eta	**1.8**	0.0003*
P40124	CAP1_MOUSE	Adenylyl cyclase-associated protein 1	**1.8**	0.7781
P62806	H4_MOUSE	Histone H4	**1.8**	0.4353
P47754	CAZA2_MOUSE	F-actin-capping protein subunit alpha-2	**1.8**	0.0128*
Q9Z0N1	IF2G_MOUSE	Eukaryotic translation initiation factor 2 subunit 3, X-linked	**1.8**	0.2354
O89079	COPE_MOUSE	Coatomer subunit epsilon	**1.8**	0.0106*

Q62167	DDX3X_MOUSE	ATP-dependent RNA helicase DDX3X	**1.8**	0.0374*
P05202	AATM_MOUSE	Aspartate aminotransferase, mitochondrial	**1.8**	0.0359*
Q9DB05	SNAA_MOUSE	Alpha-soluble NSF attachment protein	**1.8**	0.0089*
P07310	KCRM_MOUSE	Creatine kinase M-type	**1.8**	0.0655
P05064	ALDOA_MOUSE	Fructose-bisphosphate aldolase A	**1.8**	0.0031*
Q8VCR7	ABHEB_MOUSE	Protein ABHD14B	**1.8**	0.1584
P54071	IDHP_MOUSE	Isocitrate dehydrogenase [NADP], mitochondrial	**1.8**	0.0085*
Q60931	VDAC3_MOUSE	Voltage-dependent anion-selective channel protein 3	**1.8**	0.2564
Q91V41	RAB14_MOUSE	Ras-related protein Rab-14	**1.8**	0.1186
P32067	LA_MOUSE	Lupus La protein homolog	**1.8**	0.5780
P47753	CAZA1_MOUSE	F-actin-capping protein subunit alpha-1	**1.8**	0.2973
P19253	RL13A_MOUSE	60S ribosomal protein L13a	**1.8**	0.6132
Q9D819	IPYR_MOUSE	Inorganic pyrophosphatase	**1.8**	0.0001*
Q9CQE1	NPS3B_MOUSE	Protein NipSnap homolog 3B	**1.8**	0.0841
P62281	RS11_MOUSE	40S ribosomal protein S11	**1.8**	0.2019
P80314	TCPB_MOUSE	T-complex protein 1 subunit beta	**1.8**	0.0003*
O88844	IDHC_MOUSE	Isocitrate dehydrogenase [NADP] cytoplasmic	**1.8**	0.0061*
P00405	COX2_MOUSE	Cytochrome c oxidase subunit 2	**1.8**	0.7867
Q9CQV8	1433B_MOUSE	14-3-3 protein beta/alpha	**1.8**	0.0003*
P14152	MDHC_MOUSE	Malate dehydrogenase, cytoplasmic	**1.9**	0.0072*
O08547	SC22B_MOUSE	Vesicle-trafficking protein SEC22b	**1.9**	0.6657
P07758	A1AT1_MOUSE	Alpha-1-antitrypsin 1-1	**1.9**	0.9961
O55060	TPMT_MOUSE	Thiopurine S-methyltransferase	**1.9**	0.1258
P97821	CATC_MOUSE	Dipeptidyl peptidase 1	**1.9**	0.0114*
P62267	RS23_MOUSE	40S ribosomal protein S23	**1.9**	0.0022*
Q9DCH4	EIF3F_MOUSE	Eukaryotic translation initiation factor 3 subunit F	**1.9**	0.0001*
P47856	GFPT1_MOUSE	Glutamine--fructose-6-phosphate aminotransferase [isomerizing] 1	**1.9**	0.7719
Q9R0P5	DEST_MOUSE	Destrin	**1.9**	0.0025*
Q60597	ODO1_MOUSE	2-oxoglutarate dehydrogenase, mitochondrial	**1.9**	0.5798
P62821	RAB1A_MOUSE	Ras-related protein Rab-1A	**1.9**	0.6912
P14869	RLA0_MOUSE	60S acidic ribosomal protein P0	**1.9**	0.0048*
P35762	CD81_MOUSE	CD81 antigen	**1.9**	0.3778
Q9Z1Z2	STRAP_MOUSE	Serine-threonine kinase receptor-associated protein	**1.9**	0.0071*
P62852	RS25_MOUSE	40S ribosomal protein S25	**1.9**	0.3033
P51855	GSHB_MOUSE	Glutathione synthetase	**1.9**	0.0005*
Q9JM76	ARPC3_MOUSE	Actin-related protein 2/3 complex subunit 3	**1.9**	0.0015*
Q01730	RSU1_MOUSE	Ras suppressor protein 1	**1.9**	0.0013*
P84099	RL19_MOUSE	60S ribosomal protein L19	**1.9**	0.4550
P63001	RAC1_MOUSE	Ras-related C3 botulinum toxin substrate 1	**1.9**	0.1808
Q61554	FBN1_MOUSE	Fibrillin-1	**1.9**	0.0197*

P31001	DESM_MOUSE	Desmin	**1.9**	0.0242*
P52480	KPYM_MOUSE	Pyruvate kinase PKM	**1.9**	0.0000*
P10833	RRAS_MOUSE	Ras-related protein R-Ras	**1.9**	0.0004*
Q8VDN2	AT1A1_MOUSE	Sodium/potassium-transporting ATPase subunit alpha-1	**1.9**	0.8932
P62702	RS4X_MOUSE	40S ribosomal protein S4, X isoform	**1.9**	0.0829
P51885	LUM_MOUSE	Lumican	**1.9**	0.0215*
P19157	GSTP1_MOUSE	Glutathione S-transferase P 1	**2.0**	0.0025*
Q91VR2	ATPG_MOUSE	ATP synthase subunit gamma, mitochondrial	**2.0**	0.2152
P62830	RL23_MOUSE	60S ribosomal protein L23	**2.0**	0.0000*
P49817	CAV1_MOUSE	Caveolin-1	**2.0**	0.9227
Q60930	VDAC2_MOUSE	Voltage-dependent anion-selective channel protein 2	**2.0**	0.1581
O35206	COFA1_MOUSE	Collagen alpha-1(XV) chain	**2.0**	0.0566
Q9R0P9	UCHL1_MOUSE	Ubiquitin carboxyl-terminal hydrolase isozyme L1	**2.0**	0.6936
P61750	ARF4_MOUSE	ADP-ribosylation factor 4	**2.0**	0.6012
P10605	CATB_MOUSE	Cathepsin B	**2.0**	0.0427*
P61161	ARP2_MOUSE	Actin-related protein 2	**2.0**	0.0189*
Q99JI6	RAP1B_MOUSE	Ras-related protein Rap-1b	**2.0**	0.6902
Q9DB77	QCR2_MOUSE	Cytochrome b-c1 complex subunit 2, mitochondrial	**2.0**	0.0327*
Q9D8C4	IN35_MOUSE	Interferon-induced 35 kDa protein homolog	**2.0**	0.9340
P28654	PGS2_MOUSE	Decorin	**2.0**	0.0312*
P28653	PGS1_MOUSE	Biglycan	**2.0**	0.015*
A3KMP2	TTC38_MOUSE	Tetratricopeptide repeat protein 38	**2.0**	0.0277*
P17710	HXK1_MOUSE	Hexokinase-1	**2.0**	0.0034*
P46412	GPX3_MOUSE	Glutathione peroxidase 3	**2.0**	0.0051*
P06745	G6PI_MOUSE	Glucose-6-phosphate isomerase	**2.0**	0.0529
Q91VJ2	CAVN3_MOUSE	Protein kinase C delta-binding protein	**2.0**	0.0009*
Q91VD9	NDUS1_MOUSE	NADH-ubiquinone oxidoreductase 75 kDa subunit, mitochondrial	**2.0**	0.9468
Q61205	PA1B3_MOUSE	Platelet-activating factor acetylhydrolase IB subunit gamma	**2.0**	0.0128*
P35486	ODPA_MOUSE	Pyruvate dehydrogenase E1 component subunit alpha, somatic form, mitochondrial	**2.0**	0.1717
P62245	RS15A_MOUSE	40S ribosomal protein S15a	**2.0**	0.009*
P97429	ANXA4_MOUSE	Annexin A4	**2.0**	0.005*
O35129	PHB2_MOUSE	Prohibitin-2	**2.0**	0.2712
Q9Z1Q5	CLIC1_MOUSE	Chloride intracellular channel protein 1	**2.1**	0.0006*
Q60847	COCA1_MOUSE	Collagen alpha-1(XII) chain	**2.1**	0.0544
P62838	UB2D2_MOUSE	Ubiquitin-conjugating enzyme E2 D2	**2.1**	0.0015*
Q8VEM8	MPCP_MOUSE	Phosphate carrier protein, mitochondrial	**2.1**	0.6264
Q9CVB6	ARPC2_MOUSE	Actin-related protein 2/3 complex subunit 2	**2.1**	0.0042*
P25444	RS2_MOUSE	40S ribosomal protein S2	**2.1**	0.0265*
P23492	PNPH_MOUSE	Purine nucleoside phosphorylase	**2.1**	0.0028*

Q9R1P4	PSA1_MOUSE	Proteasome subunit alpha type-1	**2.1**	0.6375
P62996	TRA2B_MOUSE	Transformer-2 protein homolog beta	**2.1**	0.9607
P62918	RL8_MOUSE	60S ribosomal protein L8	**2.1**	0.002*
O55143	AT2A2_MOUSE	Sarcoplasmic/endoplasmic reticulum calcium ATPase 2	**2.1**	0.2483
P80313	TCPH_MOUSE	T-complex protein 1 subunit eta	**2.1**	0.0069*
Q9CQI6	COTL1_MOUSE	Coactosin-like protein	**2.1**	0.0000*
P27659	RL3_MOUSE	60S ribosomal protein L3	**2.1**	0.0074*
P61205	ARF3_MOUSE	ADP-ribosylation factor 3	**2.1**	0.6534
Q64105	SPRE_MOUSE	Sepiapterin reductase	**2.1**	0.1543
Q02053	UBA1_MOUSE	Ubiquitin-like modifier-activating enzyme 1	**2.1**	0.0869
P80315	TCPD_MOUSE	T-complex protein 1 subunit delta	**2.1**	0.0246*
Q61702	ITIH1_MOUSE	Inter-alpha-trypsin inhibitor heavy chain H1	**2.1**	0.7474
Q91VC3	IF4A3_MOUSE	Eukaryotic initiation factor 4A-III	**2.1**	0.0352*
P09813	APOA2_MOUSE	Apolipoprotein A-II	**2.1**	0.4634
Q9DBG6	RPN2_MOUSE	Dolichyl-diphosphooligosaccharide--protein glycosyltransferase subunit 2	**2.1**	0.3296
Q9WTP7	KAD3_MOUSE	GTP:AMP phosphotransferase AK3, mitochondrial	**2.2**	0.0034*
P10107	ANXA1_MOUSE	Annexin A1	**2.2**	0.0015*
Q61696	HS71A_MOUSE	Heat shock 70 kDa protein 1A	**2.2**	0.0001*
P70124	SPB5_MOUSE	Serpin B5	**2.2**	0.0018*
P68040	RACK1_MOUSE	Receptor of activated protein C kinase 1	**2.2**	0.0078*
O09131	GSTO1_MOUSE	Glutathione S-transferase omega-1	**2.2**	0.0153*
P07901	HS90A_MOUSE	Heat shock protein HSP 90-alpha	**2.2**	0.1495
Q5EBG6	HSPB6_MOUSE	Heat shock protein beta-6	**2.2**	0.9404
Q04857	CO6A1_MOUSE	Collagen alpha-1(VI) chain	**2.2**	0.0151*
Q9R1P0	PSA4_MOUSE	Proteasome subunit alpha type-4	**2.2**	0.2915
P49722	PSA2_MOUSE	Proteasome subunit alpha type-2	**2.2**	0.7706
Q8R059	GALE_MOUSE	UDP-glucose 4-epimerase	**2.2**	0.0021*
Q922F4	TBB6_MOUSE	Tubulin beta-6 chain	**2.3**	0.0068*
Q9JMH6	TRXR1_MOUSE	Thioredoxin reductase 1, cytoplasmic	**2.3**	0.0408*
Q80X19	COEA1_MOUSE	Collagen alpha-1(XIV) chain	**2.3**	0.0000*
Q62009	POSTN_MOUSE	Periostin	**2.3**	0.0002*
Q99KP3	CRYL1_MOUSE	Lambda-crystallin homolog	**2.3**	0.0322*
Q9D0K2	SCOT1_MOUSE	Succinyl-CoA:3-ketoacid coenzyme A transferase 1, mitochondrial	**2.3**	0.0002*
P06151	LDHA_MOUSE	L-lactate dehydrogenase A chain	**2.3**	0.0089*
P11983	TCPA_MOUSE	T-complex protein 1 subunit alpha	**2.3**	0.0001*
O35643	AP1B1_MOUSE	AP-1 complex subunit beta-1	**2.3**	0.4950
Q9DCN2	NB5R3_MOUSE	NADH-cytochrome b5 reductase 3	**2.3**	0.1310
Q9JKS4	LDB3_MOUSE	LIM domain-binding protein 3	**2.3**	0.0571
P14148	RL7_MOUSE	60S ribosomal protein L7	**2.3**	0.3608
P99024	TBB5_MOUSE	Tubulin beta-5 chain	**2.3**	0.7581

Q61166	MARE1_MOUSE	Microtubule-associated protein RP/EB family member 1	**2.3**	0.2806
Q7TPR4	ACTN1_MOUSE	Alpha-actinin-1	**2.4**	0.0046*
Q9QUM9	PSA6_MOUSE	Proteasome subunit alpha type-6	**2.4**	0.2651
P26040	EZRI_MOUSE	Ezrin	**2.4**	0.0934
O09061	PSB1_MOUSE	Proteasome subunit beta type-1	**2.4**	0.4024
P16858	G3P_MOUSE	Glyceraldehyde-3-phosphate dehydrogenase	**2.4**	0.0002*
P51881	ADT2_MOUSE	ADP/ATP translocase 2	**2.4**	0.7784
P16125	LDHB_MOUSE	L-lactate dehydrogenase B chain	**2.4**	0.0042*
P11087	CO1A1_MOUSE	Collagen alpha-1(I) chain	**2.4**	0.2014
O35679	ISK4_MOUSE	Serine protease inhibitor Kazal-type 4	**2.4**	0.0042*
O55222	ILK_MOUSE	Integrin-linked protein kinase	**2.4**	0.4624
Q60932	VDAC1_MOUSE	Voltage-dependent anion-selective channel protein 1	**2.4**	0.0054*
Q68FD5	CLH1_MOUSE	Clathrin heavy chain 1	**2.5**	0.5243
P01942	HBA_MOUSE	Hemoglobin subunit alpha	**2.5**	0.0019*
Q99JW2	ACY1_MOUSE	Aminoacylase-1	**2.5**	0.0017*
P11499	HS90B_MOUSE	Heat shock protein HSP 90-beta	**2.5**	0.0402*
Q9D8N0	EF1G_MOUSE	Elongation factor 1-gamma	**2.5**	0.0825
P14824	ANXA6_MOUSE	Annexin A6	**2.5**	0.0008*
Q91V12	BACH_MOUSE	Cytosolic acyl coenzyme A thioester hydrolase	**2.5**	0.0092*
P24472	GSTA4_MOUSE	Glutathione S-transferase A4	**2.6**	0.0167*
Q9QZD9	EIF3I_MOUSE	Eukaryotic translation initiation factor 3 subunit I	**2.6**	0.7126
Q99JY9	ARP3_MOUSE	Actin-related protein 3	**2.6**	0.009*
P80318	TCPG_MOUSE	T-complex protein 1 subunit gamma	**2.6**	0.0016*
Q8BFR5	EFTU_MOUSE	Elongation factor Tu, mitochondrial	**2.6**	0.5321
Q8VHX6	FLNC_MOUSE	Filamin-C	**2.6**	0.0032*
Q9QZJ6	MFAP5_MOUSE	Microfibrillar-associated protein 5	**2.6**	0.0087*
O70370	CATS_MOUSE	Cathepsin S	**2.6**	0.0164*
Q8CIB5	FERM2_MOUSE	Fermitin family homolog 2	**2.7**	0.9352
Q9WV54	ASAH1_MOUSE	Acid ceramidase	**2.7**	0.4657
Q62000	MIME_MOUSE	Mimecan	**2.7**	0.0016*
P19096	FAS_MOUSE	Fatty acid synthase	**2.7**	0.1080
O88342	WDR1_MOUSE	WD repeat-containing protein 1	**2.7**	0.0018*
P59999	ARPC4_MOUSE	Actin-related protein 2/3 complex subunit 4	**2.7**	0.0015*
Q91YR9	PTGR1_MOUSE	Prostaglandin reductase 1	**2.7**	0.0001*
Q9D708	S10AG_MOUSE	Protein S100-A16	**2.7**	0.0005*
Q9DAU7	WFDC2_MOUSE	WAP four-disulfide core domain protein 2	**2.7**	0.0267*
Q8K0J2	B3GN7_MOUSE	UDP-GlcNAc:betaGal beta-1,3-N-acetylglucosaminyltransferase 7	**2.7**	0.0189*
P02089	HBB2_MOUSE	Hemoglobin subunit beta-2	**2.8**	0.0032*
P13020	GELS_MOUSE	Gelsolin	**2.8**	0.0027*
Q9D154	ILEUA_MOUSE	Leukocyte elastase inhibitor A	**2.8**	0.0049*

Q9WUA3	PFKAP_MOUSE	ATP-dependent 6-phosphofructokinase, platelet type	**2.8**	0.0453*
O35639	ANXA3_MOUSE	Annexin A3	**2.8**	0.0004*
P58389	PTPA_MOUSE	Serine/threonine-protein phosphatase 2A activator	**2.8**	0.002*
P07356	ANXA2_MOUSE	Annexin A2	**2.8**	0.0054*
P48962	ADT1_MOUSE	ADP/ATP translocase 1	**2.9**	0.0895
Q9CZM2	RL15_MOUSE	60S ribosomal protein L15	**2.9**	0.9310
P19324	SERPH_MOUSE	Serpin H1	**2.9**	0.0005*
P63268	ACTH_MOUSE	Actin, gamma-enteric smooth muscle	**2.9**	0.0086*
P68368	TBA4A_MOUSE	Tubulin alpha-4A chain	**2.9**	0.8308
Q7TMM9	TBB2A_MOUSE	Tubulin beta-2A chain	**2.9**	0.8720
P30275	KCRU_MOUSE	Creatine kinase U-type, mitochondrial	**2.9**	0.0027*
P02088	HBB1_MOUSE	Hemoglobin subunit beta-1	**2.9**	0.0029*
Q60854	SPB6_MOUSE	Serpin B6	**3.0**	0.0016*
O08709	PRDX6_MOUSE	Peroxiredoxin-6	**3.0**	0.0006*
Q8BG32	PSD11_MOUSE	26S proteasome non-ATPase regulatory subunit 11	**3.0**	0.0036*
Q91WL0	ES8L3_MOUSE	Epidermal growth factor receptor kinase substrate 8-like protein 3	**3.1**	0.9594
Q8BVA4	LMOD1_MOUSE	Leiomodin-1	**3.1**	0.0247*
Q9JK53	PRELP_MOUSE	Prolargin	**3.1**	0.0008*
P47738	ALDH2_MOUSE	Aldehyde dehydrogenase, mitochondrial	**3.2**	0.0008*
P45376	ALDR_MOUSE	Aldose reductase	**3.2**	0.0001*
Q9JM14	NT5C_MOUSE	5'(3')-deoxyribonucleotidase, cytosolic type	**3.2**	0.0000*
Q61598	GDIB_MOUSE	Rab GDP dissociation inhibitor beta	**3.2**	0.0019*
Q80UG5	SEPT9_MOUSE	Septin-9	**3.2**	0.0008*
Q01149	CO1A2_MOUSE	Collagen alpha-2(I) chain	**3.3**	0.2946
Q9DCD0	6PGD_MOUSE	6-phosphogluconate dehydrogenase, decarboxylating	**3.3**	0.1011
P62962	PROF1_MOUSE	Profilin-1	**3.3**	0.0001*
O70435	PSA3_MOUSE	Proteasome subunit alpha type-3	**3.3**	0.5050
P24527	LKHA4_MOUSE	Leukotriene A-4 hydrolase	**3.3**	0.0285*
P60843	IF4A1_MOUSE	Eukaryotic initiation factor 4A-I	**3.4**	0.0001*
Q8BZF8	PGM5_MOUSE	Phosphoglucomutase-like protein 5	**3.4**	0.0112*
Q3UW53	NIBAN_MOUSE	Protein Niban	**3.5**	0.5502
P15626	GSTM2_MOUSE	Glutathione S-transferase Mu 2	**3.6**	0.0048*
Q99MQ4	ASPN_MOUSE	Asporin	**3.7**	0.0004*
Q9CZU6	CISY_MOUSE	Citrate synthase, mitochondrial	**3.7**	0.0305*
P10649	GSTM1_MOUSE	Glutathione S-transferase Mu 1	**3.7**	0.0006*
Q8BP67	RL24_MOUSE	60S ribosomal protein L24	**3.8**	0.9507
Q6GSS7	H2A2A_MOUSE	Histone H2A type 2-A	**3.8**	0.8999
P68134	ACTS_MOUSE	Actin, alpha skeletal muscle	**3.8**	0.0002*
Q9R0P3	ESTD_MOUSE	S-formylglutathione hydrolase	**3.8**	0.0288*
Q91V92	ACLY_MOUSE	ATP-citrate synthase	**3.9**	0.0095*

Q02788	CO6A2_MOUSE	Collagen alpha-2(VI) chain	**4.1**	0.0068*
Q8K0C5	ZG16_MOUSE	Zymogen granule membrane protein 16	**4.2**	0.0074*
Q9WTI7	MYO1C_MOUSE	Unconventional myosin-Ic	**4.4**	0.0018*
P84228	H32_MOUSE	Histone H3.2	**4.4**	0.8648
Q8CI94	PYGB_MOUSE	Glycogen phosphorylase, brain form	**4.4**	0.0211*
Q9Z0L8	GGH_MOUSE	Gamma-glutamyl hydrolase	**4.4**	0.0000*
Q9R1K9	CETN2_MOUSE	Centrin-2	**4.5**	0.8196
Q9D2Q8	S10AE_MOUSE	Protein S100-A14	**4.7**	0.0001*
Q05816	FABP5_MOUSE	Fatty acid-binding protein, epidermal	**4.8**	0.2314
P97430	SLPI_MOUSE	Antileukoproteinase	**4.8**	0.0001*
P00329	ADH1_MOUSE	Alcohol dehydrogenase 1	**5.2**	0.0046*
P53996	CNBP_MOUSE	Cellular nucleic acid-binding protein	**6.3**	0.9870
P11034	MCPT1_MOUSE	Mast cell protease 1	**6.6**	0.8425
Q8R1M8	MPTX_MOUSE	Mucosal pentraxin	**6.6**	0.0001*
Q11011	PSA_MOUSE	Puromycin-sensitive aminopeptidase	**6.7**	0.0194*
P02535	K1C10_MOUSE	Keratin, type I cytoskeletal 10	**6.8**	0.2255
P21550	ENOB_MOUSE	Beta-enolase	**7.2**	0.003*
Q08189	TGM3_MOUSE	Protein-glutamine gamma-glutamyltransferase E	**7.3**	0.0056*
Q9CWW6	PIN4_MOUSE	Peptidyl-prolyl cis-trans isomerase NIMA-interacting 4	**7.4**	0.2584
Q9R0Y5	KAD1_MOUSE	Adenylate kinase isoenzyme 1	**7.7**	0.7660
O54974	LEG7_MOUSE	Galectin-7	**8.6**	0.2047
Q5SX40	MYH1_MOUSE	Myosin-1	**8.6**	0.0482*
P12265	BGLR_MOUSE	Beta-glucuronidase	**8.7**	0.2710
P13412	TNNI2_MOUSE	Troponin I, fast skeletal muscle	**9.1**	0.1328
Q91Y97	ALDOB_MOUSE	Fructose-bisphosphate aldolase B	**9.4**	0.2133
Q8CIT9	SBSN_MOUSE	Suprabasin	**9.9**	0.0372*
Q9JM83	CALM4_MOUSE	Calmodulin-4	**11.0**	0.0345*
Q9QZ47	TNNT3_MOUSE	Troponin T, fast skeletal muscle	**13.3**	0.1103
Q91VC7	PP14A_MOUSE	Protein phosphatase 1 regulatory subunit 14A	**13.7**	0.5508
P97457	MLRS_MOUSE	Myosin regulatory light chain 2, skeletal muscle isoform	**21.0**	0.0995
P09542	MYL3_MOUSE	Myosin light chain 3	**32.5**	0.1648
P05977	MYL1_MOUSE	Myosin light chain 1/3, skeletal muscle isoform	**36.1**	0.1244
P11088	FILA_MOUSE	Filaggrin	**39.4**	0.1585
P20801	TNNC2_MOUSE	Troponin C, skeletal muscle	**58.2**	0.0089*

Table 2.13 Complete List of Quantified Mouse Proteins in Feces

Accession ID	Gene ID	Protein Name	Fold Change DF/PF	*p*-value
Q8K0C5	ZG16_MOUSE	Zymogen granule membrane protein 16	**-41.5**	0.8722
P43137	LIT1_MOUSE	Lithostathine-1	**-29.6**	0.2398
P16406	AMPE_MOUSE	Glutamyl aminopeptidase	**-15.0**	0.9869
Q64475	H2B1B_MOUSE	Histone H2B type 1-B	**-9.5**	0.0955
Q91XA9	CHIA_MOUSE	Acidic mammalian chitinase	**-8.5**	0.9437
P17751	TPIS_MOUSE	Triosephosphate isomerase	**-8.5**	0.3627
Q91WV7	SLC31_MOUSE	Neutral and basic amino acid transport protein rBAT	**-8.3**	0.2913
P54869	HMCS2_MOUSE	Hydroxymethylglutaryl-CoA synthase, mitochondrial	**-6.6**	0.7390
P13634	CAH1_MOUSE	Carbonic anhydrase 1	**-4.3**	0.1830
Q9D816	CP255_MOUSE	Cytochrome P450 2C55	**-3.4**	0.2342
Q8K419	LEG4_MOUSE	Galectin-4	**-3.1**	0.6688
P19001	K1C19_MOUSE	Keratin, type I cytoskeletal 19	**-3.0**	0.7369
P20029	BIP_MOUSE	78 kDa glucose-regulated protein	**-2.6**	0.0536
P62908	RS3_MOUSE	40S ribosomal protein S3	**-2.4**	0.8192
Q8R1M8	MPTX_MOUSE	Mucosal pentraxin	**-2.4**	0.3903
Q8K386	RAB15_MOUSE	Ras-related protein Rab-15	**-2.3**	0.6168
Q60997	DMBT1_MOUSE	Deleted in malignant brain tumors 1 protein	**-2.3**	0.5446
P06151	LDHA_MOUSE	L-lactate dehydrogenase A chain	**-2.2**	0.1946
Q8R1M2	H2AJ_MOUSE	Histone H2A.J	**-2.1**	0.0383*
Q921I1	TRFE_MOUSE	Serotransferrin	**-2.0**	0.5130
Q9CQC2	COL_MOUSE	Colipase	**-2.0**	0.4345
P35700	PRDX1_MOUSE	Peroxiredoxin-1	**-2.0**	0.1534
Q03265	ATPA_MOUSE	ATP synthase subunit alpha, mitochondrial	**-1.9**	0.4065
Q8VDN2	AT1A1_MOUSE	Sodium/potassium-transporting ATPase subunit alpha-1	**-1.9**	0.7178
E9Q7P9	CDHR2_MOUSE	Cadherin-related family member 2	**-1.9**	0.8836
P11679	K2C8_MOUSE	Keratin, type II cytoskeletal 8	**-1.8**	0.5118
P14094	AT1B1_MOUSE	Sodium/potassium-transporting ATPase subunit beta-1	**-1.7**	0.0116*
Q91WG0	EST2C_MOUSE	Acylcarnitine hydrolase	**-1.7**	0.0674
P19467	MUC13_MOUSE	Mucin-13	**-1.7**	0.8498
Q61847	MEP1B_MOUSE	Meprin A subunit beta	**-1.7**	0.4119
P17182	ENOA_MOUSE	Alpha-enolase	**-1.6**	0.7469
O88312	AGR2_MOUSE	Anterior gradient protein 2 homolog	**-1.6**	0.2099
P97429	ANXA4_MOUSE	Annexin A4	**-1.6**	0.9343
P30275	KCRU_MOUSE	Creatine kinase U-type, mitochondrial	**-1.5**	0.8891
Q9CQ52	CEL3B_MOUSE	Chymotrypsin-like elastase family member 3B	**-1.5**	0.7586
P17563	SBP1_MOUSE	Selenium-binding protein 1	**-1.5**	0.0383*
P62984	RL40_MOUSE	Ubiquitin-60S ribosomal protein L40	-1.4	0.6288

Q6Q473	CLA4A_MOUSE	Calcium-activated chloride channel regulator 4A	-1.4	0.5389
P56480	ATPB_MOUSE	ATP synthase subunit beta, mitochondrial	-1.4	0.2624
Q62468	VILI_MOUSE	Villin-1	-1.4	0.4644
P35230	REG3B_MOUSE	Regenerating islet-derived protein 3-beta	-1.3	0.7766
P16858	G3P_MOUSE	Glyceraldehyde-3-phosphate dehydrogenase	-1.2	0.1862
P63260	ACTG_MOUSE	Actin, cytoplasmic 2	-1.2	0.8802
P07356	ANXA2_MOUSE	Annexin A2	1.1	0.4649
Q80Z19	MUC2_MOUSE	Mucin-2	1.3	0.4363
P28843	DPP4_MOUSE	Dipeptidyl peptidase 4	1.3	0.6656
Q11136	PEPD_MOUSE	Xaa-Pro dipeptidase	1.3	0.3175
P70412	CUZD1_MOUSE	CUB and zona pellucida-like domain-containing protein 1	1.3	0.4442
P02816	PIP_MOUSE	Prolactin-inducible protein homolog	1.4	0.1653
Q60931	VDAC3_MOUSE	Voltage-dependent anion-selective channel protein 3	1.4	0.5322
P97449	AMPN_MOUSE	Aminopeptidase N	1.4	0.2856
Q9CR35	CTRB1_MOUSE	Chymotrypsinogen B	1.4	0.8202
P09803	CADH1_MOUSE	Cadherin-1	1.4	0.1031
P24822	PPBI_MOUSE	Intestinal-type alkaline phosphatase	1.4	0.7916
Q6P8U6	LIPP_MOUSE	Pancreatic triacylglycerol lipase	**1.5**	0.7247
P05208	CEL2A_MOUSE	Chymotrypsin-like elastase family member 2A	**1.5**	0.9300
P24823	PPBN_MOUSE	Alkaline phosphatase, placental-like	**1.5**	0.5241
Q60928	GGT1_MOUSE	Gamma-glutamyltranspeptidase 1	**1.5**	0.0013*
Q9Z2W0	DNPEP_MOUSE	Aspartyl aminopeptidase	**1.6**	0.1142
P08228	SODC_MOUSE	Superoxide dismutase [Cu-Zn]	**1.7**	0.7944
P18761	CAH6_MOUSE	Carbonic anhydrase 6	**1.7**	0.2613
Q9D7Z6	CLCA1_MOUSE	Calcium-activated chloride channel regulator 1	**1.7**	0.7222
Q6UGQ3	SG2B2_MOUSE	Secretoglobin family 2B member 2	**1.8**	0.2263
P17892	LIPR2_MOUSE	Pancreatic lipase-related protein 2	**1.8**	0.6553
Q3SYP2	CTRC_MOUSE	Chymotrypsin-C	**2.0**	0.6245
Q9R100	CAD17_MOUSE	Cadherin-17	**2.1**	0.4024
P07724	ALBU_MOUSE	Serum albumin	**2.1**	0.4897
P15947	KLK1_MOUSE	Kallikrein-1	**3.4**	0.9121
Q9D733	GP2_MOUSE	Pancreatic secretory granule membrane major glycoprotein GP2	**3.7**	0.9541
O09049	REG3G_MOUSE	Regenerating islet-derived protein 3-gamma	**3.8**	0.4364
P02088	HBB1_MOUSE	Hemoglobin subunit beta-1	**4.9**	0.4635
P62806	H4_MOUSE	Histone H4	**5.2**	0.0394*
P07146	TRY2_MOUSE	Anionic trypsin-2	**6.5**	0.2720
Q8BFR5	EFTU_MOUSE	Elongation factor Tu, mitochondrial	**6.8**	0.4772
P01942	HBA_MOUSE	Hemoglobin subunit alpha	**7.5**	0.5020

Table 2.1 Statistically Significant Quantified Mouse Proteins from Colon Samples

Accession Number	Gene ID	Protein Name	Fold Change DC/PC	*p*-value
P20801	TNNC2_MOUSE	Troponin C, skeletal muscle	58.25	0.009
Q08189	TGM3_MOUSE	Protein-glutamine gamma-glutamyltransferase E	7.29	0.006
P21550	ENOB_MOUSE	Beta-enolase	7.20	0.003
Q8R1M8	MPTX_MOUSE	Mucosal pentraxin	6.64	0.000
P00329	ADH1_MOUSE	Alcohol dehydrogenase 1	5.17	0.005
P97430	SLPI_MOUSE	Antileukoproteinase	4.78	0.000
Q9D2Q8	S10AE_MOUSE	Protein S100-A14	4.70	0.000
Q9Z0L8	GGH_MOUSE	Gamma-glutamyl hydrolase	4.44	0.000
Q9WTI7	MYO1C_MOUSE	Unconventional myosin-Ic	4.36	0.002
Q8K0C5	ZG16_MOUSE	Zymogen granule membrane protein 16	4.20	0.007
Q02788	CO6A2_MOUSE	Collagen alpha-2(VI) chain	4.11	0.007
Q91V92	ACLY_MOUSE	ATP-citrate synthase	3.85	0.009
P68134	ACTS_MOUSE	Actin, alpha skeletal muscle	3.81	0.000
P10649	GSTM1_MOUSE	Glutathione S-transferase Mu 1	3.71	0.001
Q99MQ4	ASPN_MOUSE	Asporin	3.68	0.000
P15626	GSTM2_MOUSE	Glutathione S-transferase Mu 2	3.62	0.005
P60843	IF4A1_MOUSE	Eukaryotic initiation factor 4A-I	3.35	0.000
P62962	PROF1_MOUSE	Profilin-1	3.30	0.000
Q80UG5	SEPT9_MOUSE	Septin-9	3.24	0.001
Q61598	GDIB_MOUSE	Rab GDP dissociation inhibitor beta	3.19	0.002
Q9JM14	NT5C_MOUSE	5'(3')-deoxyribonucleotidase, cytosolic type	3.18	0.000
P45376	ALDR_MOUSE	Aldose reductase	3.17	0.000
P47738	ALDH2_MOUSE	Aldehyde dehydrogenase, mitochondrial	3.16	0.001
Q9JK53	PRELP_MOUSE	Prolargin	3.15	0.001
Q8BG32	PSD11_MOUSE	26S proteasome non-ATPase regulatory subunit 11	3.05	0.004
O08709	PRDX6_MOUSE	Peroxiredoxin-6	3.00	0.001
Q60854	SPB6_MOUSE	Serpin B6	3.00	0.002
P02088	HBB1_MOUSE	Hemoglobin subunit beta-1	2.93	0.003
P30275	KCRU_MOUSE	Creatine kinase U-type, mitochondrial	2.93	0.003
P63268	ACTH_MOUSE	Actin, gamma-enteric smooth muscle	2.87	0.009
P19324	SERPH_MOUSE	Serpin H1	2.86	0.001
P07356	ANXA2_MOUSE	Annexin A2	2.83	0.005
P58389	PTPA_MOUSE	Serine/threonine-protein phosphatase 2A activator	2.82	0.002
O35639	ANXA3_MOUSE	Annexin A3	2.82	0.000
Q9D154	ILEUA_MOUSE	Leukocyte elastase inhibitor A	2.79	0.005
P13020	GELS_MOUSE	Gelsolin	2.76	0.003
P02089	HBB2_MOUSE	Hemoglobin subunit beta-2	2.76	0.003
Q9D708	S10AG_MOUSE	Protein S100-A16	2.71	0.000

Q91YR9	PTGR1_MOUSE	Prostaglandin reductase 1	2.70	0.000
P59999	ARPC4_MOUSE	Actin-related protein 2/3 complex subunit 4	2.69	0.001
O88342	WDR1_MOUSE	WD repeat-containing protein 1	2.68	0.002
Q62000	MIME_MOUSE	Mimecan	2.66	0.002
Q9QZJ6	MFAP5_MOUSE	Microfibrillar-associated protein 5	2.64	0.009
Q8VHX6	FLNC_MOUSE	Filamin-C	2.63	0.003
P80318	TCPG_MOUSE	T-complex protein 1 subunit gamma	2.61	0.002
Q99JY9	ARP3_MOUSE	Actin-related protein 3	2.59	0.009
Q91V12	BACH_MOUSE	Cytosolic acyl coenzyme A thioester hydrolase	2.55	0.009
P14824	ANXA6_MOUSE	Annexin A6	2.52	0.001
Q99JW2	ACY1_MOUSE	Aminoacylase-1	2.51	0.002
P01942	HBA_MOUSE	Hemoglobin subunit alpha	2.51	0.002
Q60932	VDAC1_MOUSE	Voltage-dependent anion-selective channel protein 1	2.44	0.005
O35679	ISK4_MOUSE	Serine protease inhibitor Kazal-type 4	2.41	0.004
P16125	LDHB_MOUSE	L-lactate dehydrogenase B chain	2.40	0.004
P16858	G3P_MOUSE	Glyceraldehyde-3-phosphate dehydrogenase	2.38	0.000
Q7TPR4	ACTN1_MOUSE	Alpha-actinin-1	2.35	0.005
P11983	TCPA_MOUSE	T-complex protein 1 subunit alpha	2.30	0.000
P06151	LDHA_MOUSE	L-lactate dehydrogenase A chain	2.29	0.009
Q9D0K2	SCOT1_MOUSE	Succinyl-CoA:3-ketoacid coenzyme A transferase 1, mitochondrial	2.29	0.000
Q62009	POSTN_MOUSE	Periostin	2.27	0.000
Q80X19	COEA1_MOUSE	Collagen alpha-1(XIV) chain	2.26	0.000
Q922F4	TBB6_MOUSE	Tubulin beta-6 chain	2.25	0.007
Q8R059	GALE_MOUSE	UDP-glucose 4-epimerase	2.25	0.002
P68040	RACK1_MOUSE	Receptor of activated protein C kinase 1	2.20	0.008
P70124	SPB5_MOUSE	Serpin B5	2.19	0.002
Q61696	HS71A_MOUSE	Heat shock 70 kDa protein 1A	2.17	0.000
P10107	ANXA1_MOUSE	Annexin A1	2.17	0.001
Q9WTP7	KAD3_MOUSE	GTP:AMP phosphotransferase AK3, mitochondrial	2.17	0.003
P27659	RL3_MOUSE	60S ribosomal protein L3	2.11	0.007
Q9CQI6	COTL1_MOUSE	Coactosin-like protein	2.11	0.000
P80313	TCPH_MOUSE	T-complex protein 1 subunit eta	2.10	0.007
P62918	RL8_MOUSE	60S ribosomal protein L8	2.10	0.002
P23492	PNPH_MOUSE	Purine nucleoside phosphorylase	2.07	0.003
Q9CVB6	ARPC2_MOUSE	Actin-related protein 2/3 complex subunit 2	2.06	0.004
P62838	UB2D2_MOUSE	Ubiquitin-conjugating enzyme E2 D2	2.06	0.002
Q9Z1Q5	CLIC1_MOUSE	Chloride intracellular channel protein 1	2.06	0.001
P97429	ANXA4_MOUSE	Annexin A4	2.05	0.005
P62245	RS15A_MOUSE	40S ribosomal protein S15a	2.05	0.009
Q91VJ2	CAVN3_MOUSE	Protein kinase C delta-binding protein	2.03	0.001

P46412	GPX3_MOUSE	Glutathione peroxidase 3	2.02	0.005
P17710	HXK1_MOUSE	Hexokinase-1	2.02	0.003
P81117	NUCB2_MOUSE	Nucleobindin-2	-2.00	0.000
P62077	TIM8B_MOUSE	Mitochondrial import inner membrane translocase subunit Tim8 B	-2.01	0.003
Q9CRB6	TPPP3_MOUSE	Tubulin polymerization-promoting protein family member 3	-2.01	0.000
Q64213	SF01_MOUSE	Splicing factor 1	-2.02	0.000
P11679	K2C8_MOUSE	Keratin, type II cytoskeletal 8	-2.03	0.006
Q9ERG0	LIMA1_MOUSE	LIM domain and actin-binding protein 1	-2.03	0.001
Q9JMD0	ZN207_MOUSE	BUB3-interacting and GLEBS motif-containing protein ZNF207	-2.04	0.001
Q08331	CALB2_MOUSE	Calretinin	-2.04	0.000
P62960	YBOX1_MOUSE	Nuclease-sensitive element-binding protein 1	-2.08	0.000
Q9WVA2	TIM8A_MOUSE	Mitochondrial import inner membrane translocase subunit Tim8 A	-2.09	0.000
Q91V76	CK054_MOUSE	Ester hydrolase C11orf54 homolog	-2.11	0.008
Q91WJ8	FUBP1_MOUSE	Far upstream element-binding protein 1	-2.12	0.000
Q6P9R2	OXSR1_MOUSE	Serine/threonine-protein kinase OSR1	-2.13	0.000
Q8R4U7	LUZP1_MOUSE	Leucine zipper protein 1	-2.14	0.000
P19001	K1C19_MOUSE	Keratin, type I cytoskeletal 19	-2.14	0.000
P70441	NHRF1_MOUSE	Na(+)/H(+) exchange regulatory cofactor NHE-RF1	-2.15	0.000
Q6NZJ6	IF4G1_MOUSE	Eukaryotic translation initiation factor 4 gamma 1	-2.15	0.000
P56391	CX6B1_MOUSE	Cytochrome c oxidase subunit 6B1	-2.16	0.000
P19536	COX5B_MOUSE	Cytochrome c oxidase subunit 5B, mitochondrial	-2.17	0.000
Q9Z1D1	EIF3G_MOUSE	Eukaryotic translation initiation factor 3 subunit G	-2.20	0.004
Q99LT0	DPY30_MOUSE	Protein dpy-30 homolog	-2.20	0.001
Q9Z2I0	LETM1_MOUSE	LETM1 and EF-hand domain-containing protein 1, mitochondrial	-2.21	0.001
Q02819	NUCB1_MOUSE	Nucleobindin-1	-2.23	0.000
Q61792	LASP1_MOUSE	LIM and SH3 domain protein 1	-2.23	0.000
Q62261	SPTB2_MOUSE	Spectrin beta chain, non-erythrocytic 1	-2.24	0.000
P99028	QCR6_MOUSE	Cytochrome b-c1 complex subunit 6, mitochondrial	-2.27	0.000
E9Q7P9	CDHR2_MOUSE	Cadherin-related family member 2	-2.28	0.000
P21107	TPM3_MOUSE	Tropomyosin alpha-3 chain	-2.28	0.004
O08663	MAP2_MOUSE	Methionine aminopeptidase 2	-2.28	0.002
P57016	LAD1_MOUSE	Ladinin-1	-2.28	0.000
Q9QXS1	PLEC_MOUSE	Plectin	-2.30	0.001
P52503	NDUS6_MOUSE	NADH dehydrogenase [ubiquinone] iron-sulfur protein 6	-2.30	0.000
P61022	CHP1_MOUSE	Calcineurin B homologous protein 1	-2.31	0.001
Q9JLQ0	CD2AP_MOUSE	CD2-associated protein	-2.34	0.000
P55012	S12A2_MOUSE	Solute carrier family 12 member 2	-2.34	0.001
Q9DCM0	ETHE1_MOUSE	Persulfide dioxygenase ETHE1, mitochondrial	-2.34	0.000
Q91WQ9	CALL4_MOUSE	Calmodulin-like protein 4	-2.39	0.001
P14733	LMNB1_MOUSE	Lamin-B1	-2.39	0.000

Q6IRU5	CLCB_MOUSE	Clathrin light chain B	-2.40	0.000
P15379	CD44_MOUSE	CD44 antigen	-2.40	0.000
Q80VJ2	SRA1_MOUSE	Steroid receptor RNA activator 1	-2.41	0.004
O70400	PDLI1_MOUSE	PDZ and LIM domain protein 1	-2.41	0.000
Q9D8Y0	EFHD2_MOUSE	EF-hand domain-containing protein D2	-2.46	0.000
O88312	AGR2_MOUSE	Anterior gradient protein 2 homolog	-2.46	0.003
Q6PDG5	SMRC2_MOUSE	SWI/SNF complex subunit SMARCC2	-2.48	0.004
Q9DBG5	PLIN3_MOUSE	Perilipin-3	-2.50	0.000
P09541	MYL4_MOUSE	Myosin light chain 4	-2.51	0.001
P47212	GALA_MOUSE	Galanin peptides	-2.58	0.000
Q80W00	PP1RA_MOUSE	Serine/threonine-protein phosphatase 1 regulatory subunit 10	-2.58	0.002
Q4VAA2	CDV3_MOUSE	Protein CDV3	-2.64	0.001
Q9DCV7	K2C7_MOUSE	Keratin, type II cytoskeletal 7	-2.75	0.000
Q9D1L0	CHCH2_MOUSE	Coiled-coil-helix-coiled-coil-helix domain-containing protein 2	-2.75	0.000
Q99KN9	EPN4_MOUSE	Clathrin interactor 1	-2.75	0.002
Q99PL5	RRBP1_MOUSE	Ribosome-binding protein 1	-2.77	0.000
Q8BI84	TGO1_MOUSE	Melanoma inhibitory activity protein 3	-2.88	0.000
P05784	K1C18_MOUSE	Keratin, type I cytoskeletal 18	-2.90	0.000
Q8VDM6	HNRL1_MOUSE	Heterogeneous nuclear ribonucleoprotein U-like protein 1	-2.98	0.001
Q62393	TPD52_MOUSE	Tumor protein D52	-3.04	0.000
E9Q7G0	NUMA1_MOUSE	**Nuclear mitotic apparatus protein 1**	-3.05	0.003
Q80Z19	MUC2_MOUSE	Mucin-2	-3.07	0.000
Q60598	SRC8_MOUSE	Src substrate cortactin	-3.25	0.000
Q99K28	ARFG2_MOUSE	ADP-ribosylation factor GTPase-activating protein 2	-3.28	0.008
Q99K30	ES8L2_MOUSE	Epidermal growth factor receptor kinase substrate 8-like protein 2	-3.56	0.001
P16014	SCG1_MOUSE	Secretogranin-1	-3.66	0.001
Q9JIX8	ACINU_MOUSE	Apoptotic chromatin condensation inducer in the nucleus	-3.79	0.004
P55095	GLUC_MOUSE	Glucagon	-3.82	0.000
P59242	CING_MOUSE	Cingulin	-3.96	0.003
P20065	TYB4_MOUSE	Thymosin beta-4	-4.02	0.001
P29391	FRIL1_MOUSE	Ferritin light chain 1	-4.09	0.000
Q6URW6	MYH14_MOUSE	Myosin-14	-4.10	0.007
Q8VI24	SATB2_MOUSE	DNA-binding protein SATB2	-4.12	0.004
Q9D279	MISP_MOUSE	Mitotic interactor and substrate of PLK1	-4.17	0.000
Q9ES28	ARHG7_MOUSE	Rho guanine nucleotide exchange factor 7	-5.07	0.009
P13634	CAH1_MOUSE	Carbonic anhydrase 1	-6.83	0.000
P09528	FRIH_MOUSE	Ferritin heavy chain	-7.42	0.001
Q9D312	K1C20_MOUSE	Keratin, type I cytoskeletal 20	-7.51	0.000
P55050	FABPI_MOUSE	Fatty acid-binding protein, intestinal	-11.29	0.000
P97816	S100G_MOUSE	Protein S100-G	-12.89	0.000

Table 2.14 Species Identifiied Across Distal and Proximal Fecal Samples and their Characteristics

Species Code	Species	Phylum	Class	Genus	Gram Stain	Oxygen Requirements	Pathogenicity
ACET2	Acetivibrio thermocellus	Bacillota	Clostridia	Acetivibrio	+	Anaerobic	Non-pathogenic
AGARV	Agathobacter rectalis	Bacillota	Clostridia	Agathobacter	+	Anaerobic	Non-pathogenic
ALISL	Aliivibrio salmonicida	Proteobacteria	Gammaproteobacteria	Allivibrio	-	Facultative	Non-pathogenic
ANAPI	Anaerotignum propionicum	Bacillota	Clostridia	Anaerotignum	+	Anaerobic	Pathogenic
BACFR	Bacteroides fragilis	Bacteroidetes	Bacteroidia	Bacteroides	-	Anaerobic	Pathogenic
BACLD	Bacillus licheniformis	Bacillota	Bacilli	Bacillus	+	Facultative	Non-pathogenic
BACME	Bacillus megaterium	Bacillota	Bacilli	Bacillus	+	Aerobic	Non-pathogenic
BACTN	Bacteroides thetaiotaomicron	Bacteroidetes	Bacteroidia	Bacteroides	-	Anaerobic	Non-pathogenic
CARHZ	Carboxydothermus hydrogenoformans	Bacillota	Clostridia	Carboxydothermus	+	Anaerobic	Non-pathogenic
CELJU	Cellvibrio japonicus	Proteobacteria	Gammaproteobacteria	Cellvibrio	-	Aerobic	Non-pathogenic
CLOAB	Clostridium acetobutylicum	Bacillota	Clostridia	Clostridium	+	Anaerobic	Non-pathogenic
CLOB8	Clostridium beijerinckii	Bacillota	Clostridia	Clostridium	+	Anaerobic	Non-pathogenic
CLOBB	Clostridium botulinum	Bacillota	Clostridia	Clostridium	+	Anaerobic	Pathogenic
CLOPE/CLOP1 /CLOPS	Clostridium perfringens	Bacillota	Clostridia	Clostridium	+	Anaerobic	Pathogenic
CLOSY	Clostridium symbiosum	Bacillota	Clostridia	Lachnoclostridium	-	Anaerobic	Non-pathogenic
CLOTE	Clostridium tetani	Bacillota	Clostridia	Clostridium	+	Anaerobic	Pathogenic
CORDI	Corynebacterium diphtheriae	Actinobacteria	Actinobacteria	Corynebacterium	+	Aerobic	Pathogenic
COREF* /CORGL*	Corynebacterium efficiens*/glutamicum*	Actinobacteria	Actinobacteria	Corynobacterium	+	Facultative	Non-pathogenic
CORGL	Corynebacterium glutamicum	Actinobacteria	Actinobacteria	Corynobacterium	+	Anaerobic	Pathogenic
CYTH3	Cytophaga hutchinsonii	Bacteroidetes	Cytophagia	Cytophaga	-	Aerobic	Non-pathogenic
DEHMC	Dehalococcoides mccartyi	Chloroflexi	Dehalococcoidetes	Dehalococcoides	+	Anaerobic	Non-pathogenic
DICTD	Dictyoglomus turgidum	Dictyoglomi	Dictyoglomia	Dictyoglomus	+	Anaerobic	Non-pathogenic
ECOLI	Escherichia coli	Proteobacteria	Gammaproteobacteria	Eschereschia	-	Facultative	Pathogenic
FLAJ1	Flavobacterium johnsoniae	Bacteroidetes	Flavobacteria	Flavobacterium	-	Aerobic	Non-pathogenic
FUSNN	Fusobacterium nucleatum subsp. nucleatum	Fusobacteria	Fusobacteria	Fusobacterium	-	Anaerobic	Pathogenic
GEOUR	Geobacter uraniireducens	Proteobacteria	Deltaproteobacter	Geobacter	-	Microaerophilic	Non-pathogenic
LACDB	Lactobacillus delbrueckii	Bacillota	Bacilli	Lactobacillus	+	Facultative	Non-pathogenic
LACE2	Lachnospira eligens	Bacillota	Clostridia	Lachnospira	+	Anaerobic	Non-pathogenic
LACLM	Lactococcus lactis subsp. Cremoris	Bacillota	Bacilli	Lactococcus	+	Anaerobic	Non-pathogenic
LACP7	Lachnoclostridium phytofermentans	Bacillota	Clostridia	Clostridium	+	Anaerobic	Non-pathogenic
LEPBP	Leptospira biflexa serovar Patoc	Spirochaetota	Spirochaetia	Leptospira	-	Aerobic	Non-pathogenic
LEUMM* /LEUCK*	Leuconostoc mesenteroides/citreum	Bacillota	Bacilli	Leuconostoc	+	Facultative	Non-pathogenic
LISIN*/LISMO*	Listeria innocua/monocytogenes	Bacillota	Bacilli	Listeria	+	Anaerobic	Pathogenic
OCEIH	Oceanobacillus iheyensis	Bacillota	Bacilli	Oceanobacillus	+	Aerobic	Non-pathogenic
PARD8	Parabacteroides distasonis	Bacteroidetes	Bacteroidia	Parabacteroides	-	Anaerobic	Pathogenic
PORGI*	Porphyromonas gingivalis	Bacteroidetes	Bacteroidia	Porphyromonas	-	Anaerobic	Pathogenic

/PORG3*							
PROM4	Prochlorococcus marinus	Cyanobacteria	N/A	Prochlorococcus	-	Aerobic	Non-pathogenic
PSEAE	Pseudomonas aeruginosa	Proteobacteria	Gammaproteobacteria	Pseudomonas	-	Aerobic	Pathogenic
RUMCH	Ruminiclostridium cellulolyticum	Bacillota	Clostridia	Clostridium	+	Anaerobic	Non-pathogenic
SELRU	Selenomonas ruminantium	Bacillota	Negativicutes	Selenomonas	-	Anaerobic	Non-pathogenic
SHEAM* /SHELP*	Shewanella amazonensis/loihica	Proteobacteria	Gammaproteobacteria	Shewanella	-	Facultative	Non-pathogenic
SPITD	Spirochaeta thermophila	Spirochaetota	Spirochaetia	Spirochaeta	-	Anaerobic	Pathogenic
STRP6/STRP8/ STRPQ	Streptococcus pyogenes	Bacillota	Bacilli	Streptococcus	+	Facultative	Pathogenic
SYNJB	Synechococcus sp.	Cyanobacteria	Cyanophyceae	Synechococcus	-	Facultative	Non-pathogenic
SYNS3	Synechococcus sp.	Cyanobacteria	Cyanophyceae	Synechococcus	-	Facultative	Non-pathogenic
SYNY3	Synechocystis sp.	Cyanobacteria	Cyanophyceae	Synechocystis	-	Facultative	Non-pathogenic
THEP3	Thermoanaerobacter pseudethanolicus	Bacillota	Clostridia	Thermoanaerobacter	+	Anaerobic	Non-pathogenic

*Peptide quantified sourced back to two species of the same family

CHAPITRE 3
GENERAL DISCUSSION

This chapter summarizes and discusses results previously described in Chapter 2, as well as offers additional results pertaining to the metabolomic, proteomic and metaproteomic analyses of healthy mouse colon and fecal samples.

3.1 Metabolomic Analysis of Colon and Fecal Samples

Metabolomic analysis was performed to characterize the metabolome coverage from fecal and colon samples using an untargeted LC-MS/MS approach with two complementary chromatographic methods in electrospray positive and negative mode. Sample preparation was employed followed by peak picking, library searching for identification of putative metabolites and verification of peak integrations and finally, statistical analysis between distal and proximal samples. Although quantitation is employed for both metabolomic and proteomic analysis, the process is quite different between the two types of analyses. Quantitation in metabolomic analysis requires a more tedious approach to proteomics (where SWATH analysis software allows for automated quantitation) in which manual verification of metabolites is necessary to ensure quantitation and statistical analysis is accurate. Statistically significant metabolites also need to undergo extra verifications of peak integrations as these metabolites are often considered to be biomarkers in many different cases in which it is critical to ensure that peak integrations of metabolites are performed correctly. Often in metabolomic analysis, follow-up targeted analyses are required to confirm the identification and significance of metabolomites.

Untargeted metabolomics can yield useful information on observed phenotypes originating from changes at the genomic, transcriptomic, and proteomic levels. An important goal of this work was to identify distinct groups of metabolites and pathways that differ between distal and proximal colon regions in healthy mice. This study allowed us to understand baseline heterogeneity within the colon, serving for further studies when intestinal diseases are involved. The fecal metabolome was studied for the same purposes as well as to characterize how it compares to the colon metabolome in a healthy mouse model. As shown in Figure 3.1, there is a high number of metabolites that are shown to overlap between colon and fecal sample matrices, but there remains many metabolites unique to the respective sample types. With 335 common metabolites, 174 and 289 remain unique to the colon and feces respectively. Proximal and distal samples originating

from five healthy mice were subjected to homogenisation and protein precipitation followed by data processing of raw LC-MS/MS data (Figure 2.1). Although the data processing of colon and fecal samples followed the same steps, slight differences in sample preparation were employed in order to initially normalize. Higher weights (mg) of colon samples were available compared to the weights (mg) of fecal samples. The initial volume of buffer added to colon therefore corresponded to 0.5 µL of buffer per mg of tissue collected whereas 1 µL/mg was used for feces samples. Although the colon and fecal samples received are wet weights and the water content throughout the colon is unknown, normalization based on the weights of samples received was performed. Additionally, during data processing, an additional normalization step was employed after peak integration using MarkerView software where MLR normalization was employed as mentioned in Chapter 2. Although the latter step was not performed for proteomic analysis, a Bradford protein quantification was done as mentioned in Chapter 2 to normalize protein content ensuring the same conditions in all samples prior the digestion.

Another difference employed was the need for probe sonication of tissue samples for adequate homogenisation, whereas feces samples did not necessitate this step. Fecal samples were able to homogenize well with the addition of ammonium bicarbonate (ABC) buffer and 100% MeOH and vortexing, but the tissue samples being of much higher weights and the nature of whole tissue, addition of ABC buffer and MeOH with subsequent vortexing was not enough to homogenize the samples hence the necessity for probing.

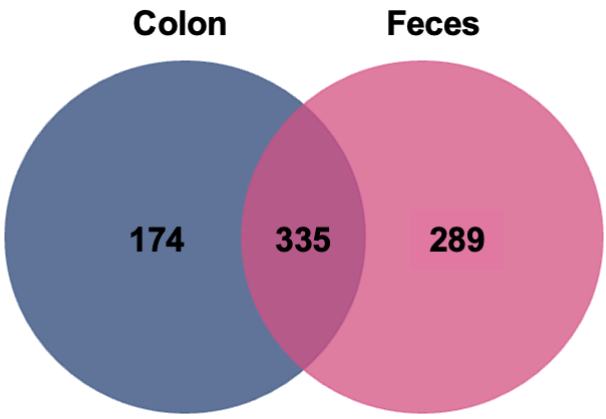

Figure 3.1 Overlap of colon and fecal metabolites identified

To maximize the number of metabolites putatively identified, two chromatographic columns were employed for metabolite separation by liquid chromatography prior to mass spectrometry analysis.

These were a mixed mode column with ion exchange and reverse phase stationary phase (Scherzo SM-C18) and a pentafluorophenyl (Luna PFP) column to separate compounds based on different properties and provide complementary metabolites. This was shown to be effective as shown in Figure 2.2 where, in both sample types, that there a large portion of putative metabolites identified uniquely from each column.

This work was able to putatively identify a large number of metabolites using LC-HRMS/MS from colon and fecal samples. Statistical analysis was then performed to find out which metabolites were higher in one of the colon regions. The colon dataset demonstrated important heterogeneity of 153 metabolites in the two regions, but the same pattern was not seen from the fecal samples with only 23 metabolites shown to be significant, even though a high initial number of putative metabolites were found in feces. Considering the larger number of changing metabolite levels in the colon, pathway analyses were performed to visualize which biological pathways could be playing important roles specifically in one of the regions. Although the dataset is quite complex and much more can be extracted from these results, we were able to identify two specific classes of metabolites and highlight their heterogeneity in the colon. Prostaglandins as well as tryptophan metabolites were found to increase in the distal and proximal regions, respectively. Tryptophan metabolism can be broken down into three main pathways: kynurenine pathway, serotonin pathway and the indole pathway in which the metabolites involved are largely implicated in colonic motility and gut signalling and have a large presence in the GI tract (Roth *et al.*, 2021). More specifically, serotonin is abundant in the gut where its presence in the gut accounts for more than 90% of the body's serotonin production, although research is largely focused on serotonin in the context of neurological disorders (Appleton, 2018). Although it has been described how changing levels of serotonin in the gut can be implicated in the pathogenesis of intestinal diseases, such as IBS-C and IBS-D, its levels in the gut can also be implicated in the manifestation of neurological disorders. Literature has shown that altered levels of GI metabolites, such as serotonin, can lead to several neurological disorders, such as anxiety and depression through the gut-brain axis (Appleton, 2018; Irum *et al.*, 2023). Serotonin is a key neurotransmitter involved in the central nervous system and in the GI tract, highlighting its potential implication in a plethora of diseases. Although several selective serotonin reuptake inhibitors (SSRIs) exist as treatment options for neurological disorders such as anxiety and depression, research has shown that certain specific bacterial species able to produce neurotransmitters, such as serotonin, populating the gut microbiome can also lead to beneficial results in this context (Potter *et al.*, 2023). It was also found that many patients suffering from intestinal diseases from gut dysbiosis, involving tryptophan

metabolism and more specifically serotonin levels, also present symptoms of neurological disorders (Potter *et al.*, 2023). The key findings that serotonin is highly upregulated in the proximal region of the colon in healthy subjects is an important result of this study. This finding indicates that monitoring serotonin levels specifically from the proximal colon could show more clear differences in the context of disease. As serotonin is much less expressed in the distal region of the colon, the proximal portion likely yields much more accurate information regarding the changing levels of serotonin in the gut. This information can be very useful to diagnose and determine the levels of serotonin needed on a patient-by-patient basis to potentially remediate symptoms of both neurological and intestinal disorders.

Several prostaglandin molecules showed increased levels in the distal portion of the colon (Table 2.2). Prostaglandins are long chain fatty acids prevalent in the gut, notably in the gut mucosa, with either anti-inflammatory or pro-inflammatory properties, making them a group of metabolites of interest in the context of GI inflammation or disease. The higher expression of several prostaglandins in the distal colon could lead to several theories about the nature of intestinal disease prognosis between the two regions of the colon, as well as the region-specific perturbations. Due to the fact that prostaglandins are heavily involved in mucosal defence, they will often be involved in the inflammatory response to resolve injury or infection in the body along with immune cells, but concurrently can also contribute to chronic inflammatory conditions by continuous recruitment of cytokines and chemokines (Aoki et Narumiya, 2012; Ricciotti et FitzGerald, 2011; Semble et Wu, 1989). Regarding CRC, the presence of several prostaglandin molecules in the distal colon could be linked to why prognosis in the proximal region of the colon is worse than in the distal region due to increase in pro-inflammatory action. In the context of CRC, prostaglandin molecules could potentially play an important role in mediating inflammation in the distal colon, whereas the same cannot be said for the proximal region. On the contrary, ulcerative colitis which is more often expressed in the distal colon could be a result of pro and chronic inflammatory action by the several prostaglandins found to be region specific in the distal portion. The findings of regional specificity of prostaglandins in healthy subjects can serve as an important baseline to further understand the prevalence, diagnosis, and treatment options for various intestinal conditions. The metabolomic analysis has demonstrated key metabolite groups that can be measured in the gut as well as which ones show regional specificity.

3.2 Proteomic Analysis of Colon Samples

Untargeted proteomics was performed on colon samples from the proximal and distal regions for protein identification and relative quantitation between the two regions studied. Proteomic analysis of colon samples was performed for identifying and quantifying mouse proteins, however, when fecal samples were analysed in the same manner, the coverage of mouse proteins was extremely low, due to most proteins being from microorganisms in feces. Therefore, a metaproteomic analysis was performed on fecal samples to identify and quantify microbial proteins as opposed to mouse proteins.

By combining both data-dependent (IDA) and data-independent (SWATH) data acquisition, a comprehensive proteomic profile was obtained for colon samples with a total of 1103 colon mouse proteins quantified. The extraction procedure previously described in Chapter 2 allows for extraction of several proteins including intracellular, membrane, and extracellular proteins. Membrane proteins are often more difficult to extract due to their lipid bilayer, notably when working with complex sample matrices but does not mean it is not possible. It is based on whether or not certain types of proteins are abundant enough in a given sample to be detected by the mass spectrometer (Lai, X., 2013; Vuckovic *et al.*, 2013). For example, highly abundant proteins are easily detected but lower abundant membrane proteins that are present in the sample are not likely to be detected. In cases like these, there are certain procedures that can be performed to enrich low abundance proteins for their detection. Procedures such a fractionation, differential centrifugation, and targeted mass spectrometry analysis can be performed to overcome high-abundant proteins to be able to detect and quantify lower abundant proteins (Sarihan *et al.*, 2023; Vuckovic *et al.*, 2013).

Performing statistical analysis revealed many changing proteins between the proximal and distal regions, with 158 proteins being differentially expressed when using strict statistical parameters ($p < 0.01$, *fold-change* > |2|), demonstrating high protein heterogeneity between the two regions. The online tool Reactome was used to map these proteins to specific pathways dominating in the distal and proximal colon, respectively. Proteins involved in both axon guidance and innate immune response were increased in the distal colon. On the other hand, in the proximal region, proteins involved in keratinization were increased.

Performing an analysis of the changing colon proteins using Panther, a different online software, showed additional pathways of interest, notably to the distal region of the colon. Using the list of

proteins changing by at least 50% with 281 statistically significant proteins, 129 proteins were shown have higher levels in the distal region, compared to 152 proteins for the proximal group. Although, less proteins were increased in the distal colon, these proteins were able to map more pathways, including glycolysis, integrin signalling and cytoskeletal regulation. Table 3.1 summarizes the proteins of interest from these three pathways. Although a lower fold change criteria was used for the Panther analysis, proteins changing by at least 50% with *p*-values below 0.05 are still considered to be statistically significant.

Table 3.1 Proteins with Higher Levels in Distal Colon Involved in A) Cytoskeletal Regulation, B) Integrin Signalling Pathway, and C) Glycolysis

A)

Cytoskeletal Regulation by Rho GTPase			
Accession Number	**Protein Name**	**Fold Change DC vs. PC**	***p*-value**
P45591	Cofilin-2	1.7	8.9×10^{-3}
Q9JM76	Actin-related protein 2/3 complex subunit 3	1.9	1.5×10^{-3}
Q922F4	Tubulin beta-6 chain	2.3	6.8×10^{-3}
P62962	Profilin-1	3.3	1.1×10^{-4}
P59999	Actin-related protein 2/3 complex subunit 4	2.7	1.5×10^{-3}
P68134	Actin, alpha skeletal muscle	3.8	1.9×10^{-4}
P63268	Actin, gamma-enteric smooth muscle	2.9	8.6×10^{-3}
Q9CVB6	Actin-related protein 2/3 complex subunit 2	2.1	4.2×10^{-3}

B)

Integrin Signalling Pathway			
Accession Number	**Protein Name**	**Fold Change DC vs. PC**	***p*-value**
Q9JM76	Actin-related protein 2/3 complex subunit 3	1.9	1.5×10^{-3}
Q02788	Collagen alpha-2(VI) chain	4.1	6.8×10^{-3}
P10833	Ras-related protein R-Ras	1.9	4.0×10^{-4}
Q7TPR4	Alpha-actinin-1	2.4	4.6×10^{-3}
P68134	Actin, alpha skeletal muscle	3.8	1.9×10^{-4}
P63268	Actin, gamma-enteric smooth muscle	2.9	8.6×10^{-3}
P11688	Integrin alpha-5	1.7	9.2×10^{-4}
Q9CVB6	Actin-related protein 2/3 complex subunit 2	2.1	4.2×10^{-3}
P02468	Laminin subunit gamma-1	1.6	9.4×10^{-3}
Q80X19	Collagen alpha-1(XIV) chain	2.3	4.5×10^{-5}
Q9D898	Actin-related protein 2/3 complex subunit 5-like protein	1.7	2.8×10^{-3}

C)

Glycolysis			
Accession Number	**Protein Name**	**Fold Change DC vs. PC**	***p*-value**
P17710	Hexokinase-1	2.0	3.4×10^{-3}
P05064	Fructose-bisphosphate aldolase A	1.8	3.1×10^{-3}
P16858	Glyceraldehyde-3-phosphate dehydrogenase	2.4	2.4×10^{-4}
P52480	Pyruvate kinase PKM	1.9	2.9×10^{-5}
P09411	Phosphoglycerate kinase 1	1.7	4.9×10^{-4}

As shown in Table 3.1, eight and eleven proteins, respectively, are implicated in cytoskeletal regulation by Rho GTPases and integrin signalling, having three proteins in common. Integrins comprise a large group of cell adhesion molecules that can bind to soluble ligands, extracellular matrix (ECM) ligands as well as cell surface ligands (Takada *et al.*, 2007). By binding to various ligands, they can participate in critical signalling by allowing interactions between cells and the ECM. This makes integrins a key component in various functions such as cell homeostasis, inflammation, cell survival and proliferation (Cooper et Giancotti, 2019). A possible explanation for the overlap between the integrin signalling and cytoskeletal regulation pathways is that integrins can allow cytoskeletal cells to bind to their targets in the ECM, a process that would involve both pathways (Ramovs *et al.*, 2017).

Although only one integrin was quantified in this dataset (integrin-alpha 5), there are several proteins that are involved in the overall binding with integrins resulting in their downstream signalling. For example, laminin is a protein that was quantified as part of the integrin signalling pathway and is implicated in the early stages of the signalling cascade. Laminins are cell adhesion glycoproteins as well and are a main target of specific integrins. The same relationship is seen with collagen proteins (which have also been quantified) in which different integrins and their subunits can bind to different ligands i.e., collagen ligands or laminin ligands depending on their binding affinities (Cooper et Giancotti, 2019). Depending on which ligands integrins will bind to, different roles can be carried out.

This analysis demonstrates that integrin and laminin binding is likely occurring more in the distal colon. Laminin and collagen proteins along with a multitude of other glycoproteins and glycosaminoglycans are found in basement membranes that are present in nearly all tissues. They are composed of thin ECM and are responsible for acting as a barrier between stroma and parenchymal cells (Mylonas et Lazaris, 2014). It has been shown that certain diseases such as cancer can alter basement membrane composition or even mutations in basement membrane proteins can be the cause of disease in tissues (Mylonas et Lazaris, 2014; Schmehl *et al.*, 2000; Spenlé *et al.*, 2014). Interestingly, Schmehl *et al.* studied the colonic tissues of patients with ulcerative colitis and found an under expression of laminin proteins combined with an overexpression of collagen type IV and V proteins. This reorganization of the basement membrane led to the possibility of loss of function of the basement membrane (Schmehl *et al.*, 2000). This is an interesting finding considering many ulcerative colitis cases are mainly found in the distal colon,

making proteins involved in integrin signalling notably, laminin and collagen proteins an area of research to consider in future studies.

Performing proteomic analysis allowed comprehensive profiling of the distinct regions of the colon, thus showing certain pathways being dominant in respective regions. Complementary pathway analyses (Panther, Reactome and MetaboAnalyst) also proved beneficial.

3.3 Metaproteomics of Fecal Samples

Metaproteomics is a growing area of research notably for the study of the gut microbiome as it allows for the identification and quantification of proteins from microbial species also offering strain specific information in certain cases (Kleiner, 2019). Although genomic approaches such as 16S rRNA analysis are widely utilized for identifying microorganism species, metaproteomics by LC-MS/MS offers advantages such as yielding information about the proteins being expressed from specific microbial species and revealing the functions that are being played out by these species allowing for a more comprehensive view of the protein network and interactions between species (Petriz et Franco, 2017). Metaproteomics also has the added advantage of higher resolution of species compared to 16S rRNA, allowing for strain specific, as well as having inherently better quantitative potential (Cortes *et al.*, 2019).

To perform metaproteomics, fecal samples undergoing protein digests directly following metabolite extraction and protein precipitation were necessary due to the high likelihood of degradation of proteins in stored fecal extracts during storage. Considering fecal matter is largely made up of microorganisms such as bacteria, the original fecal samples from five healthy female mice used for the metabolomic and proteomic analyses unfortunately did not have substantial protein amount for performing metaproteomics analysis. Considering that metabolomic sample preparation was performed prior to proteomic sample preparation and underwent subsequent storage at -80ºC for several weeks, there was a considerable loss of protein in the samples. Therefore, for the purpose of a metaproteomic analysis for microorganism identification in the respective regions, additional fecal samples were used from six healthy mice, 3 females and 3 males. Upon procurement of these samples, sample preparation was performed immediately to avoid any problem associated to protein degradation in the fecal extracts. The loss of protein in the original samples was observed when protein normalization was performed using a Bradford protein assay. In the original samples about 68 µg/ml of protein per sample was recorded whereas in the new freshly prepared samples about 1400 µg/ml of protein per sample was recorded. When

the low protein concentrations were observed for the original samples that underwent protein degradation, they were discarded, and the analysis was then performed on the additional samples that were prepared immediately after metabolite extraction.

To gain a deeper understanding of proteins present in fecal samples, metaproteomics was conducted. OneOmics Software was employed for data processing, similar to the previous proteomics analysis without initial specifying a species for database searching. The primary objective of the metaproteomics analysis was to identify distinct bacterial species present in the colon and verify if any of these showed differences in abundances between the two regions. The identification of unique bacterial species was only feasible at the peptide level rather than the protein level since most proteins quantified could be attributed to at least three different bacterial species. The critical factor distinguishing a protein's association with a specific bacterial species was found to be the quantified peptide, with a sequence uniquely attributed to that species. Table 2.7 summarizes the bacterial species identified, along with associated proteins and peptides from IDA acquisition in the distal and proximal regions

To conduct this analysis, pooled samples (from distal and proximal feces separately) were initially subjected to IDA acquisition for protein identification, followed by individual sample injections in SWATH mode for quantification. While IDA acquisition provided an initial impression of regional specificity, subsequent analysis of quantification data revealed that the identified peptides did not exhibit such specificity. SWATH quantification, represented in a heatmap, provided a more accurate depiction of the samples, emphasizing its superiority over IDA for quantitation. The distinction between IDA and SWATH lies in their ion selection mechanisms. IDA relies on selecting the higher intensity precursor ions for fragmentation, while SWATH utilizes small mass windows for comprehensive fragmentation. Our results underscore the advantages of SWATH in terms of quantitative measurements and reproducibility of measuring peptides throughout a sample set (Fernández-Costa *et al.*, 2020). The complexity of fecal samples further emphasizes the need for reliable results. Subsequent work is planned to develop a targeted method for these peptides specifically for a rapid quantitative assessment of changes in the microbiome of fecal samples in the context of disease or changes in diet. Performing an MRM assay is a good way to target these peptides and confirm their presence in fecal samples. MRM is a robust analysis method and allows for lower abundant peptides/proteins to be detected. The quantitation aspect also becomes much more accurate if a targeted MRM acquisition is performed due to the higher selectivity obtained compared to SWATH, yielding better chromatographic peak shapes and thus more accurate

statistical analysis to determine abundance of the proteins/peptides in each sample group (Brioschi *et al.*, 2021).

The limitations presented with IDA acquisition is also demonstrated throughout literature. Fernández-Costa *et al.*, as well as Barkovitz *et al.*, have both demonstrated better reproducibility between replicate samples for peptide and protein quantification when employing DIA/SWATH acquisition mode for samples due to the fact that quantification in SWATH mode utilizes MS1 (precursor ion without fragmentation) and MS2 (fragment ions) data, as opposed to only MS1 data in IDA acquisition (Barkovits *et al.*, 2020; Fernández-Costa *et al.*, 2020). The quantification on MS1 level employed with IDA acquisition leads to several caveats such as: loss of quantification power of low-abundant species and high interference of background signals that can also hinder peptide quantification (Willems *et al.*, 2021). This is especially important as sample complexity increases, as is the case with fecal samples, increasing chemical noise and background signals, affecting the robustness of the data (Willems *et al.*, 2021). Concerning bacterial peptides and proteins, Willems *et al.,* compared identification and quantification results of different dilutions of host proteins using HeLa protein lysates and *Salmonella* protein lysates to assess the efficiencies of both acquisition modes. DIA/SWATH acquisition proved to be especially beneficial for *Salmonella* protein and peptides identifications and quantification at lower dilutions compared to IDA (Willems *et al.*, 2021).

Although through this study was able to quantify differences, or lack thereof between proximal and distal feces, quantification relative to species amount/abundance was not able to be performed as absolute quantification is needed. That being said, there is extensive literature describing what has been quantified on the species level by metaproteomics and 16S rRNA, which is notably useful to consider for future experiments. A study performed by *Liu et al*. found that the most prevalent phyla from the fecal microbiome in control mice were *Bacteroidetes* and *Bacillota* (*Firmicutes*) by 16S rRNA sequencing (Liu *et al.*, 2022). Additionally, a study performed by *Qin, J et al.* reported as well that *Bacteroidetes* and *Bacillota* make up over 90% of the phyla found in the human distal colon from 16S rRNA as well (Qin *et al.*, 2010). Interestingly, *Thuy-Boun et al.* found large discrepancies between the results obtained from metaproteomic and 16S rRNA analysis on the detected levels of *Bacteroidetes* and *Bacillota (Firmicutes)* phyla from stool samples in a study comparing healthy and ulcerative colitis patients. In this study they reported 22.7% *Bacillota* composition in samples compared to 86.2% composition from 16S rRNA, along with much lower detection of *Bacteroidetes* from 16S rRNA (around 0.86%) contrary to 4.2% found

from metaproteomic analysis (Thuy-Boun *et al.*, 2022). The challenges and discrepancies shown from the study performed by *Thuy-Boun et al.* highlight the challenges and complementarity associated with two popular techniques for studying the microbiome and highlights the additional work that needs to be done to further understand and identify the gut microbiome composition.

While the study couldn't draw definitive conclusions regarding regional specificity of bacterial species, our metaproteomics via LC-HRMS/MS offered extensive microbiome coverage at the species and strain levels based on the quantified proteins and peptides monitored. This will undoubtedly serve for future projects implicating perturbations at the microbiome level. This is an exciting new area of proteomics that is applicable to many studies involving gut health and these results will serve as a starting point for our group to continue research in this field.

CONCLUSION

The GI tract, more specifically the colon has been of great interest over the last few decades due to the prevalence of intestinal diseases. Although many studies have shown how disease affects the metabolomic, proteomic, and transcriptomic profile of the colon, very few studies have shown the metabolome and proteome coverage of a healthy colon, notably with the absence of disease to further understand baseline variations in the colon prior to introduction of disease.

This work aimed to study the overall metabolomic and proteomic coverage from colon and feces of healthy mice, as well as investigate if certain of these molecules show region specificity in the colon. High overall metabolite and protein coverage was found in the colon, with many significantly changing molecules in both datasets. Regarding fecal samples, a high metabolite coverage was found, but metaproteomics was required to properly characterize the proteome of these samples. On both metabolite and protein levels, the feces did not show the same region heterogeneity as the colon samples in healthy mice. Metaproteomics revealed several advantages including the specificity of microbial species able to be quantified. Limitations encountered such as the less accurate data obtained from IDA identification regarding which species were present in the distinct regions of the colon was evident from our results.

The information revealed in this project is especially important as it has highlighted key molecular groups that can be targeted for more detailed follow-up studies involving specific diseases affecting the gut. For example, prostaglandins and tryptophan metabolites and well as keratin proteins show regional specificity in healthy subjects, where they can potentially aid in understanding the prevalence, prognosis and treatments options for intestinal diseases affecting specific regions more aggressively.

BIBLIOGRAPHIE

Agrawal, M. et Jess, T. (2022). Implications of the changing epidemiology of inflammatory bowel disease in a changing world. *United European Gastroenterol J*, *10*(10), 1113-1120. https://doi.org/10.1002/ueg2.12317

Ang, C. S., Rothacker, J., Patsiouras, H., Burgess, A. W. et Nice, E. C. (2010). Murine fecal proteomics: a model system for the detection of potential biomarkers for colorectal cancer. *J Chromatogr A*, *1217*(19), 3330-3340. https://doi.org/10.1016/j.chroma.2009.10.007

Aoki, T. et Narumiya, S. (2012). Prostaglandins and chronic inflammation. *Trends in Pharmacological Sciences*, *33*(6), 304-311. https://doi.org/https://doi.org/10.1016/j.tips.2012.02.004

Appleton, J. (2018). The Gut-Brain Axis: Influence of Microbiota on Mood and Mental Health. *Integr Med (Encinitas)*, *17*(4), 28-32.

Armengaud, J. (2023). Metaproteomics to understand how microbiota function: The crystal ball predicts a promising future. *Environ Microbiol*, *25*(1), 115-125. https://doi.org/10.1111/1462-2920.16238

Arnold, D., Lueza, B., Douillard, J. Y., Peeters, M., Lenz, H. J., Venook, A., Heinemann, V., Van Cutsem, E., Pignon, J. P., Tabernero, J., Cervantes, A. et Ciardiello, F. (2017). Prognostic and predictive value of primary tumour side in patients with RAS wild-type metastatic colorectal cancer treated with chemotherapy and EGFR directed antibodies in six randomized trials. *Ann Oncol*, *28*(8), 1713-1729. https://doi.org/10.1093/annonc/mdx175

Azzouz, L. L. et Sharma, S. (2023). Physiology, Large Intestine. Dans *StatPearls*.

Banerjee, S. et Mazumdar, S. (2012). Electrospray ionization mass spectrometry: a technique to access the information beyond the molecular weight of the analyte. *Int J Anal Chem*, *2012*, 282574. https://doi.org/10.1155/2012/282574

Baribault, H., Penner, J., Iozzo, R. V. et Wilson-Heiner, M. (1994). Colorectal hyperplasia and inflammation in keratin 8-deficient FVB/N mice. *Genes Dev*, *8*(24), 2964-2973. https://doi.org/10.1101/gad.8.24.2964

Barkovits, K., Pacharra, S., Pfeiffer, K., Steinbach, S., Eisenacher, M., Marcus, K. et Uszkoreit, J. (2020). Reproducibility, Specificity and Accuracy of Relative Quantification Using Spectral Library-based Data-independent Acquisition. *Mol Cell Proteomics*, *19*(1), 181-197. https://doi.org/10.1074/mcp.RA119.001714

Baxter, B. A., Parker, K. D., Nosler, M. J., Rao, S., Craig, R., Seiler, C. et Ryan, E. P. (2020). Metabolite profile comparisons between ascending and descending colon tissue in healthy adults. *World J Gastroenterol*, *26*(3), 335-352. https://doi.org/10.3748/wjg.v26.i3.335

Bird, I. M. (1989). High performance liquid chromatography: principles and clinical applications. *Bmj*, *299*(6702), 783-787. https://doi.org/10.1136/bmj.299.6702.783

Bishnupuri, K. S., Alvarado, D. M., Khouri, A. N., Shabsovich, M., Chen, B., Dieckgraefe, B. K. et Ciorba, M. A. (2019). IDO1 and Kynurenine Pathway Metabolites Activate PI3K-Akt Signaling in the Neoplastic Colon Epithelium to Promote Cancer Cell Proliferation and Inhibit Apoptosis. *Cancer Res*, *79*(6), 1138-1150. https://doi.org/10.1158/0008-5472.Can-18-0668

Bonetto, S., Fagoonee, S., Battaglia, E., Grassini, M., Saracco, G. M. et Pellicano, R. (2021). Recent advances in the treatment of irritable bowel syndrome. *Pol Arch Intern Med*, *131*(7-8), 709-715. https://doi.org/10.20452/pamw.16067

Brioschi, M., Gianazza, E., Agostoni, P., Zoanni, B., Mallia, A. et Banfi, C. (2021). Multiplexed MRM-Based Proteomics Identified Multiple Biomarkers of Disease Severity in Human Heart Failure. *Int J Mol Sci*, *22*(2). https://doi.org/10.3390/ijms22020838

Busi, S. B., Lei, Z., Sumner, L. W. et Amos-Landgraf, J. M. (2023). Integrated multi-omic analyses provide insight into colon adenoma susceptibility modulation by the gut microbiota. *mSystems*, *8*(4), e0015123. https://doi.org/10.1128/msystems.00151-23

Chandel, N. S. (2021). Carbohydrate Metabolism. *Cold Spring Harb Perspect Biol*, *13*(1). https://doi.org/10.1101/cshperspect.a040568

Cheng, L. K., O'Grady, G., Du, P., Egbuji, J. U., Windsor, J. A. et Pullan, A. J. (2010). Gastrointestinal system. *Wiley Interdiscip Rev Syst Biol Med*, *2*(1), 65-79. https://doi.org/10.1002/wsbm.19

Cleveland, J. P. et Rose, J. R. (2013). Identification of b-/y-ions in MS/MS spectra using a two stage neural network. *Proteome Sci*, *11*(Suppl 1), S4. https://doi.org/10.1186/1477-5956-11-s1-s4

Clish, C. B. (2015). Metabolomics: an emerging but powerful tool for precision medicine. *Cold Spring Harb Mol Case Stud*, *1*(1), a000588. https://doi.org/10.1101/mcs.a000588

Cooper, J. et Giancotti, F. G. (2019). Integrin Signaling in Cancer: Mechanotransduction, Stemness, Epithelial Plasticity, and Therapeutic Resistance. *Cancer Cell*, *35*(3), 347-367. https://doi.org/10.1016/j.ccell.2019.01.007

Corfe, B. M., Majumdar, D., Assadsangabi, A., Marsh, A. M. R., Cross, S. S., Connolly, J. B., Evans, C. A. et Lobo, A. J. (2015). Inflammation decreases keratin level in ulcerative colitis; inadequate restoration associates with increased risk of colitis-associated cancer. *BMJ Open Gastroenterology*, *2*(1), e000024. https://doi.org/10.1136/bmjgast-2014-000024

Cortes, L., Wopereis, H., Tartiere, A., Piquenot, J., Gouw, J. W., Tims, S., Knol, J. et Chelsky, D. (2019). Metaproteomic and 16S rRNA Gene Sequencing Analysis of the Infant Fecal Microbiome. *Int J Mol Sci*, *20*(6). https://doi.org/10.3390/ijms20061430

Coskun, O. (2016). Separation techniques: Chromatography. *North Clin Istanb*, *3*(2), 156-160. https://doi.org/10.14744/nci.2016.32757

Cosnes, J., Gower-Rousseau, C., Seksik, P. et Cortot, A. (2011). Epidemiology and natural history of inflammatory bowel diseases. *Gastroenterology*, *140*(6), 1785-1794. https://doi.org/10.1053/j.gastro.2011.01.055

Dambrova, M., Makrecka-Kuka, M., Kuka, J., Vilskersts, R., Nordberg, D., Attwood, M. M., Smesny, S., Sen, Z. D., Guo, A. C., Oler, E., Tian, S., Zheng, J., Wishart, D. S., Liepinsh, E. et Schiöth, H. B. (2022). Acylcarnitines: Nomenclature, Biomarkers, Therapeutic Potential, Drug Targets, and Clinical Trials. *Pharmacol Rev*, *74*(3), 506-551. https://doi.org/10.1124/pharmrev.121.000408

Deng, K., Han, P., Song, W., Wang, Z., Zhang, F., Xie, H., Zhao, W., Xu, H., Cai, Y., Rong, Z., Yu, X., Cui, B. B. et Li, K. (2018). Plasma metabolomic profiling distinguishes right-sided from left-sided colon cancer. *Clin Chim Acta*, *487*, 357-362. https://doi.org/10.1016/j.cca.2018.10.010

Deng, Y., Zhou, M., Wang, J., Yao, J., Yu, J., Liu, W., Wu, L., Wang, J. et Gao, R. (2021). Involvement of the microbiota-gut-brain axis in chronic restraint stress: disturbances of the kynurenine metabolic pathway in both the gut and brain. *Gut Microbes*, *13*(1), 1-16. https://doi.org/10.1080/19490976.2020.1869501

Dent, E. W., Gupton, S. L. et Gertler, F. B. (2011, Mar 1). The growth cone cytoskeleton in axon outgrowth and guidance. *Cold Spring Harb Perspect Biol*, *3*(3). https://doi.org/10.1101/cshperspect.a001800

Dettmer, K., Aronov, P. A. et Hammock, B. D. (2007). Mass spectrometry-based metabolomics. *Mass Spectrom Rev*, *26*(1), 51-78. https://doi.org/10.1002/mas.20108

Di Tommaso, N., Gasbarrini, A. et Ponziani, F. R. (2021). Intestinal Barrier in Human Health and Disease. *Int J Environ Res Public Health*, *18*(23). https://doi.org/10.3390/ijerph182312836

Dieterich, W., Schink, M. et Zopf, Y. (2018). Microbiota in the Gastrointestinal Tract. *Med Sci (Basel)*, *6*(4). https://doi.org/10.3390/medsci6040116

Dupree, E. J., Jayathirtha, M., Yorkey, H., Mihasan, M., Petre, B. A. et Darie, C. C. (2020). A Critical Review of Bottom-Up Proteomics: The Good, the Bad, and the Future of this Field. *Proteomes*, *8*(3). https://doi.org/10.3390/proteomes8030014

Duraes, L. C., Steele, S. R., Valente, M. A., Lavryk, O. A., Connelly, T. M. et Kessler, H. (2022). Right colon, left colon, and rectal cancer have different oncologic and quality of life

outcomes. *International Journal of Colorectal Disease*, *37*(4), 939-948. https://doi.org/10.1007/s00384-022-04121-x

Fabregat, A., Sidiropoulos, K., Viteri, G., Forner, O., Marin-Garcia, P., Arnau, V., D'Eustachio, P., Stein, L. et Hermjakob, H. (2017). Reactome pathway analysis: a high-performance in-memory approach. *BMC Bioinformatics*, *18*(1), 142. https://doi.org/10.1186/s12859-017-1559-2

Fernández-Costa, C., Martínez-Bartolomé, S., McClatchy, D. B., Saviola, A. J., Yu, N. K. et Yates, J. R., 3rd. (2020). Impact of the Identification Strategy on the Reproducibility of the DDA and DIA Results. *J Proteome Res*, *19*(8), 3153-3161. https://doi.org/10.1021/acs.jproteome.0c00153

Feuerstein, J. D., Moss, A. C. et Farraye, F. A. (2019). Ulcerative Colitis. *Mayo Clin Proc*, *94*(7), 1357-1373. https://doi.org/10.1016/j.mayocp.2019.01.018

Folz, J., Culver, R. N., Morales, J. M., Grembi, J., Triadafilopoulos, G., Relman, D. A., Huang, K. C., Shalon, D. et Fiehn, O. (2023). Human metabolome variation along the upper intestinal tract. *Nat Metab*, *5*(5), 777-788. https://doi.org/10.1038/s42255-023-00777-z

Fouquet, G., Coman, T., Hermine, O. et Côté, F. (2019). Serotonin, hematopoiesis and stem cells. *Pharmacological Research*, *140*, 67-74. https://doi.org/https://doi.org/10.1016/j.phrs.2018.08.005

Gao, J., Xiong, T., Grabauskas, G. et Owyang, C. (2022). Mucosal Serotonin Reuptake Transporter Expression in Irritable Bowel Syndrome Is Modulated by Gut Microbiota Via Mast Cell-Prostaglandin E2. *Gastroenterology*, *162*(7), 1962-1974.e1966. https://doi.org/10.1053/j.gastro.2022.02.016

Garg, E. et Zubair, M. (2023). Mass Spectrometer. Dans *StatPearls*. StatPearls Publishing, Copyright © 2023, StatPearls Publishing LLC.

Geng, Z. H., Zhu, Y., Li, Q. L., Zhao, C. et Zhou, P. H. (2022). Enteric Nervous System: The Bridge Between the Gut Microbiota and Neurological Disorders. *Front Aging Neurosci*, *14*, 810483. https://doi.org/10.3389/fnagi.2022.810483

Gershon, M. D. et Tack, J. (2007, 2007/01/01/). The Serotonin Signaling System: From Basic Understanding To Drug Development for Functional GI Disorders. *Gastroenterology*, *132*(1), 397-414. https://doi.org/https://doi.org/10.1053/j.gastro.2006.11.002

Gonzalez-Covarrubias, V., Martínez-Martínez, E. et Del Bosque-Plata, L. (2022). The Potential of Metabolomics in Biomedical Applications. *Metabolites*, *12*(2). https://doi.org/10.3390/metabo12020194

Gorospe, M., Wang, X., Guyton, K. Z. et Holbrook, N. J. (1996). Protective role of p21(Waf1/Cip1) against prostaglandin A2-mediated apoptosis of human colorectal carcinoma cells. *Mol Cell Biol*, *16*(12), 6654-6660. https://doi.org/10.1128/mcb.16.12.6654

Greenwood-Van Meerveld, B., Johnson, A. C. et Grundy, D. (2017). Gastrointestinal Physiology and Function. *Handb Exp Pharmacol*, *239*, 1-16. https://doi.org/10.1007/164_2016_118

Gremel, G., Wanders, A., Cedernaes, J., Fagerberg, L., Hallström, B., Edlund, K., Sjöstedt, E., Uhlén, M. et Pontén, F. (2015). The human gastrointestinal tract-specific transcriptome and proteome as defined by RNA sequencing and antibody-based profiling. *J Gastroenterol*, *50*(1), 46-57. https://doi.org/10.1007/s00535-014-0958-7

Gross, J. r. H. (2010). *Mass spectrometry : a textbook* (2nd ed.). Springer. https://doi.org/10.1007/978-3-642-10711-5

Guijas, C., Montenegro-Burke, J. R., Warth, B., Spilker, M. E. et Siuzdak, G. (2018). Metabolomics activity screening for identifying metabolites that modulate phenotype. *Nat Biotechnol*, *36*(4), 316-320. https://doi.org/10.1038/nbt.4101

Haag, A. M. (2016). Mass Analyzers and Mass Spectrometers. *Adv Exp Med Biol*, *919*, 157-169. https://doi.org/10.1007/978-3-319-41448-5_7

Habtezion, A., Toivola, D. M., Butcher, E. C. et Omary, M. B. (2005). Keratin-8-deficient mice develop chronic spontaneous Th2 colitis amenable to antibiotic treatment. *J Cell Sci*, *118*(Pt 9), 1971-1980. https://doi.org/10.1242/jcs.02316

Hao, F., Guo, H., Zhong, J., Geng, Q., Yang, Y., Chen, B. et Guo, C. (2018). Effects of Prostaglandin E1 on Patients Undergoing Major Gastrointestinal Surgery. *Ann Surg*, *267*(4), 759-765. https://doi.org/10.1097/SLA.0000000000002152

Hillman, E. T., Lu, H., Yao, T. et Nakatsu, C. H. (2017). Microbial Ecology along the Gastrointestinal Tract. *Microbes Environ*, *32*(4), 300-313. https://doi.org/10.1264/jsme2.ME17017

Ho, C. S., Lam, C. W., Chan, M. H., Cheung, R. C., Law, L. K., Lit, L. C., Ng, K. F., Suen, M. W. et Tai, H. L. (2003). Electrospray ionisation mass spectrometry: principles and clinical applications. *Clin Biochem Rev*, *24*(1), 3-12.

Hoffmann, E. d. et Stroobant, V. (2007). *Mass spectrometry : principles and applications* (Third edition. ed.). J. Wiley.

Holland, A. M., Bon-Frauches, A. C., Keszthelyi, D., Melotte, V. et Boesmans, W. (2021). The enteric nervous system in gastrointestinal disease etiology. *Cell Mol Life Sci*, *78*(10), 4713-4733. https://doi.org/10.1007/s00018-021-03812-y

Hou, K., Wu, Z. X., Chen, X. Y., Wang, J. Q., Zhang, D., Xiao, C., Zhu, D., Koya, J. B., Wei, L., Li, J. et Chen, Z. S. (2022). Microbiota in health and diseases. *Signal Transduct Target Ther*, *7*(1), 135. https://doi.org/10.1038/s41392-022-00974-4

Huang, Y., Duanmu, J., Liu, Y., Yan, M., Li, T. et Jiang, Q. (2021). Analysis of multi-omics differences in left-side and right-side colon cancer. *PeerJ*, *9*, e11433. https://doi.org/10.7717/peerj.11433

Huang, Z., Liu, K., Ma, W., Li, D., Mo, T. et Liu, Q. (2022). The gut microbiome in human health and disease-Where are we and where are we going? A bibliometric analysis. *Front Microbiol*, *13*, 1018594. https://doi.org/10.3389/fmicb.2022.1018594

Hugenholtz, F. et de Vos, W. M. (2018). Mouse models for human intestinal microbiota research: a critical evaluation. *Cell Mol Life Sci*, *75*(1), 149-160. https://doi.org/10.1007/s00018-017-2693-8

Imperial, R., Ahmed, Z., Toor, O. M., Erdoğan, C., Khaliq, A., Case, P., Case, J., Kennedy, K., Cummings, L. S., Melton, N., Raza, S., Diri, B., Mohammad, R., El-Rayes, B., Pluard, T., Hussain, A., Subramanian, J. et Masood, A. (2018). Comparative proteogenomic analysis of right-sided colon cancer, left-sided colon cancer and rectal cancer reveals distinct mutational profiles. *Mol Cancer*, *17*(1), 177. https://doi.org/10.1186/s12943-018-0923-9

Irum, N., Afzal, T., Faraz, M. H., Aslam, Z. et Rasheed, F. (2023). The role of gut microbiota in depression: an analysis of the gut-brain axis [Review]. *Frontiers in Behavioral Neuroscience*, *17*. https://doi.org/10.3389/fnbeh.2023.1185522

James, S. L., Irving, P. M., Gearry, R. B. et Gibson, P. R. (2008). Management of distal ulcerative colitis: frequently asked questions analysis. *Intern Med J*, *38*(2), 114-119. https://doi.org/10.1111/j.1445-5994.2007.01601.x

Jara-Gutiérrez, Á. et Baladrón, V. (2021). The Role of Prostaglandins in Different Types of Cancer. *Cells*, *10*(6). https://doi.org/10.3390/cells10061487

Johnson, C. H., Ivanisevic, J. et Siuzdak, G. (2016). Metabolomics: beyond biomarkers and towards mechanisms. *Nat Rev Mol Cell Biol*, *17*(7), 451-459. https://doi.org/10.1038/nrm.2016.25

Kahai, P., Mandiga, P., Wehrle, C. J. et Lobo, S. (2023). Anatomy, Abdomen and Pelvis: Large Intestine. Dans *StatPearls*.

Karpievitch, Y. V., Polpitiya, A. D., Anderson, G. A., Smith, R. D. et Dabney, A. R. (2010). Liquid Chromatography Mass Spectrometry-Based Proteomics: Biological and Technological Aspects. *Ann Appl Stat*, *4*(4), 1797-1823. https://doi.org/10.1214/10-aoas341

Kessmann, J. (2006). Hirschsprung's disease: diagnosis and management. *Am Fam Physician*, *74*(8), 1319-1322.

Klein, M. et Varga, I. (2020). Hirschsprung's Disease-Recent Understanding of Embryonic Aspects, Etiopathogenesis and Future Treatment Avenues. *Medicina (Kaunas)*, *56*(11). https://doi.org/10.3390/medicina56110611

Kleiner, M. (2019). Metaproteomics: Much More than Measuring Gene Expression in Microbial Communities. *mSystems*, *4*(3). https://doi.org/10.1128/mSystems.00115-19

Koutroubakis, I. E. (2010). Recent advances in the management of distal ulcerative colitis. *World J Gastrointest Pharmacol Ther*, *1*(2), 43-50. https://doi.org/10.4292/wjgpt.v1.i2.43

Kuipers, E. J., Grady, W. M., Lieberman, D., Seufferlein, T., Sung, J. J., Boelens, P. G., van de Velde, C. J. et Watanabe, T. (2015). Colorectal cancer. *Nat Rev Dis Primers*, *1*, 15065. https://doi.org/10.1038/nrdp.2015.65

Kunkel, S. L., Thrall, R. S., Kunkel, R. G., McCormick, J. R., Ward, P. A. et Zurier, R. B. (1979, Nov). Suppression of immune complex vasculitis in rats by prostaglandin. *J Clin Invest*, *64*(5), 1525-1529. https://doi.org/10.1172/jci109611

Lai, L. A., Tong, Z., Chen, R. et Pan, S. (2019). Metaproteomics Study of the Gut Microbiome. *Methods Mol Biol*, *1871*, 123-132. https://doi.org/10.1007/978-1-4939-8814-3_8

Lai, X. (2013). Reproducible method to enrich membrane proteins with high purity and high yield for an LC-MS/MS approach in quantitative membrane proteomics. *Electrophoresis*, *34*(6), 809-817. https://doi.org/10.1002/elps.201200503

Lee, M. S., Menter, D. G. et Kopetz, S. (2017). Right Versus Left Colon Cancer Biology: Integrating the Consensus Molecular Subtypes. *J Natl Compr Canc Netw*, *15*(3), 411-419. https://doi.org/10.6004/jnccn.2017.0038

Lehman, H. K. et Segal, B. H. (2020). The role of neutrophils in host defense and disease. *J Allergy Clin Immunol*, *145*(6), 1535-1544. https://doi.org/10.1016/j.jaci.2020.02.038

Levin, G., Duffin, K. L., Obukowicz, M. G., Hummert, S. L., Fujiwara, H., Needleman, P. et Raz, A. (2002). Differential metabolism of dihomo-gamma-linolenic acid and arachidonic acid by cyclo-oxygenase-1 and cyclo-oxygenase-2: implications for cellular synthesis of prostaglandin E1 and prostaglandin E2. *Biochem J*, *365*(Pt 2), 489-496. https://doi.org/10.1042/bj20011798

Li, J., Smith, L. S. et Zhu, H. J. (2021). Data-independent acquisition (DIA): An emerging proteomics technology for analysis of drug-metabolizing enzymes and transporters. *Drug Discov Today Technol*, *39*, 49-56. https://doi.org/10.1016/j.ddtec.2021.06.006

Liu, J., Qi, M., Qiu, C., Wang, F., Xie, S., Zhao, J., Wu, J. et Song, X. (2022). Integrative analysis of the mouse fecal microbiome and metabolome reveal dynamic phenotypes in the development of colorectal cancer. *Front Microbiol*, *13*, 1021325. https://doi.org/10.3389/fmicb.2022.1021325

Livovsky, D. M., Pribic, T. et Azpiroz, F. (2020). Food, Eating, and the Gastrointestinal Tract. *Nutrients*, *12*(4). https://doi.org/10.3390/nu12040986

Lotfollahzadeh, S., Taherian, M. et Anand, S. (2023). Hirschsprung Disease. Dans *StatPearls*. StatPearls Publishing, Copyright © 2023, StatPearls Publishing LLC.

Loupakis, F., Yang, D., Yau, L., Feng, S., Cremolini, C., Zhang, W., Maus, M. K., Antoniotti, C., Langer, C., Scherer, S. J., Muller, T., Hurwitz, H. I., Saltz, L., Falcone, A. et Lenz, H. J. (2015). Primary tumor location as a prognostic factor in metastatic colorectal cancer. *J Natl Cancer Inst*, *107*(3). https://doi.org/10.1093/jnci/dju427

Macklin, A., Khan, S. et Kislinger, T. (2020). Recent advances in mass spectrometry based clinical proteomics: applications to cancer research. *Clin Proteomics*, *17*, 17. https://doi.org/10.1186/s12014-020-09283-w

Majumdar, D., Tiernan, J. P., Lobo, A. J., Evans, C. A. et Corfe, B. M. (2012). Keratins in colorectal epithelial function and disease. *Int J Exp Pathol*, *93*(5), 305-318. https://doi.org/10.1111/j.1365-2613.2012.00830.x

Malone, J. C., Arbor, T. C. et Shah, A. B. (2023). Embryology, Midgut. Dans *StatPearls*. StatPearls Publishing, Copyright © 2023, StatPearls Publishing LLC.

Mandal, A. K., Zhang, Z., Kim, S. J., Tsai, P. C. et Mukherjee, A. B. (2005). Yin-yang: balancing act of prostaglandins with opposing functions to regulate inflammation. *J Immunol*, *175*(10), 6271-6273. https://doi.org/10.4049/jimmunol.175.10.6271

Manocha, M. et Khan, W. I. (2012). Serotonin and GI Disorders: An Update on Clinical and Experimental Studies. *Clin Transl Gastroenterol*, *3*(4), e13. https://doi.org/10.1038/ctg.2012.8

Marshall, J., Yoshino, T., Rha, S. Y., Church, D. N., Coutinho, A. K., Sampaio-Filho, C. A., Gallagher, D. J., García-Foncillas, J., Heyde, S. v. d., Juhl, H., Woodsmith, J. et Kerr, D. J. (2021). Multi-omics characterization of left-right colorectal cancer. *Journal of Clinical Oncology*, *39*(15_suppl), 3542-3542. https://doi.org/10.1200/JCO.2021.39.15_suppl.3542

Mason, K. L., Huffnagle, G. B., Noverr, M. C. et Kao, J. Y. (2008). Overview of gut immunology. *Adv Exp Med Biol*, *635*, 1-14. https://doi.org/10.1007/978-0-387-09550-9_1

Matthiesen, R. et Bunkenborg, J. (2013). Introduction to mass spectrometry-based proteomics. *Methods Mol Biol*, *1007*, 1-45. https://doi.org/10.1007/978-1-62703-392-3_1

Mawe, G. M. et Hoffman, J. M. (2013). Serotonin signalling in the gut--functions, dysfunctions and therapeutic targets. *Nat Rev Gastroenterol Hepatol*, *10*(8), 473-486. https://doi.org/10.1038/nrgastro.2013.105

Meier, K. H. U., Trouillon, J., Li, H., Lang, M., Fuhrer, T., Zamboni, N., Sunagawa, S., Macpherson, A. J. et Sauer, U. (2023). Metabolic landscape of the male mouse gut identifies different niches determined by microbial activities. *Nat Metab*, *5*(6), 968-980. https://doi.org/10.1038/s42255-023-00802-1

Monteiro, M. P. et Batterham, R. L. (2017). The Importance of the Gastrointestinal Tract in Controlling Food Intake and Regulating Energy Balance. *Gastroenterology*, *152*(7), 1707-1717.e1702. https://doi.org/10.1053/j.gastro.2017.01.053

Mun, J., Hur, W. et Ku, N. O. (2022). Roles of Keratins in Intestine. *Int J Mol Sci*, *23*(14). https://doi.org/10.3390/ijms23148051

Mylonas, C. C. et Lazaris, A. C. (2014). Colorectal cancer and basement membranes: clinicopathological correlations. *Gastroenterol Res Pract*, *2014*, 580159. https://doi.org/10.1155/2014/580159

Nguyen, T. L., Vieira-Silva, S., Liston, A. et Raes, J. (2015). How informative is the mouse for human gut microbiota research? *Dis Model Mech*, *8*(1), 1-16. https://doi.org/10.1242/dmm.017400

Ogobuiro, I., Gonzales, J., Shumway, K. R. et Tuma, F. (2023). Physiology, Gastrointestinal. Dans *StatPearls*.

Pang, Z., Chong, J., Zhou, G., de Lima Morais, D. A., Chang, L., Barrette, M., Gauthier, C., Jacques, P.-É., Li, S. et Xia, J. (2021). MetaboAnalyst 5.0: narrowing the gap between raw spectra and functional insights. *Nucleic Acids Research*, *49*(W1), W388-W396. https://doi.org/10.1093/nar/gkab382

Parigi, S. M., Larsson, L., Das, S., Ramirez Flores, R. O., Frede, A., Tripathi, K. P., Diaz, O. E., Selin, K., Morales, R. A., Luo, X., Monasterio, G., Engblom, C., Gagliani, N., Saez-Rodriguez, J., Lundeberg, J. et Villablanca, E. J. (2022). The spatial transcriptomic landscape of the healing mouse intestine following damage. *Nat Commun*, *13*(1), 828. https://doi.org/10.1038/s41467-022-28497-0

Petrelli, F., Tomasello, G., Borgonovo, K., Ghidini, M., Turati, L., Dallera, P., Passalacqua, R., Sgroi, G. et Barni, S. (2017). Prognostic Survival Associated With Left-Sided vs Right-Sided Colon Cancer: A Systematic Review and Meta-analysis. *JAMA Oncol*, *3*(2), 211-219. https://doi.org/10.1001/jamaoncol.2016.4227

Petriz, B. A. et Franco, O. L. (2017). Metaproteomics as a Complementary Approach to Gut Microbiota in Health and Disease. *Front Chem*, *5*, 4. https://doi.org/10.3389/fchem.2017.00004

Potter, K., Gayle, E. J. et Deb, S. (2023, 2023/11/03). Effect of gut microbiome on serotonin metabolism: a personalized treatment approach. *Naunyn-Schmiedeberg's Archives of Pharmacology*. https://doi.org/10.1007/s00210-023-02762-5

Qin, J., Li, R., Raes, J., Arumugam, M., Burgdorf, K. S., Manichanh, C., Nielsen, T., Pons, N., Levenez, F., Yamada, T., Mende, D. R., Li, J., Xu, J., Li, S., Li, D., Cao, J., Wang, B., Liang, H., Zheng, H., Xie, Y., Tap, J., Lepage, P., Bertalan, M., Batto, J. M., Hansen, T., Le Paslier, D., Linneberg, A., Nielsen, H. B., Pelletier, E., Renault, P., Sicheritz-Ponten, T., Turner, K., Zhu, H., Yu, C., Li, S., Jian, M., Zhou, Y., Li, Y., Zhang, X., Li, S., Qin, N., Yang, H., Wang, J., Brunak, S., Doré, J., Guarner, F., Kristiansen, K., Pedersen, O., Parkhill, J., Weissenbach, J., Bork, P., Ehrlich, S. D. et Wang, J. (2010). A human gut microbial gene catalogue established by metagenomic sequencing. *Nature*, *464*(7285), 59-65. https://doi.org/10.1038/nature08821

Rajakariar, R., Hilliard, M., Lawrence, T., Trivedi, S., Colville-Nash, P., Bellingan, G., Fitzgerald, D., Yaqoob, M. M. et Gilroy, D. W. (2007). Hematopoietic prostaglandin D2 synthase controls the onset and resolution of acute inflammation through PGD2 and 15-deoxyDelta12 14 PGJ2. *Proc Natl Acad Sci U S A*, *104*(52), 20979-20984. https://doi.org/10.1073/pnas.0707394104

Ramovs, V., Te Molder, L. et Sonnenberg, A. (2017). The opposing roles of laminin-binding integrins in cancer. *Matrix Biol*, *57-58*, 213-243. https://doi.org/10.1016/j.matbio.2016.08.007

Reigstad, C. S., Salmonson, C. E., Rainey, J. F., 3rd, Szurszewski, J. H., Linden, D. R., Sonnenburg, J. L., Farrugia, G. et Kashyap, P. C. (2015). Gut microbes promote colonic serotonin production through an effect of short-chain fatty acids on enterochromaffin cells. *FASEB J*, *29*(4), 1395-1403. https://doi.org/10.1096/fj.14-259598

Ricciotti, E. et FitzGerald, G. A. (2011). Prostaglandins and inflammation. *Arterioscler Thromb Vasc Biol*, *31*(5), 986-1000. https://doi.org/10.1161/atvbaha.110.207449

Rinninella, E., Raoul, P., Cintoni, M., Franceschi, F., Miggiano, G. A. D., Gasbarrini, A. et Mele, M. C. (2019). What is the Healthy Gut Microbiota Composition? A Changing Ecosystem across Age, Environment, Diet, and Diseases. *Microorganisms*, *7*(1). https://doi.org/10.3390/microorganisms7010014

Roscilli, G., Marra, E., Mori, F., Di Napoli, A., Mancini, R., Serlupi-Crescenzi, O., Virmani, A., Aurisicchio, L. et Ciliberto, G. (2013). Carnitines slow down tumor development of colon cancer in the DMH-chemical carcinogenesis mouse model. *J Cell Biochem*, *114*(7), 1665-1673. https://doi.org/10.1002/jcb.24508

Rossi, A., Kapahi, P., Natoli, G., Takahashi, T., Chen, Y., Karin, M. et Santoro, M. G. (2000). Anti-inflammatory cyclopentenone prostaglandins are direct inhibitors of IkappaB kinase. *Nature*, *403*(6765), 103-108. https://doi.org/10.1038/47520

Roth, W., Zadeh, K., Vekariya, R., Ge, Y. et Mohamadzadeh, M. (2021). Tryptophan Metabolism and Gut-Brain Homeostasis. *Int J Mol Sci*, *22*(6). https://doi.org/10.3390/ijms22062973

Russell, S. A. et Bashaw, G. J. (2018). Axon guidance pathways and the control of gene expression. *Dev Dyn*, *247*(4), 571-580. https://doi.org/10.1002/dvdy.24609

Ryan, M. C., Stucky, M., Wakefield, C., Melott, J. M., Akbani, R., Weinstein, J. N. et Broom, B. M. (2019). Interactive Clustered Heat Map Builder: An easy web-based tool for creating sophisticated clustered heat maps. *F1000Res*, *8*. https://doi.org/10.12688/f1000research.20590.2

Saha, L. (2014, Jun 14). Irritable bowel syndrome: pathogenesis, diagnosis, treatment, and evidence-based medicine. *World J Gastroenterol*, *20*(22), 6759-6773. https://doi.org/10.3748/wjg.v20.i22.6759

Sarihan, M., Bal Albayrak, M. G., Kasap, M., Akpinar, G. et Kocyigit, E. (2023). An experimental workflow for enrichment of low abundant proteins from human serum for the discovery of serum biomarkers. *J Biol Methods*, *10*, e99010001. https://doi.org/10.14440/jbm.2023.394

Sasaki, H. et Fukushima, M. (1994). Prostaglandins in the treatment of cancer. *Anticancer Drugs*, *5*(2), 131-138. https://doi.org/10.1097/00001813-199404000-00002

Scalbert, A., Brennan, L., Fiehn, O., Hankemeier, T., Kristal, B. S., van Ommen, B., Pujos-Guillot, E., Verheij, E., Wishart, D. et Wopereis, S. (2009, Dec). Mass-spectrometry-based metabolomics: limitations and recommendations for future progress with particular focus on nutrition research. *Metabolomics*, *5*(4), 435-458. https://doi.org/10.1007/s11306-009-0168-0

Schmehl, K., Florian, S., Jacobasch, G., Salomon, A. et Körber, J. (2000). Deficiency of epithelial basement membrane laminin in ulcerative colitis affected human colonic mucosa. *Int J Colorectal Dis*, *15*(1), 39-48. https://doi.org/10.1007/s003840050006

Schröder, O., Yudina, Y., Sabirsh, A., Zahn, N., Haeggström, J. Z. et Stein, J. (2006). 15-deoxy-Delta12,14-prostaglandin J2 inhibits the expression of microsomal prostaglandin E synthase type 2 in colon cancer cells. *J Lipid Res*, *47*(5), 1071-1080. https://doi.org/10.1194/jlr.M600008-JLR200

Schröder, R., Xue, L., Konya, V., Martini, L., Kampitsch, N., Whistler, J. L., Ulven, T., Heinemann, A., Pettipher, R. et Kostenis, E. (2012). PGH1, the precursor for the anti-inflammatory prostaglandins of the 1-series, is a potent activator of the pro-inflammatory receptor CRTH2/DP2. *PLoS One*, *7*(3), e33329. https://doi.org/10.1371/journal.pone.0033329

Semble, E. L. et Wu, W. C. (1989). Prostaglandins in the gut and their relationship to non-steroidal anti-inflammatory drugs. *Baillière's Clinical Rheumatology*, *3*(2), 247-269. https://doi.org/https://doi.org/10.1016/S0950-3579(89)80020-2

Simon, L. S. (1999). Role and regulation of cyclooxygenase-2 during inflammation. *Am J Med*, *106*(5b), 37s-42s. https://doi.org/10.1016/s0002-9343(99)00115-1

Sleno, L. (2012). The use of mass defect in modern mass spectrometry. *J Mass Spectrom*, *47*(2), 226-236. https://doi.org/10.1002/jms.2953

Snyder, L. R., Kirkland, J. J. et Dolan, J. W. (2010). *Introduction to modern liquid chromatography* (3rd / ed.). Wiley. https://doi.org/10.1002/9780470508183

Soret, R., Schneider, S., Bernas, G., Christophers, B., Souchkova, O., Charrier, B., Righini-Grunder, F., Aspirot, A., Landry, M., Kembel, S. W., Faure, C., Heuckeroth, R. O. et Pilon, N. (2020, Nov). Glial Cell-Derived Neurotrophic Factor Induces Enteric Neurogenesis and Improves Colon Structure and Function in Mouse Models of Hirschsprung Disease. *Gastroenterology*, *159*(5), 1824-1838.e1817. https://doi.org/10.1053/j.gastro.2020.07.018

Spenlé, C., Lefebvre, O., Lacroute, J., Méchine-Neuville, A., Barreau, F., Blottière, H. M., Duclos, B., Arnold, C., Hussenet, T., Hemmerlé, J., Gullberg, D., Kedinger, M., Sorokin, L., Orend, G. et Simon-Assmann, P. (2014). The laminin response in inflammatory bowel disease: protection or malignancy? *PLoS One*, *9*(10), e111336. https://doi.org/10.1371/journal.pone.0111336

Spiller, R. (2008, 2008/11/01/). Serotonin and GI clinical disorders. *Neuropharmacology*, *55*(6), 1072-1080. https://doi.org/https://doi.org/10.1016/j.neuropharm.2008.07.016

Srinivas, S. R., Prasad, P. D., Umapathy, N. S., Ganapathy, V. et Shekhawat, P. S. (2007). Transport of butyryl-L-carnitine, a potential prodrug, via the carnitine transporter OCTN2 and the amino acid transporter ATB(0,+). *Am J Physiol Gastrointest Liver Physiol*, *293*(5), G1046-1053. https://doi.org/10.1152/ajpgi.00233.2007

Straus, D. S. et Glass, C. K. (2001). Cyclopentenone prostaglandins: new insights on biological activities and cellular targets. *Med Res Rev*, *21*(3), 185-210. https://doi.org/10.1002/med.1006

Su, M. W., Chang, C. K., Lin, C. W., Chu, H. W., Tsai, T. N., Su, W. C., Chen, Y. C., Chang, T. K., Huang, C. W., Tsai, H. L., Wu, C. C., Chou, H. C., Shiu, B. H. et Wang, J. Y. (2022). Genomic and Metabolomic Landscape of Right-Sided and Left-Sided Colorectal Cancer: Potential Preventive Biomarkers. *Cells*, *11*(3). https://doi.org/10.3390/cells11030527

Surh, Y.-J., Na, H.-K., Park, J.-M., Lee, H.-N., Kim, W., Yoon, I.-S. et Kim, D.-D. (2011). 15-Deoxy-Δ12,14-prostaglandin J2, an electrophilic lipid mediator of anti-inflammatory and pro-resolving signaling. *Biochemical Pharmacology*, *82*(10), 1335-1351. https://doi.org/https://doi.org/10.1016/j.bcp.2011.07.100

Takada, Y., Ye, X. et Simon, S. (2007). The integrins. *Genome Biol*, *8*(5), 215. https://doi.org/10.1186/gb-2007-8-5-215

Taketo, M., Schroeder, A. C., Mobraaten, L. E., Gunning, K. B., Hanten, G., Fox, R. R., Roderick, T. H., Stewart, C. L., Lilly, F., Hansen, C. T. et et al. (1991). FVB/N: an inbred mouse strain preferable for transgenic analyses. *Proc Natl Acad Sci U S A*, *88*(6), 2065-2069. https://doi.org/10.1073/pnas.88.6.2065

Thursby, E. et Juge, N. (2017). Introduction to the human gut microbiota. *Biochem J*, *474*(11), 1823-1836. https://doi.org/10.1042/bcj20160510

Thuy-Boun, P. S., Wang, A. Y., Crissien-Martinez, A., Xu, J. H., Chatterjee, S., Stupp, G. S., Su, A. I., Coyle, W. J. et Wolan, D. W. (2022). Quantitative Metaproteomics and Activity-based Protein Profiling of Patient Fecal Microbiome Identifies Host and Microbial Serine-type Endopeptidase Activity Associated With Ulcerative Colitis. *Mol Cell Proteomics*, *21*(3), 100197. https://doi.org/10.1016/j.mcpro.2022.100197

Tuli, L. et Ressom, H. W. (2009). LC-MS Based Detection of Differential Protein Expression. *J Proteomics Bioinform*, *2*, 416-438. https://doi.org/10.4172/jpb.1000102

Vadlamudi, H. C., Raju, Y. P., Yasmeen, B. R. et Vulava, J. (2012). Anatomical, biochemical and physiological considerations of the colon in design and development of novel drug delivery systems. *Curr Drug Deliv*, *9*(6), 556-565. https://doi.org/10.2174/156720112803529774

van der Post, S. et Hansson, G. C. (2014). Membrane protein profiling of human colon reveals distinct regional differences. *Mol Cell Proteomics*, *13*(9), 2277-2287. https://doi.org/10.1074/mcp.M114.040204

Venkateswaran, N. et Conacci-Sorrell, M. (2020). Kynurenine: an oncometabolite in colon cancer. *Cell Stress*, *4*(1), 24-26. https://doi.org/10.15698/cst2020.01.210

Venkateswaran, N., Lafita-Navarro, M. C., Hao, Y. H., Kilgore, J. A., Perez-Castro, L., Braverman, J., Borenstein-Auerbach, N., Kim, M., Lesner, N. P., Mishra, P., Brabletz, T., Shay, J. W., DeBerardinis, R. J., Williams, N. S., Yilmaz, O. H. et Conacci-Sorrell, M. (2019). MYC promotes tryptophan uptake and metabolism by the kynurenine pathway in colon cancer. *Genes Dev*, *33*(17-18), 1236-1251. https://doi.org/10.1101/gad.327056.119

Viggiano, D., Ianiro, G., Vanella, G., Bibbò, S., Bruno, G., Simeone, G. et Mele, G. (2015). Gut barrier in health and disease: focus on childhood. *Eur Rev Med Pharmacol Sci*, *19*(6), 1077-1085.

Vuckovic, D., Dagley, L. F., Purcell, A. W. et Emili, A. (2013). Membrane proteomics by high performance liquid chromatography-tandem mass spectrometry: Analytical approaches and challenges. *Proteomics*, *13*(3-4), 404-423. https://doi.org/10.1002/pmic.201200340

Wang, B., Wu, L., Chen, J., Dong, L., Chen, C., Wen, Z., Hu, J., Fleming, I. et Wang, D. W. (2021). Metabolism pathways of arachidonic acids: mechanisms and potential therapeutic targets. *Signal Transduct Target Ther*, *6*(1), 94. https://doi.org/10.1038/s41392-020-00443-w

Wang, D. et DuBois, R. N. (2008). Pro-inflammatory prostaglandins and progression of colorectal cancer. *Cancer Lett*, *267*(2), 197-203. https://doi.org/10.1016/j.canlet.2008.03.004

Wang, S., van Schooten, F.-J., Jin, H., Jonkers, D. et Godschalk, R. (2023). The Involvement of Intestinal Tryptophan Metabolism in Inflammatory Bowel Disease Identified by a Meta-Analysis of the Transcriptome and a Systematic Review of the Metabolome. *Nutrients*, *15*(13), 2886.

Wang, W., Zhong, X. et Guo, J. (2021). Role of 2-series prostaglandins in the pathogenesis of type 2 diabetes mellitus and non-alcoholic fatty liver disease (Review). *Int J Mol Med*, *47*(6). https://doi.org/10.3892/ijmm.2021.4947

Wang, Z. et Yu, B. (2019). Chapter 15 - Metabolomics, Proteomics, and Genomics: An Introduction to a Clinician. Dans V. Nambi (dir.), *Biomarkers in Cardiovascular Disease* (p. 159-170). Elsevier. https://doi.org/https://doi.org/10.1016/B978-0-323-54835-9.00015-6.

Wei, L., Singh, R., Ha, S. E., Martin, A. M., Jones, L. A., Jin, B., Jorgensen, B. G., Zogg, H., Chervo, T., Gottfried-Blackmore, A., Nguyen, L., Habtezion, A., Spencer, N. J., Keating, D. J., Sanders, K. M. et Ro, S. (2021, Jun). Serotonin Deficiency Is Associated With Delayed Gastric Emptying. *Gastroenterology*, *160*(7), 2451-2466.e2419. https://doi.org/10.1053/j.gastro.2021.02.060

Weiss, G. A. et Hennet, T. (2017). Mechanisms and consequences of intestinal dysbiosis. *Cell Mol Life Sci*, *74*(16), 2959-2977. https://doi.org/10.1007/s00018-017-2509-x

West, R. M. (2021). Best practice in statistics: Use the Welch t-test when testing the difference between two groups. *Annals of Clinical Biochemistry*, *58*(4), 267-269. https://doi.org/10.1177/0004563221992088

Willems, P., Fels, U., Staes, A., Gevaert, K. et Van Damme, P. (2021). Use of Hybrid Data-Dependent and -Independent Acquisition Spectral Libraries Empowers Dual-Proteome Profiling. *J Proteome Res*, *20*(2), 1165-1177. https://doi.org/10.1021/acs.jproteome.0c00350

Wishart, D. S. (2008). Applications of metabolomics in drug discovery and development. *Drugs R D*, *9*(5), 307-322. https://doi.org/10.2165/00126839-200809050-00002

Wu, H. J. et Wu, E. (2012). The role of gut microbiota in immune homeostasis and autoimmunity. *Gut Microbes*, *3*(1), 4-14. https://doi.org/10.4161/gmic.19320

Xu, X., Ocansey, D. K. W., Hang, S., Wang, B., Amoah, S., Yi, C., Zhang, X., Liu, L. et Mao, F. (2022). The gut metagenomics and metabolomics signature in patients with inflammatory bowel disease. *Gut Pathog*, *14*(1), 26. https://doi.org/10.1186/s13099-022-00499-9

Zhang, X., Liu, X., Zhou, W., Du, Q., Yang, M., Ding, Y. et Hu, R. (2021). Blockade of IDO-Kynurenine-AhR Axis Ameliorated Colitis-Associated Colon Cancer via Inhibiting Immune Tolerance. *Cell Mol Gastroenterol Hepatol*, *12*(4), 1179-1199. https://doi.org/10.1016/j.jcmgh.2021.05.018

Zhang, Y., Liu, Y., Sun, J., Zhang, W., Guo, Z. et Ma, Q. (2023). Arachidonic acid metabolism in health and disease. *MedComm (2020)*, *4*(5), e363. https://doi.org/10.1002/mco2.363

Zhao, Z., Bai, J., Liu, C., Wang, Y., Wang, S., Zhao, F. et Gu, Q. (2023). Metabolomics analysis of amino acid and fatty acids in colorectal cancer patients based on tandem mass spectrometry. *J Clin Biochem Nutr*, *73*(2), 161-171. https://doi.org/10.3164/jcbn.22-110

Zhu, X., Chen, Y. et Subramanian, R. (2014). Comparison of information-dependent acquisition, SWATH, and MS(All) techniques in metabolite identification study employing ultrahigh-performance liquid chromatography-quadrupole time-of-flight mass spectrometry. *Anal Chem*, *86*(2), 1202-1209. https://doi.org/10.1021/ac403385y

Zwittink, R. D., van Zoeren-Grobben, D., Martin, R., van Lingen, R. A., Groot Jebbink, L. J., Boeren, S., Renes, I. B., van Elburg, R. M., Belzer, C. et Knol, J. (2017). Metaproteomics reveals functional differences in intestinal microbiota development of preterm infants. *Mol Cell Proteomics*, *16*(9), 1610-1620. https://doi.org/10.1074/mcp.RA117.000102